ESSENTIALS OF THE THEORY OF FLIGHT AND ELEMENTS OF DESIGNING ARTIFICIAL EARTH SATELLITES

M. K. Tikhonravov, I. K. Bazhinov, O. V. Gurko et al.

(NASA-TT-F-16220) ESSENTIALS OF THE THEORY OF FLIGHT AND ELEMENTS OF DESIGNING ARTIFICIAL EARTH SATELLITES (Kanner (Leo) Associates) 365 p HC $10.00 CSCL 22C N75-23637
G3/13 22161 Unclas

Translation of "Osnovy Teorii Poleta i Elementy Proyektirovaniya Iskusstvennykh Sputnikov Zemli", 2nd Edition, Revised and Expanded, Moscow, "Mashinostroyeniye" Press, 1974, pp. 1-331

NATIONAL AERONAUTICS AND SPACE ADMINISTRATION
WASHINGTON, D.C. 20546 JUNE 1975

STANDARD TITLE PAGE

1. Report No. NASA TT F-16,220	2. Government Accession No.	3. Recipient's Catalog No.
4. Title and Subtitle ESSENTIALS OF THE THEORY OF FLIGHT AND ELEMENTS OF DESIGNING ARTIFICIAL EARTH SATELLITES		5. Report Date June 1975 6. Performing Organization Code
7. Author(s) M. K. Tikhonravov (deceased), I. K. Bazhinov, O. V. Gurko et al.		8. Performing Organization Report No. 10. Work Unit No.
9. Performing Organization Name and Address Leo Kanner Associates, Redwood City, CA 94063		11. Contract or Grant No. NASw 2481 13. Type of Report and Period Covered Translation
12. Sponsoring Agency Name and Address NATIONAL AERONAUTICS AND SPACE ADMINISTRATION, WASHINGTON, D.C. 20546		14. Sponsoring Agency Code

15. Supplementary Notes

Translation of "Osnovy Teorii Poleta i Elementy Proyektirovaniya Iskusstvennykh Sputnikov Zemli", 2nd Edition, Revised and Expanded, Moscow, "Mashinostroyeniye" Press, 1974, pp. 1-331

16. Abstract

The book gives the basic concepts of the unperturbed (Keplerian) motion of a satellite. The effect on satellite motion of the following principal perturbing factors is analyzed: errors of satellite insertion into orbit, noncentrality of the Earth's gravitational field, air drag, anomalies of gravitational force, attraction of Moon and Sun, and solar wind pressure. The basic methods of determining satellite orbits from measurements are given. Problems of inserting artificial earth satellites into orbit and deorbiting to the Earth's surface are examined. The essentials of flight theory are expounded with reference to the necessity of selecting the optimal ballistic-design parameters when designing spacecraft.

17. Key Words (Selected by Author(s))	18. Distribution Statement
	Unclassified - Unlimited

19. Security Classif. (of this report)	20. Security Classif. (of this page)	21. No. of Pages	22. Price
Unclassified	Unclassified	365	

NASA-HQ

Annotation

Osnovy teorii poleta i elementy proyektirovaniya iskusstvennykh sputnikov zemli [Essentials of Flight Theory and Elements of Designing Artificial Earth Satellites, M.K. Tikhonravov, I.K. Bazhinov, O.V. Gurko, G.Yu. Maksimov, and I.M. Yatsunskiy, 2nd Edition, Revised and Expanded, Moscow, "Mashinostroyeniye" Press, 1974, 322 pages.

The book gives the basic concepts of the unperturbed (Keplerian) motion of a satellite. The effect on satellite motion of the following principal perturbing factors is analyzed: errors of satellite insertion into orbit, noncentrality of the Earth's gravitational field, air drag, anomalies of gravitational force, attraction of Moon and Sun, and solar wind pressure. The basic methods of determining satellite orbits from measurements are presented here. Problems of inserting artificial earth satellites into orbit and deorbiting to the Earth's surface are examined.

The essentials of flight theory are expounded with reference to the necessity of selecting the optimal ballistic-design parameters when designing spacecraft.

The book will prove useful to specialists in space technology as well as the students and instructors at the related higher educational institutions. 6 Tables, 68 Figures, 83 References.

PREFACE

After a severe illness, on 4 March 1972 Mikhail Klavdiyevich /5
Tikhonravov succumbed: one of the pioneers in Soviet rocket and space technology, Honored Leader in Science and Technology of the RSSR, Doctor of Technical Sciences, professor, and Corresponding Member of the International Astronomical Academy.

M.K. Tikhonravov was born in 1900 in the city of Vladimir in a school teacher's family. In 1919 he volunteered for the Red Army. In 1925, after graduating from the Air Force Academy imeni N.Ye. Zhukovskiy, Mikhail Klavdiyevich began working at aviation industry enterprises. He was one of the pioneers in domestic glider construction. A number of all-Union records were set on gliders of his design.

From 1931, M.K. Tikhonravov worked as part of the Group for the Study of Jet Propulsion (GIRD [Gruppa izucheniya reaktivnogo dvizheniya] 1932-1934) in Moscow. Here M.K. Tikhonravov's team built and launched the first domestic liquid-fueled rocket, the GIRD-09, in August 1933.

During the prewar years and in the Great Patriotic War, M.K. Tikhonravov worked at the RNII [Space Scientific Research Institute of Jet Propulsion], where he engaged in theoretical and experimental research on liquid-propellant rocket engines, developing rockets for investigating the upper atmospheric layers, and achieving closer fire patterns of the jet rockets of the legendary Katyusha.

Following the war, Mikhail Klavdiyevich worked on problems of designing composite rockets and artificial satellites. In /6
1948-1950, M.K. Tikhonravov presented papers on the technical feasibilities of building launch vehicles and artificial satellites in our country in the immediate future.

M.K. Tikhonravov worked in the design bureau under the supervision of the Chief Designer, Academician S.P. Korolev. With the direct participation of Mikhail Klavdiyevich, plans for the first artificial Earth satellite and manned spacecraft, and the first plans of automatic interplanetary and lunar landing craft were developed.

M.K. Tikhonravov gave much attention to educating and training young scientific co-workers, engineers, and designers. From 1947 to the last years of his life, he gave lectures to students at higher education institutions.

On becoming acquainted with K.E. Tsiolkovskiy in the early 1930's, Mikhail Klavdiyevich was struck by the great idea of interplanetary flight and all of his later life was devoted to

bringing this about. His theoretical and design work are priceless landmarks along this road. One can state without overexaggeration that the selfless scientific, educational, design, public informational, and organizing activities of M.K. Tikhonravov in great measure promoted the emergence of our country as first in the mastery of space.

Mikhail Klavdiyevich was repeatedly honored with high governmental awards: he was awarded the title of Hero of Socialist Labor; he was honored with the orders of Lenin, Red Banner, Patriotic War, and with medals. He was bestowed the Lenin Prize.

We will always cherish the glowing memory of Mikhail Kavdiyevich Tikhonravov, selflessly serving his homeland, a man of great heart.

Authors' group

FOREWORD TO FIRST EDITION

Rapid strides in the past decade made in rocket and space technology are leading to the gradual practical mastery by man of space foreseen by the great Russian scientist K. E. Tsiolkovskiy, the pioneer of spaceflight theory. /7

In this book are examined the essentials of flight theory inseparably linked to several elements of the designing of artificial Earth satellites (AES), since without studying the flight theory of the latter a grasp of space technology and spaceflight in the broader aspects is inconceivable.

Underlying the book are the theoretical studies carried out by the authors in 1950-1959 and supplemented by the results of studies in the past several years. Begun long before the beginning of the satellite age, they were directed at extending the theory of spaceflight. These studies met with a profound understanding and enjoyed the support of the Academician S. P. Korolev, the most eminent Soviet scientist and designer in rocket-space systems and studies of space.

The first chapter of the book deals with problems of satellite insertion into orbit. The methods of inserting into orbit a maximum-weight satellite developed in this chapter have been extended to engineering calculations. This chapter also gives fundamental concepts of the unperturbed motion of a satellite used in the subsequent chapters of the book.

The second chapter acquaints the reader with the problem of the deorbiting of spacecraft to Earth. Ballistic and gliding descents are examined, ensuring admissible g-loads and temperatures during aerodynamic heating.

The third chapter gives the theory of flight of AES [artificial Earth satellites] in orbit in a formulation convenient for engineering use. Besides simple formulas that make it possible to consider, when calculating satellite motion, the effect of the noncentrality of the Earth's gravity fields, attraction of the Moon and the Sun, atmospheric drag, and light pressure, when necessary techniques of calculations employing electronic computers are presented. This chapter, as in the two preceding (and also in Chapter 4), the methods worked out obey a single rule: the accuracy of the calculations must accord with the problems posed. It is to be noted that the derivation of some formulas are given in condensed form.

Chapter Four analyzes errors of satellite insertion into orbit resulting from inaccurate control of the spacecraft during the powered trajectory sections. One of the possible variants of the problem of two satellites meeting in orbit is solved. Changes in orbit by means of applied impulse forces are considered. Here

are derived the equations of perturbed motion in a near-circular orbit, obtained as early as 1954 by linearization. Subsequently these equations were elaborated by other authors.

Chapter Five sets forth the main principles of determining the orbits of artificial satellites and any other spacecraft from measurements.

The concluding, sixth chapter, highlights several special problems of satellite motion around the mass center when affected by applied forces and control moments.

FOREWORD TO SECOND EDITION /9

Seven years have passed since the book first appeared. During this time, new advances have been gained in mastering space through further progress in space technology. Along with flights of spacecraft to the moon and unmanned spacecraft to the planets of our solar system, mastery of near-Earth space by means of the large orbital stations of the Salyut and Skylab have become quite significant. As we know, one of the main aims of these flights is studying the possibilities of man's normal existence in space for extended periods, numbering many months or even years. In particular, this study is a necessity for expeditions even to the closest planet.

The first flights of artificial Earth satellites, followed by the first lunar probes, the automatic craft to Mars and to Venus, and finally, the first manned flights in space are the consequence of the progress made in the theory of flight of spacecraft. Well known is the determining role of flight theory in the initial stage of designing a given space complex in order to select orbital parameters of the AES and the main ballistic-design characteristics of the craft. Flight theory is also determining in planning the sessions of measurement and control of flights. In the latter case it is vital to predict motion over an extended period with an estimate of the possible orbital errors that are a consequence of errors in measurements or inaccurate allowance for applied forces.

The growing role of studies in flight theory and designing of /10
AES was responsible for the changes and expansion that were made in the book in the preparation of its second edition. The authors endeavored to reflect as far as possible all the fundamental problems in AES flight theory.

All chapters were revised.

Chapter One additionally includes material on the overall problem of optimizing the trajectories of inserting AES into orbit by using various kinds of engines.

The second chapter, on the errors of insertion into orbit, is somewhat shortened by dropping materials that have now become outdated. Still, in this chapter the section dealing with linearization of equations of motion of AES in a circular orbit was expanded.

Chapter Three is supplemented with revised methods of calculating satellite motion in orbit.

The fourth chapter was written anew and contains methods of determining orbits for navigations employing new techniques of estimating measurement errors and optimizing their distribution in orbit.

Chapter Five, dealing with problems of deorbiting, was considerably revised. Materials on control descent and the methods of aerodynamic landing are included in it.

The sixth chapter is supplemented with a treatment of problems of the dependence of the information content of radio communication links from measuring stations on the accuracy of AES orientation.

Participating in writing the book were A.A. Pivovarchik. He wrote Section 1.2 of Chapter I (except for the last subsection). V.N. Pochukayev participated in developing and writing Chapter IV, and N.I. Ivanov participated in developing and writing Chapter V.

The authors are grateful for any comments. They should be sent to this address: Moscow, B-78, No. 1-y Basmannyy per., d.3, "Mashinostroyeniye" Press.

ESSENTIALS OF FLIGHT THEORY AND ELEMENTS OF DESIGNING ARTIFICIAL EARTH SATELLITES

M.K. Tikhonravov, I.K. Bazhinov, O.V. Gurko,
G.Yu. Maksimov, and I.M. Yatsunskiy

CHAPTER I

/11*

INSERTION OF SATELLITE INTO ORBIT

We will define as an artificial satellite a body (or craft) capable of executing at least several orbits around the Earth under the effect of initial velocity imparted to it. Therefore, in order for the body to be converted into a satellite, it must be given a specific velocity at a high enough altitude at which atmospheric drag becomes negligible. Imparting this velocity to the craft will be referred to in the following as insertion of the satellite into orbit.

Insertion of the satellite into orbit can be achieved in two fundamentally different ways.

The first method is for the engine to operate continuously until the last rocket stage acquires the required velocity. Here the entire last stage is converted into a satellite. This method is the simplest, but to achieve high orbits it either leads to the necessity of substantially changing the engine operating conditions or else becomes energetically disadvantageous.

The second method is for the engine to operate with an interruption. After completing the first part of the powered flight the rocket will travel in an elliptical orbit (transfer ellipse). At one of the points of this ellipse the engine will again be fired (final fuel combustion is carried out) and the last rocket stage will now arrive at the required or some intermediate orbit, if the insertion into the given orbit is assumed to be conducted with several engine firings.

In the following we will refer to the first method as insertion into orbit without final combustion, and the second -- with final combustion of fuel.

We will refer to the first part of the powered section (before the interruption) in the following as the powered section of the trajectory, and to the second -- as the final-combustion section.

---

* Numbers in the margin indicate pagination in the foreign text.

This chapter examines the main regularities of unperturbed motion and solves several problems on the insertion of the satellite into orbit using liquid-propellant rocket engines and ramjet engines.

By unperturbed (design) motion we will mean the motion of the satellite considered under the condition that the only force applied on the orbit is the force of Earth's gravity. The Earth is assumed to be a sphere with concentric distribution of density (Keplerian motion). This point of view corresponds to that adopted in celestial mechanics. /12

Besides deriving the basic formulas of unperturbed motion, this chapter presents a method for determining the projection of the satellite trajectory onto the surface of the rotating Earth and formulates a problem of selecting the attitude of the orbital plane.

1.1. Unperturbed Satellite Motion

Derivation of Main Functions

Suppose that a system of fixed rectangular coordinates Oxyz is chosen, in which a heavy material point[1] with mass m. During its motion it is attracted by n celestial bodies with masses $m_0, m_1, \ldots, m_{n-1}$, likewise considered as material points. According to Newton's Law of Universal Gravity, the force of attraction that is experienced by each heavy point acting from a body j with mass m_j is expressed by the formula

$$f = k^2 m m_j \Delta_j^{-2},$$

where k^2 is the gravitational constant; and Δ_j is the distance from the point in question to the body with number j.

Referring to the component of force f along the coordinate axes

$$k^2 m m_j \frac{x_j - x}{\Delta_j^3}, \quad k^2 m m_j \frac{y_j - y}{\Delta_j^3}, \quad k^2 m m_j \frac{z_j - z}{\Delta_j^3}$$

$$\left(\frac{x_j - x}{\Delta_j}, \quad \frac{y_j - y}{\Delta_j}, \quad \frac{z_j - z}{\Delta_j} \right| \text{are the direction cosines),}$$

the differential equations describing the motion of a point with mass m can be represented in the form

[1] A spacecraft or satellite is what is referred to here.

Page Intentionally Left Blank

Pages 3 through 68

different, but magnitude-constant fuel consumption. Let us write out the working formulas for a three-stage rocket:

1. $$\tau_0 = \frac{-n_{01}g_0t_1I_1^{I} - n_{02}g_0t_2I_1^{II} + g_0t_f + w_f - \Delta w}{-n_{01}g_0t_1I_2^{I} - n_{02}g_0t_2I_2^{II} + u_f - \Delta u}; \qquad (1.143)$$

2. $$v_0^2 = w_0^2 + u_0^2;$$

$$\Delta w = 2\nu^2 \int_0^{t_f} y\,dt;$$

$$\Delta u = -\nu^2 \int_0^{t_f} x\,dt;$$

3. $$\tilde{x}_f = x_0 + u_0t_f + n_{01}g_0t_1^2I_4^{I} + n_{02}g_0t_2^2I_4^{II} + n_{01}g_0t_1t_2I_2^{I};$$

$$\tilde{y}_f = y_0 + w_0t_f + n_{01}g_0t_1^2I_3^{I} + n_{02}g_0t_2^2I_3^{II} - g_0\frac{t_f^2}{2} + n_{01}g_0t_1t_2I_1^{I};$$

4. $$x_f = x_0' + u_0't_f + n_{01}g_0t_1^2(I_4^{I})' + n_{02}g_0t_2^2(I_4^{II})' + \Delta x + n_{01}g_0t_1t_2(I_2^{I})';$$

/72

$$y_f = y_0' + w_0't_f + n_{01}g_0t_1^2(I_3^{I})' + n_{02}g_0t_2^2(I_3^{II})' - g_0\frac{t_f^2}{2} + n_{01}g_0t_1t_2I_1^{I} + \Delta y;$$

$$\Delta y = 2\nu^2 \int_0^{t_f} dt \int_0^{t} y\,d\eta;$$

$$\Delta x = -\nu^2 \int_0^{t_f} dt \int_0^{t} x\,d\eta;$$

5. $$w_f = -u_f\frac{x_f}{R + y_f};$$

6. $$h_f = y_f + \frac{x_f^2}{2R}.$$

Here the superscripts "I" and "II" refer to the first and second trajectory sections, respectively:

t_1 and t_2 is the time of flight in the first and section sections;

$$t_f = t_1 + t_2;$$

n_{01}, n_{02} are the initial g-loads calculated for the first and second trajectory sections.

Integrals with the superscript "I" are calculated with respect to the variables a_1, b_1 and τ_1, where

$$a_1=\beta_1 t_1; \quad b_1=b\frac{t_1}{t_f}.$$

The integrals with the superscript "II" are calculated with respect to the quantities $\tilde{b}$ and τ_0':

$$\tilde{b}=b\frac{t_2}{t_f}; \quad \tau_0'=b\frac{t_1}{t_f}+\tau_0.$$

From these equations the parameters b and τ_0 determining the optimal program as follows are calculated, as in the case of one stage:

$$\operatorname{tg}\dot{\varphi}(t)=b\xi+\tau_0,$$

where

$$\xi=\frac{t}{t_f}.$$

Let us reduce the control formulas (see (1.132)) to dimensionless form:

$$I=\int_0^1 \frac{\sin\operatorname{arctg}\left(\frac{\xi}{\bar{C}_2}+\tau_0\right)}{1-a_1\xi}d\xi= \qquad /73$$

$$=\frac{\bar{C}_2}{b^2}\left[\frac{1}{a^{1/2}}\ln\left|\frac{2(aX_1)^{1/2}+2ax_1+b}{2(aX_0)^{1/2}+2ax_0+b}\right|+\right.$$

$$\left.+\frac{\bar{a}}{c^{1/2}}\ln\left|\frac{\frac{2(cX_1)^{1/2}}{x_1}+\frac{2c}{x_1}+b}{\frac{2(cX_0)^{1/2}}{x_0}+\frac{2c}{x_0}+b}\right|\right]; \qquad (1.144)$$

$$I_2=\int_0^1 \frac{\cos\operatorname{arctg}\left(\frac{\xi}{\bar{C}_2}+\tau_0\right)}{1-a_1\xi}d\xi=$$

$$=-\frac{\bar{C}_2}{bc^{1/2}}\ln\left|\frac{\frac{2(cX_1)^{1/2}}{x_1}+\frac{2c}{x_1}+b}{\frac{2(cX_0)^{1/2}}{x_0}+\frac{2c}{x_0}+b}\right|. \qquad (1.145)$$

Here $1/\bar{C}_2$ corresponds to the programmed coefficient b in the tables, and a_1 corresponds to the fuel filling factor a

$$\left.\begin{aligned} &X_1=ax_1^2+bx_1+c; \quad X_0=ax_0^2+bx_0+c;\\ &x_1=\bar{a}+\bar{b}\left(\frac{1}{\bar{C}_2}+\tau_0\right); \; x_0=\bar{a}+\bar{b}\tau_0;\\ &\bar{a}=1+a_1\bar{C}_2\tau_0; \quad \bar{b}=-a_1\bar{C}_2;\\ &a=\frac{1}{\bar{b}^2}; \; b=-2\frac{\bar{a}}{\bar{b}^2}; \; c=1+\frac{\bar{a}^2}{\bar{b}^2}. \end{aligned}\right\} \qquad (1.146)$$

Let us present the final formulas for computing the integrals I_1, I_2, ..., I_4 when b = 0:

$$I_1=\frac{\sin\tau_0}{a}\ln\frac{1}{1-a}; \qquad (1.147)$$

$$I_2=\frac{\cos\tau_0}{a}\ln\frac{1}{1-a}; \qquad (1.148)$$

$$I_3=\frac{\sin\tau_0}{a^2}\left[-(1-a)\ln\frac{1}{1-a}+a\right]; \qquad (1.149)$$

$$I_4=\frac{\cos\tau_0}{a^2}\left[-(1-a)\ln\frac{1}{1-a}+a\right]. \qquad (1.150)$$

In conclusion we note that program (1.126) and, even more so, the simplified tg ϕ = bt + τ, can prove to be unsuitable for very lengthy powered sections (longer than 3000 km), since the errors arising due to the incompleteness of allowing for the noncentrality of the gravity field become appreciable. /74

1.4. Insertion of Satellite into Orbit with Final Combustion of Fuel

The method of inserting an artificial Earth satellite considered in the preceding section is the simplest. However, it does not ensure sufficiently high orbits. At the same time, these orbits can be of interest both for a large manned satellite-station, as well as for other, simpler AES.

We will assume that the procedure in obtaining some specified orbit is as follows in the general case. After completion of the power section, the last rocket stage or part of it will move along some elliptical orbit, which we will in the following refer to as the transfer ellipse. At some point of this ellipse, which we will call the transfer point, the engine is again fired and the rocket acquires the velocity components that ensure its further motion along the assigned orbit. Here let us neglect the variations

in the launch vehicle coordinates in the period of final fuel combustion, that is, let us assume that the final-combustion section will be contracted to a point. We will characterize the final-combustion section only by the modulus of the velocity vector that must be added to the existing vector in order for the new velocity to coincide in magnitude and direction to the assigned orbit. It is natural to assume that the smaller this additional velocity vector will be in terms of the magnitude of the modulus, the smaller the fuel outlays will be required for the transfer to the assigned orbit, and therefore, the satellite weight will be greater.

Thus, the problem of the optimal attainment of the assigned elliptical orbit essentially reduces to two problems: selecting the powered section and determining the transfer point ensuring the maximum satellite weight for the assigned orbit.

Determination of Optimal Transfer Point

Let us examine the problem when there is some transfer ellipse along which the rocket will move with unfired engine. Let us determine the point on this ellipse for which a minimum additional velocity is required for transfer in this ellipse to some assigned orbit. This point determines the instant of rocket engine firing. Here it is obvious that the transfer is possible only in the range of distances to the center of the Earth at which both orbits are located (Fig. 1.10).

Let us expand the velocity vector at the ellipse in two directions: along the vector radius drawn from the center of attraction to the given point, and perpendicular to this radius. Let us denote these components by v_r and v_n, respectively. To determine these components we have Eqs. (1.23) and (1.24), in which μ is the gravitational constant ($\mu \approx 398{,}600$ km^3/sec^2 for Earth). /75

Using the polar equation of an ellipse, we can bring these formulas to the form

$$v_r^2 = \frac{\mu}{p}\left[e^2 - \left(\frac{p}{\rho} - 1\right)^2\right]; \qquad (1.151)$$

$$v_n^2 = \frac{\mu}{p}\left(\frac{p}{\rho}\right)^2, \qquad (1.152)$$

where ρ is the instantaneous radius-vector of the ellipse.

We denote with the subscript "1" the parameters pertaining to the transfer ellipse, and by the subscript "2" -- to the orbit that we must obtain. Let us write the expression for the necessary increment in the velocity in the form

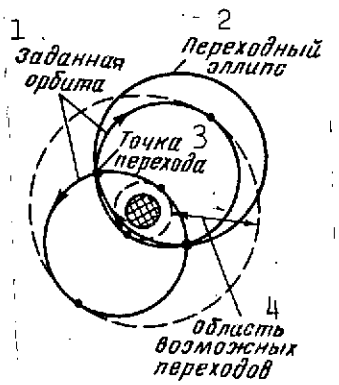

Fig. 1.10. Scheme of AES transfer from one orbit to another.

Key: 1. Assigned orbit; 2. Transfer ellipse; 3. Transfer point; 4. Domain of possible transfer.

$$\Delta v^2=(v_{n1}-v_{n2})^2+(v_{r1}-v_{r2})^2. \qquad (1.153)$$

We preliminarily assume that we will characterize the assigned orbit to which the transfer is to be made only by its shape, that is, by the parameter p and eccentricity e, or by the apogee distance R and perigee distance r. It is possible to draw two elliptical orbits with assigned parameter and eccentricity through any point in the transfer ellipse within the range of possible transfers. In addition, motion in either one or the other direction is possible in each of these orbits. However, only in one of the orbits for a specific direction of motion at the transfer point will the velocity components v_r and v_n have the same sign as in the transfer ellipse. Therefore, the transfer to this orbit requires a minimum amount of fuel compared to transfer to other orbits. Bearing in mind that we can always obtain a specific (required) orientation of the new orbit by suitably selecting the power trajectory section, in the following we will assume that the transfer is executed precisely into the orbit requiring the minimum fuel outlay for transfer at a given point.

According to the foregoing, the values of v_r and v_n for both elliptical orbits we will assume positive. By substituting in (1.153) instead of v_r and v_n their expressions(1.151) and (1.152) written, respectively, for two ellipses, we get /76

$$\frac{\Delta v^2}{\mu}=\frac{(\sqrt{p_1}-\sqrt{p_2})^2}{\varrho^2}+\left[\frac{1}{\sqrt{p_1}}\sqrt{e_1^2-\left(\frac{p_1}{\varrho}-1\right)^2}-\right.$$
$$\left.-\frac{1}{\sqrt{p_2}}\sqrt{e_2^2-\left(\frac{p_2}{\varrho}-1\right)^2}\right]^2. \qquad (1.154)$$

The eccentricity e and parameter p can be expressed in terms of the apogee distance R and perigee distance r of the elliptical orbits to the center of attraction:

$$e=\frac{R-r}{R+r}; \qquad (1.155)$$

$$p=\frac{2rR}{R+r}. \qquad (1.156)$$

Using these formulas, let us reduce Eq. (1.154) to the form

$$\frac{\Delta v^2}{\mu}=(\sqrt{p_1}-\sqrt{p_2})^2x^2+$$
$$+\left[\sqrt{p_1\left(\frac{1}{r_1}-x\right)\left(x-\frac{1}{R_1}\right)}-\sqrt{p_2\left(\frac{1}{r_2}-x\right)\left(x-\frac{1}{R_2}\right)}\right]^2, \quad (1.157)$$

where

$$\frac{1}{p_i}=\frac{1}{2}\left(\frac{1}{R_i}+\frac{1}{r_i}\right),$$
$$x=\frac{1}{\varrho};\ i=1,2.$$

Thus, we have formulated the problem of finding the x that provides a minimum for the quantity $\Delta v^2/\mu$. The quantity x varies within the range

$$\min\left(\frac{1}{R_1},\ \frac{1}{R_2}\right)<x<\max\left(\frac{1}{r_1},\ \frac{1}{r_2}\right). \quad (1.58)$$

The direct determination of the minimum for expression (1.157) by setting the first derivative in x equal to zero bring us to a complex equation in the variable x. To simplify the problem, let us turn to the geometrical analogy. We will assume that $p_1 \neq p_2$ and we will write Eq. (1.157) in the form

$$\frac{\Delta v^2}{\mu(\sqrt{p_1}-\sqrt{p_2})^2}=x^2+y^2, \quad (1.159)$$

where

$$y=\frac{|y_1(x)|-|y_2(x)|}{|\sqrt{p_1}-\sqrt{p_2}|};$$

/77

$$y_1^2(x)=p_1\left(\frac{1}{r_1}-x\right)\left(x-\frac{1}{R_1}\right); \quad (1.160)$$

$$y_2^2(x)=p_2\left(\frac{1}{r_2}-x\right)\left(x-\frac{1}{R_2}\right). \quad (1.161)$$

Eq. (1.159) is the equation of a circle with its center at the point x = y = 0 and with a radius equal to $\frac{\Delta v}{\sqrt{\mu}(\sqrt{p_1}-\sqrt{p_2})}$,

and Eqs. (1.160) and (1.161) are equations of ellipses. These ellipses have their centers at the points $\left(x=\frac{1}{p_1},\ y=0\right)$

and $\left(x = \frac{1}{p_2},\ y = 0\right)$, respectively, that is, at the points lying midway between the points $\frac{1}{r_1}$, $\frac{1}{R_1}$ and $\frac{1}{r_2}$, $\frac{1}{R_2}$. The semi-axes of these ellipses will be expressed by the following formulas:

$$a_i = \frac{1}{2}\left(\frac{1}{r_i} - \frac{1}{R_i}\right);$$

$$b_i = \frac{1}{2}\frac{\left(\frac{1}{r_i} - \frac{1}{R_i}\right)}{\sqrt{\frac{1}{p_i}}}, \qquad (1.162)$$

where i = 1,2.

The optimal value of x realizing a minimum for the quantity $|\Delta v|$ is defined as the coordinate of the point of tangency of the circle (1.159) that has the minimum of the possible radii, to curve y(x) in the range of condition (1.158). The radius of this circle will determine the minimum increment in velocity Δv (Fig. 1.11).

The position of this point of tangency will depend on the mutual position of the ellipses (1.160) and (1.161), which in turn depends on r_1, r_2, R_1, and R_2. From this geometrical picture it is clear that at the point at which the circle is tangent to the curve y(x), the following conditions is satisfied:

$$y\dot{y} = -x. \qquad (1.63)$$

Using the geometrical interpretation, we will show that when $r_1 \neq r_2$ and $R_1 \neq R_2$, the optimal values of x lie within the domain (1.158). Let $r_2 > r_1$ and $R_2 < R_1$, that is, the transfer is executed in an ellipse whose perigee distance is greater than in the transfer ellipse, and the apogee distance is smaller. Then ellipse (1.161) lies within ellipse (1.160), as shown in Fig. 1.12, and /78

$$\dot{y}_1(x_0) - \dot{y}_2(x_0) = -\infty = \dot{y}(x_0);$$
$$\dot{y}_1(x_f) - \dot{y}_2(x_f) = +\infty = \dot{y}(x_f).$$

Since in this case y > 0 over the entire interval $[x_0, x_f]$, we have

$$y(x_0)\dot{y}(x_0) = -\infty;$$
$$y(x_f)\dot{y}(x_f) = +\infty.$$

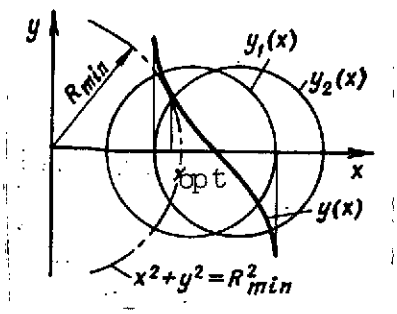

Fig. 1.11. For the derivation of the formula for the optimal velocity impulse Δv.

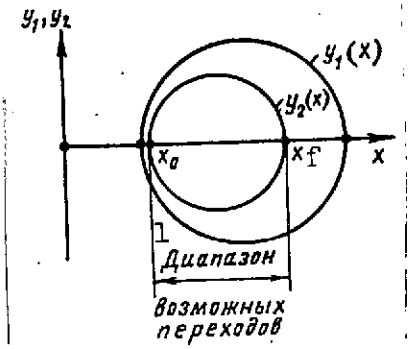

Fig. 1.12. For the determination of x_{opt}.

Key: 1. Range of possible transitions.

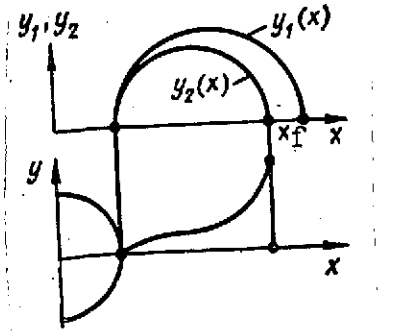

Fig. 1.13. For determination of Δv_{min} by formula (1.164).

In the open interval (x_0, x_f) the function $(y\dot{y})$ is continuous, and therefore it can be concluded that condition (1.163) will be satisfied at some point in this interval, that is, the value x_{opt} will exist that does not coincide with any of the endpoints of the interval $[x_0, x_f]$. We can readily show this to be true also of other cases of the relation between r_1, r_2, R_1, and R_2 if $R_1 \neq R_2$ and $r_1 \neq r_2$.

Let us examine the case when the apogee distances of both ellipses coincide, and the perigee of the new ellipse is higher than the perigee of the transfer ellipse.

Independently of r_1 and r_2, if $R_1 = R_2$, when $x = 1/R_1 = 1/R_2$ condition $y = 0$ will always obtain, since at this point both ellipses will intersect with the x axis (Fig. 1.13). In this case the point of tangency of the minimum-radius circle will coincide with the left endpoint of the interval, and the minimum Δv will be determined from the condition /79

$$\frac{\Delta v^2}{\mu(\sqrt{p_1}-\sqrt{p_2})^2} = x_0^2 = \frac{1}{R_1^2},$$

whence we get

$$\Delta v_{min} = \sqrt{\mu}\,\frac{|\sqrt{p_1}-\sqrt{p_2}|}{R_1}. \qquad (1.164)$$

Thus, to raise the perigee of the transfer ellipse while preserving the former apogee distance constant, it is advantageous to have an additional final combustion of the fuel at the apogee of the transfer ellipse. This conclusion also applies to the case when the perigee of the new ellipse must lie below the perigee of the starting ellipse, for example, during deorbiting.

Let us examine another particular case when the resulting orbit is circular.

Then $r_2 = R_2 = R$ and the range of possible transitions is contracted to a point corresponding to the radius of the circular orbit. Here Eq. (1.157) is brought to the form

$$\frac{\Delta v^2}{\mu}=\frac{(\sqrt{p_1}-\sqrt{R})^2}{R^2}+p_1\left(\frac{1}{r_1}-\frac{1}{R}\right)\left(\frac{1}{R}-\frac{1}{R_1}\right). \qquad (1.165)$$

Let us examine how Δv changes with change in the radius of the circular orbit within the range $r_1 \leq R \leq R_1$.

Eq. (1.165) can be written in the following form:

$$\frac{\Delta v^2}{\mu}=3z^2-2\sqrt{\frac{2R_1r_1}{R_1+r_1}}z^3-\frac{2}{R_1+r_1}, \qquad (1.166)$$

where

$$z=\frac{1}{\sqrt{R}}.$$

From the last equation it follows that the derivative of $\Delta v^2/\mu$ with respect to z tends to zero at the point

$$z_1=0,\ z_2=\sqrt{\frac{R_1+r_1}{2r_1R_1}}=\frac{1}{\sqrt{p_1}},\quad R=p_1.$$

Analysis of Eq. (1.166) shows that at the point $z = 1/\sqrt{p_1}$ the maximum of $\Delta v^2/\mu$ is realized, while the minimum value of this quantity can occur only at one of the endpoints of the interval (r_1 or R_1), that is, at the apogee or perigee of the transfer ellipse. Let us compare $\Delta v^2/\mu$ for the apogee and perigee of the transfer ellipse.

Based on Eq. (1.166) let us write /80

$$\Delta=\left(\frac{\Delta v^2}{\mu}\right)_{R=R_1}-\left(\frac{\Delta v^2}{\mu}\right)_{R=r_1}=$$

$$=\frac{r_1}{\alpha}\left[-3(\alpha-1)+2\sqrt{2}\left(\alpha\sqrt{\frac{\alpha}{\alpha+1}}-\sqrt{\frac{1}{\alpha+1}}\right)\right], \qquad (1.167)$$

where

$$\alpha=\frac{R_1}{r_1}.$$

In the graph (Fig. 1.14) is shown the dependence of Δ/r_1 on the parameter α. The graph shows that for any transfer ellipses

$\Delta < 0$, therefore the minimum of Δv is realized at the apogee of the ellipse. This conclusion can be obtained also in general form for any values of the parameter α.

Let us examine one more particular case when $p_1 = p_2$, that is, the ellipse parameter remains unchanged during a transfer to another ellipse. Here the optimal point of transfer is obtained most simply as follows.

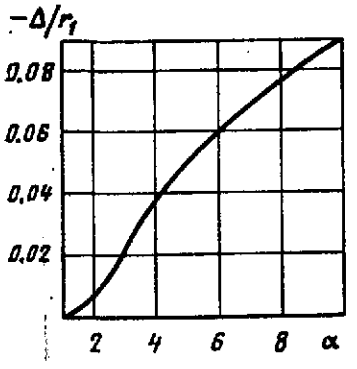

Fig. 1.14. Δ/r_1 as a function of parameter α in Eq. (1.167).

From Eqs. (1.151) and (1.152) let us find a relation between the velocity components in the ellipse

$$\left(v_n - \sqrt{\frac{\mu}{p}}\right)^2 + v_r^2 = \frac{\mu}{p} e^2. \qquad (1.168)$$

This is the equation of a circle in the axes v_n and v_r with its center at the point $v_r = 0$, $v_n = \sqrt{\mu/p}$ and with the radius $\sqrt{\mu/p}\cdot e$. Obviously, the circle intersects with the v_n axis at the points corresponding to the points of the perigee and apogee of the given ellipse. The radius-vector of the moving body ρ will be related to the variable v_n by formula (1.152):

$$\rho = \sqrt{\frac{\mu p}{v_n}}. \qquad (1.169)$$

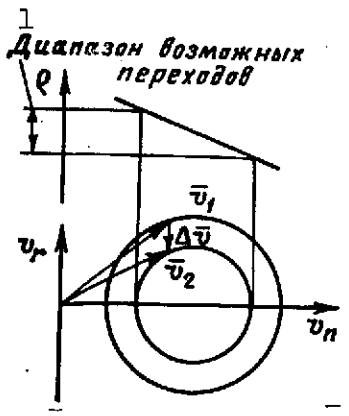

Fig. 1.15. For determining the increment in velocity Δv necessary for transfer from one orbit to another when p = const.

Key: 1. Range of possible transfers.

If the parameters of both ellipses coincide, the circles characterizing the relationship between v_n and v_r for both ellipses have a common center and differ only in radius.

Since the function $\rho(v_n)$ is the same for both ellipses, the value of the increment in velocity required for transfer is determined as shown in Fig. 1.15. From the figure it follows that $|\Delta\bar{v}|$ is at a minimum at the point corresponding to the center of the circles, that is, when $v_n = \sqrt{\mu/p}$. As follows from Eq. (1.152), to this point there corresponds

$$\rho_{opt} = p \text{ or } \vartheta = \frac{\pi}{2}.$$

Here the minimum increment in velocity necessary for transfer will be determined thusly: /81

$$\Delta v_{\min} = \sqrt{\frac{\mu}{p}}\,|e_1 - e_2|. \qquad (1.170)$$

Δv was calculated for several orbits to illustrate other cases. The calculation was carried out using the following formula, which can be readily derived from Eq. (1.157):

$$\Delta\tilde{v}^2 = \left(\frac{\Delta v}{v_{\mathrm{pr}_1}}\right)^2 = \frac{1}{y^2}\left\{\left(\sqrt{\frac{\alpha}{1+\alpha}} - \sqrt{\frac{\beta\gamma}{1+\alpha}}\right)^2 + \left[\sqrt{\frac{1}{1+\alpha}(y-1)(\alpha-y)} - \sqrt{\frac{1}{\beta+\gamma}(y-\beta)(\gamma-y)}\right]^2\right\},$$

where

$$y = \frac{\varrho}{r_1}; \quad \beta = \frac{r_2}{r_1};$$
$$\alpha = \frac{R_1}{r_1}; \quad \gamma = \frac{R_2}{r_1};$$

$v_{\mathrm{pr}\ r_1}$ is the parabolic velocity at distance r_1.

In all the calculations $\alpha = 1.20$ was assumed. Fig. 1.16 shows the functions $\Delta\tilde{v}^2(y)$ for the case when the perigee of the new ellipse is at the same altitude as the perigee of the initial transfer ellipse ($\beta = 1$). The plots show that in this case the optimal point of transfer coincides with the perigee of the transfer ellipse. From Fig. 1.17 and 1.18 we see how the transfer point is shifted when there is a change in the perigee distance of the new ellipse for a fixed apogee. Therefore, the more strongly the perigee distances of both ellipses differ, the closer is the optimal transfer point to the apogee of the initial ellipse. Calculations show that the transfer at the optimal point provides a substantial advantage in the magnitude of Δv, therefore, in the satellite weight. /82

Selection of Powered Trajectory Section for Insertion of Satellite into Circular Orbit with Final Combustion of Fuel

Let us assume that the satellite is inserted into orbit by means of a three-stage rocket[2], where the entire third stage goes

[2] This assumption is not mandatory. The same orbit can be obtained also for a two-stage rocket by using final fuel combustion, but with lesser satellite weight.

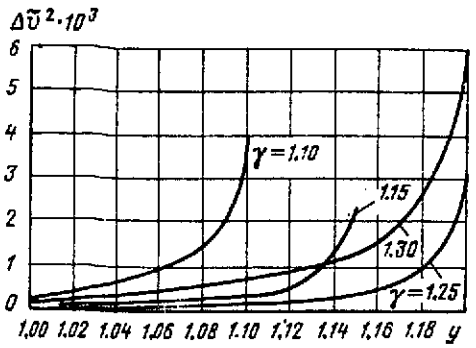

Fig. 1.16. $\Delta\tilde{v}^2$ as a function of y when the altitudes of the perigee of the new and the transfer ellipses coincide (α = = 1.2; β = 1.0).

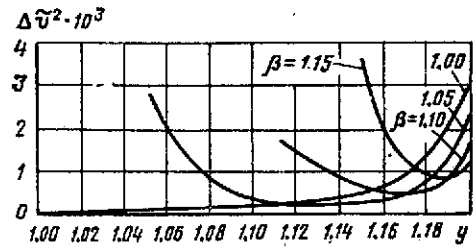

Fig. 1.17. $\Delta\tilde{v}^2$ as a function of y when β is varied from 1 to 1.15 (α = 1.2; γ = 1.25).

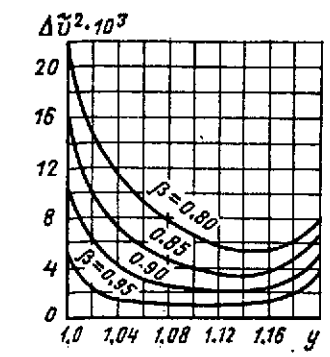

Fig. 1.18. $\Delta\tilde{v}^2$ as a function of y when β is varied from 0.8 to 0.95 (α = 1.2; γ = 1.25).

into orbit. Part of the fuel in the in the third stage is expended in the principal power trajectory section and part is expended in the transfer from the transfer ellipse to the circular orbit. Under the condition that the parameters of the third stage and also of the entire rocket are known, the parameters of motion at the end of the powered section will be determined only by the time of completion of the powered section t_f and by the program of variation in the rocket angle of pitch. Here the time of completion of the powered section will characterize the fraction of the third-stage fuel expended in the principal powered section. Suppose that the time Δt is required for the final combustion of the fuel in the transfer from the ellipse to the circular orbit. Bearing in mind that the parameters of the third stage are fixed, we can conclude that the satellite weight will be the largest when the following quantity is at a minimum: /83

$$T=t_f+\Delta t. \qquad (1.171)$$

Suppose that for some instant of time t_f the rocket at the end of the powered section has the motion parameters v_f, θ_f, and r_f. In order for the apogee of the transfer ellipse to be at position R from the center of attraction, these parameters must satisfy the condition:

$$v_f^2=2\mu\frac{\frac{1}{r_f}-\frac{1}{R}}{1-\left(\frac{r_f\cos\theta_f}{R}\right)^2}. \qquad (1.172)$$

As was shown, it is best to transfer to a circular orbit from a transfer ellipse that is tangent to the given circular orbit. Therefore, in Eq. (1.172) we will assume by

r to refer to the radius of the assigned circular orbit. In order to determine the increment in velocity necessary to transfer to the circular orbit at the apogee of the ellipse, we can use the following formula:

$$\Delta v = \sqrt{\frac{\mu}{R}} - \frac{r_f \cos\theta_f}{R} \sqrt{2\mu \frac{\frac{1}{r_f} - \frac{1}{R}}{1 - \left(\frac{r_f \cos\theta_f}{R}\right)^2}}. \qquad (1.173)$$

Let us proceed to selecting the optimal program for the powered section. Here we will neglect the variation in r_f. This assumption means that we do not take into account the condition of the previous section on the insertion of the satellite with maximum velocity at the assigned altitude (r_f) or with assigned velocity at maximum altitude. As a result, the number of boundary conditions imposed become one fewer. In this problem this is advantaneous since here we have the optimal transfer ellipse, not the trajectory of insertion into a given orbit with a continuous powered section.

We will assume the value of the angle θ_f to be fixed in selecting the program. Then for a fixed altitude of the circular orbit the quantities v_f and Δv will be determined for each value of the angle θ_f. Therefore, we can formulate the problem thusly: for assigned values θ_f and v_f we are to select the program for the powered section c so that t_f will be at a minimum. /84

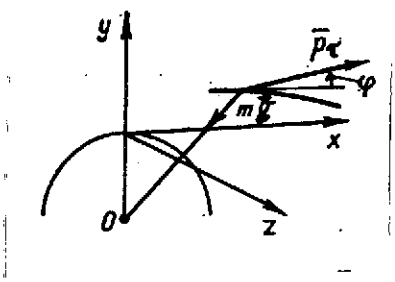

Fig. 1.19. For the derivation of the linearized equation of motion of an AES in the system of coordinates xyz.

The smallest t_f ensures maximum satellite weight for an assigned orbit, since we assumed Δv to be fixed. We can modify the problem formulated so as to seek the maximum velocity at the end of the powered section with fixed t_f and θ_f. The assumption of constancy of r_f as variations are carried out under the program refers only to the selection of the kind of change in the angle of pitch with time.

Let us divide the powered section into two sections, the first of which we will arbitrary assume to be in the atmosphere, and the second -- to be entirely in vacuum. We will assume the family of trajectories of the first section to depend on a single parameter

-- the angle θ_0 at the end of the first section, since the selection of the program for this section is determined mainly by other considerations.

We will determine for each θ_0 the optimal program in the second section.

We will consider the motion of the rocket in the second section in the system x, y, z as not participating in the rotational motion of the Earth (Fig. 1.19). We will assume that in the second section motion occurs in the plane $(\dot{x}, \dot{y})$ coinciding with the vector of the absolute velocity at the instant of completion of the first section and extending through the Earth's center. By denoting the parameters of motion at the end of the first section with respect to the Earth v_0, θ_0, and h_0, the parameters of satellite motion at this same instant relative to the system x, y, and z can be expressed by the formula

$$\left.\begin{aligned} v_{x_1} &= v_1 \cos\theta_1, \\ v_{y_1} &= v_1 \sin\theta_1; \\ y_1 &= h_0; \\ x_1 &= 0, \end{aligned}\right\} \qquad (1.74)$$

where

$$v_1 = \sqrt{v_0^2 + v_{ci}^2 + 2v_0 v_{ci} \cos\theta_0 \sin\delta_0};$$

$$\sin\theta_1 = \frac{v_0}{v_1}\sin\theta_0; \quad v_{ci} = \Omega_E (R_E + h_0)\cos\psi_0;$$

δ_0, ψ_0 are the azimuth and latitude at the end of the first section, respectively

$\Omega_E = 7.29 \cdot 10^{-2}$ sec^{-1} is the angular velocity of rotation of the Earth, and

$R_E = 6371$ km is the radius of the Earth.

Let us write the equations of motion in the second section in the form /85

$$\left.\begin{aligned} \dot{v}_x + \nu^2 x - p\cos\varphi &= 0; \\ \dot{v}_y - 2\nu^2 y - p\sin\varphi + g_0 &= 0; \\ \dot{x} - v_x &= 0; \\ \dot{y} - v_y &= 0, \end{aligned}\right\} \qquad (1.175)$$

where

$$p = \frac{P_c}{m}; \quad \nu^2 = \frac{g_0}{R_E}.$$

We will seek the extremum of the functional

$$I=v_f+\int_{t_1}^{t_f}[\lambda_1(\dot{v}_x+\nu^2x-p\cos\varphi)+\lambda_2(\dot{v}_y-2\nu^2y- \\ -p\sin\varphi+g_0)+\lambda_3(\dot{x}-v_x)+\lambda_4(\dot{y}-v_y)]\,dt, \tag{1.176}$$

where

$$v_f=\sqrt{v_{xf}^2+v_{yf}^2}.$$

This functional is analogous to the one considered in [46]. The equations of the extremal will include the equations of the system (1.175) and the auxiliary equation:

$$\left.\begin{aligned}&\dot{\lambda}_1+\lambda_3=0;\\&\dot{\lambda}_2+\lambda_4=0;\\&\dot{\lambda}_3-\nu^2\lambda_1=0;\\&\dot{\lambda}_4+2\nu^2\lambda_2=0;\\&\operatorname{tg}\varphi=\frac{\lambda_2}{\lambda_1}.\end{aligned}\right\} \tag{1.177}$$

We introduce one more assumption. We will assume the inclination of the velocity vector at the end of the powered section θ_{f0} to be fixed with respect to the x axis, and not to the local horizon. Bearing in mind that the parameters of the beginning of the second section are fixed, to determine the constants λ_{1f}, λ_{2f}, λ_{3f} and λ_{4f} in (1.177), let us use the condition

$$\left(\frac{v_{xf}}{v_f}+\lambda_{1f}\right)\delta v_{xf}+\left(\frac{v_{yf}}{v_f}+\lambda_{2f}\right)\delta v_{yf}+\lambda_{3f}v_{xf}+\lambda_{4f}\delta y_f=0,$$

whence under these assumptions we have

$$\lambda_{3f}=\lambda_{4f}=0; \tag{1.178}$$

$$\frac{v_{xf}}{v_f}+\lambda_{1f}+\left(\frac{v_{yf}}{v_f}+\lambda_{2f}\right)\operatorname{tg}\theta_{f0}=0. \tag{1.179}$$

Integrating Eqs. (1.177) under the initial conditions (1.178), /86 we get the following law of variation in the angle φ

$$\operatorname{tg}\varphi=\operatorname{tg}\varphi_f\frac{\operatorname{ch}\sqrt{2}\nu(t_f-t)}{\cos\nu(t_f-t)}. \tag{1.180}$$

Expanding this expression in a series, we get,

$$\operatorname{tg}\varphi=\operatorname{tg}\varphi_f\left[1+\frac{3}{2}v^2(t_f-t)^2+\frac{7}{8}v^4(t_f-t)^4+\right.$$
$$\left.+\frac{31}{80}v^6(t_f-t)^6+\ldots\right].$$

Considering that $t_f - t < 300$ sec, with adequate accuracy we can assume

$$\varphi=\varphi_f+\delta\varphi(t), \tag{1.181}$$

where $$\delta\varphi(t)=\frac{3}{4}v^2(t_f-t)^2\sin 2\varphi_f.$$

In accordance with Eq. (1.180) we have

$$\operatorname{tg}\varphi_f=\frac{\lambda_2 f}{\lambda_1 f}.$$

Condition (1.179) does not impose constraints on tg ϕ_f. Obviously, ϕ_f is best selected from the condition that the angle θ_{f0} at the end of the powered section is equal to the assigned value. Since it is assumed that θ_f is varied as a parameter, instead of θ_{f0} we can assign the value of ϕ_f. With sufficient accuracy the system (1.175) can be integrated in its final form as the angle ϕ is varied according to the law (1.181). The parameters of motion at the end of the powered section were calculated with reference to the addition of the angle $\delta\phi(t)$ and without this angle, where in the latter case the parameter ϕ_f was varied so that the angle ϕ_{f0} remained as before. The results showed that allowing for the increment has virtually no effect on the velocity at the end of the powered section (the deviation is less than 1 m/sec). So to the first approximation we can assume ϕ to be constant in the powered section.

Let us present formulas for calculating the parameters of motion at the end of the powered section with $\phi = \phi_f = \text{const}$[3], assuming that the first section of the trajectory corresponds to the flight of the first rocket stage:

---

[3] The formulas were derived from the solution of system (1.175) with ϕ = const by expanding sin, cos, sh, and ch in series, retaining the terms of the first and second order of smallness, inclusively.

$$\left.\begin{aligned}
x_f &= \frac{\dot{x}_1}{\nu}\sin \nu t_f + I_1 \cos\varphi_f;\\
\dot{x}_f &= \dot{x}_1 \cos\nu t_f + B_1 \cos\varphi_f;\\
y_f &= \frac{\dot{y}_1}{\sqrt{2}\nu}\operatorname{sh}\sqrt{2}\nu t_f + y_1 \operatorname{ch}\sqrt{2}\nu t_f + I_1 \sin\varphi_f - \frac{g_0}{2\nu^2}(\operatorname{ch}\sqrt{2}\nu t_f - 1);\\
\dot{y}_f &= \dot{y}_1 \operatorname{ch}\sqrt{2}\nu t_f + y_1\sqrt{2}\nu \operatorname{sh}\sqrt{2}\nu t_f + D_1 \sin\varphi_f - \frac{g_0}{\sqrt{2}\nu}\operatorname{sh}\sqrt{2}\nu t_f,
\end{aligned}\right\} \qquad (1.182)$$

where

$$B_1 = I_3 - \frac{\nu^2}{2} I_2;\quad D_1 = I_3 + \nu^2 I_2;$$

$$I_1 = \frac{q_1}{\beta_1^2}[\beta_1 t_2 + (1-\beta_1 t_f)\ln f_1] + \frac{q_2}{\beta_2^2}[\beta_2(t_f - t_2) + f_2 \ln f_2];$$

$$I_2 = -\frac{q_1}{\beta_1^3}(1-\beta_1 t_f)^2 \ln f_1 + \frac{2q_1 t_f t_2}{\beta_1} -$$

$$-\frac{q_1}{\beta_1^3}\left(\frac{f_1^2-1}{2} + 2\beta_1 t_2\right) - \frac{q_2}{\beta_2^3} f_2^2 \ln f_2 +$$

$$+ 2q_2 t_f \frac{t_f - t_2}{\beta_2} - \frac{q_2}{\beta_2^3}\left[\frac{f_2^2-1}{2} + 2\beta_2 \cdot (1+\beta_2 t_2)(t_f - t_2)\right];$$

$$I_3 = -\frac{q_1}{\beta_1}\ln f_1 - \frac{q_2}{\beta_2}\ln f_2;$$

$$f_1 = 1 - \beta_1 t_2;$$

$$f_2 = 1 - \beta_2 (t_f - t_2);$$

t_2 is the firing time of the engines in the second stage

t_f is the total flight time in the powered section from the instant of separation of the first stage

β_1, β_2 are the mass flow rate of fuel for the second and third stages related to the initial weight of the corresponding stage:

$$q_1 = p_{II},\quad q_2 = p_{III}.$$

Based on the parameters of motion at the end of the powered section we can calculate the radius of the circular orbit R and Δt. To do this, let us use the following formulas:

$$
\left.
\begin{aligned}
&R = r_f \frac{k\cos^2\theta_f}{1-e};\\
&e = \sqrt{1-(2-k)k\cos^2\theta_f};\\
&k = \frac{r_f v_f^2}{\mu};\ \mu = 398600\,\frac{\text{km}^3}{\text{sec}^2}\\
&\Delta t = \left(1-e^{-\frac{\Delta v}{w}}\right)\left[\frac{1}{\beta_2}-(t_f-t_2)\right];\\
&\Delta v = \sqrt{\frac{\mu}{R}-\frac{r_f v_f\cos\theta_f}{R}};\quad w = \frac{q_2}{\beta_2};\\
&v_f = \sqrt{\dot{x}_f^2+\dot{y}_f^2};\ \theta_f = \theta_{f0}+\varepsilon;\ \operatorname{tg}\theta_{f0} = \frac{\dot{y}_f}{\dot{x}_f};\\
&\sin\varepsilon = \frac{x_f}{r_f};\quad r_f = \sqrt{x_f^2+(6371+y_f)^2}.
\end{aligned}
\right\} \qquad (1.183)
$$

For the final solution to the problem, we must express the radius of the circular orbit and Δt as functions of the angle ϕ_f for different values of the parameters θ_0. Further, based on the functions (1.183), we can determine the function T (see Eq. (1.171)) as dependent on ϕ_f for different θ_0, for insertion into several fixed circular orbits.

These results lead to the following conclusions.

1. There exists a specific optimal point for transfer from one elliptical orbit to another. Achieving a transfer at this point gives a major advantage in satellite weight.

2. In order to obtain a circular orbit at a specific altitude with maximum satellite weight, the additional final fuel combustion is best effected at the apogee of the transfer ellipse. Here the angle of pitch at the powered section of the trajectory of insertion into the transfer ellipse lying outside the atmosphere can be assumed constant.

CHAPTER II

DEVIATIONS OF ORBIT CAUSED BY ERRORS OF INSERTION

When inserting a spacecraft into orbit, due to the action of various random factors not taken into account, the values of the actual parameters of motion may not coincide with the design parameters. The deviations in the parameters of motion at the moment of satellite insertion into orbit will cause the corresponding deviations in the elements of the latter.

The main causes of errors in the insertion of a spacecraft into orbit are the following:

1) imprecision in the functioning of the launch vehicle control system over the powered section, deviations from the nominal values of the design and weight characteristics of the rocket, and deviations in the characteristics of its power plant; and

2) random deviations in the characteristics of the systems participating in the final acceleration of the spacecraft during insertion into orbit (with final combustion of fuel, see Chapter I).

For satellites which are inserted into orbit without final acceleration, only perturbations caused by errors in the first group can arise. Obviously, orbital perturbations in this case are analogous to perturbations of the transfer ellipse of the satellite with final acceleration. Therefore the results of analyzing errors of insertion in the first case can be entirely transferred to the transfer satellite in the second insertion method.

This chapter analysis the nature of the dependence of orbital perturbations on the insertion errors for both spacecraft inserted into orbit with a continuous powered section, as well as for spacecraft inserted into orbit with final acceleration. Based on the resulting functions, we can determine the rational method and the accuracy of the control for each specific type of spacecraft. The material presented here can also assist in solving the problem of the rational control when maneuvers are executed in orbit.

These problems are solved under the following assumptions:

1. The field of terrestrial gravity is central and the Earth is a sphere with radius R = 6371 km.

2. The end of the powered section, the transfer ellipse, and the resulting orbit are outside the Earth's atmosphere.

3. The effect of celestial bodies on satellite motion is absent.

4. The satellite acquires additional velocity during final acceleration instantaneously, and the final acceleration is executed in the plane of the transfer ellipse.

2.1. Orbital Deviations Due to Deviations in the Parameters of Motion at the End of the Powered Section /90

Errors in the operation of the launch vehicle over the powered section of spacecraft insertion into orbit leads to the parameters of motion differing from the design values at the end of the powered section. We will characterize these deviations in the parameters of the motion by the deviations in the flight altitude and the velocity and also by the deviation in the inclination of the velocity vector to the local horizon, which we denote by the following, respectively:

$$\Delta r_1 = r_1 - \tilde{r}_1;\ \Delta v_1 = v_1 - \tilde{v}_1;\ \Delta\theta_1 = \theta_1 - \tilde{\theta}_1, \tag{2.1}$$

where the sign ~ signifies the design values of the corresponding parameters. A change in the distance of the powered section influences only the position of the line of apsides of the resulting orbit, and the possible deviations here are relatively small. Therefore, analysis of the effect of the distance of the powered section is not presented below.

Let us examine how the deviations in the principal orbital parameters depend approximately on Δr_1, Δv_1, and $\Delta\theta_1$.

1. Deviations of altitudes of orbital perigee and orbital apogee. Errors in the altitude of the orbital perigee are most important when a spacecraft is inserted into orbit without final acceleration, since this method of insertion is characterized, as pointed out in Chapter I, by relatively small perigee altitudes of the resulting orbits. For these orbits, random deviations in the perigee altitudes must be small, since they can lead to appreciable reduction in the lifetime of satellites through an increase in the effect of the Earth's atmosphere.

The perigee and apogee distances from the Earth's center are determined from the formulas (see Chapter I):

$$\frac{r_{\pi 1}}{r_1} = \frac{k_1 \cos^2\theta_1}{1+e_1} = \frac{1-e_1}{2-k_1}; \tag{2.2}$$

$$\frac{r_{\alpha 1}}{r_1} = \frac{k_1 \cos^2\theta_1}{1-e_1} = \frac{1+e_1}{2-k_1}, \tag{2.3}$$

where

$$k_1 = \frac{r_1 v_1^2}{\mu}; \quad e_1 = \sqrt{1 - k_1(2 - k_1)\cos^2\theta_1}; \tag{2.4}$$

r_1 is the distance from the Earth's center to the end of the powered section. The values $r = r_{\pi 1}$ and $r = r_{\alpha 1}$ defined by formulas (2.2) and (2.3) are two solutions to the following equation:

$$\left(\frac{r}{r_1} - \frac{1}{2 - k_1}\right)^2 - \frac{k_1}{2 - k_1}\sin^2\theta_1 = \left(\frac{k_1 - 1}{2 - k_1}\right)^2. \tag{2.5}$$

When $k_1 < 2$, this equation in the system of coordinates $\sin\theta_1$, r/r_1 defines a family of hyperbolas with a real axis coinciding with the coordinate axis r/r_1, and with the center displaced along this axis by the amount $1/(2 - k_1)$ (Fig. 2.1). When $k_1 = 1$, the hyperbola degenerates into a pair of straight lines intersecting at the point $r/r_1 = 1$, $\sin\theta_1 = 0$ and having a slope $\operatorname{tg}\xi = 1$. /91

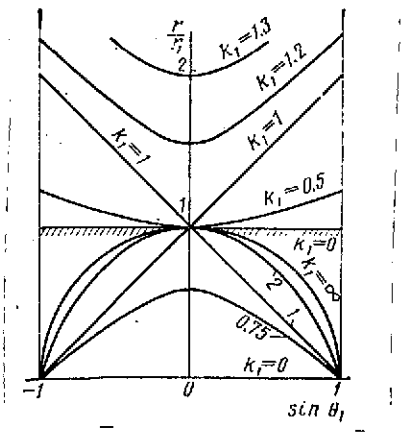

Fig. 2.1. For the solution of Eq. (4.1).

When $k_1 = 0$, the hyperbola degenerates into a pair of parallel lines: $r/r_1 = 1$ and $r/r_1 = 0$. The line $r/r_1 = 1$ (with oblique hatching) divides this domain into two parts. Below this line ($r/r_1 < 1$) extend the curves for the perigee distance, and above this line ($r/r_1 \geq 1$) -- the curves for the apogee distance.

When $k = 2$, Eq. (2.5) defines a parabola with its vertex at the point $r/r_1 = 1$, $\sin\theta_1 \neq 0$ and with a symmetry axis coinciding with the axis r/r_1.

When $k_1 = \infty$, Eq. (2.5) characterizes a circle with a radius equal to unity, and with its center at the origin of coordinates.

When $2 < k_1 < \infty$, Eq. (2.5) defines a family of ellipses. For convenience in later analysis of the deviations of the perigee distance, let us introduce a new variable:

$$\beta_\pi = 1 - \frac{r_{\pi 1}}{r_1}. \tag{2.6}$$

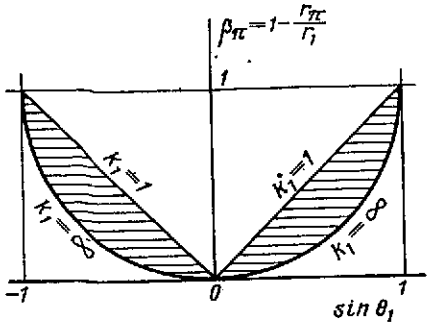

Fig. 2.2. Domain of existence of β_π.

For any values $k_1 \geq 1$, β_π as functions of $\sin\theta_1$ can be represented by curves lying within the hatched domain (Fig. 2.2). The larger k_1, the smaller β_π, when $\sin\theta_1$ is kept constant. We note that the dependence of β_π on $\sin\theta_1$ in the domain about $\theta_1 = 0$ is substantially nonlinear. The dependence of β_π on θ_1 in the domain of small θ_1 angles is shown in Fig. 2.3. As the curves in Fig. 2.3 show, the parameter k_1 strongly influences $1 - \beta_\pi$ and therefore, $r_{\pi 1}$ for a given angle $\theta_1 \neq 0$.

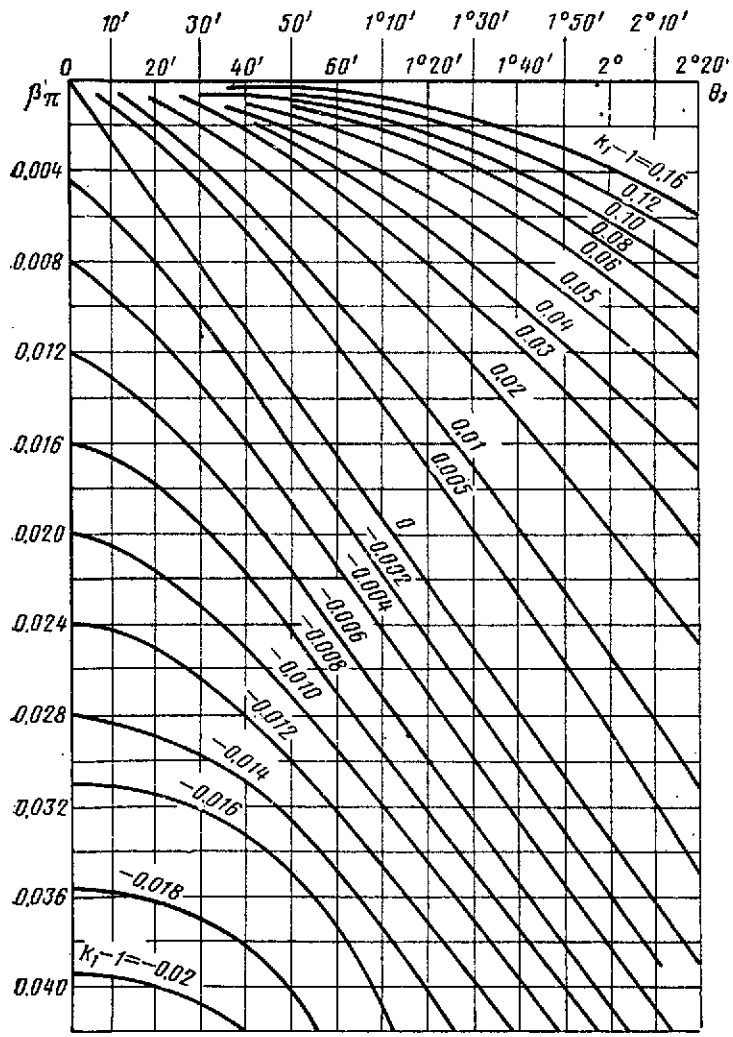

Fig. 2.3. Function $\beta_\pi(\theta_1, k_1)$.

Let us examine the relation between deviations of parameters at the end of the powered section and changes in perigee altitude. /92

Using Eq. (2.6), we can write

$$\Delta r_{\pi 1} = \Delta r_1 (1 - \beta_\pi) - \Delta\beta_\pi (r_1 + \Delta r_1). \quad (2.7)$$

Generally, $k_1 \geq 1.03$, $|\theta_1| \leq 2°$ obtains for orbits of spacecraft inserted without final acceleration. Corresponding to this, $\beta_\pi \leq 0.0165$ (see Fig. 2.3). In addition, if $\Delta r_1 \leq 50$ km, then instead of Eq. (2.7) we can write the following, with an error of less than 1 km in the determination of $\Delta r_{\pi 1}$: /93

$$\Delta r_{\pi 1} \approx \Delta r_1 - r_1 \Delta\beta_\pi. \quad (2.8)$$

The quantity $\Delta\beta_\pi$ is defined by the deviations Δv_1, $\Delta\theta_1$, and Δr_1 and can

be determined by means of, for instance, Fig. 2.3. For approximate estimates we have

$$\Delta\beta_\pi \leqslant \Delta\beta_{\pi\max} = \beta_\pi(\sin\theta_{1\max},\ k_{1\min}) - \beta_\pi(\sin\tilde{\theta}_1,\ \tilde{k}_1).$$

If $\tilde{\theta}_1 = 0$, the second term in the last formula drops out. Then from (2.8), by assuming the deviation $\Delta\theta_1$ to be small, we get

$$\Delta r_{\pi 1} \leqslant |\Delta r_1| + r_1\beta_\pi(\Delta\theta_{1\max},\ k_{1\min}). \tag{2.9}$$

To illustrate the effect of the deviations $\Delta\theta_1$ and Δv_1 on the deviations in the perigee altitude, let us make several calculations.

1. We will assume that the elements at the end of the powered section have the following values: $\tilde{v}_1 = 8$ km/sec, $\tilde{r}_1 = 6540$ km, and $\tilde{\theta}_1 = 0$. We will assume that when the angle θ_1 is varied by the amount $\Delta\theta_1$, the velocity and altitude at the end of the powered section remain unchanged. Then $k_1 \approx 1.05$. If $\Delta\theta_1 = 2$ and $1°$, from the graph in Fig. 2.3 we have

$$\Delta r_{\pi 1} \approx 74.5 \text{ km and } \Delta r_{\pi 1} \approx 21 \text{ km}.$$

2. We will assume that the design velocity at the end of the powered section is increased to 8.1 km/sec, and then given our former assumptions we find that when $\Delta\theta_1 = 1$ and $2°$ we will corresponding have $\Delta r_{\pi 1} = 14.4$ and 55 km. In this case a 1.2% increase in velocity gives a reduction in the error of the perigee altitude, when $\Delta\theta_1 = 2°$ of about 27%.

3. Let us find at which $\Delta\theta_1$ the orbit will intersect the Earth's surface if $v_1 = 8$ km/sec. We set

$$\frac{r_1 - r_{\pi 1}}{r_1} = \frac{170}{6540} = 0.026.$$

This deviation in the orbital perigee will occur when $\Delta\theta_1 = 3.15°$, as follows from the curves in Fig. 2.3. We note that if the velocity were circular (for $h_{\pi 1} = 170$ km, $v_1 \approx 7.80$ km/sec), a deviation in the perigee altitude of 0.026 would correspond to $\Delta\theta_1 \approx 1.5°$.

Let us examine the deviations in the apogee distance. First, we note that at small θ_1 at which the dependence of r_α on θ_1 is substantially nonlinear, the deviation Δr_α due to $\Delta\theta_1$ can be

found by the same technique as for the deviation Δr_{π} examined above, since due to $\Delta\theta_1$, the deviation $\Delta r_{\alpha} = -\Delta r_{\pi}$.

The estimate of the deviations Δr_{α} due to the deviations Δv_1 and Δr_1 and also due to $\Delta\theta_1$, with $\theta_1 > 3^{\circ}$[1], can be satisfactorily made by means of the first derivatives. The formulas for the first derivatives can be derived from Eq. (2.2) and are as follows: /94

$$\frac{\partial r_{\alpha}}{\partial v_1} = \frac{2k_1 a_1}{v_1}\left[\frac{r_{\alpha}}{r_1} + \frac{1}{e_1}(k_1 - 1)\cos^2\theta_1\right]; \tag{2.10}$$

$$\frac{\partial r_{\alpha}}{\partial r_1} = \frac{k_1 a_1}{r_1}\left[\frac{r_{\alpha}}{r_1} + \frac{1}{e_1}(k_1 - 1)\cos^2\theta_1\right] + \frac{r_{a1}}{r_1}; \tag{2.11}$$

$$\frac{\partial r_{\alpha}}{\partial \theta_1} = \frac{k_1}{2e_1}\sin 2\theta_1, \tag{2.12}$$

where

$$a_1 = (r_{\pi 1} + r_{a1})\frac{1}{2}.$$

For small orbits, near-circular, and when $\theta_1 = 0$, we have

$$\frac{\partial r_{\alpha}}{\partial v_1} = 3.2\text{-}3.5 \text{ [km/m/sec]}; \quad \frac{\partial r_{\alpha}}{\partial r_1} \approx 3.0\text{-}3.3 \text{ [km/km]}.$$

2. Deviations in the parameters of spacecraft motion at orbital apogee. To estimate the deviations in the orbital element when a spacecraft is inserted into the orbit with final acceleration in the region of the transfer-ellipse apogee, it is essential that we know the deviations in the parameters of spacecraft motion in the region of final acceleration due to errors in the principal powered section. We will estimate these deviations in the linear approximation, indicating the domain of the value of the elements of the transfer ellipse in which the linear approximation yields satisfactory results. Deviations in one of the important transfer-ellipse parameters -- the altitude of its apogee -- were examined above and are defined by Eqs. (2.10)-(2.12).

The deviation in the parameter $k_2 = \frac{1}{\mu} v_a^2 r_{\alpha}^2$ at the apogee of the transfer ellipse is another essential deviation. Considering that $k_2 = 1 - e_1$ (e_1 is the eccentricity of the ellipse, we find

$$\Delta k_2 = -\left[\frac{k_1 - 1}{e_1}\cos^2\theta_1 \Delta k_1 + \frac{r_1}{2a_1}\frac{k_1}{e_1}\sin 2\theta_1 \Delta\theta_1\right], \tag{2.13}$$

[1] The value was obtained from estimates of the quantities of the second derivatives.

where the subscript "1" denotes the values of the corresponding parameters at the end of the main powered section.

For cases when the moment of final acceleration is determined by the assigned flight time from the end of the powered section to the moment the spacecraft transits the apogee of the transfer ellipse, deviations in this time due to errors in spacecraft insertion into the transfer ellipse are also essential. /95
This time T is determined from the formula

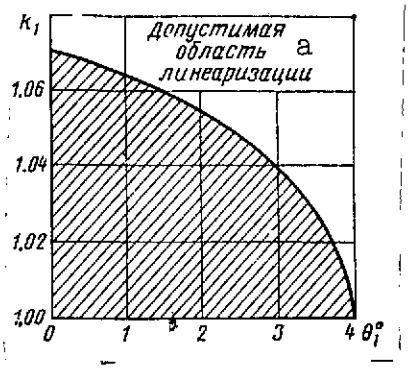

Fig. 2.4. Domain of values k_1 and θ_1 (not hatched) in which the error in the calculation of the deviations ΔT and $\Delta\vartheta$ from linear relationships does not exceed 10-15%.

Key: a. Admissible domain of linearization

$$T = \frac{\mu^{1/2}}{r_1^{3/2}}\overline{T}, \tag{2.14}$$

where

$$\overline{T} = \frac{1}{(2-k_1)^{3/2}}(E + e_1 \sin E); \tag{2.15}$$

$$E = \pi - 2\operatorname{arctg}\left(\sqrt{\frac{1-e_1}{1+e_1}}\operatorname{tg}\frac{\vartheta}{2}\right); \tag{2.16}$$

$$\vartheta = \operatorname{arctg}\frac{k_1 \cos\theta_1 \sin\theta_1}{k_1\cos^2\theta_1 - 1}. \tag{2.17}$$

The angle E can also be determined from the following expressions:

$$\sin E = \frac{1}{e_1}\sqrt{k_1(2-k_1)}\sin\theta_1;\quad \cos E = -\frac{k_1-1}{e_1}, \tag{2.18}$$

obtained from the main relations of elliptical theory. Expressions for the corresponding derivatives are of the following form:

$$\frac{\partial\overline{T}}{\partial k_1} = \frac{\sin\theta_1}{(2-k_1)^2\sqrt{k_1}}\left[\frac{1}{e_1^2} - (k_1-1)\right] + \frac{3}{2}\frac{\overline{T}}{2-k_1}; \tag{2.19}$$

$$\frac{\partial\overline{T}}{\partial\theta_1} = \frac{\sqrt{k_1}\cos\theta_1}{2-k_1}\left(1 - \frac{k_1-1}{e_1^2}\right). \tag{2.20}$$

The expressions of the derivatives $\frac{\partial T}{\partial \theta_1}$, $\frac{\partial T}{\partial \vartheta_1}$ and $\frac{\partial T}{\partial r_1}$ can be readily obtained by means of Eqs. (2.14), (2.19), and (2.20).

Fig. 2.4 shows the domain of k_1 and θ_1 values (unhatched) in which the estimate of the errors in the time T by means of the first derivatives gives an error not greater than 10-15%. This domain was obtained by estimating the quantities of the second derivatives.

Let us examine, finally, the deviations in the angular position of the transfer-ellipse apogee relative to the end of the powered section of spacecraft insertion into the transfer ellipse. We will characterize this position of the apogee by the angle

$$\vartheta_a = \pi - \vartheta_1, \tag{2.21}$$

where ϑ_1 is the true anomaly of the end of the powered section.

From the equation of the ellipse we have /96

$$\vartheta_a = \arccos\left\{\frac{1}{e_1}\left[k_1 \sin^2\theta_1 - (k_1 - 1)\right]\right\}. \tag{2.22}$$

Differentiating this formula, we find

$$\frac{\partial \vartheta_a}{\partial k_1} = \frac{1}{2e_1}\sin^2\theta_1; \tag{2.23}$$

$$\frac{\partial \vartheta_a}{\partial \theta_1} = -\frac{k_1 - 1}{e_1^2} - 1. \tag{2.24}$$

The estimate of the deviations $\Delta\vartheta_a$ by means of Eqs. (2.23) and (2.24) in the domain of k_1 and θ_1 values shown in Fig. 2.4 leads to errors of not more than 10-15%.

2.2. Determination of Initial Orbital Perturbations Due to Deviations in Final Acceleration Parameters

By final acceleration parameters we will mean the following quantities (Fig. 2.5):

u is the additional velocity
λ is the angle between the vector of the additional velocity u and the velocity vector prior to final acceleration v_2, and
T is the moment at which final acceleration is carried out.

Deviations in the final acceleration parameters cause deviations in the parameters of motion after final acceleration. The latter can be considered as initial perturbations. Therefore, the investigation of the effect of deviations in the final

acceleration parameters on the resulting orbit can be divided into two problems:

1) determining the initial perturbations of motion due to deviations in the final acceleration parameters; and

2) examining motion along the orbit when there are initial perturbations due to final acceleration errors.

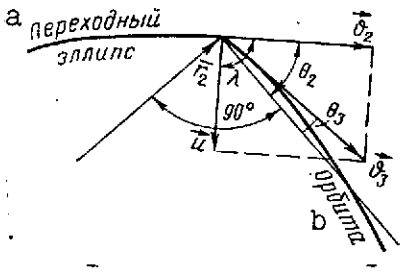

Fig. 2.5. For determining the equation of spacecraft motion during final acceleration.

Key: a. Transfer ellipse; b. Orbit

Deviations in the parameters of satellite motion in the transfer ellipse are also perturbations. Thus, if the final acceleration takes place at the apogee of the transfer ellipse, the deviations in the apogee altitude and the variation of the velocity at the apogee will be directly reflected in subsequent motion. If the instant of final acceleration is determined by means of a clock type mechanism onboard the satellite, (that is, final acceleration is carried out over the period T_{cal} [cal = calculated] after the end of the powered section, /97 where T_{cal} is constant and equal to the time of motion from the end of the powered section to the apogee for design motion), deviations in the flight time to the apogee will cause final acceleration to occur at a point not coincident with the apogee of the transfer ellipse. This also leads to the appearance of deviations in the velocity, altitude and direction of the velocity vector at the moment of final acceleration and will be a cause for the occurrence of deviations in motion after final acceleration. However, the effect of deviations in the transfer-ellipse parameters on motion after final acceleration will differ, depending on the method of final acceleration control. Therefore, a quantitative analysis of this effect can be made only for a specific method of control. For this analysis we can use, for instance, the formulas presented here for the derivatives; the analysis itself is not set forth.

As we know, the shape of an orbit in a central force field is defined by the quantities r, θ, and $k = v^2r/\mu$, which are known at any point of the trajectory. At the final acceleration point, after its completion, we have

$$r=r_3,\ \theta=\theta_3,\ k=k_3=\frac{v_3^2 r_3}{\mu}. \qquad (2.25)$$

The subscript "3" refers to the parameters of motion after final acceleration. Let us determine the deviations in these

quantities from the design values due to the action of deviations in the final acceleration parameters.

By virtue of the assumption made of instantaneous final acceleration, we have

$$r_3 = r_2; \quad \Delta r_3 = \Delta r_2. \tag{2.26}$$

The quantities v_3 and θ_3 are defined by the formula

$$v_3^2 = v_2^2 + 2v_2 u \cos\lambda + u^2; \tag{2.27}$$

$$\sin(\theta_2 - \theta_3) = \frac{u}{v_3} \sin\lambda. \tag{2.28}$$

In addition, we have the following relations:

$$\sin\theta_3 = \frac{1}{v_3}[v_2 \sin\theta_2 - u\cos(\lambda - \theta_2)]; \tag{2.29}$$

$$\cos\theta_3 = \frac{1}{v_3}[v_2 \cos\theta_2 + u\cos(\lambda - \theta_2)]. \tag{2.30}$$

The position of the spacecraft in the transfer ellipse characterized by the true anomaly ϑ_2 depends on the moment of time at which final acceleration takes place.

The deviation in time δT is associated with the deviation in the angle ϑ_2 by the relation

$$\delta\vartheta_2 \approx \frac{\partial\vartheta_2}{\partial T}\delta T, \tag{2.31}$$

where

$$\frac{\partial\vartheta_2}{\partial T} = \frac{\sqrt{\mu p_1}}{r_2^2}; \quad p_1 = r_1 k_1 \cos^2\theta_1.$$

Instead of ϑ_2, it is convenient to use the quantity /98

$$\Delta\vartheta = \pi - \vartheta_2. \tag{2.32}$$

The dependence of the parameters of motion on $\Delta\vartheta$ is expressed by the following formulas of celestial mechanics:

$$\left.\begin{aligned} v_2^2 &= \frac{\mu}{p_1}(1 - 2e_1\cos\Delta\vartheta + e_1^2); \quad r_2 = \frac{1}{1 - e_1\cos\Delta\vartheta}; \\ \sin\theta_2 &= \frac{e_1\sin\Delta\vartheta}{\sqrt{1 - 2e_1\cos\Delta\vartheta + e_1^2}}; \quad \cos\theta_2 = \frac{1 - e_1\cos\Delta\vartheta}{\sqrt{1 - 2e_1\cos\Delta\vartheta + e_1^2}}. \end{aligned}\right\} \tag{2.33}$$

The angle $\Delta\vartheta$ defines the position of the spacecraft during final acceleration relative to the transfer ellipse apogee. If in the calculated case the final acceleration is effected at the transfer ellipse apogee, this angle characterizes the deviation of the spacecraft position at this instant due to change in the moment of final acceleration relative to the design value.

Let us denote the deviations in the final acceleration parameters from the design values as follows:

δu is the deviation in the additional velocity
$\delta\lambda$ is the deviation in the angle λ, and
$\delta\Delta\vartheta$ are the deviations in the angle $\Delta\vartheta$.

With these deviations, the following obtain:

$$\delta\theta_3=\theta_3-\tilde{\theta}_3;\quad \delta k_3=k_3-\tilde{k}_3,$$

The formulas for the first derivatives are of the form

$$\begin{aligned}
&\frac{\partial\theta_3}{\partial u}=-\frac{v_2}{v_3^2}\sin\lambda;\quad \frac{\partial k_3}{\partial u}=\frac{2k_2}{v_2}\left(\frac{u}{v_2}+\cos\lambda\right);\\
&\frac{\partial\theta_3}{\partial\lambda}=\frac{1}{2}\left[-1+\frac{v_2^2}{v_3^2}-\frac{u^2}{v_3^2}\right];\quad \frac{\partial k_3}{\partial\lambda}=-\frac{2}{\mu}uv_2r_2\sin\lambda;\\
&\frac{\partial k_3}{\partial\Delta\vartheta}=\frac{v_3^2}{\mu}\frac{\partial r_2}{\partial\Delta\vartheta}+\frac{2r_2}{\mu}(v_2+u\cos\lambda)\frac{\partial v_2}{\partial\Delta\vartheta};\\
&\frac{\partial\theta_3}{\partial\Delta\vartheta}=\frac{\partial\theta_2}{\partial\Delta\vartheta}+\frac{u}{v_3^2}\frac{\partial v_2}{\partial\Delta\vartheta}\sin\lambda,
\end{aligned}\qquad (2.34)$$

where

$$\frac{\partial v_2}{\partial\Delta\vartheta}=\sqrt{\frac{\mu}{p_1}}\sin\theta_2;\quad \frac{\partial r_2}{\partial\Delta\vartheta}=-r_2\operatorname{tg}\theta_2;$$
$$\frac{\partial\theta_2}{\partial\Delta\vartheta}=-\frac{e_1(e_1-\cos\Delta\vartheta)}{1+e_1^2-2e_1\cos\Delta\vartheta}.$$

Let us examine more closely the case when the design orbit is circular. Here the final acceleration is completed at the apogee of the transfer ellipse when $\lambda = 0$. It is not difficult to obtain u, required for transfer to the circular orbit form the relation $k_3 = 1$. The formula for k_3 is of the following form: /99

$$k_3=1-e_1+2u\sqrt{\frac{r_1k_1\cos^2\theta_1}{\mu}}+\frac{1+e_1}{2-k_1}\frac{u^2r_1}{\mu},\qquad (2.35)$$

where

$$u=\sqrt{\frac{\mu}{r_a}}(1-\sqrt{1-e_1}).\qquad (2.36)$$

Referring to Eq. (2.36) and also to the conditions $\lambda = 0$ and $\Delta\vartheta = 0$, we can reduce the formulas for the derivatives to the following form:

$$\left.\begin{aligned} &\frac{\partial\theta_3}{\partial u}=0; && \frac{\partial k_3}{\partial u}=2\sqrt{\frac{r_2}{\mu}};\\ &\frac{\partial\theta_3}{\partial\lambda}=\sqrt{1-e_1}-1; && \frac{\partial k_3}{\partial\lambda}=0;\\ &\frac{\partial\theta_3}{\partial\Delta\vartheta}=\frac{e_1}{1-e_1}; && \frac{\partial k_3}{\partial\Delta\vartheta}=0. \end{aligned}\right\} \qquad (2.37)$$

The estimate of the orbital deviations dependent on the second derivatives in the case when the design orbit is circular shows that their effect is slight and can be neglected. In this case,

$$\delta k_3=\frac{\partial k_3}{\partial u}\delta u; \qquad (2.38)$$

$$\delta\theta_3=\frac{\partial\theta_3}{\partial\lambda}\delta\lambda+\frac{\partial\theta_3}{\partial\Delta\vartheta}\delta\Delta\vartheta; \qquad (2.39)$$

$$\delta r_3=\delta r_{a1}. \qquad (2.40)$$

Let us define the deviation δk_3 due to deviations in the transfer ellipse parameters, for small $\delta\Delta\vartheta$ and $\delta\lambda$, using Eqs. (2.35) and (2.36), as follows:

$$\delta k_3'=(1-e_1)\delta k_2,$$

where δk_2 is found from Eq. (2.13).

In this case, the total deviation Δk_3 can be expressed as:

$$\Delta k_3=\frac{\partial k_3}{\partial u}\delta u+(1+e_1)\delta k_2. \qquad (2.41)$$

2.3. Deviations of Circular Orbit

Let us examine the perturbed [disturbed] motion of the satellite after the additional velocity has been imparted to it.

The approach to the problem adopted in this section and consisting in linearizing the equations of motion is justified by the fact that it enables us to obtain simple, although less exact, expressions for the variation in time of the deviations of motion parameters. For generality, we will assume that the satellite is acted on, in addition to the gravitational force, by some force $\overline{P}$, which can either be a perturbing or a controlling force. In /100

both cases we will assume that the magnitude and direction of this force are given functions of time. In deriving the necessary equations we will also assume that the force $\bar{P}$ is situated in the orbital plane defined by the initial velocity components. Here we first consider the case when the perturbed motion occurs in the plane of the design orbit.

The equations of satellite motion in a polar system of coordinates are as follows:

$$\left.\begin{aligned} \frac{dv_\tau}{dt} &= p\sin\theta - \frac{1}{r}v_\tau v_n;\\ \frac{dv_n}{dt} &= p\cos\theta - g + \frac{1}{r}v_\tau^2;\\ \frac{dr}{dt} &= v_n, \end{aligned}\right\} \qquad (2.42)$$

where $p = |\bar{P}|/m$; $g = \mu/r^2$
θ is the angle between $\bar{P}$ and $\bar{r}$
v_n is the radial component of velocity, and
v_τ is the transversal velocity component.

Let us write the equations of perturbed motion in variations. To do this we set

$$\left.\begin{aligned} v_\tau &= v_{\tau 0} + \Delta v_\tau;\\ v_n &= v_{n0} + \Delta v_n;\\ r &= r_0 + \Delta r, \end{aligned}\right\} \qquad (2.43)$$

where $v_{\tau 0}$, $v_{n\,0}$, and r_0 are the parameters of motion in the design orbit. By substituting Eqs. (2.43) into Eqs. (2.42) and leaving only the terms of the first order of smallness, we get the equations of motion in variation

$$\left.\begin{aligned} \Delta\dot{v}_\tau + \frac{v_{n0}}{r_0}\Delta v_\tau + \frac{v_{\tau 0}}{r_0}\Delta v_n + \frac{v_{n0}v_{\tau 0}}{r_0^2}\Delta r &= p\sin\theta;\\ \Delta\dot{v}_n - \frac{2v_{\tau 0}}{r_0}\Delta v_\tau + \frac{v_{\tau 0}^2}{r_0^2}\Delta r &= p\cos\theta - g_r'\Delta r;\\ \Delta\dot{r} &= \Delta v_n, \end{aligned}\right\} \qquad (2.44)$$

where

$$g_r' = -2\frac{\mu}{r_0^3} = -\frac{2g}{r_0}.$$

Let us further assume that the design orbit is circular. Then /101 in Eqs. (2.44) we can set: $v_{n\,0} = 0$, $v_{\tau 0} = \text{const}$, $r_0 = \text{const}$ and $g_r' = -2\frac{v_{\tau 0}^2}{r_0^2}$.

The system of equations we have obtained defines the deviations in the motion parameters Δv_τ, Δv_n, and Δr from their values corresponding to motion in the circular orbit:

$$\left.\begin{aligned} \Delta\dot{v}_\tau + \frac{v_{\tau 0}}{r_0}\Delta v_n &= p\sin\theta; \\ \Delta\dot{v}_n - \frac{2v_{\tau 0}}{r_0}\Delta v_\tau - \frac{v_{\tau 0}^2}{r_0^2}\Delta r &= p\cos\theta; \\ \Delta\dot{r} &= \Delta v_n. \end{aligned}\right\} \qquad (2.44')$$

This system is a system of linear equations with constant coefficients and with right-hand sides that are given functions of time. Let us substitute the last equation into the first and integrate the result. We get

$$\Delta v_\tau + \frac{v_{\tau 0}}{r_0}\Delta r = \int_0^t p\sin\theta dt + C, \qquad (2.45)$$

where

$$C = \Delta v_{\tau 0} + \frac{v_{\tau 0}}{r_0}\Delta r_0,$$

$\Delta v_{\tau 0}$ and Δr_0 are the initial values in the deviations corresponding to the instant t = 0.

Substituting Eq. (2.45) into the second equation of system (2.44) and using the third equation, we get

$$\Delta\ddot{r} + \left(\frac{v_{\tau 0}^2}{r_0^2}\right)\Delta r = p\cos\theta + \frac{2v_{\tau 0}}{r_0}\left[\int_0^t p\sin\theta\, dt + C\right]. \qquad (2.46)$$

Let us transform the equation appearing in the parentheses. Since the design orbit is circular,

$$\frac{v_{\tau 0}}{r_0} = \frac{2\pi}{T},$$

where T is the period of revolution of the satellite in the design circular orbit.

With reference to this relation, we can write Eq. (2.46) as

$$\Delta\ddot{r} + \left(\frac{2\pi}{T}\right)^2\Delta r = p\cos\theta + \frac{4\pi}{T}\left[\int_0^t p\sin\theta\, dt + C\right]. \qquad (2.47)$$

For given initial deviations and known functions of time $\dot{p}$ and θ, /102
the last equation can be integrated. As a result of integration, we will find the function $\Delta r(t)$. Here Eq. (2.45) will define the velocity deviation Δv_τ and the second equation of the system (2.44') -- Δv_n. It is not difficult to obtain as well a formula for the deviation of the central angle ϕ

$$\Delta\varphi = \Delta\varphi_0 + \frac{1}{r_0}\int_0^t \left(\Delta v_\tau - \frac{2\pi}{T}\Delta r\right) dt. \tag{2.48}$$

We must show that the resulting equations and the formulas make it possible to solve the problem of the control of motion and fuel expenditures for the approach of two satellites. In this section we do not examine these problems, therefore for the following we will set p = 0. As a result Eq. (2.47) becomes simplified. By solving this equation, let us determine the relation between the deviations of satellite altitude and the initial deviations in motion parameters:

$$\Delta r = 2\Delta r_0 + \frac{T}{\pi}\Delta v_{\tau 0} + A\sin\left(\frac{2\pi}{T}t + \psi_0\right), \tag{2.49}$$

where

$$A = \sqrt{\left(\Delta r_0 + \frac{T}{\pi}\Delta v_{\tau 0}\right)^2 + \left(\frac{T}{2\pi}\right)^2 \Delta v_{n0}^2};$$

$$\sin\psi_0 = -\frac{1}{A}\left(\Delta r_0 + \frac{T}{\pi}\Delta v_{\tau 0}\right);$$

$$\cos\psi_0 = \frac{1}{A}\frac{T}{2\pi}\Delta v_{n0}.$$

Using this result, Eqs. (2.45) and (2.48), and the second equation of the system 92.44'), we can arrive at an expression for the deviations in the other motion parameters.

Omitting the derivations, we present the final formulas:

$$\left.\begin{aligned}
&\Delta\varphi = \Delta\varphi_0 - \omega\frac{\Delta T}{T}t + \frac{2}{v_{\tau 0}}B\cos[\omega t + \gamma_0] - \frac{2}{v_{\tau 0}}\Delta v_{n0};\\
&\Delta v_n = B\cos[\omega t + \gamma_0];\\
&\Delta v_\tau = -\frac{v_{\tau 0}}{3T}\Delta T - B\sin[\omega t + \gamma_0],
\end{aligned}\right\} \tag{2.50}$$

where

$$B = \sqrt{\Delta v_{n0}^2 + (\omega\Delta r_0 + 2\Delta v_{\tau 0})^2};$$

$$\sin\gamma = -\frac{1}{B}(\omega\Delta r_0 + 2\Delta v_{\tau 0});$$

$$\cos\gamma = -\frac{1}{B}\Delta v_{n0};$$

$$\Delta T = \frac{3T}{2r_0}\left(2\Delta r_0 + \frac{T}{\pi}\Delta V_{\tau 0}\right);$$

$$\omega = \frac{2\pi}{T};$$

r_0, $v_{\tau 0}$ and T are the altitude, velocity, and period of revolution for the design circular orbit.

The initial deviations Δr_0, $\Delta\phi_0$, $\Delta v_{n\,0}$, and $\Delta v_{\tau 0}$ correspond to t = 0.

Let us present the formulas for calculating the deviations in the satellite altitude when insertion errors are present. These formulas can be readily obtained from Eqs. (2.50), by assuming, successfully, that all the deviations, except for one, are equal to zero:

1) when $\Delta r_0 \neq 0$

$$\Delta r = \Delta r_0(2 - \cos\omega t), \quad |\Delta r|_{\max} = 3|\Delta r_0|;$$

2) when $\Delta v_{\tau 0} \neq 0$

$$\Delta r = 2\frac{1}{\omega}\Delta v_{\tau 0}(1 - \cos\omega t), \quad |\Delta r|_{\max} = 4\frac{1}{\omega}(\Delta v_{\tau 0});$$

3) when $\Delta v_{n0} \neq 0$

$$\Delta r = \frac{1}{\omega}\Delta v_{n0}\sin\omega t, \quad |\Delta r|_{\max} = \frac{1}{\omega}(\Delta v_{n0}).$$

Let us examine further the lateral deviations of the circular orbit from its design plane originating only due to initial deviations.

Denoting by z the satellite deviation from the plane of the design orbit and assuming this deviation to be small, for this case we can write the following equation:

or

$$\left.\begin{aligned} \ddot{z} + \frac{g_0}{r_0}z = 0 \\ \ddot{z} + \left(\frac{2\pi}{T}\right)^2 z = 0, \end{aligned}\right\} \qquad (2.51)$$

where g_0 and r_0 is the acceleration due to the gravity and the radius of the design circular orbit.

Solving this equation, let us find the dependence of the lateral deviation of the circular orbit on flight time

$$z = z_0 \cos \omega t + V_{z0} \frac{1}{\omega} \sin \omega t, \tag{2.52}$$

where z_0 and $V_{z\,0}$ are the lateral deviation and lateral velocity when $t = 0$.

Since in the other sections of this chapter we considered the deviations Δk_3 and $\Delta\theta_1$ instead of the deviations $\Delta v_{n\,0}$ and $\Delta v_{\tau 0}$, let us transform Eqs. (2.50). /104

The relation between the deviations for the case of a circular design orbit is determined by the formulas

$$\Delta v_{\tau 0} = \frac{v_3}{2} \Delta k_3 - \frac{v_3}{2r_3} \Delta r_3; \tag{2.53}$$

$$\Delta v_{n0} = v_3 \Delta \theta_3. \tag{2.54}$$

Here Eq. (2.49) becomes

$$\Delta r = \Delta r_3 + r_3 \Delta k_3 + r_3 \sqrt{\Delta k_3^2 + \Delta \theta_3^2} \sin\left(\frac{2\pi}{T} t + \psi_0\right). \tag{2.55}$$

Using Eqs. (2.50) and substituting therein the expressions for the deviation Δk_3 and $\Delta\theta_3$ caused by deviations in the final acceleration parameters, we get

$$|\Delta r_u| = 4r_2 \sqrt{r_2/\mu}\, |\Delta u|;$$

$$|\Delta r_\lambda| = r_2 |(\sqrt{1 - e_1} - 1)\, \Delta\lambda|;$$

$$|\Delta r_\vartheta| = r_2 \frac{e_1}{1 - e_1} |\Delta\vartheta|.$$

For the transfer ellipses characterized by $1.05 \leq \frac{r_{\alpha 1}}{r_1} \leq 1.5$ we have

$$3650\,|\Delta u| < |\Delta r_u| < 6320\,|\Delta u|;$$

$$87\,|\Delta\lambda| < |\Delta r_\lambda| < 2500\,|\Delta\lambda|;$$

$$178\,|\Delta\vartheta| < |\Delta r_\vartheta| < 7500\,|\Delta\vartheta|.$$

The last estimate shows that the deviation Δu equal to 1 m/sec causes an altitude deviation from 3.65 to 6.32 km, depending on the altitude of the design orbit and the angle θ_1. A deviation $\Delta\lambda$ of 1° leads to a deviation of the orbit from the design orbit by the amount 1.5-44 km. Finally, $\Delta\theta$ = 1° causes the changes r 3.1-130 km.

These estimates lead to the following conclusions.

1. If we must ensure small orbital deviations from the design orbit, the control system must provide for final acceleration at the transfer ellipse apogee. This is particularly true of cases when the angle θ_1 is large and the transfer ellipse has a large eccentricity.

2. The necessary accuracy of spacecraft orientation during final acceleration increases with increasing in θ_1. In order that when θ_1 = 25° and r_3 = 7000 km the deviation in the orbital altitude due to orientation error not to exceed 10 km, this error must not be more than 15', while when θ_1 = 0 and for the same r_2, the error of orientation must be not more than 5°. /105

3. For the effect of deviations in the final acceleration parameters to be the smallest, the angle of inclination of the velocity vector to the horizon at the end of the powered section must be close to zero.

CHAPTER III

/106

ANALYSIS OF EFFECT OF PERTURBING FORCES ACTING ON AN ORBIT

When in an orbit, a satellite is affected by small or, as they are called, perturbing forces. The effect of these forces causes deviations (perturbations) of satellite coordinates and velocity relative to unperturbed motion. Study of these perturbations is one of the fundamental problems in the theory of satellite motion. Perturbing forces and their effect on an orbit must be allowed for in design-project work and especially when determining orbits from measurements.

This chapter presents information on the main perturbing forces and derives equations by which their effect on the satellite mass center can be calculated if the initial conditions of motion are known.

Forces acting on a satellite in flight can be divided into gravitational forces, which are massive conservative forces, and surface forces. Also, electromagnetic forces can act on a satellite, but they are very weak and have no practical importance.

Among the gravitational forces affecting the motion of the center of mass is the auxiliary force of attraction appearing due to the oblateness of the Earth, the anomaly of the Earth's gravity field, and the attraction of Moon and Sun.

Surface forces, in contrast to gravitational forces, cannot have a potential function. We will consider two of these forces: the decelerating force caused by the air drag, and the force of solar wind pressure. The action of the remaining forces can be neglected.

3.1. Method of Osculating Elements

The differential equations of satellite motion in an absolute system of rectangular coordinates with its origin at the Earth's center are of the form [56]:

$$\left.\begin{aligned} \ddot{x}+\mu\frac{x}{r^3}&=F_x;\\ \ddot{y}+\mu\frac{y}{r^3}&=F_y;\\ \ddot{z}+\mu\frac{z}{r^3}&=F_z. \end{aligned}\right\} \qquad (3.1)$$

The right-hand sides of the equations are projections on the corresponding axes of the resultant of all forces acting on the satellite in flight, with the exception of the main force of the Earth's central field of attraction, whose projections onto the coordinate axes have been singled out and shown in the left-hand part of this system. If no other forces except for the central force acts on the satellite, zeroes will appear in the right-hand sides. As was explained in Chapter I, these equations are called the equations of unperturbed motion. They are integrated to completion, and depending on the initial conditions of motion, the resulting trajectories can be ellipses, parabolas, or hyperbolas. Let us examine only the elliptical trajectories (orbits), and their particular case -- circular orbits. /107

The forces added to the right-hand parts of the equations alter the orbit in a specific way. These forces are small, the orbital variations are also small. Actually, all forces acting on the satellite are small compared with the primary central force, therefore they are perturbing forces.

To calculate these motions, it is useful to employ the method of osculating elements familiar in celestial mechanics. Its concept is the use of six constants of integration (a, e, ω, i, Ω, τ) of the system of equations of unperturbed motion as new variables. From the mathematical standpoint, system (3.1) of perturbed motion is solved by the method of variations of arbitrary constants. As a result, a system of six first-order differential equations in six unknown functions of time is obtained -- the former arbitrary constants a, e, ω, i, Ω, and τ. These equations, like Eqs. (3.1) are not integrated in final form. Their advantage is that for small perturbing forces the new variables vary little and the method of successive approximations can be used for solutions of the system.

The solution of system (3.1) in the new variables for each instant of time yields six parameters (elements) defining some fictive elliptical orbit ("osculating ellipses"). If at each instant of time t_1 the perturbing forces cease to be in effect, further motion will continue along an ellipse that has the elements $a(t_1)$, $e(t_1)$, $\omega(t_1)$, $\Omega(t_1)$, $i(t_1)$, and $\tau(t_1)$ and is tangent to the actual orbit at a point where the perturbing forces no longer have an effect. The orbit is the envelope of these ellipses. The variable elements of the orbit $a(t)$, $e(t)$, $\omega(t)$, $\Omega(t)$, $i(t)$, and $\tau(t)$ are called the osculating elements.

The satellite coordinates and velocities in a rectangular system of coordinates are calculated by the same formulas as for unperturbed motion (see Chapter I), but the values of the elements a, e, ω, ..., appearing in these formulas, must correspond to the given moment of time. /108

Let us proceed to the derivation of the differential equations for osculating elements. Formally, we could simply substitute into the equations of perturbed motion (3.1) the solution for the unperturbed system of equations (see Chapter I), assuming the constants of integration a, e, ... as functions of time. However, this is too involved. We can use several methods [23, 29] that enable us to much more simply obtain the desired equations. Let us dwell on one of them.

Derivation of Equations for Orbital Elements Ω, p and i

In Chapter I, the following functions were obtained for unperturbed motion:

$$C_1 = C \sin \Omega \sin i;$$
$$C_2 = -C \cos \Omega \sin i;$$
$$C_3 = C \cos i,$$

where C_1, C_2 and C_3 are the projections of the vector of the kinetic moment $\bar{C}$ on the coordinate axes Ox, Oy, and Oz.

Under the method of variations of arbitrary constants, the kinetic moment and thus its projections C_1, C_2, and C_3 for perturbed motion become functions of time. On the other hand, from mechanics we know that the derivative of the kinetic moment in time is equal to the moment of the resultant of all forces, that is,

$$\frac{d\bar{G}}{dt} = \bar{r} \times \bar{F}. \tag{3.2}$$

By applying this formula to the projections of the kinetic moment C_1, C_2, and C_3, we get

$$\left.\begin{aligned}
\frac{dC_1}{dt} &= \frac{dC}{dt} \sin \Omega \sin i + C \cos \Omega \sin i \frac{d\Omega}{dt} + C \sin \Omega \cos i \frac{di}{dt};\\
\frac{dC_2}{dt} &= -\frac{dC}{dt} \cos \Omega \sin i + C \sin \Omega \sin i \frac{d\Omega}{dt} - C \cos \Omega \cos i \frac{di}{dt};\\
\frac{dC_3}{dt} &= \frac{dC}{dt} \cos i - C \sin i \frac{di}{dt}.
\end{aligned}\right\} \tag{3.3}$$

Fig. 3.1 shows the projections of the perturbing force (per unit mass) on the orbital coordinate axes: S -- on the radius-vector; T -- on the transversal; and W -- on the binormal.

Let us rotate the coordinate axes Oxyz about the Oz axis so that the angle Ω disappears, that is, let us orient the Ox axes along the nodal line Ok. Then the system of equations (3.3) becomes /109

$$\left.\begin{aligned}\frac{dC_1'}{dt}&=C\sin i\frac{d\Omega}{dt};\\ \frac{dC_2'}{dt}&=-\frac{dC}{dt}\sin i-C\cos i\frac{di}{dt};\\ \frac{dC_3}{dt}&=\frac{dC}{dt}\cos i-C\sin i\frac{di}{dt}.\end{aligned}\right\}\qquad(3.4)$$

The stroke shows that the kinetic moment $\overline{C}$ is projected onto the rotated axes.

For the first equation, the projection of the moment of applied forces (on the Ok axis) will be Wr sin u (the moments of the forces S and T do not yield to projections, since these forces intersect the Ok axis). By setting Wr sin u equal to dC_1'/dt, under this theorem on the kinetic moment we get

$$\frac{dC_1'}{dt}=C\sin i\frac{d\Omega}{dt}=Wr\sin u.$$

But $C=\sqrt{\mu p}$ for both the unperturbed as well as perturbed motion, and therefore

$$\frac{d\Omega}{dt}=W\frac{r}{\sqrt{\mu p}}\frac{\sin u}{\sin i}.\qquad(3.5)$$

Further, by rotating the Oz and Oy axes about Ok by the angle i + 90° (the Oy axis will be directed toward the vector $\overline{C}$), we get for the last two equations (3.4)

$$\left.\begin{aligned}\frac{dC_2'}{dt}&=\frac{dC}{dt};\\ \frac{dC_3'}{dt}&=C\frac{di}{dt}.\end{aligned}\right\}\qquad(3.6)$$

The first of the equalities (3.6) shows that the derivative of the kinetic-moment projections $\overline{C}$ onto the axis colinear to the moment as such is equal in absolute value to the derivative in time of

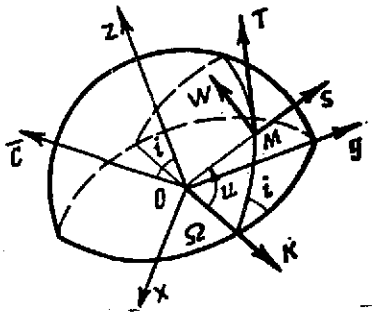

Fig. 3.1. For the derivatives of equations for osculating elements.

the modulus of this moment. By setting dC_2''/dt equal to the projection of the moment of the applied forces on the same axis, we get /110

$$\frac{dC_2^*}{dt}=\frac{dC}{dt}=\frac{\sqrt{\mu}}{2\sqrt{p}}\frac{dp}{dt}=rT.$$

The components W and S of the perturbing force, as we can easily see, do not yield moments on this axis. Hence, for dp/dt we have

$$\frac{dp}{dt}=2\sqrt{\frac{p}{\mu}}rT. \tag{3.7}$$

The second equality (3.6), considering that the projection of the moment of applied forces on the Oz' axis will be Wr cos u, enables us to obtain

or

$$\left.\begin{aligned} C\frac{di}{dt}&=Wr\cos u\\ \frac{di}{dt}&=\frac{r}{\sqrt{\mu p}}W\cos u. \end{aligned}\right\} \tag{3.8}$$

The orbital inclination i and the position of the node Ω, that is, the orientation of the orbital plane depend only on the lateral forces W, since the two other components T and S always lie in the plane of the osculating ellipse (see (3.5) and (3.8)).

Derivation of Equations for Orbital Elements e and ω

As was shown in Chapter I, the velocity components v in unperturbed elliptical motion are:

$$v_r=\dot{r}=\sqrt{\frac{\mu}{p}}e\sin\vartheta; \tag{3.9}$$

$$v_n=\sqrt{\frac{\mu}{p}}(1+e\cos\vartheta), \tag{3.10}$$

where v_r is the projection v onto the radius-vector of the orbit, and v_n is the projection of v onto the transversal.

For perturbed motion, Eqs. (3.9) and (3.10) are of the same form, but the elements p and e in this case apply to the osculating ellipse at the orbital point under consideration. By equating the transversal components v_n in the perturbed motion equal to $r \frac{d\sigma}{dt}$, where $d\sigma/dt$ is the angular rate of the radius-vector r [47], we get

$$v_n = r\frac{d\sigma}{dt} = \sqrt{\frac{\mu}{p}}(1+e\cos\vartheta). \tag{3.11}$$

We can show that the angular rate of the radius-vector r in perturbed motion consists of the two summands du/dt and $\cos i \frac{d\Omega}{dt}$. Actually, the component of angular velocity du/dt appears due to satellite motion in the orbital plane (osculating ellipse) without reference to the rotation of the plane itself. This second component $\cos i \frac{d\Omega}{dt}$ arises due to rotation of the actual orbital plane about the Earth's axis of rotation. These two motions then determine the angular translation of the satellite in absolute space per unit time. /111

Thus,

$$\frac{d\sigma}{dt} = \frac{du}{dt} + \cos i\frac{d\Omega}{dt} = \frac{d\omega}{dt} + \frac{d\vartheta}{dt} + \cos i\frac{d\Omega}{dt}, \tag{3.12}$$

since

$$u = \omega + \vartheta.$$

Multiplying (3.11) by $r = \frac{p}{1+e\cos\vartheta}$, we have

$$r^2\frac{d\sigma}{dt} = \sqrt{\mu p} = C, \tag{3.13}$$

that is, the modulus of the kinetic moment or twice the sectorial velocity is expressed in terms of the total angular velocity of the radius-vector r, and not in terms of $d\vartheta/dt$, as in unperturbed motion [23, 47].

By differentiating with respect to time the expression $r(1 + e\cos\vartheta) = p$, and also (3.9), we get

$$\dot{r}\frac{p}{r}+e\dot{r}\cos\vartheta-\dot{\vartheta}re\sin\vartheta=\dot{p}$$

or

$$e\sin\vartheta\sqrt{\frac{\mu}{p}}\frac{p}{r}+r\cos\vartheta\,\dot{e}-re\sin\vartheta\cdot\dot{\vartheta}=\dot{p} \qquad (3.14)$$

and

$$\ddot{r}=\dot{e}\sin\vartheta\sqrt{\frac{\mu}{p}}+e\cos\vartheta\sqrt{\frac{\mu}{p}}\dot{\vartheta}-\frac{e}{2}\sin\vartheta\sqrt{\frac{\mu}{p}}\frac{\dot{p}}{p}.$$

Since the equation of satellite motion in projections onto the radius-vector is of the form

$$\ddot{r}-r\dot{\sigma}^2=S-\frac{\mu}{r^2}, \qquad (3.15)$$

then after substitution of $\ddot{r}$ and $\dot{\sigma}$ we get

$$\dot{e}\sin\vartheta\sqrt{\frac{\mu}{p}}+e\cos\vartheta\sqrt{\frac{\mu}{p}}\dot{\vartheta}-e\sin\vartheta\sqrt{\frac{\mu}{p}}\frac{\dot{p}}{2p}-\frac{\mu p}{r^3}=S-\frac{\mu}{r^2}. \qquad (3.16)$$

Canceling out $\dot{\vartheta}$ from the two equations (3.14) and (3.16), we find /112

$$\sqrt{\frac{\mu}{p}}\dot{e}=S\sin\vartheta+2T\cos\vartheta+e\sin^2\vartheta\frac{r}{p}T+\frac{\mu p}{r^3}\sin\vartheta-e\frac{\mu}{r^2}\sin\vartheta\cos\vartheta-\frac{r}{r^2}\sin\vartheta,$$

or

$$\sqrt{\frac{\mu}{p}}\dot{e}=S\sin\vartheta+T\cos\vartheta+\frac{r}{p}T\cos\vartheta+e\frac{r}{p}T+T\cos\vartheta-\frac{r}{p}T\cos\vartheta-e\frac{r}{p}T\cos^2\vartheta+\frac{\mu p}{r^3}\sin\vartheta-e\frac{\mu}{r^2}\sin\vartheta\cos\vartheta-\frac{\mu}{r^2}\sin\vartheta=S\sin\vartheta+T\cos\vartheta+\frac{r}{p}T\cos\vartheta+e\frac{r}{p}T.$$

Finally, we have

$$\frac{de}{dt}=\sqrt{\frac{p}{\mu}}\left[S\sin\vartheta+\left(1+\frac{r}{p}\right)T\cos\vartheta+e\frac{r}{p}T\right]. \qquad (3.17)$$

To determine the value of $\dot{\vartheta}$, let us substitute this expression for de/dt into Eq. (3.14)

$$e\sin\vartheta\sqrt{\frac{\mu}{p}}\frac{p}{r}+r\cos\vartheta\sqrt{\frac{p}{\mu}}\times$$
$$\times\left[S\sin\vartheta+\left(1+\frac{r}{p}\right)T\cos\vartheta+e\frac{r}{p}T\right]-re\sin\vartheta\dot{\vartheta}=\dot{p}.$$

Further, using (3.7), after transformation we get

$$\sqrt{\frac{\mu}{p}}\frac{p}{r^2}+\frac{\cos\vartheta}{e}\sqrt{\frac{p}{\mu}}S+\left(1+\frac{r}{p}\right)\sqrt{\frac{p}{\mu}}\frac{1-\sin^2\vartheta}{e\sin\vartheta}T+$$
$$+\frac{\cos\vartheta}{\sin\vartheta}\sqrt{\frac{p}{\mu}}\frac{r}{p}T-\dot{\vartheta}=2\sqrt{\frac{p}{\mu}}\frac{T}{e\sin\vartheta},$$

whence

$$\dot{\vartheta}=\frac{\sqrt{\mu p}}{r^2}+\sqrt{\frac{p}{\mu}}\left[\frac{S\cos\vartheta}{e}-\left(1+\frac{r}{p}\right)\frac{T\sin\vartheta}{e}+\right.$$
$$\left.+\left(1+\frac{r}{p}\right)\frac{T}{e\sin\vartheta}+\frac{\cos\vartheta}{\sin\vartheta}\frac{r}{p}T-\frac{2T}{e\sin\vartheta}\right].$$

The last two terms in total are equal to zero. Therefore

$$\dot{\vartheta}=\frac{\sqrt{\mu p}}{r^2}+\sqrt{\frac{p}{\mu}}\left[\frac{S\cos\vartheta}{e}-\left(1+\frac{r}{p}\right)\frac{\sin\vartheta}{e}T\right]. \qquad (3.18)$$

Using (3.5), (3.12) and (3.18) for dω/dt (angular velocity of rotation of the perigee), we get /113

$$\frac{d\omega}{dt}=\sqrt{\frac{p}{\mu}}\left[-\frac{S\cos\vartheta}{e}+\left(1+\frac{r}{p}\right)\frac{\sin\vartheta}{e}T-W\frac{r}{p}\operatorname{ctg}i\sin u\right]. \qquad (3.19)$$

For small eccentricities e, Eqs. (3.17) and (3.19) are best replaced by the following:

$$\frac{d\lambda_1}{dt}=\sqrt{\frac{p}{\mu}}\left[-S\cos u+T\left(1+\frac{r}{p}\right)\sin u+\right.$$
$$\left.+\frac{r}{p}(T\lambda_1-W\lambda_2\operatorname{ctg}i\sin u)\right]; \qquad (3.20)$$

$$\frac{d\lambda_2}{dt}=\sqrt{\frac{p}{\mu}}\left[S\sin u+T\left(1+\frac{r}{p}\right)\cos u+\right.$$
$$\left.+\frac{r}{p}(T\lambda_2+W\lambda_1\operatorname{ctg}i\sin u)\right], \qquad (3.21)$$

where

$$\lambda_1 = e\sin\omega;\ \lambda_2 = e\cos\omega;\ e = \sqrt{\lambda_1^2+\lambda_2^2};\ \operatorname{tg}\omega = \frac{\lambda_1}{\lambda_2}.$$

Eqs. (3.20) and (3.21) can be easily derived by differentiating the expressions for λ_1 and λ_2 and by substituting the derivatives de/dt and dω/dt from (e.17) and (3.19). These equations can be used for calculating orbits (including circular) with any eccentricities.

It remains to find the last, sixth, equation determining the satellite flight time. Usually this is the equation for τ -- the time of transit through the perigee of the osculating ellipse. However, there is not need for it. It can be replaced by the equation setup for du/dt on the basis of (3.12) and (3.13). By excluding the principal motion, instead of u we can have the slow-varying deviation of the perturbed u from its unperturbed value. The main advantage of the osculating elements -- their small variability -- is retained. Let us write out this equation:

$$\frac{d\bar{u}}{dt} = \frac{d\sigma}{dt} - \cos i\frac{d\Omega}{dt} - \frac{d(u)}{dt}, \tag{3.22}$$

or

$$\frac{d\bar{u}}{dt} = \frac{\sqrt{\mu p}}{r^2}\left(1 - \frac{r^2}{(r)^2}\sqrt{\frac{(p)}{p}}\right) - \frac{r}{\sqrt{\mu p}}W\operatorname{ctg} i\sin u. \tag{3.23}$$

Here (u) is the unperturbed value of u; $\bar{u} = u - (u)$. Similarly, (r) and (p) are the unperturbed values of parameter p and the satellite radius-vector r.

Since in orbital calculation procedure the equation for τ is encountered quite frequently, we present it without derivation [20]: /114

$$\frac{d\tau}{dt} = \frac{r^2}{e\mu}\left[-(\cos\vartheta - e\sin\vartheta N)S + \frac{p}{r}NT\right], \tag{3.24}$$

where

$$N = 2\frac{p^2}{r^2}\int_0^{\vartheta}\frac{\cos\vartheta d\vartheta}{(1+e\cos\vartheta)^3}.$$

The true anomaly ϑ and the time t are associated by the equation

$$t - \tau = \frac{p^{3/2}}{\sqrt{\mu}}\int_0^{\vartheta}\frac{d\vartheta}{(1+e\cos\vartheta)^2}.$$

The system of six equations (3.5), (3.7), (3.8), (3.17), (3.19) and (3.23) or (3.24) is a closed first-order system in six unknown functions $\Omega(t)$, $p(t)$, $i(t)$, $e(t)$, $\omega(t)$, $\bar{u}(t)$ or $\tau(t)$. For each moment of time these functions make it possible to determine the coordinates and the satellite velocity components based on the formulas of unperturbed motion (see Chapter I).

For convenience, let us write all six equations in osculating elements together:

$$\left.\begin{aligned}
&\frac{d\Omega}{dt}=W\frac{r}{\sqrt{\mu p}}\frac{\sin u}{\sin i};\\
&\frac{dp}{dt}=2\sqrt{\frac{p}{\mu}}rT;\\
&\frac{di}{dt}=\frac{r}{\sqrt{\mu p}}W\cos u;\\
&\frac{de}{dt}=\sqrt{\frac{p}{\mu}}\left[S\sin\vartheta+\left(1+\frac{r}{p}\right)T\cos\vartheta+e\frac{r}{p}T\right];\\
&\frac{d\omega}{dt}=\sqrt{\frac{p}{\mu}}\left[-\frac{1}{e}S\cos\vartheta+\frac{1}{e}\left(1+\frac{r}{p}\right)T\sin\vartheta-\right.\\
&\qquad\left.-\frac{r}{p}W\operatorname{ctg}i\sin u\right];\\
&\frac{d\bar{u}}{dt}=\frac{\sqrt{\mu p}}{r^2}\left(1-\frac{r^3}{\mu p}W\operatorname{ctg}i\sin u-\frac{r^2}{(r)^2}\sqrt{\frac{(p)}{p}}\right),
\end{aligned}\right\}\qquad(3.25)$$

where

$$u=\omega+\vartheta;\quad \bar{u}=u-(u).$$

For unperturbed motion, we have /115

$$(u)=(\omega)+(\vartheta);\quad (r)=\frac{(p)}{1+(e)\cos(\vartheta)};$$

$$\operatorname{tg}\frac{(\vartheta)}{2}=\sqrt{\frac{1+(e)}{1-(e)}}\operatorname{tg}\frac{(E)}{2};$$

$$(E)-(e)\sin(E)-(E_0)+(e)\sin(E_0)=\sqrt{\mu}(a)^{-3/2}(t-t_0),$$

where t_0 is the initial moment of time; and (E_0) is the initial eccentric anomaly (unperturbed) corresonding to t_0.

The system (3.25) of equations of motion in osculating elements is integrated for known initial (when $t=t_0$) values of the six orbital elements: Ω_0, p_0, i_0, e_0, ω_0, and $\bar{u}_0$.

This system enables us to obtain approximate formulas for Ω, p, i, ... corresponding to several kinds of perturbing forces.

First let us transform from the independent variable t to u or ϑ. Using the expression

$$\frac{du}{dt}=\frac{\sqrt{\mu p}}{\gamma r^2}, \quad \text{or} \quad \frac{dt}{du}=\gamma\frac{r^2}{\sqrt{\mu p}}, \tag{3.26}$$

which follows from (3.23) and where

$$\gamma=\frac{1}{1-\frac{r^3}{\mu p}W\operatorname{ctg} i\sin u},$$

it is easy to transform from Eqs. (3.25) to the following equations in the variable u [47]:

$$\left.\begin{aligned}
&\frac{d\Omega}{du}=W\frac{r^3\gamma}{\mu p}\frac{\sin u}{\sin i};\\
&\frac{dp}{du}=\frac{2\gamma}{\mu}r^3T;\\
&\frac{di}{du}=\frac{r^3\gamma}{\mu p}W\cos u;\\
&\frac{de}{du}=\frac{r^2\gamma}{\mu}\left[S\sin\vartheta+\left(1+\frac{r}{p}\right)T\cos\vartheta+e\frac{r}{p}T\right];\\
&\frac{d\omega}{du}=\frac{r^2\gamma}{\mu e}\left[-S\cos\vartheta+\left(1+\frac{r}{p}\right)T\sin\vartheta-e\frac{r}{p}W\operatorname{ctg} i\sin u\right];\\
&\frac{dt}{du}=1-\frac{r^2\gamma}{\sqrt{p}}\frac{\sqrt{(p)}}{(r)^2}.
\end{aligned}\right\} \tag{3.27}$$

To derive the equations in the variable ϑ that are convenient to use in studying air drag, we will start from Eqs. (3.12) and (3.13). The latter give us /116

$$\frac{d\vartheta}{dt}=\frac{\sqrt{\mu p}}{r^2}-\frac{d\omega}{dt}-\cos i\frac{d\Omega}{dt}=$$
$$=\frac{\sqrt{\mu p}}{r^2}\left(1-\frac{r^2}{\sqrt{\mu p}}\frac{d\omega}{dt}-\frac{r^2}{\sqrt{\mu p}}\cos i\frac{d\Omega}{dt}\right).$$

Using Eqs. (3.25), we get [47]

$$\frac{dt}{d\vartheta}=\frac{r^2\gamma_1}{\sqrt{\mu p}},$$

where

$$\gamma_1=\frac{1}{1+\frac{r^2}{\mu e}S\cos\vartheta-\frac{r^2}{\mu e}\left(1+\frac{r}{p}\right)T\sin\vartheta}.$$

Thus, equations in ϑ_1 have exactly the same form as (3.27), but the multiplier γ is replaced by γ_1.

3.2. Orbital Perturbations Caused by the Effect of Compression of the Terrestrial Ellipsoid

Additional gravitational masses situated in the plane of the equator and the consequence of the oblateness of the Earth, strongly affect satellite motion. These forces, like the attractive force of the Earth's central field, have a potential which (instead of the potential of the central field b_0/r) can be written by the following series:

$$V = \frac{b_0}{r} - \frac{b_2}{r^3} p_2(\sin\psi) + \frac{b_4}{r^5} p_4(\sin\psi) - \ldots . \tag{3.28}$$

where b_0, b_2 are constant coefficients
$p_2(\sin\psi)$, $p_4(\sin\psi)$ are Legendre polynomials, and
ψ is the geocentric latitute.

The series rapidly converges and it is in practice sufficient to delimit it to two, and at the maximum three expansion terms.

Many studies have dealt with the field of the terrestrial spheroid (or ellipsoid of revolution) represented by potential (3.28) and its effect on satellite motion. The studies [32, 82] reduce this problem to quadratures. Convenient approximate formulas permitting permitting qualitative analysis without resorting to a computer, and also quite accurately performing orbital calculations, were found possible to obtain by means of Eqs. (3.27), by using the classical methods of celestial mechanics. The accuracy of these formulas is only satisfactory not only for qualitative/117 analysis, but in many instances also in determining orbits from measurements.

If one considers that an Earth satellite is continuously acted on by poorly considered forces (anomalies, air drag, solar light pressure, and so on) and, in addition, the accuracy of the determination of orbits depends on measurement errors, the necessity of determining the boundary, on the one hand, of the suitability of approximate formulas becomes clear and on the other -- the utility of using exact theories (see Section 3.5).

Let us proceed to deriving the formulas for the osculating elements based on Eqs. (3.27). We will assume in the first

approximation that the osculating elements in the right-hand parts of these equations are constant. Here, the system breaks down into individual equations, which can be solved with quadratures:

$$
\begin{aligned}
&\delta\Omega = \Omega - (\Omega) = \int \frac{r^3\gamma}{\mu p} W \frac{\sin u}{\sin i}\, du;\\
&\delta p = p - (p) = \int \frac{2\gamma}{\mu} r^3 T\, du;\\
&\delta i = i - (i) = \int \frac{r^3\gamma}{\mu p} W \cos u\, du;\\
&\delta e = e - (e) = \int \frac{r^2\gamma}{\mu}\left[S\sin\vartheta + \left(1+\frac{r}{p}\right)T\cos\vartheta + e\frac{r}{p}T\right] du;\\
&\delta\omega = \omega - (\omega) = \int \frac{r^2\gamma}{\mu e}\left[-S\cos\vartheta + \left(1+\frac{r}{p}\right)T\sin\vartheta - e\frac{r}{p}W\operatorname{ctg} i\sin u\right] du;\\
&\delta\bar{u} = \bar{u} - (\bar{u}_0) = \int \left(1 - \frac{r^2\gamma}{\sqrt{p}}\frac{\sqrt{(p)}}{(r)^2}\right) du.
\end{aligned}
\qquad (3.29)
$$

Here (Ω), (p), (i), (e) and (ω) are the unperturbed orbital elements, defined as follows

$$
(\Omega) = \Omega_0 - \int_0 W \frac{r^3\gamma \sin u}{\mu p \sin i}\, du = \Omega_0 + \frac{\varepsilon\cos i}{\mu p^2}\left\{u_0 - \frac{1}{2}\sin 2u_0 + e\left[\sin(u_0-\omega) - \frac{1}{2}\sin(u_0+\omega) - \frac{1}{6}\sin(3u_0-\omega)\right]\right\} \text{ and so on;}
$$

Ω_0, p_0, ..., ω_0 are the initial values of the elements.

To obtain the unperturbed elements, it is useful to employ iterations.

The method of solving Eqs. (3.29) presupposes that after we have obtained the first approximation we proceed to the next approximation, that is, we substitute the first-approximation results into the initial equations and integrate again, and so on. /118 Here we will limit ourselves only to the first approximation.

Preliminarily, we represent the potential V of the terrestrial spheroid as

$$
V = \frac{\mu}{r} - \frac{\varepsilon}{r^3}\left(\sin^2\psi - \frac{1}{3}\right), \qquad (3.30)
$$

and by discarding in Eq. (3.28) the term containing $p_4(\sin\psi)$, by replacing $p_2(\sin\psi)$ by its value

$$p_2(\sin\psi)=\frac{1}{2}(3\sin^2\psi-1)$$

and by assuming

$$b_0=\mu;\ \varepsilon=\frac{3}{2}b_2.$$

The first term in the expression for V is the potential of the central field. In the second term, that allows for the effect of the noncentrality of the gravitational field, the coefficient ε, in accordance with the theory of Earth's figure is of the form [47]

$$\varepsilon=\mu\bar{a}^2\left(\alpha-\frac{m}{2}\right),$$

where $\bar{a}$ is the radius of the equator
α is the compression of the Earth
$m = \dfrac{\Omega_E^2\bar{a}}{g_e}$
($\Omega_E^2\bar{a}$ is the centrifugal force at the equator; g_e is the gravitational force at the equator); and
$\alpha - \dfrac{m}{2} = 0.001633$.

The term discarded in (3.28) is of the order of $\alpha - \frac{m}{2}$. Compared with the second term, it does not yield accelerations greater than 0.05 mm/sec^2, which is smaller than the effect of the anomalies in the gravitational force (see Section 3.3). When necessary, this term can be allowed for together with the anomalies. By replacing $\sin\psi$ in (3.30) by the formula

$$\sin\psi=\sin i\sin u, \tag{3.31}$$

(from the spherical triangle, see Fig. 3.1) and by singling out the perturbing potential V', we get

$$V'=-\frac{\varepsilon}{r^3}\left(\sin^2 i\sin^2 u-\frac{1}{3}\right). \tag{3.32}$$

Hence, for the components of the force brought about by the oblateness of the Earth S_1, T_1, and W_1, we have

$$\left.\begin{aligned} S_1 &= \frac{\varepsilon}{r^4}(3\sin^2 i \sin^2 u - 1);\\ T_1 &= -\frac{\varepsilon}{r^4}\sin^2 i \sin 2u;\\ W_1 &= -\frac{\varepsilon}{r^4}\sin 2i \sin u. \end{aligned}\right\} \qquad (3.33)$$

In this case, the multiplier γ in (3.26) becomes

$$\gamma = \left(1 - \frac{r^3}{\mu p}\operatorname{ctg} i \sin u W\right)^{-1} = \left(1 + \frac{2\varepsilon}{\mu p r}\cos^2 i \sin^2 u\right)^{-1}. \qquad (3.34)$$

For any orbits, this multiplier never deviates from unity by more than ≈ 0.003. Errors of the same order can originate due to averaging of the values of the osculating elements p, e, ..., τ. Therefore, it is not meaningful to complicate the problem by allowing for γ, in spite of the fact that in the first approximation this multiplier is not difficult to allow for. We will assume $\gamma = 1$, with the exception of the formula for calculating the flight time (see text p. 127 [translation page 127]).

Perturbations of Longitude of Node Ω

We have for the position of the orbital node, that is, for Ω,

$$\delta\Omega = \int \frac{r^3 \sin u}{\mu p \sin i}\left(-\frac{\varepsilon}{r^4}\sin 2i \sin u\right) du =$$

$$= -\frac{2\varepsilon \cos i}{\mu p^2}\int (1 + e\cos\vartheta)\sin^2 u\, du = -\frac{2\varepsilon\cos i}{\mu p^2}\times$$

$$\times \int \left\{\sin^2 u + \frac{e}{4}[\cos(u-\omega) - \cos(u+\omega) + \cos\vartheta - \cos(2u+\vartheta)]\right\} du =$$

$$= -\frac{\varepsilon\cos i}{\mu p^2}\int \left\{2\sin^2 u + \frac{e}{2}[2\cos(u-\omega) - \cos(u+\omega) - \cos(3u-\omega)]\right\} du.$$

Integrating this expression for any u, we get

$$\left.\begin{aligned} \delta\Omega &= -\frac{\varepsilon\cos i}{\mu p^2}\left\{u - \frac{1}{2}\sin 2u + e\left[\sin(u-\omega) - \right.\right.\\ &\left.\left. - \frac{1}{2}\sin(u+\omega) - \frac{1}{6}\sin(3u-\omega)\right]\right\};\\ \Omega &= (\Omega) + \delta\Omega. \end{aligned}\right\} \qquad (3.35)$$

After integrating within the limits u_0 to $u_0 + 2\pi$, Eq. (3.35) /120 becomes

$$\delta\Omega_{2\pi} = -\frac{2\pi\varepsilon}{\mu p^2}\cos i, \qquad (3.36)$$

that is, the node in the first approximation experiences secular perturbations proportional to the cosine of the angle of accumulation and inversely proportional to the square of the orbital parameter.

For direct satellites with $i < 90°$, the node travels in the direction inverse to the increase in Ω (westerly), while for reverse satellites ($i > 90°$) -- toward the side of increasing Ω (easterly). This motion -- rotation of the orbital plane about the axis of rotation of the Earth -- is called the precession of the orbital node. The precession attains appreciable values. For example, for a Vostok type satellite the diurnal precession is $-4°$.

Perturbations of Orbital Parameter p

For the orbital parameter p we have

$$\delta p = \int \frac{2r^3}{\mu} T du = \frac{2}{\mu} \int r^3 \left(-\frac{\varepsilon}{r^4} \sin^2 i \sin 2u \right) du =$$

$$= -\frac{2\varepsilon \sin^2 i}{\mu p} \int (1 + e\cos\vartheta) \sin 2u du = -\frac{2\varepsilon \sin^2 i}{\mu p} \times$$

$$\times \int \left\{ \sin 2u + \frac{e}{2} [\sin(2u - \vartheta) + \sin(2u + \vartheta)] \right\} du =$$

$$= -\frac{2\varepsilon \sin^2 i}{\mu p} \left\{ -\frac{1}{2} \cos 2u - \frac{e}{2} \left[\cos(u + \omega) + \frac{1}{3} \cos(3u - \omega) \right] \right\}.$$

Finally,

$$\delta p = \frac{\varepsilon \sin^2 i}{\mu p} \left\{ \cos 2u + e \left[\cos(u + \omega) + \frac{1}{3} \cos(3u - \omega) \right] \right\}; \qquad (3.37)$$

$$p = (p) + \delta p.$$

As we can see from the formula, the orbital parameter in the first approximation does not have secular perturbations. Over a single rotation around the Earth (to the accuracy of the eccentricity it experiences two complete fluctuations with amplitude $A_p = \frac{\varepsilon \sin^2 i}{\mu p}$.

The amplitude is equal to zero for the equatorial orbits (p_{eq} = const) and has a maximum for the polar orbits $A_{p\,max} = \frac{\varepsilon}{\mu p}$. Since ε/μ = 66,432.78 and $p_{min} \approx$ 6550 km, the maximum amplitude for all orbits $A_{p\,max} < 10$ km.

We have

$$\delta i = \int \frac{r^3}{\mu p} \cos u W du = \int \frac{r^3}{\mu p} \cos u \left(-\frac{\varepsilon}{r^4} \sin 2i \sin u \right) du =$$
$$= -\frac{\varepsilon \sin 2i}{2\mu p^2} \int (1 + e\cos\vartheta) \sin 2u du =$$
$$= -\frac{\varepsilon \sin 2i}{2\mu p^2} \int \left\{ \sin 2u + \frac{e}{2} [\sin(u+\omega) + \sin(3u-\omega)] \right\} du =$$
$$= \frac{\varepsilon \sin 2i}{2\mu p^2} \left\{ \frac{1}{2} \cos 2u + \frac{e}{2} \left[\cos(u+\omega) + \frac{1}{3} \cos(3u-\omega) \right] \right\}$$

or

$$\delta i = \frac{\varepsilon \sin 2i}{4\mu p^2} \left\{ \cos 2u + e \left[\cos(u+\omega) + \frac{1}{3} \cos(3u-\omega) \right] \right\}, \qquad (3.38)$$
$$i = (i) + \delta i.$$

The inclination to the first approximation, like the orbital parameter p, does not have secular perturbations. In one revolution the parameter i, just like p, executes (with an accuracy to e) two complete oscillations with amplitude $A_i = \frac{\varepsilon \sin 2i}{4\mu p^2}$. The maximum amplitude attained when i = 45° or 135° is

$$|A_{i\,\max}| = \frac{\varepsilon}{4\mu p^2} \approx 0{,}0004,$$

which corresponds to the maximum deviation of the satellite in the lateral direction due to i:

$$0.004r = 0.0004 \cdot 6550 = 2.6 \text{ km}.$$

Perturbations of Eccentricity e

The most complex expressions are obtained for the eccentricity and argument of the perigee, but even they can be derived by using series expansions in e, which has to be done if we use the equations of osculating elements and independent variable t [61]:

$$\delta e = \int \frac{r^2}{\mu} \left[S \sin\vartheta + \left(1 + \frac{r}{p}\right) T \cos\vartheta + e \frac{r}{p} T \right] du =$$
$$= \int \frac{\varepsilon}{\mu r^2} \left\{ (3\sin^2 i \sin^2 u - 1) \sin\vartheta - \left(1 + \frac{r}{p}\right) \sin^2 i \sin 2u \cos\vartheta - \right.$$
$$\left. - e \frac{r}{p} \sin^2 i \sin 2u \right\} du = \frac{\varepsilon}{\mu p^2} \int \left\{ (1 + e\cos\vartheta)^2 \times \right.$$

$$\times(3\sin^2 i\sin^2 u-1)\sin\vartheta-(1+e\cos\vartheta)^2\sin^2 i\sin 2u\times$$
$$\times\cos\vartheta-(1+e\cos\vartheta)\sin^2 i\sin 2u\cos\vartheta-$$
$$-e(1+e\cos\vartheta)\sin^2 i\sin 2u\}\,du=$$
$$=\frac{\epsilon}{\mu p^2}\int\Big\{(1+e\cos\vartheta)^2[3\sin^2 i\sin^2 u\sin\vartheta-\sin\vartheta+$$
$$+\frac{3}{2}e\sin^2 i\sin^2 u\sin 2\vartheta-e\sin\vartheta\cos\vartheta-2\sin^2 i\sin 2u\cos\vartheta-$$
$$-e\sin^2 i\sin 2u\cos^2\vartheta-e\sin^2 i\sin 2u]\Big\}\,du.$$

After simple transformations similar to those used in deriving the formulas for Ω, p, and i, we get

$$\delta e=\frac{\epsilon}{\mu p^2}\{D_1\cos(u-\omega)+D_2\cos(u+\omega)+D_3\cos(3u-\omega)+$$
$$+e[D_4\cos 2u+D_5\cos 2(u-\omega)+D_6\cos(4u-2\omega)]+$$
$$+e^2[D_7\cos 3(u-\omega)+D_8\cos(u-3\omega)+D_9\cos(5u-3\omega)]\},\qquad(3.39)$$

where

$$D_1=-\left(1+\frac{e^2}{4}\right)\left(\frac{3}{2}\sin^2 i-1\right);\quad D_5=-\frac{1}{2}\left(\frac{3}{2}\sin^2 i-1\right);$$
$$D_2=\frac{1}{4}\left(1+\frac{11}{4}e^2\right)\sin^2 i;\qquad D_6=\frac{3}{8}\sin^2 i;$$
$$D_3=\frac{1}{12}\left(7+\frac{17}{4}e^2\right)\sin^2 i;\qquad D_7=-\frac{1}{12}\left(\frac{3}{2}\sin^2 i-1\right);$$
$$D_4=\frac{5}{4}\sin^2 i;\qquad D_8=\frac{1}{16}\sin^2 i;$$
$$e=(e)+\delta e.$$

Eq. (3.39) shows that eccentricity has no secular perturbations in the first approximation. The periodic fluctuations (with accuracy to e) occur with a period equal to the period of satellite rotation around the Earth (two harmonics), and with a period that is three times smaller. The oscillatory process for e is determined mainly by the sum of these harmonics.

The amplitude of the oscillations -- of the order α - m/2 -- in fact depends on i and ω.

The smaller the eccentricity, the more it fluctuates, relatively. When e is of the order 0.001633, variations in eccentricity during a single revolution can reach 100%.

To calculate the perturbations of the semi-axis δa, we can use the formula

$$\delta a = \frac{(p) + \delta p}{1 - ((e) + \delta e)^2} - (a).$$

Perturbations of Argument of Perigee ω /123

For the argument of the perigee ω we have

$$\delta\omega = \int \frac{r^2}{\mu e}\left[-S\cos\vartheta + \left(1+\frac{r}{p}\right)T\sin\vartheta - \frac{er}{p}\operatorname{ctg} i\sin uW\right]du =$$
$$= \int \frac{\varepsilon}{r^2\mu e}\left[-\cos\vartheta(3\sin^2 i\sin^2 u - 1) - \sin\vartheta\left(1+\frac{r}{p}\right)\sin^2 i\sin 2u + \right.$$
$$\left. + e\frac{r}{p}\operatorname{ctg} i\sin^2 u\sin 2i\right]du = \frac{\varepsilon}{\mu p^2 e}\int[\cos\vartheta + 2e\cos^2\vartheta + e^2\cos^3\vartheta -$$
$$- 3\sin^2 i\sin^2 u\cos\vartheta - 6e\sin^2 i\sin^2 u\cos^2\vartheta - 3e^2\sin^2 i\sin^2 u\cos^3\vartheta -$$
$$- 2\sin^2 i\sin 2u\sin\vartheta - 3e\sin^2 i\cos\vartheta\sin\vartheta\sin 2u - e^2\sin^2 i \times$$
$$\times\sin\vartheta\cos^2\vartheta\sin 2u + 2e\cos^2 i\sin^2 u + 2e^2\cos^2 i\cos\vartheta\sin^2 u]du.$$

Replacing, as in the preceding cases, the products of the trignometric functions by sums, after integration, we get

$$\delta\omega = \frac{\varepsilon}{\mu p^2}\left\{S_0 u + \frac{1}{e}[S_1\sin(u-\omega) + S_2\sin(u+\omega) + S_3\sin(3u-\omega)] - \right.$$
$$+ \left(D_4 - \frac{1}{2}\right)\sin 2u + D_5\sin 2(u-\omega) + D_6\sin(4u-2\omega) +$$
$$\left. + e[D_7\sin 3(u-\omega) + D_8\sin(u-3\omega) + D_9\sin(5u-3\omega)]\right\}, \qquad (3.40)$$

where

$$S_0 = 2 - \frac{5}{2}\sin^2 i;$$
$$S_1 = 1 + \frac{7}{4}e^2 - \left(\frac{3}{2} + \frac{17}{8}e^2\right)\sin^2 i;$$
$$S_2 = -\frac{1}{4}\left(1 - \frac{15}{4}e^2\right)\sin^2 i - \frac{1}{2}e^2;$$
$$S_3 = \frac{1}{12}\left(7 + \frac{19}{4}e^2\right)\sin^2 i - \frac{1}{6}e^2.$$

When u is varied by 2π, $\delta\omega$ becomes

$$\delta\omega_{2\pi} = \frac{2\pi\varepsilon}{\mu p^2}\left(2 - \frac{5}{2}\sin^2 i\right), \qquad (3.41)$$

that is, to the first approximation the perigee has, under the effect of the terrestrial compression, a secular drift calculated by

Eq. (3.41). The main periodic terms of the perigee argument fluctuate just as the periodic terms of the eccentricity, but with a phase shift of 90°.

When e = 0, Eq. (3.40) becomes unsuitable, which is to be expected since the actual concept of the perigee argument is associated with the presence of eccentricity. /124

Thus, formulas have been obtained for the elements of the elliptical orbits p, e, ω, Ω, and i as a function of the argument of the latitude u. For a given u and the orbit element corresponding to it calculated based on these formulas, we can compute the rectangular coordinates x, y, and z and the velocities $\dot{x}$, $\dot{y}$ and $\dot{z}$ (see Chapter I). Here the error in coordinates must not exceed several tens of meters.

Using the equations for λ_1 and λ_2, we can readily obtain formulas suitable for near-circular orbits ($k = \sin^2 i$):

$$\delta\lambda_1 = \frac{e}{\mu p^2}\left\{\left[1-\frac{7}{4}k+\lambda_1^2\left(\frac{1}{4}-\frac{9}{8}k\right)+\lambda_2^2\left(\frac{5}{4}-\frac{9}{8}k\right)\right]\sin u+\right.$$
$$+\left[\frac{7}{12}k+\lambda_1^2\left(-\frac{1}{12}+\frac{23}{48}k\right)+\lambda_2^2\left(-\frac{1}{12}+\frac{13}{48}k\right)\right]\sin 3u+$$
$$+\lambda_1\left[\left(-\frac{1}{2}+2k\right)\cos 2u-\frac{3}{8}k\cos 4u\right]+\lambda_2\left[\left(2-\frac{5}{2}k\right)u+\right.$$
$$\left.+\frac{1}{2}k\sin 2u+\frac{3}{8}k\sin 4u\right]+\frac{1}{16}k(\lambda_2^2-\lambda_1^2)\sin 5u+$$
$$\left.+\lambda_1\lambda_2\left[\left(-2+\frac{13}{4}k\right)\cos u+\frac{5}{24}k\cos 3u-\frac{1}{8}k\cos 5u\right]\right\}.$$

$$\delta\lambda_2 = \frac{e}{\mu p^2}\left\{\left[1-\frac{5}{4}k+\lambda_1^2\left(\frac{9}{4}-\frac{25}{8}k\right)+\lambda_2^2\left(\frac{1}{4}+\frac{3}{8}k\right)\right]\cos u+\right.$$
$$+\left[\frac{7}{12}k+\lambda_1^2\left(-\frac{1}{4}+\frac{25}{48}k\right)+\lambda_2^2\left(\frac{1}{12}+\frac{11}{48}k\right)\right]\cos 3u+$$
$$+\lambda_1\left[-\left(2-\frac{5}{2}k\right)u+(1-2k)\sin 2u+\frac{3}{8}k\sin 4u\right]+$$
$$+\lambda_2\left[\left(\frac{1}{2}+\frac{1}{2}k\right)\cos 2u+\frac{3}{8}k\cos 4u\right]+\frac{1}{16}k(\lambda_2^2-\lambda_1^2)\cos 5u+$$
$$\left.+\lambda_1\lambda_2\left[\left(\frac{1}{4}k-1\right)\sin u+\left(\frac{1}{3}-\frac{7}{24}k\right)\sin 3u+\frac{1}{8}k\sin 5u\right]\right\}.$$

The elements λ_1 and λ_2 can be calculated by the formula

$$\lambda_1 = (\lambda_1)+\delta\lambda_1;\ \lambda_2 = (\lambda_2)+\delta\lambda_2,$$

where (λ_1) and (λ_2) are their unperturbed values.

The perturbations in the remaining elements expressed in terms /125 of the elements λ_1 and λ_2 become

$$\delta\Omega = -\frac{\varepsilon\cos i}{\mu p^2}\left[u - \frac{1}{2}\sin 2u + \lambda_1\left(-\frac{3}{2}\cos u + \frac{1}{6}\cos 3u\right) + \right.$$
$$\left. + \lambda_2\left(\frac{1}{2}\sin u - \frac{1}{6}\sin 3u\right)\right];$$
$$\delta i = \frac{\varepsilon\sin 2i}{4\mu p^2}\left[\cos 2u + \lambda_1\left(-\sin u + \frac{1}{3}\sin 3u\right) + \right.$$
$$\left. + \lambda_2\left(\cos u + \frac{1}{3}\cos 3u\right)\right];$$
$$\delta p = \frac{\varepsilon k}{\mu p}\left[\cos 2u + \lambda_1\left(-\sin u + \frac{1}{3}\sin 3u\right) + \right.$$
$$\left. + \lambda_2\left(\cos u + \frac{1}{3}\cos 3u\right)\right].$$

In the case of circular orbits ($\lambda_1 = \lambda_2 = 0$), the formulas for the perturbations in the motion parameters are considerably simplified:

$$\delta\Omega_{ci} = -\frac{\varepsilon\cos i}{\mu r^2}\left(u - \frac{1}{2}\sin 2u\right);$$
$$\delta i_{ci} = \frac{\varepsilon\sin 2i}{4\mu r^2}\cos 2u;$$
$$\delta p_{ci} = \frac{\varepsilon\sin^2 i}{\mu r}\cos 2u;$$
$$\delta\lambda_1 = \frac{\varepsilon}{\mu r^2}\left[\left(1 - \frac{7}{4}\sin^2 i\right)\sin u + \frac{7}{12}\sin^2 i\sin 3u\right];$$
$$\delta\lambda_2 = \frac{\varepsilon}{\mu r^2}\left[\left(1 - \frac{5}{4}\sin^2 i\right)\cos u + \frac{7}{12}\sin^2 i\cos 3u\right].$$

Here r is the radius of the unperturbed circular orbit.

For converting to rectangular coordinates, let us use Eqs. (3.9) and (3.10), where

$$r = \frac{p}{1 + \lambda_1\sin u + \lambda_2\cos u};$$
$$v_r = \dot{r} = \sqrt{\frac{\mu}{p}}(\lambda_2\sin u - \lambda_1\cos u);$$
$$v_n = r\dot{\sigma} = \sqrt{\frac{\mu}{p}}(1 + \lambda_1\sin u + \lambda_2\cos u).$$

If the elements x, y, z, v_x, v_y, and v_z are given, then we have /126

$$\lambda_1 = \sqrt{\frac{p}{\mu}}\left[\left(v_n - \sqrt{\frac{\mu}{p}}\right)\sin u - v_r \cos u\right];$$

$$\lambda_2 = \sqrt{\frac{p}{\mu}}\left[\left(v_n - \sqrt{\frac{\mu}{p}}\right)\cos u + v_r \sin u\right];$$

$$v_r = \frac{1}{r}(xv_x + yv_y + zv_z);$$

$$v_n = \sqrt{v^2 - v_r^2};$$

$$\sin u = \frac{z}{r \sin i} = \frac{-x \sin \Omega + y \cos \Omega}{r \cos i};$$

$$\cos u = \frac{1}{r}(x \cos \Omega + y \sin \Omega);$$

$$\sin \Omega = \frac{C_1}{C \sin i};\quad \cos \Omega = -\frac{C_2}{C \sin i};\quad \cos i = \frac{C_3}{C};\quad p = \frac{C^2}{\mu},$$

where C_1, C_2, and C_3 are the projections of the kinetic moment $\overline{C}$ calculated from the assigned x, y, ..., z.

These formulas enable us to calculate from the known initial values of the orbital elements in the absolute rectangular coordinate system the osculating elements λ_{10}, λ_{20}, p_0, Ω_0 and i_0 need for calculating the perturbations caused by the compression of the terrestrial ellipsoid.

Perturbations of the Radius-Vector r and the Flight Altitude h

The radius-vector of a satellite is calculated by the formula

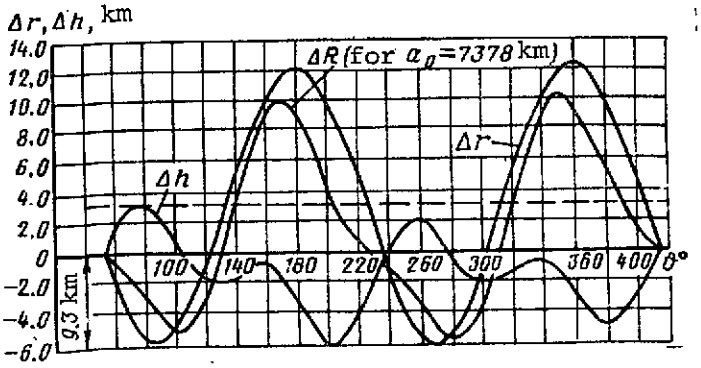

Fig. 3.2. Perturbation of radius-vector r and flight altitude h as functions of true anomaly.

$$r = \frac{p}{1 + e \cos(u - \omega)},$$

as for unperturbed motion, but p, e, and ω are calculated by Eq. (3.37), (3.39) and (3.40).

The flight altitude is

$$h = r - R,$$

where $R = \bar{a}(1 - \bar{\alpha}\sin^2 i \sin^2 u)$ is the Earth's radius.

The maximum error of the last formula is 40 m.

Fig. 3.2 presents, as an example, the results of calculating the perturbed values of r and h using the first-approximation formulas. The radius-vector r fluctuates with greater amplitude than does the flight altitude h. The satellite as it were "follows" the Earth's surface, although it does not in fact attain total compensation. This makes it easier to set up simplified methods of calculating motion with reference to the air drag forces (see Section 3.5). /127

Calculation of Flight Time

To determine the flight time, let us use the differential equation that associates time t and the latitude argument u:

$$\frac{dt}{du}=\frac{r^2}{\sqrt{\mu p}\left(1-\frac{r^2}{\mu p}\operatorname{ctg} i\sin uW\right)}. \tag{3.42}$$

From Eq. (3.42) we get the time

$$t-t_0=\int_{u_0}^{u}\frac{r^2du}{\sqrt{\mu p}\left(1+\frac{2\varepsilon}{\mu pr}\cos^2 i\sin^2 u\right)}. \tag{3.43}$$

Here the acceleration component W is replaced by its value based on Eq. (3.33).

In the case of unperturbed motion $\varepsilon = 0$, p = const and e = = const, therefore for the flight time we get the familiar Kepler's equation

$$E-e\sin E-E_0+e\sin E_0=\sqrt{\mu}a^{-\frac{3}{2}}(t-t_0). \tag{3.44}$$

Differences in time t calculated by Eqs. (3.43) and (3.44) are of the order of $(\alpha - m/2)(t - t_0)$ and amount to several seconds per orbit.

For orbits with small eccentricities (but with $e \neq 0$), based on Eqs. (3.42) and (3.43) we can easily obtain the final formula for calculating time. Expanding Eqs. (3.42) in series in ω, p, e, and ε_1 $\left(\varepsilon_1 = \frac{2\varepsilon}{\mu pr}\cos^2 i\sin^2 u\right)$ and leaving only the linear terms, we get (by discarding the unperturbed part dt/du) /128

$$\frac{d\bar{t}}{du}=\frac{3r^2}{2p\sqrt{\mu p}}\Delta p-\frac{2r^3}{p\sqrt{\mu p}}\cos\vartheta\Delta e-\frac{2r^3e}{p\sqrt{\mu p}}\sin\vartheta\Delta\omega-$$
$$-\frac{2r\varepsilon}{(\mu p)^{3/2}}\cos^2 i\sin^2 u.$$

Replacing δp, δe, and $e\delta\omega$ by their values according to Eqs. (3.37), (3.39) and (3.40), we get

$$\frac{d\bar{l}}{du}=\frac{3r^2\varepsilon\sin^2 i}{2p(\mu p)^{3/2}}\left(\cos 2u+e\cos(u+\omega)+\frac{e}{3}\cos(3u-\omega)\right)-$$
$$-\frac{2r^3\varepsilon}{p^2(\mu p)^{3/2}}\cos\vartheta\left[D_1\cos\vartheta+D_2\cos(u+\omega)+D_3\cos(3u-\omega)+\right.$$
$$+eD_4\cos 2u+eD_5\cos 2\vartheta+eD_6\cos(4u-2\omega)]-$$
$$-\frac{2r^3\varepsilon}{p^2(\mu p)^{3/2}}\sin\vartheta\left[S_0ue+S_1\sin\vartheta+S_2\sin(u+\omega)+\right.$$
$$+S_3\sin(3u-\omega)+e\left(D_4-\frac{1}{2}\right)\sin 2u+eD_5\sin 2\vartheta+$$
$$\left.+eD_6\sin(4u-2\omega)\right]-\frac{2r\varepsilon}{(\mu p)^{3/2}}\cos^2 i\sin^2 u.$$

Here the terms containing e^2 are discarded. Considering that

$$r=\frac{p}{1+e\cos\vartheta}=p(1-e\cos\vartheta)+O(pe^2),$$

after integration we have

$$\overline{\delta l}=\frac{\varepsilon}{\mu\sqrt{\mu p}}\left|(1-4\cos^2 i)u+\left(\frac{1}{2}-\frac{7}{12}k\right)\sin 2u+\right.$$
$$+e\left[\frac{1}{8}k\sin(u+\omega)+\left(\frac{5}{12}k-\frac{1}{2}\right)\sin(3u-\omega)+\right.$$
$$+\left(2-\frac{7}{2}k+\frac{3}{4}\cos 2\omega\right)\sin\vartheta-(1-5\cos^2 i)u\cos\vartheta-$$
$$\left.\left.-\frac{3}{8}k\sin(u-3\omega)\right]\right|_{u_0}^{u}. \qquad (3.45)$$

For large e (without series expansion in e) we can also obtain a working formula if Eq. (3.43) is represented as follows: /129

$$t-t_0=\int_{u_0}^{u}\frac{r^2du}{\sqrt{\mu p}\left(1+\frac{2\varepsilon}{\mu pr}\cos^2 i\sin^2 u\right)}=$$

$$=\int_{u_0}^{u}F(u)du=\int_{u_0}^{u}\left[F_0+\left(\frac{\partial F}{\partial p}\right)_0\Delta p+\left(\frac{\partial F}{\partial e}\right)_0\Delta e+\right.$$

$$\left.+\left(\frac{\partial F}{\partial \omega}\right)_0\Delta\omega+\left(\frac{\partial F}{\partial \varepsilon_1}\right)_0\varepsilon_1+O\left(T\left(\alpha-\frac{m}{2}\right)^2\right)\right]du, \qquad (3.45')$$

where

$$F_0=\frac{p^2}{\sqrt{\mu p}\,[1+e\cos(u-\omega)]^2}=\left(\frac{\partial F}{\partial \varepsilon_1}\right)_0;$$

$$\left(\frac{\partial F}{\partial p}\right)_0=\frac{3\sqrt{p}}{2\sqrt{\mu}\,[1+e\cos(u-\omega)]^2};$$

$$\left(\frac{\partial F}{\partial e}\right)_0=1-\frac{2p\sqrt{p}\cos(u-\omega)}{\sqrt{\mu}\,[1+e\cos(u-\omega)]^3};$$

$$\left(\frac{\partial F'}{\partial \omega}\right)_0=1-\frac{2p\sqrt{p}\,e\sin(u-\omega)}{\sqrt{\mu}\,[1+e\cos(u-\omega)]^3};$$

$$\varepsilon_1=-\frac{2\varepsilon}{\mu pr}\cos^2 i\sin^2 u.$$

We will take the orbital elements p, e, and ω as unperturbed values, that is, (p), (e), and (ω), which gives us the highest accuracy.

By replacing in Eq. (3.45') the quantities Δp, Δe and Δω from (3.37), (3.39) and (3.40), respectively, after integration we have

$$\overline{\delta t}=\frac{2\varepsilon}{\mu\sqrt{\mu p}}\left|(1-e)^{-\frac{5}{2}}\left[-\left(D_5+\frac{3}{2}D_6e^2+\frac{9}{16}ke^2\cos 2\omega\right)E+\right.\right.$$

$$+(S_4+S_5\cos 2\omega)\sin E+(S_6+S_7\cos 2\omega)\sin 2E]+$$

$$\left.+(1-e^2)^{-2}\left[-\frac{1}{2}S_0u+\frac{1}{4}\sin 2\omega\left(\frac{13}{12}k-1-\frac{k}{e^2}+\frac{2}{3e^2}\right)\right]\theta^2+\right.$$

$$\left.+\frac{k\sin 2\omega}{6e^2}\theta+\frac{1-k}{3e}\sin(u+\omega)\right|_{u_0}^{u}, \qquad (3.46)$$

where

$$S_4=-ke+\frac{1}{2}e+\frac{7}{6}e^3-\frac{3}{2}ke^3;$$

$$S_5=\frac{19}{24}ke^3-\frac{1}{2}e^3-\frac{3}{8}ke+\frac{2}{3}e-\frac{1}{3e}+\frac{k}{3e};$$

$$S_6=\left(\frac{5}{24}-\frac{3}{16}k-\frac{5}{12}e^2+\frac{1}{2}ke^2\right)e^2;$$

$$S_7=\frac{1}{2}\left(\frac{1}{6}-\frac{1}{4}k-\frac{1}{3}e^2+\frac{19}{48}ke^2+\frac{1}{6}e^4-\frac{1}{3}ke^4\right);$$

$$\theta=1-e\cos E.$$

/130

Applying Eqs. (3.45) and (3.46), with sufficient accuracy we can calculate the flight time in an orbit with any eccentricity e if the angle u or E is given, and conversely, we can find these angles for known time by interpolation, using the Keplerian orbit in the first approximation.

In Eqs. (3.45) and (3.46) the additional time which the satellite spends in flight from the equator (when $u_0 = 0$) to the point of orbit with latitude argument u is calculated, compared to the time of flight in an unperturbed orbit. The total flight time will be

$$t = \bar{t} + \delta t, \tag{3.47}$$

where $\bar{t}$ is the flight time in the unperturbed orbit.

If we set $u = 2\pi$ in Eq. (3.46), the additional flight time in an orbit (secular term) will be

$$\delta\bar{T} = \frac{2\pi\varepsilon}{\mu\sqrt{\mu a}(1-e^2)^{5/2}}\left[\left(1+\frac{3}{2}e^2\right)\left(\frac{3}{2}\sin^2 i - 1\right) - \frac{9}{8}e^2\sin^2 i\cos 2\omega + \right.$$
$$\left. + (1-e^2)^{1/2}\left(\frac{5}{2}\sin^2 i - 2\right)(1-e\cos E_0)^2\right], \tag{3.48}$$

where E_0 is the eccentric anomaly corresponding to u_0;

$$E_0 = 2\operatorname{arctg}\sqrt{\frac{1-e}{1+e}}\operatorname{tg}\frac{1}{2}(u_0-\omega).$$

The accuracy of Eq. (3.45) is of the order of e^2. Since $\delta\bar{t}$ is several seconds, the error can reach hundredths of a second if $e < 0.1$. By substituting $u = 2\pi$ into Eq. (3.45), we can single out the corresponding secular term

$$\delta\bar{T} = \frac{2\pi\varepsilon}{\mu\sqrt{\mu p}}\left[-(4\cos^2 i - 1) + e(5\cos^2 i - 1)\cos(u_0 - \omega)\right]. \tag{3.48'}$$

The quantity $\delta\bar{T}$ obtained by Eq. (3.46) or (3.45) is the difference between the draconic period of satellite rotation and the period of revolution in the unperturbed orbit. The flight time of the /131
the satellites from equator to equator (one revolution) is called the draconic period T_d

$$T_d = \bar{T} + \delta\bar{T}, \tag{3.49}$$

where $\overline{T} = \frac{2\pi}{\sqrt{\mu}} (a)^{3/2}$ is the period for the unperturbed orbit, and $\delta\overline{T}$ can be calculated both by Eq. (3.48') for small e as well as by (3.48') for any eccentricities (when e > 0).

If we neglect the terms of the order of e in Eq. (3.48'), then by equating the term in the parentheses ($4\cos^2 i - 1$) to zero, we find the orbital inclination for which the draconic period is equal to the unperturbed orbit (the critical inclination):

$$4\cos^2 i - 1 = 0;$$
$$\cos i = \pm 0.5,$$

that is, the orbital inclination i = 60° and 120°.

For near-circular orbits with inclination less than 60° (or greater than 120°), the draconic period is less than the perturbed period calculated based on unperturbed elements determined above for orbits with inclinations in the range 120 > i > 60° and greater. The presence of the critical inclination is accounted for by the fact that the potential of the gravity field of the terrestrial ellipsoid is constructed as the sum of a series, the first term in which, being the central field, already includes the entire mass of the ellipsoid. The remaining terms are corrections that change sign as they pass through a specific latitude. Closer to the equator where large gravitational masses are concentrated, as follows from the expression for the potential, the force of attraction is greater and, therefore, the flight time is shorter. The closer to the poles, the less the attractive force and the longer the flight time. At some mean inclination, the overall action of the gravitational forces on the satellite become equal to the action of the spherical Earth with a mass equal to the mass of the terrestrial ellipsoid, and for a selected unperturbed orbit (mean with respect to the perturbed motion) the critical period sets in.

3.3. Perturbing Influence of Anomalies in Gravity on Satellite Orbit

In addition to the oblateness of the Earth, which determines basically the noncentrality of the gravity field, satellite motion is affected by gravitational anomalies. These forces are caused by the nonuniform distribution of the masses of different density in the Earth's crust and have their own potential. In addition to the potential of the normal gravity field which allows for the effect of the compression of the Earth, the potential of the gravitational anomalies represent the true potential of a geoid.

Due to the large nonuniformity in the distribution of masses, /132
the potential of the anomalies depends both on the geographical

latitude as well as on the longitude of the points on the Earth's surface. Usually it can be written together with the terms that allow for the compression of the Earth, as an expansion in spherical functions [29]:

$$T' = \gamma_m \sum_{n=2}^{\infty} \sum_{m=0}^{n} \left(\frac{R}{\rho}\right)^{n+1} (\alpha_{nm} \cos m\lambda + \beta_{nm} \sin m\lambda) p_{nm}(\sin \varphi), \qquad (3.50)$$

where
- ρ is the radius-vector of the point in space (from the Earth's center), for example, the point at which the satellite is at a given moment
- ϕ is latitude
- λ is longitude of the same point
- R is the mean Earth radius
- γ_m is the mean acceleration of gravity at the surface of the terrestrial ellipsoid
- α_{nm}, β_{nm} are constant numbers -- coefficients of the expansion and
- $p_{nm}(\sin\phi)$ are spherical functions.

If $m = 0$, $\sin m\lambda = 0$; $\cos m\lambda = 1$, and the harmonics thus obtained are called zonal harmonics. They do not depend on longitude. If $m \neq 0$, the harmonics depend on longitude and are called tesseral harmonics.

The effect of anomalies is small compared with the effect of the compression (α_{20}) of the Earth.

Deviations in coordinates due to anomalies are of the order of hundreds of meters, and deviations in velocity components due to anomalies -- of the order of hundredths of a meter, and at the maximum, tenths of a meter per second over a period of several orbits.

For the projections of forces caused by the effect of anomalies onto the orbital axes we can readily obtain

$$\left.\begin{aligned} T &= \Delta g_Q^{\rho} \cos\delta + \Delta g_Q^{\lambda} \sin\delta; \\ W &= -\Delta g_Q^{\lambda} \cos\delta + \Delta g_Q^{\varphi} \sin\delta; \\ S &= -\Delta g_Q. \end{aligned}\right\} \qquad (3.51)$$

where S, T, W are the components of the perturbing force caused by the anomalies (per unit mass)

Δg_ρ^ϕ, Δg_ρ^λ are the projections of the acceleration caused by anomalies in the direction of the meridian (toward the north ϕ) and in the direction of the parallel (toward the east λ) at a given point, and

Δg_ρ as above, toward the center of the Earth.

Differentiating the expressions for the potential t' in the directions ρ, ϕ, and λ, we have: /133

$$\left.\begin{aligned}
\Delta g_\varrho &= \frac{\gamma_m}{R}\sum_{n=2}^{\infty}(n+1)\left(\frac{R}{\varrho}\right)^{n+2}\sum_{m=0}^{n}\times \\
&\times(\alpha_{nm}\cos m\lambda+\beta_{nm}\sin m\lambda)\,p_{nm}\sin\varphi); \\
\Delta g_\varrho^\varphi &= \frac{\gamma_m}{R}\sum_{n=2}^{\infty}\left(\frac{R}{\varrho}\right)^{n+2}\sum_{m=0}^{n}\times \\
&\times(\alpha_{nm}\cos m\lambda+\beta_{nm}\sin m\lambda)\,p'_{nm}(\sin\varphi); \\
\Delta g_\varrho^\lambda &= \frac{\gamma_m}{R\cos\varphi}\sum_{n=2}^{\infty}\left(\frac{R}{\varrho}\right)^{n+2}\sum_{m=0}^{n}\times \\
&\times(-\alpha_{nm}\sin m\lambda+\beta_{nm}\cos m\lambda)\,m p_{nm}(\sin\varphi).
\end{aligned}\right\} \qquad (3.52)$$

Substituting the values of Δg_ρ, Δg_ρ^ϕ, and Δg_ρ^λ obtained to the equations of motion in the osculating elements, after integration of the system of perturbation of these elements we find Eq. (3.29).

The integration can be carried out by using the smallness of the perturbations, assuming the elements a, ..., i to be constant in the right-hand side.

Thus, the problem reduces to the following quadratures (see text page 117 [translation page 116]):

$$\left.\begin{aligned}
\Delta\Omega &= \Omega-\Omega_0=\int_0^t\frac{r}{\sqrt{\mu p}}\frac{\sin u}{\sin i}\left(-\Delta g_\varrho^\lambda\cos\delta+\Delta g_\varrho^\varphi\sin\delta\right)dt; \\
\Delta p &= p-p_0=2\int_{t_0}^{t}\sqrt{\frac{p}{\mu}}\,r\left(\Delta g_\varrho^\varphi\cos\delta+\Delta g_\varrho^\lambda\sin\delta\right)dt; \\
\Delta i &= i-i_0=\int_{t_0}^{t}\frac{r}{\sqrt{\mu p}}\cos u\left(-\Delta g_\varrho^\lambda\cos\delta+\Delta g_\varrho^\varphi\sin\delta\right)dt, \\
\Delta e &= e-e_0=\int_{t_0}^{t}\sqrt{\frac{p}{\mu}}\left\{-\sin\vartheta\,\Delta g_\varrho+\left[\cos\vartheta+\frac{r}{p}(\cos\vartheta+e)\right]\times\right. \\
&\left.\times\left(\Delta g_\varrho^\varphi\cos\delta+\Delta g_\varrho^\lambda\sin\delta\right)\right]dt;
\end{aligned}\right\} \qquad (3.53)$$

$$\Delta\omega=\omega-\omega_0=\int_{t_0}^{t}\sqrt{\frac{\overline{p}}{\mu}}\left[\frac{1}{e}\cos\vartheta\Delta g_Q+\frac{1}{e}\left(1+\frac{r}{p}\right)\times\right.$$

$$\times\sin\vartheta\left(\Delta g_Q^{\varphi}\cos\delta+\Delta g_Q^{\lambda}\sin\delta\right)-$$

$$\left.-\frac{r}{p}\operatorname{ctg} i\sin u\left(-\Delta g_Q^{\lambda}\cos\delta+\Delta g_Q^{\varphi}\sin\delta\right)\right]dt;$$

$$\Delta\overline{u}=\overline{u}-\overline{u}_0=\int_{t_0}^{t}\frac{\sqrt{\mu\overline{p}}}{r^2}\left[1-\frac{r^2}{(r)^2}\sqrt{\frac{(\overline{p})}{p}}-\right.$$

$$\left.-\frac{r^3}{\mu p}\operatorname{ctg} i\sin u\left(-\Delta g_Q^{\lambda}\cos\delta+\Delta g_Q^{\varphi}\sin\delta\right)\right]dt. \qquad (3.53)$$

/134

The solution can also be obtained by another method, be replacing dt with $\frac{r^2}{\sqrt{\mu p}}du$, that is, by converting to the variable u or ϑ. Next, the time is obtained by the quadrature

$$t=t_0+\int_{u_0}^{u}\frac{r^2\left[1+\frac{r^3}{\mu p}\operatorname{ctg} i\sin u\left(\Delta g_Q^{\lambda}\cos\delta-\Delta g_Q^{\varphi}\sin\delta\right)\right]^{-1}}{\sqrt{\mu p}}du.$$

The cosine and the sine of the azimuth δ of the orbit can be calculated by the formulas of spherical trignometry

$$\cos\delta=\sin i\frac{\cos u}{\cos\varphi};$$

$$\sin\delta=\frac{\cos i}{\cos\varphi}.$$

In computing the quadratures, all the osculating elements appearing under the sign of the integral can be assumed to be constant (when e > 0). The corresponding error in the quantity $\Delta\Omega$, Δi, ..., Δp, for eccentricity values that are not too small -- is of the order of a tenth of a percent. This accuracy is more than sufficient, since the reliability of the numerical values of most of the coefficients of the anomaly field α_{nm} and β_{nm} is of the order of 50%.

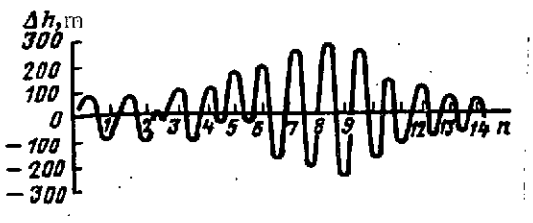

Fig. 3.3. Periodic fluctuations in altitude of AES flight Δh as a function of the number of its orbits.

For the approximate calculations, by making several extra assumptions, from Eq. (3.53) we can obtain the final formulas for $\Delta\Omega$, ..., Δp [78, 79, 80]. It is important to note that the anomalies produce both periodic and secular orbital perturbations. Also observed are long-periodic fluctuations in

orbital elements caused largely by the fact that the time of revolution of the Earth is not an exact multiple of the time of revolution of the satellite around it. The point is that the satellite imprecisely repeats its "diurnal track" relative to the field of anomalies and the Earth's surface.

The long-periodic fluctuations are very small and the main deviations in the coordinates and velocity occur within a day. The approximate trend of their variation with altitude is shown in Fig. 3.3. /135

By the end of the day the displacements Δh become nearly zero, and in subsequent days the fluctuations are approximately repeated. the displacements along the orbit can be accumulated. This accumulation can occur for actual orbits (if we do not consider air drag) also due to an imprecise knowledge of the coefficient μ that allows for the effect of the central field.

3.4. Perturbations Caused by the Influence of Moon and Sun

In the particular case considered in this study when the artificial satellite is close to the Earth, it proves possible to obtain a simple approximate solution quite suitable not only for quantitative analysis, but also for the solution of numerous practical problems.

Let us write out the equations of satellite motion in the following form:

$$\left.\begin{aligned} \ddot{x}+\frac{fM_0}{r^3}x&=\sum_{j=1}^{n-1}\frac{\partial R_j}{\partial x}=\frac{\partial R}{\partial x};\\ \ddot{y}+\frac{fM_0}{r^3}y&=\sum_{j=1}^{n-1}\frac{\partial R_j}{\partial y}=\frac{\partial R}{\partial y};\\ \ddot{z}+\frac{fM_0}{r^3}z&=\sum_{j=1}^{n-1}\frac{\partial R_j}{\partial z}=\frac{\partial R}{\partial z}, \end{aligned}\right\} \qquad (3.54)$$

where M_0 is the mass of the principal attracting sphere (we neglect the mass of the satellite compared to M_0)

$R=\sum_{j=1}^{n-1}R_j$ is the disturbing [perturbative] function, and

r is the radius-vector of the satellite.

The origin of coordinates is at the center of gravity M_0. In the derivative for R_j, it was intended that in accordance with the main laws of mechanics the center of inertia of a system of bodies associated only by internal forces will move in space uniformly and rectilinearly. Let us write the equations of motion of the system of bodies in an absolute system of coordinates ξ, η, and ζ [56]: /136

$$\left.\begin{aligned} M_i\ddot{\xi}_i &= f\sum_j M_iM_j\frac{\xi_j-\xi_i}{\Delta_{ij}^3}=\frac{\partial U}{\partial \xi_i};\\ M_i\ddot{\eta}_i &= f\sum_j M_iM_j\frac{\eta_j-\eta_i}{\Delta_{ij}^3}=\frac{\partial U}{\partial \eta_i},\ (j\neq i);\\ M_i\ddot{\zeta}_i &= f\sum_j M_iM_j\frac{\zeta_j-\zeta_i}{\Delta_{ij}^3}=\frac{\partial U}{\partial \zeta_i}\cdot(i=0,\ 1,\ \ldots,\ n). \end{aligned}\right\} \qquad (3.55)$$

Here the right-hand sides present the mutual forces of attraction of the bodies ($fM_iM_j\Delta_{ij}^{-2}$) after they have been projected onto the axes of the fixed coordinates; Δ_{ij} is the distance of the i-th and j-th bodies; and U is the force function.

The equations of motion (3.55) have been written for the i-th body. After summation over i we have

$$\sum_i M_i\ddot{\xi}_i=0;\ \sum_i M_i\ddot{\eta}_i=0;\ \sum_i M_i\ddot{\zeta}_i=0, \qquad (3.56)$$

which then proves the premise that the motion of the center of inertia of the system is uniform. By integrating these equations, we get six integrals of the motion of the system's inertia center:

$$\left.\begin{aligned} &\sum_i M_i\dot{\xi}_i=\alpha_1;\ \sum_i M_i\dot{\eta}_i=\beta;\ \sum_i M_i\dot{\zeta}_i=\gamma;\\ &\sum_i M_i\xi_i=\alpha_1 t+\alpha_2;\ \sum_i M_i\eta_i=\beta_1 t+\beta_2;\\ &\sum_i M_i\zeta_i=\gamma_1 t+\gamma_2, \end{aligned}\right\} \qquad (3.57)$$

where t is time, and α_1, α_2, β_1, β_2, γ_1 and γ_2 are the constants of integration.

Using these integrals, let us convert to a system of equations of relative motion, by setting in (3.55)

$$\xi_i=\xi_0+x_i;\quad \eta_i=\eta_0+y_i;\quad \zeta_i=\zeta_0+z_i,$$

where ξ_0, η_0, and ζ_0 are the absolute coordinates of the body M_0.

Since $x_0 = y_0 = z_0 = 0$, we find

$$\left.\begin{aligned}
&\ddot{x}_i+f(M_0+M_i)\frac{x_i}{r_i^3}=f\sum_j M_j\left(\frac{x_j-x_i}{\Delta_{ij}^3}-\frac{x_j}{r_j^3}\right)=\frac{\partial R}{\partial x_i}=\sum_j\frac{\partial R_j}{\partial x_i};\\
&\ddot{y}_i+f(M_0+M_i)\frac{y_i}{r_i^3}=f\sum_j M_j\left(\frac{y_j-y_i}{\Delta_{ij}^3}-\frac{y_i}{r_j^3}\right)=\frac{\partial R}{\partial y_i}=\sum_j\frac{\partial R_j}{\partial y_i};\\
&\ddot{z}_i+f(M_0+M_i)\frac{z_i}{r_i^3}=f\sum_j M_j\left(\frac{z_j-z_i}{\Delta_{ij}^3}-\frac{z_j}{r_j^3}\right)=\frac{\partial R}{\partial z_i}=\sum_j\frac{\partial R_j}{\partial z_i}.
\end{aligned}\right\}\qquad(3.58)$$

Hence it follows that the disturbing function is

$$R=\sum_j R_j=f\sum_j M_j\left(\frac{1}{\Delta_{ij}}-\frac{x_ix_j+y_iy_j+z_iz_j}{r_j^3}\right).\qquad(3.59)$$

Let us introduce the angle ϕ_j between the radii-vectors r_i and r_j drawn from the origin of coordinates to the satellite and to the j-th body. Then R can be written as

$$R=f\sum_j M_j\left(\frac{1}{\Delta_{1j}}-\frac{r_1\cos\varphi_j}{r_j^2}\right),\qquad(3.60)$$

where

$$\Delta_{1j}^2=(x_1-x_j)^2+(y_1-y_j)^2+(z_1-z_j)^2;$$
$$r_1^2=x_1^2+y_1^2+z_1^2;$$
$$r_j^2=x_j^2+y_j^2+z_j^2.$$

The subscript "1" here refers to the spacecraft (satellite). In addition, it must be considered that when $r_1 < r_j$, we have

$$\frac{1}{\Delta_{1j}}=\frac{1}{r_j\sqrt{1-2\frac{r_1}{r_j}\cos\varphi_j+\left(\frac{r_1}{r_j}\right)^2}}=$$
$$=\frac{1}{r_j}\sum_{k=0}^{\infty}\left(\frac{r_1}{r_j}\right)^k P_k(\cos\varphi_j),\qquad(3.61)$$

and when $r_j < r_i$

$$\frac{1}{\Delta_{ij}} = \frac{1}{r_1\sqrt{1-2\frac{r_j}{r_1}\cos\varphi_j+\left(\frac{r_j}{r_1}\right)^2}} = \frac{1}{r_1}\sum_{k=0}^{\infty}\left(\frac{r_j}{r_1}\right)^k p_k(\cos\varphi_j), \tag{3.62}$$

where $p_k(\cos\phi_j)$ is the Legendre polynomial.

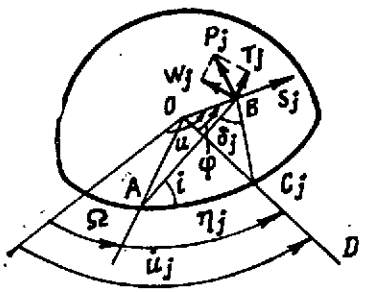

Fig. 3.4. For the derivation of the equation of perturbed motion of AES with allowance for the influence of Moon and Sun.

Since we are interested in the influence on the AES motion of the Moon and Sun, the distance to these bodies from the Earth (M_0) being greater than from the Earth to the satellite, in the following we will use Eq. (3.61). /138

Let us adopt as the principal coordinate plane the plane drawn through the orbit of the perturbed body M_j. Obviously, the vector of the perturbed acceleration caused by the body M_j lies in the plane OBC_j (Fig. 3.4). Let us decompose this sector into components, of which the first S_j coincides with the direction r_1 and the second P_j is perpendicular to r_1 and lies in the plane OBC_j. To determine these components, we have the following functions:

$$S_j = \frac{\partial R_j}{\partial r_1}; \quad P_j = \frac{\partial R_j}{r_1 \partial \varphi_j},$$

or based on Eqs. (3.60) and (3.61)

$$S_j = fM_j \frac{\partial}{\partial r_1}\left(\frac{1}{r_j}\sum_{k=0}^{\infty}\left(\frac{r_1}{r_j}\right)^k p_k(\cos\varphi_j) - \frac{r_1\cos\varphi_j}{r_j^2}\right) \approx$$
$$\approx fM_j \frac{r_1}{r_j^3}(3\cos^2\varphi_j - 1); \tag{3.63}$$

$$P_j = fM_j \frac{\partial}{r_1 \partial\varphi_j}\left(\frac{1}{r_j}\sum_{k=0}^{\infty}\left(\frac{r_1}{r_j}\right)^k p_k(\cos\varphi_j) - \frac{r_1\cos\varphi_j}{r_j^2}\right) \approx$$
$$\approx -3fM_j \frac{r_1}{r_j^3}\cos\varphi_j \sin\varphi_j. \tag{3.64}$$

(In the following, we will limit ourselves to the third term of the expansion in Legendre polynomials.)

The components T_j and W_j are determined by the formulas

$$T_j = P_j \cos\delta_j; \quad W_j = P_j \sin\delta_j.$$

From the triangle ABC_j we get

$$\left.\begin{aligned} \sin\delta_j \sin\varphi_j &= \sin\eta_j \sin i_j, \\ \cos\delta_j \sin\varphi_j &= \sin u_j \cos\eta_j - \cos u_j \sin\eta_j \cos i_j. \end{aligned}\right\} \tag{3.65}$$

With reference to Eqs. (3.64) and (3.65) we find: /139

$$W_j = -3fM_j \frac{r_1}{r_j^3} \sin i_j \sin\eta_j \cos\varphi_j; \tag{3.66}$$

$$T_j = -3fM_j \frac{r_1}{r_j^3} \cos\varphi_j (\cos\eta_j \sin u_j - \cos u_j \sin\eta_j \cos i_j). \tag{3.67}$$

In addition, from the triangle ABC_j we have

$$\cos\varphi_j = \cos u_j \cos\eta_j + \sin u_j \sin\eta_j \cos i_j. \tag{3.69}$$

The radius-vector of the satellite can be expressed in terms of the elements of the osculating orbit (a, e) and the true anomaly ϑ by the formula

$$r_1 = \frac{a(1-e^2)}{1+e\cos\vartheta}. \tag{3.69}$$

Thus, Eqs. (3.63), (3.66), (3.67), (3.68), and (3.69) express the disturbing function for the body M_j and the components of the perturbing acceleration in terms of the parameters of the osculating orbit of the satellite and the angle η_j characterizing the position of the perturbing body. The perturbing action of other bodies on satellites motion can be allowed for in similar fashion. The result of the combined action is found by superpositioning.

Let us determine the perturbations of the first order for the orbital elements Ω, ω, e, a, and e.

The equations determining the changes in the osculating elements of the orbit to the first approximation, after the use of the formulas derived above are of the form:

$$\frac{dq}{dt}=F(\vartheta, \eta),$$

where q is some element of the osculating orbit.

In place of the independent variable t (time), let us introduce the variable ϑ (true anomaly). Here, as in the case when we used u as an argument, we obtain quadratures for determining the variations in the osculating elements q. These quadratures of course enable us to use the full value of S_j, T_j, and W_j (without the assumption that the r_1/r_j ratios are small).

The solution of the equations can be much simplified if we note that the angle η_j varies very slightly (for small r_1/r_j) over a single satellite revolution around the Earth (or other planet). For example, for a circular orbit with radius $r_1 \leq 8000$ km, in a single revolution of the satellite the angle η changes for the Moon by $\Delta\eta_M \simeq 1°$, and for the Sun $\Delta\eta_S \simeq 0.1°$. For an orbit with radius $r_1 = 40{,}000$ km, $\Delta\eta_M \simeq 12°$ and $\Delta\eta_S \simeq 1°$. Because of this, we can set η = const during a single revolution for satellites close to the Earth. The variation in an element thus obtained in a single revolution will be a function of the angle η.

To determine the variation in some orbital element q in m integral revolutions, we can use the formula /140

$$q-q_0=\sum_{k=1}^{m}\Delta q_k(\eta_{k\,\mathrm{av}}), \qquad (3.70)$$

where q_k is the variation in the orbital element during the k-th satellite revolution, and $\eta_{k\,av}$ is some mean value of η during the k-th revolution.

Within the limits of this assumption $r_1/r_j < 1$, Eq.(3.70) can be replaced by the following formula:

$$q-q_0=\int_{t_0}^{t}\Delta q\frac{dt}{T_{sa}}, \qquad (3.71)$$

where Δq is the variation in the element during a single satellite revolution, and T_{sa} is the period of revolution of the satellite.

Noting that the perturbing body will move along a near-circular orbit with nearly constant velocity, we can write

$$q-q_0=\frac{1}{2\pi}\frac{T_j}{T_{sa}}\int_{\eta_0}^{\eta_0+\dot{\Omega}_p(t-t_0)}\Delta q\,d\eta, \tag{3.72}$$

where $\dot{\Omega}_p$ is the angular velocity of the perturbing body, and t_j is the period of revolution of the body around the Earth.

In Eq. (3.72), the sign of T_j must coincide with that of $\dot{\Omega}_p$. The variation in the orbital elements during a single complete revolution of a perturbing body, that is, a secular variation, if the deviation of T_j/T_{sa} is an integer, will be determined by the formula:

$$\Delta q_p=\frac{1}{2\pi}\left|\frac{T_j}{T_{sa}}\right|\int_{\eta_0}^{\eta_0+2\pi}\Delta q_T\,d\eta, \tag{3.73}$$

where q_T is the variation in an element during one satellite revolution around the Earth.

We can use this formula also when T_j/T_{sa} is fractional if we neglect the variation in the element in a single revolution of the satellite.

Variation in Longitude of Mode Ω and Position of Perigee ω /141

The changes in the longitude of the node Ω and the position of the perigee ω are determined by the following equations [20]:

$$\frac{d\Omega}{dt}=\frac{1}{na^2\sqrt{1-e^2}\sin i}\cdot\frac{\partial R}{\partial i}; \tag{3.74}$$

$$\frac{d\bar{\omega}}{dt}=\frac{1-\cos i}{na^2\sqrt{1-e^2}\sin i}\cdot\frac{\partial R}{\partial i}+\frac{\sqrt{1-e^2}}{na^2e}\cdot\frac{\partial R}{\partial e}, \tag{3.75}$$

where

$$\bar{\omega}=\omega+\Omega;\quad n=\frac{\sqrt{\mu}}{a^{3/2}};\quad \mu=fM_0.$$

To determine the variation in the longitude of the node, by differentiating Eq. (3.60) with reference to the linear expansion of $1/\Delta_{1j}$, that is,

$$R=\frac{fM_j}{r_j}\left[1+\frac{1}{2}\left(\frac{r_1}{r_j}\right)^2(3\cos^2\varphi-1)\right], \tag{3.76}$$

we find

$$\frac{\partial R}{\partial i} = -3\frac{fM_j}{r_j^3} r_1^2 \cos\varphi \sin i \sin u \sin\eta. \qquad (3.77)$$

In Eqs. (3.74), by converting to the variable ϑ and using the formula

$$\frac{d\vartheta}{dt} = \frac{\sqrt{\mu a(1-e^2)}}{r_1^2},$$

we get

$$\frac{d\Omega}{d\vartheta} = -3\xi(1-e^2)^3 \frac{\sin\eta\cos\varphi\sin u}{(1+e\cos\vartheta)^1}, \qquad (3.78)$$

where

$$\xi = \frac{M_j}{M_0}\left(\frac{a}{r_j}\right)^3 = \frac{M_j}{M_0}\left(\frac{\bar{a}}{r_j}\right)^3\left(\frac{a}{\bar{a}}\right)^3;$$

$\bar{a}$ is the equatorial radius of the Earth.

The coefficients ξ_M for the Moon and ξ_S for the Sun, when $\bar{a}$ = = 6378 km, have the following numerical values:

$$\xi_M \approx 0.56\cdot 10^{-7}\left(\frac{a}{\bar{a}}\right)^3; \quad \xi_S \approx 0.26\cdot 10^{-7}\left(\frac{a}{\bar{a}}\right)^3$$

Since first-order perturbations are being determined, in the right-hand side of Eq. (3.78) we will assume the orbital elements to be constant.

The variation in the longitude of the node $\Delta\Omega$ of the perturbed orbit in a single satellite revolution is expressed by the formula (under the condition that at the instant t_0 the angle $\vartheta = 0$) /142

$$\Delta\Omega = -3\xi(1-e^2)^3 \sin\eta \int_0^{2\pi} \frac{\cos\varphi\sin u}{(1+e\cos\vartheta)^4}\, d\vartheta. \qquad (3.79)$$

Based on the familiar formulas

$$\cos\varphi = \cos u\cos\eta + \sin u\sin\eta\cos i;$$
$$u = \omega + \vartheta$$

we have

$$\cos\varphi\sin u = A\cos^2\vartheta + B\sin^2\vartheta + C\sin\vartheta\cos\vartheta, \tag{3.80}$$

where

$$A = \frac{1}{2}\cos\eta\sin 2\omega + \sin\eta\cos i\sin^2\omega;$$

$$B = \sin\eta\cos i\cos^2\omega - \frac{1}{2}\sin 2\omega\cos\eta;$$

$$C = \cos\eta\cos 2\omega + \sin\eta\sin 2\omega\cos i.$$

Similarly, let us find

$$\cos^2\varphi = D\cos^2\vartheta + E\sin^2\vartheta + F\sin\vartheta\cos\vartheta, \tag{3.80'}$$

where

$$D = \cos^2\eta\cos^2\omega + \sin^2\eta\sin^2\omega\cos^2 i + \frac{1}{2}\sin 2\eta\cos i\sin 2\omega;$$

$$E = \cos^2\eta\sin^2\omega + \sin^2\eta\cos^2\omega\cos^2 i - \frac{1}{2}\sin 2\eta\cos i\sin 2\omega;$$

$$F = \sin^2\eta\cos^2 i\sin 2\omega - \cos^2\eta\sin 2\omega + \sin 2\eta\cos i\cos 2\omega.$$

Substituing Eqs. (3.80) into expression (3.79) and carrying out the necessary transformations, we obtain

$$\Delta\Omega = -3\xi\frac{\pi}{(1-e^2)^{1/2}}\left\{\cos i\sin^2\eta + e^2\left[\frac{5}{2}\sin 2\omega\sin\eta\cos\eta + \right.\right.$$
$$\left.\left. + (4 - 5\cos^2\omega)\cos i\sin^2\eta\right]\right\}. \tag{3.81}$$

On analogy to $\Delta\Omega$, we get

$$\Delta\omega = 3\pi\xi\sqrt{1-e^2}\,[4(\cos\eta\cos\omega + \sin\eta\sin\omega\cos i)^2 -$$
$$-(-\cos\eta\sin\omega + \sin\eta\cos\omega\cos i)^2 - 1] - \Delta\Omega\cos i. \tag{3.82}$$

Integrating Eqs. (3.81) and (3.82) in accordance with (3.73), we finally find /143

$$\Delta\omega_p = \frac{15}{2}\xi\frac{\pi}{(1-e^2)^{1/2}}\cdot\frac{T_J}{T_{sa}}\left[(\cos^2 i - 1 + e^2)\sin^2\omega + \frac{2}{5}(1-e^2)\right]; \tag{3.83}$$

$$\Delta\Omega_p = -\frac{3}{2}\xi\frac{\pi}{(1-e^2)^{1/2}}\cdot\frac{T_J}{T_{sa}}(1 - e^2 + 5e^2\sin^2\omega)\cos i. \tag{3.84}$$

Variation in Orbital Inclination i

To compute the variation in the orbital inclination, let us use the following equation [20]

$$\frac{di}{d\vartheta} = \frac{r_1^3}{p\sqrt{\mu p}} W_1 \cos u, \tag{3.85}$$

where

$$p = a(1-e^2); \quad W_1 = \sqrt{\frac{p}{\mu}}\, W. \tag{3.85'}$$

Substituting Eq. (3.66) into (3.85), after transformations we get

$$\frac{di}{d\vartheta} = -3\xi(1-e^2)^3 \sin i \sin\eta \frac{\cos u \cos\varphi}{(1+e\cos\vartheta)^4}. \tag{3.86}$$

Assuming, as earlier, that η = const, to determine the variation in the orbital inclination in a single satellite revolution we obtain the expression

$$\Delta i = -3\xi(1-e^2)^3 \sin i \sin\eta \int_0^{2\pi} \frac{\cos u \cos\varphi\, d\vartheta}{(1+e\cos\vartheta)^4}. \tag{3.87}$$

expanding cos ϕ, we find

$$\cos u \cos\varphi = A' \cos^2\vartheta + B' \sin^2\vartheta + C' \sin\vartheta\cos\vartheta, \tag{3.88}$$

where

$$A' = \frac{1}{2}\cos i \sin\eta \sin 2\omega + \cos\eta\cos^2\omega;$$

$$B' = \cos\eta \sin^2\omega - \frac{1}{2}\sin\eta\cos i \sin 2\omega;$$

$$C' = \sin\eta\cos i\cos 2\omega - \cos\eta \sin 2\omega.$$

Substituting Eq. (3.88) into Eq. (3.87), after uncomplicated transformations we find

$$\Delta i = -\frac{3\xi\pi}{(1-e^2)^{1/2}}\left\{\sin i \sin\eta\cos\eta + e^2 \sin i \sin\eta \times \right.$$
$$\left. \times\left[\frac{5}{2}\cos i \sin\eta \sin 2\omega + \cos\eta\,(5\cos^2\omega - 1)\right]\right\}. \tag{3.89}$$

Integrating this expression in accordance with Eq. (.373), let us determine the change in the orbital inclination in one revolution of the perturbing body: /144

$$\Delta i_{\text{p}} = -\frac{15}{8}\xi\frac{e^2}{(1-e^2)^{1/2}}\cdot\frac{T_J}{T_{\text{sa}}}\pi\sin 2i\sin 2\omega. \tag{3.90}$$

Note that if we assume e and i to be small, the variation we have found in the orbital inclination is a quantity of the third order of smallness relative to inclination and eccentricity.

Change in Semi-Major Axis a of Orbit

Let us use the following equations [20]:

$$\frac{da}{d\vartheta} = \frac{r_1^2}{\sqrt{\mu p}}\left[\frac{2a^2 e\sin\vartheta}{p}\sqrt{\frac{p}{\mu}}S + \frac{2a^2}{r_1}\sqrt{\frac{p}{\mu}}T\right]. \tag{3.91}$$

Substituting S, T and r_1 from Eqs. (3.63), (3.67), and (3.69) into this equation, after transformations we find

$$\frac{da}{d\vartheta} = 2\xi e(1-e^2)^2\left[e\frac{(3\cos^2\varphi-1)\sin\vartheta}{(1+e\cos\vartheta)^3} - 3\frac{\cos\varphi(\cos\eta\sin u - \cos u\sin\eta\cos i)}{(1+e\cos\vartheta)^2}\right]. \tag{3.92}$$

Under the former assumption, let us determine the variation in the semi-major axis of the satellite in one revolution:

$$\Delta a = 2\xi a(1-e^2)^2[I_1 e - 3I_2], \tag{3.93}$$

where

$$I_1 = \int_0^{2\pi}\frac{(3\cos^2\varphi-1)\sin\vartheta d\vartheta}{(1+e\cos\vartheta)^3};$$

$$I_2 = \int_0^{2\pi}\frac{\cos\varphi(\cos\eta\sin u - \cos u\sin\eta\cos i)d\vartheta}{(1+e\cos\vartheta)^2}.$$

For the integral I_1 we have

$$I_1=3F\left(\int_0^{2\pi}\frac{\cos\vartheta d\vartheta}{(1+e\cos\vartheta)^3}-\int_0^{2\pi}\frac{\cos^3\vartheta d\vartheta}{(1+e\cos\vartheta)^3}\right)=$$

$$=3F\left(\int_0^{2\pi}\frac{\cos\vartheta d\vartheta}{(1+e\cos\vartheta)^3}-\frac{1}{e^3}\int_0^{2\pi}d\vartheta+\frac{1}{e^3}\int_0^{2\pi}\frac{d\vartheta}{(1+e\cos\vartheta)^3}+\right.$$

$$\left.+\frac{3}{e^2}\int_0^{2\pi}\frac{\cos\vartheta d\vartheta}{(1+e\cos\vartheta)^3}+\frac{3}{e}\int_0^{2\pi}\frac{\cos^2\vartheta d\vartheta}{(1+e\cos\vartheta)^3}\right).$$

The integrals in the last formula computed by means of the substitution $\operatorname{tg}\frac{\vartheta}{2}=\sqrt{\frac{1+e}{1-e}}\operatorname{tg}\frac{E}{2}$, that is, after converting to the eccentric anomaly, are: /145

$$\left.\begin{aligned}&\int_0^{2\pi}\frac{\cos\vartheta d\vartheta}{(1+e\cos\vartheta)^3}=-\frac{3\pi e}{(1-e^2)^{5/2}};\quad\int_0^{2\pi}\frac{d\eta}{(1+e\cos\vartheta)^3}=\pi\frac{2+e^2}{(1-e^2)^{5/2}};\\&\int_0^{2\pi}\frac{\cos^2\vartheta d\vartheta}{(1+e\cos\vartheta)^3}=\pi\frac{1+2e^2}{(1-e^2)^{5/2}}.\end{aligned}\right\}\qquad(3.94)$$

Based on these formulas let us find

$$I_1=3F\pi\left[-\frac{3e}{(1-e^2)^{5/2}}-\frac{2}{e^3}+\frac{1}{e^3}\cdot\frac{2+e}{(1-e^2)^{5/2}}-\right.$$

$$\left.-\frac{9}{e}\cdot\frac{1}{(1-e^2)^{5/2}}+\frac{3}{e}\cdot\frac{1+2e^2}{(1-e^2)^{5/2}}\right].\qquad(3.95)$$

Further, we can get

$$\cos\varphi(\cos\eta\sin u-\cos u\sin\eta\cos i)=M\cos^2\vartheta+$$

$$+N\sin^2\vartheta+L\sin\vartheta\cos\vartheta,\qquad(3.96)$$

where

$$M=\frac{1}{2}(\cos^2\eta\sin2\omega-\sin^2\eta\cos^2 i\sin2\omega-\sin2\eta\cos i\cos2\omega);$$

$$N=\frac{1}{2}(\sin^2\eta\cos^2 i\sin2\omega-\cos^2\eta\sin2\omega+\sin2\eta\cos i\cos2\omega);$$

$$L=(\cos^2\eta-\sin^2\eta\cos^2 i)\cos2\omega+\sin2\eta\cos i\sin2\omega.$$

The second integral in Eq. (3.93) here can be reduced to the form

$$I_2=2\pi\frac{M-N}{e^2}+\left(N-\frac{M-N}{e^2}\right)\int_0^{2\pi}\frac{d\vartheta}{(1+e\cos\vartheta)^2}+$$

$$+\frac{2(N-M)}{e}\int_0^{2\pi}\frac{\cos\vartheta d\vartheta}{(1+e\cos\vartheta)^2}.$$

Computing the integrals, we find

$$I_2=2\pi\left[\frac{M-N}{e^2}+\left(N-\frac{M-N}{e^2}\right)\frac{1}{(1-e^2)^{3/2}}+2(M-N)\frac{1}{(1-e^2)^{3/2}}\right]. \qquad (3.97)$$

Now, after uncomplicated transformations we can write /146

$$\frac{1}{\pi}(I_1e-3I_2)=-\frac{6}{e^2}(M-N+F)+\frac{1}{(1-e^2)^{5/2}}\times$$
$$\times\left[(9F+12M-6N)e^2+\frac{6}{e^2}(F+M-N)+(-15F+12N-18M)\right].$$

We can easily see that all the expressions in the parentheses in the right-hand side of the formula tend to zero. This follows from the obvious conditions given below (see Eqs. (3.96) and (3.80!)):

$$\left.\begin{aligned}M+N&=0;\\ F+2M&=0.\end{aligned}\right\} \qquad (3.98)$$

Thus, we get the following result, which is valid for any values of all nodes:

$$\Delta a=0. \qquad (3.99)$$

Note that this result coincides with the derivation of the general theory -- in the first approximation the semi-major axes of the osculating planetary orbits do not have secular perturbations.

Variation in Orbital Eccentricity e

Differentiating with respect to ϑ, Eq. (3.85') that relates the orbital parameter, semi-major axis, and eccentricity, we get

$$\frac{de}{d\vartheta}=\frac{1}{2ae}\left[(1-e^2)\frac{d\varpi}{d\vartheta}-\frac{dp}{d\vartheta}\right]. \qquad (3.100)$$

The eccentricity in one satellite revolution will vary by the quantity,

$$\Delta e=\frac{1-e^2}{2ae}\Delta a-\frac{1}{2ae}\Delta p,$$

or, since $\Delta a=0$,

$$\Delta e=-\frac{1}{2ae}\Delta p. \qquad (3.101)$$

The variation in the orbital parameter is determined by the equation

$$\frac{dp}{dt} = 2r_1 \sqrt{\frac{\overline{p}}{\mu}} T. \qquad (3.102)$$

Substituting into this expression T from Eq. (3.67) and using the new variable ϑ, we get the following equation:

$$\frac{dp}{d\vartheta} = -6\xi a(1-e^2)^4 \frac{M\cos^2\vartheta + N\sin^2\vartheta + L\sin\vartheta\cos\vartheta}{(1+e\cos\vartheta)^4}, \qquad (3.103)$$

whence we find

$$\Delta p = -6\xi a(1-e^2)^{1/2}\pi e^2 |5M|. \qquad (3.104)$$

Substituting this expression we have obtained into Eq. (3.101) we find /147

$$\Delta e = \frac{15}{2}\xi\pi e(1-e^2)^{1/2} \times$$
$$\times [\cos^2\eta \sin 2\omega - \sin^2\eta\cos^2 i \sin 2\omega - \sin 2\eta \cos i \cos 2\omega]. \qquad (3.105)$$

The variation in eccentricity in one revolution of the perturbing body will be determined by the formula

$$\Delta e_p = \frac{15}{4}\xi\pi e \frac{T_j}{T_{sa}}(1-e^2)^{1/2}\sin^2 i \sin 2\omega. \qquad (3.106)$$

If we assume that the eccentricity and orbital inclination are small (of the same order as ξ), just as in the case of Δi, the resulting change in eccentricity will be quantity of the third order of smallness.

Eqs. (3.90) and (3.106), just like Eqs. (3.83) and (3.84), determine the secular variations in orbital inclination and eccentricity if the period of satellite revolution is an integral number of times smaller than the period of revolution of the perturbing body. With lesser accuracy, the perturbations can be calculated also if this condition is not satisfied.

In conclusion we note that these formulas can be used for an approximate calculation of perturbations in the orbital elements of satellites of other planets (including the Moon) if T_j/T_{sa} is large enough for these satellites.

More exact methods of calculation are given in the study [22].

Numerical Example of Calculation of Perturbations of Orbital Elements of AES Caused by Influence of Moon and Sun

As an example, let us examine the orbit of the satellite with a semi-major axis a = 7350 km and eccentricity e = 0.1:

$$\xi_M \approx 0.85 \cdot 10^{-7}; \quad \xi_S = 0{,}40 \cdot 10^{-7};$$

$$\left(\frac{T_M}{T_{sa}}\right) = 410; \quad \left(\frac{T_S}{T_{sa}}\right) \approx 5000.$$

The results of the calculations are given in Table 3.1.

Analysis of the data in Table 3.1 shows that the influence of Moon and Sun on the orbit of a satellite close to the Earth is very small. However, in a year the perigee altitude can vary by several kilometers, and the position of the node can vary by 5-7 minutes of arc.

TABLE 3.1 /148

Element	Changes in one satellite revolution		Changes in one revolution of perturbing body	
	Influence of Moon	Influence of Sun	Influence of Moon	Influence of Sun
Longitude of node Ω	$<0.17''$	$<0{,}08''$	$<34''$	$<3.2'$
Angular distance of perigee from node ω	$<0{,}29''$	$<0{,}14''$	$<2'$	$<11.3'$
Orbital inclination i	$<0{,}17''$	$<0.08''$	$<0.43''$	$<2{,}4''$
Orbital eccentricity e	$<2 \cdot 10^{-7}$ <1.5 m	$<0.93 \cdot 10^{-7}$ $<0{,}6$ m	$<0.41 \cdot 10^{-4}$ $<0{,}3$ km	$<2{,}31 \cdot 10^{-4}$ <1.7 km
Perigee distance of satellite orbit	Overall action ≈ 2.1 m		Overall action in one year ≈ 5.1 km	

Refinement of Approximate Method

Above we obtained formulas for calculating the variations in the case when the third term (n = 2) of the expansion of the disturbing function is retained. By the same approach we can obtain the following formulas corresponding to the n-th term of the expansion, in the interval from ϑ_1 to ϑ_2 :

$$\Delta\Omega_n=\frac{\mu_1 p^{n+1}\sin\eta}{\mu r_1^{n+1}2^n\,n!}\sum_{i=0}^{E\left(\frac{n-1}{2}\right)}\sum_{k=0}^{n-2i-1}(-1)^{i+1}\binom{n}{i}\frac{(2n-2i)!}{(n-2i-1)!}\times$$

$$\times\binom{n-2i-1}{k}\cos^{\sigma}\varphi_1\cos^{k}\varphi_2\left[\sin\omega\sum_{j=0}^{\frac{k}{2}}\sum_{\nu=0}^{\sigma+1+2j}(-1)^{\sigma+1+3j+\nu}\times\right.$$

$$\times\binom{\frac{k}{2}}{j}e^{-\sigma-1-2j}\binom{\sigma+1+2j}{\nu}I_{n+2-\nu}+\cos\omega\sum_{j=0}^{\frac{k+1}{2}}\sum_{\nu=0}^{\sigma+2j}(-1)^{\sigma+\nu+3j}\times$$

$$\left.\times\binom{\frac{k+1}{2}}{j}e^{-\sigma-2j}\binom{\sigma+2j}{\nu}I_{n+2-\nu}\right];$$

$$\Delta\omega_n=\frac{\mu_1}{\mu e}\frac{p^{n+1}}{r_1^{n+1}}\sum_{m=0}^{n}\sum_{i=0}^{E\left(\frac{n-m}{2}\right)}(-1)^{i}\frac{b_{nm}\binom{n}{i}(2n-2i)!}{2^n\,n!(n-m-2i)!}\times$$

$$\times\sum_{k=1,\ l=0}^{2,1}\sum_{j+\nu=0}^{\frac{m}{2}+l,\delta-1}(-1)^{\delta-1+j+\nu}\binom{\frac{m}{2}+l}{j}\binom{\delta-1}{\nu}\times$$

$$\times e^{-\delta+1}\xi_{kl}I_{n+k-\nu}-\Delta\Omega_n\cos i;$$

$$\Delta p_n=\frac{\mu_1 p^{n+2}}{\mu r_1^{n+1}}\sum_{m=0}^{n}\sum_{i=0}^{E\left(\frac{n-m}{2}\right)}(-1)^{i}\frac{b_{nm}\binom{n}{i}(2n-2i)!}{2^{n-1}\,n!(n-m-2i)!}\sum_{l=0}^{1}\eta_l\times$$

$$\times\sum_{j=0}^{\frac{m-1}{2}+l}\sum_{\nu=0}^{\delta-1}(-1)^{\delta-1+j+\nu}\binom{\frac{m-1}{2}+l}{j}e^{-\delta+1}\binom{\delta-1}{\nu}I_{n+2-\nu};$$

$$\Delta e_n=\frac{\mu_1 p^{n+1}}{\mu r_1^{n+1}}\sum_{m=0}^{n}\sum_{i=0}^{E\left(\frac{n-m}{2}\right)}(-1)^{i}\frac{b_{nm}\binom{n}{i}(2n-2i)!}{2^n\,n!(n-m-2i)!}\times$$

$$\times\left[\sum_{l=0}^{1}\zeta_l\sum_{j=0}^{\frac{m-1}{2}+l}\sum_{\nu=0}^{\delta}(-1)^{\delta+j+\nu}\binom{\frac{m-1}{2}+l}{j}e^{-\delta}\times\right.$$

$$\times\binom{\delta}{\nu}I_{n+1-\nu}+\sum_{l=k=0}^{1,1}\eta_l e^{k}\sum_{j=0}^{\frac{m-1}{2}+l}\sum_{\nu=0}^{\delta-k}(-1)^{\delta-k+j+\nu}\times$$

$$\left.\times\binom{\frac{m-1}{2}+l}{j}e^{-\delta+k}\binom{\delta-k}{\nu}I_{n+2-\nu}\right];$$

$$\cos\varphi_1=\cos\eta\cos\omega+\sin\eta\sin\omega\cos i;$$

$$\cos\varphi_2=-\cos\eta\sin\omega+\sin\eta\cos\omega\cos i.$$

/149

(3.107)

Setting n = 1 and $\mu_1 = -\Delta\mu_\odot$ (see Eq. (3.218)), we find the perturbation of the orbital element caused by the pressure of sunlight on the hull of the spacecraft.

The variation in the orbital inclination Δi_n is determine from the formula for $\Delta\Omega_n$ after sin ω has been replaced by cos ω and after cos ω has been replaced by -sin ω and the entire expression has been multiplied by sin i.

In Eqs. (3.107) the following are assumed:

$$\delta = n - m - 2i + 2j; \quad \sigma = n - 2i - 1 - k;$$

$$\eta_0 = m; \quad \eta_1 = 2i - n; \quad \zeta_0 = m; \quad \zeta_1 = 2i; \quad \xi_{10} = m - n;$$

$$\xi_{11} = 2i; \quad \xi_{21} = 2i - n; \quad \xi_{20} = m;$$

$$b_{nm} = 2\,\frac{(n-m)!}{(n+m)!}\,p_{nm}(\cos\varphi_1)\cos m\psi; \quad b_{n_0} = p_n(\cos\varphi_1);$$

$$\sin\psi = \frac{\sin i \sin\eta}{\sin\varphi_1};$$

$r_1 = \frac{p_1}{1 + e_1\cos(\Omega_1 + \eta)}$ is the radius-vector of the perturbing body (the subscript at the elements is "1") with respect to the central body.

The quantity $I_{n+k-\nu}$ is an integral of the form

$$I_{n+1} = \int_{\vartheta_1}^{\vartheta_2} \frac{d\vartheta}{(1+e\cos\vartheta)^{n+1}} = \frac{1}{n(1-e^2)}\left[-\frac{e\sin\vartheta}{(1+e\cos\vartheta)^n} + (2n-1)\times\right.$$
$$\left.\times\int\frac{d\vartheta}{(1+e\cos\vartheta)^n} - (n-1)\int\frac{d\vartheta}{(1+e\cos\vartheta)^{n-1}}\right]_{\vartheta_1}^{\vartheta_2}. \qquad (3.108)$$

These expressions for the integral of $I_{n+k-\nu}$ are valid for any nonfractional indexes of sums or combinations [for example, $\left[\binom{\frac{k+1}{2}}{j}\right]$, which is meaningful only in this case.

If these quantities prove to be fractional, the values of k or m appearing in them are reduced by unity, and the integrals $I_{n+k-\nu}$ become

$$I_{n+k-\nu} = -\int_{\vartheta_1}^{\vartheta_2}\frac{d\cos\vartheta}{(1+e\cos\vartheta)^{n+k-\nu}} =$$
$$= \frac{1}{e(1+e\cos\vartheta)^{n+k-\nu-1}(n+k-\nu-1)}\Bigg|_{\vartheta_1}^{\vartheta_2}. \qquad (3.109)$$

Here $n + k - \nu = 1 \quad I_1 = -\frac{1}{e}\ln(1+e\cos\vartheta)\Big|_{\vartheta_1}^{\vartheta_2}.$

Let $\Delta\eta$ be an interval of which we can still regard the perturbing body to be fixed[1]; and let Δt be the corresponding time interval. Then, by assuming the variations in the orbital elements of the spacecraft during the time Δt to be derivatives with respect /151 to time, and considering that the perturbing body will move in the general case along an elliptical orbit, based on Eqs. (3.107) we get the following formulas for computing the averaged increments of these elements:

$$J_{mn}=\frac{T_1(1-e_1^2)^{3/2}}{2\pi\Delta t}\frac{2^*}{p_1^{n+1}}\frac{(n-m)!}{(n+m)!}\sum_{\varkappa=\lambda=0}^{E\left(\frac{n-m}{2}\right),E\left(\frac{m}{2}\right)}\sum_{s=0}^{n-m-2\varkappa}\sum_{\tau=0}^{m-2\lambda}\times$$
$$\times(-1)^{m+\varkappa-\lambda-\tau}\frac{\binom{n}{\varkappa}\binom{m}{2\lambda}(2n-2i)!}{2^n n!(n-m-2\varkappa)!}\binom{n-m-2\varkappa}{s}\times$$
$$\times\binom{m-2\lambda}{\tau}\sum_{t-\theta=0}^{n-1,t}(-1)^{\theta}\binom{n-1}{t}\binom{t}{\theta}e_1^t\cos^{t-\theta}\Omega_1\sin^{\theta}\Omega_1\cdot J_1, \tag{3.110}$$

where

$J_1=\int_{\eta_1}^{\eta_2}\sin^{\alpha}\eta\cos^{\beta}\eta d\eta$ is the tabulated integral, $\alpha = s + \tau + \theta$, $\beta = n - 2x - 2\lambda + t - \alpha$

2^* is replaced by unity with $m = 0$

T_1 and e_1 are the period of revolution of the perturbing body about the central body and the eccentricity, respectively

$$J_{nk}=\frac{T_1(1-e_1)^{3/2}}{2\pi\Delta t p_1^{n+1}}\sum_{t-\theta=0}^{n-1,t}\sum_{q-p=0}^{\gamma,k}(-1)^{\theta+p}\binom{n-1}{t}\binom{t}{\theta}e_1^t\binom{\gamma}{q}\binom{k}{p}\times$$
$$\times\cos^{t-\theta}\Omega_1\sin^{\theta}\Omega_1\sin^{q+k-p}\omega\cos^{\gamma-q+p}\omega\cos^{q+p}i\cdot J_2. \tag{3.110!}$$

Here $J_2=\int_{\eta_1}^{\eta_2}\sin^{a}\eta\cos^{b}\eta d\eta$ is the tabulated integral, $a = \theta + q + p + l$, $b = t - \theta + \gamma - q + k - p$, $\gamma = n - 2i - k - l$.

To obtain the averaged $\overline{\Delta p_n}$, $\overline{\Delta e_n}$, and $\overline{\Delta\omega_n}$, which are the increments of the orbital elements, it is necessary that in the corresponding formulas (3.17) we replace the complex $\frac{b_{nm}}{r_1^{n+1}}$ by J_{nm}, and for the elements $\overline{\Delta\Omega_n}$ and $\overline{\Delta i_n}$ we replace the complex $\frac{\sin\eta\cos^{\sigma}\varphi_1\cos^{k}\varphi_2}{r_1^{n+1}}$ by the quantity J_{nk}.

When the equations of motion are integrated with respect to ϑ within the limits 0 to 2π, Eqs. (3.107) become simplified. All the

[1] The effect of displacement of the attracting body can be estimated with formulas (see [47]).

summands containing an integral of the type (3.109) become equal to zero, and the integral of the type (3.108) is converted to

$$I_{n+1}=\frac{2\pi}{(1-e^2)^{\frac{n+1}{2}}}P_n\left(\frac{1}{\sqrt{1-e^2}}\right).$$

We obtain (the result does not depend on Ω_1) the following expression for perturbations during the period of the revolution of the perturbing body that is moving along an elliptical orbit /152

$$J_{nm}=\frac{T_1(1-e_1^2)^{3/2}}{2\pi T p_1^{n+1}}2^*\frac{(n-m)!}{(n+m)!}\sum_{\varkappa=\lambda=0}^{E\left(\frac{n-m}{2}\right),E\left(\frac{m}{2}\right)}\sum_{s=0}^{n-m-2i}\sum_{\tau=0}^{m-2\lambda}\times$$
$$\times(-1)^{m+\varkappa-\lambda-\tau}\frac{\binom{n}{\varkappa}\binom{m}{2\lambda}(2n-2i)!}{2^n n!(n-m-2\varkappa)!}\binom{n-m-2\varkappa}{s}\binom{m-2\lambda}{\tau}\times$$
$$\times\sum_{t=0}^{n-1}\binom{n-1}{t}e_1^t J_1,$$

where T is the period of revolution of the satellite around the central body;

$$J_{nk}=\frac{T_1(1-e_1)^{3/2}}{2\pi T p_1^{n+1}}\sum_{t=0}^{n-1}\sum_{q=p=0}^{\gamma,k}(-1)^p\binom{n-1}{t}e_1^t\binom{\gamma}{q}\binom{k}{p}\sin^{q+k-p}\omega\times$$
$$\times\cos^{\gamma-q+p}\omega\cos^{q+p}i\cdot J_2.$$

As in the general case, to obtain the average increments of the orbital elements (during the period of revolution of the perturbing body), we must replace the corresponding elements in Eqs. (3.107) by J_{nm} and J_{nk}.

3.5. Estimate of Perturbing Action of Atmosphere. Determination of Satellite Lifetime

Let us examine the main perturbations of an orbit, that is, secular changes in semi-axis (or parameter) and in eccentricity determining satellite lifetime.

The drag occurring as a body moves in a molecular stream of gas can be calculated by the familiar formula

$$R_x=c_x\frac{\varrho v^2}{2}S_{\text{mol}}. \qquad (3.111)$$

Here the coefficient of aerodynamic drag c_x, as a rule, is assumed constant for the entire possible range of satellite velocities and flight altitudes.

The maximum cross section S_M in the case of a nonoriented satellite can be assumed to be constant on the average over long time intervals and equal to approximately 1/4 of the total surface area of the body [39]. Thus, a satellite of any shape can be replaced by a sphere with equivalent surface area.

The coefficient c_x is assumed to be equal to the drag coefficient for the sphere. From the data of the theory of the drag experienced by bodies in a molecular gas flow, the c_x of the sphere is 2.1-2.15 [62]. /153

For an oriented satellite, we must calculate the maximum cross section in accordance with the satellite orientation relative to the incident stream. The coefficient c_x also changes as a function of the orientation of the body relative to the gas stream and can be calculated from available theoretical methods of calculation [62].

The density of air ρ is a function of flight altitudes and also depends on the position of the Sun relative to the orbital plane (perigee), geographical latitude of the satellite, physical processes occurring on the Sun (changes in solar activity), and rotation of the Sun about its own axis. Up to altitudes 250-300 km, the density in the region of an orbit depends only little on the position of the Sun relative to the perigee[2] (the part of the orbit where atmospheric drag is most evident). For perigee altitudes above 300 km, the density depends strongly on whether the perigee is on the day side or night side of the Earth. At the altitudes 400, 500, 600 and 700 km, the density of air in the daytime is greater than at night by 1.6, 3, 6, and 11 times, respectively. At altitudes above 500 km, latitudinal variability of density appears [34].

From recent data, the main cause of variation in density is the warming of the atmosphere due to the absorption of solar electromagnetic radiation, however fluxes of corpuscles coming from the Sun during periods of geomagnetic storms also have an influence. Formulas were proposed for allowing for the variation in ρ as a function of solar activity and diurnal trend, but the reliability of these formulas is not known [34].

It is of interest to note that from the data of studies presented in the collection [37], the omission of the "swelling" of the atmosphere due to solar warming does not yield errors in the position of an AES in an orbit of more than 25 m for all flight altitudes.

---

[2] This refers to the maximum solar activity for the 1959-1960 period.

Many studies have dealt with the problem of determining the density of the upper atmospheric layers. Here use was made principally of data on satellite deceleration [33, 39, 68].

Numerous atmospheric models were proposed in which changes in density as a function of altitude above sea level were taken into account. In this study, use was made of the model of the provisional standard atmosphere VSA-60 (up to altitudes of 200 km) used in the USSR and the M-1 atmospheric model (up to altitudes of 400 km) coinciding with the altitude of 200 km with the American atmospheric model ARDC-1959 [34].

The deviations between the models in the region of overlapping altitudes are of the order of 20 percent. This quantity can characterize the accuracy with which the mean density values were /154
obtained for the entire globe at these altitudes. Observations of the deceleration of the first three Soviet satellites [70] yield exactly these deviations. The higher the altitude, the less exactly density is known. In addition, amplitudes of fluctuations in ρ increase, which show up clearly based on data on the change in the period of satellite rotation about the Earth.

The study [33] presents the curves of variation in density related to one altitude with respect to the hour angle of the perigee (λ). The dependence of ρ on hour angle, that is, on the position of the Sun relative to the orbital perigee, which determines the extent of air heating in this area, is not as well-defined as the fluctuations with the period of 27-28 days coincident with the period of the Sun's rotation about its axis.

If we replot the curves for flight time, the coincidence of phases over this period becomes a general law for all satellites. In amplitude these fluctuations reach 15 percent at altitudes 200-225 km, and 40-50 percent at altitudes 350-370 km. Slower and more irregular fluctuations in density are also observed, which can be seen from the same study [33].

Selection of Type of Approximating Function for Density ρ

It is expedient to be limited to the most probable atmospheric model for calculating satellite motion with reference to drag of the medium.

It is not meaningful to allow for fluctuations until they have been adequately studied, all the more so because when calculations are made over lengthy time intervals the deviations in the position of the satellite in orbit resulting from the effect of density fluctuations will be averaged in some way.

For short time intervals the errors will be much larger owing to a lack of knowledge of the phase of fluctuations in ρ before satellite launch. Errors in the preliminary prediction in the latter case can be as high as 50 percent for perigee altitudes 200-225 km and more than 100 percent for an altitude of 350 km.

In spite of these errors, it appears useful for the selected atmospheric model to choose the most exact approximating function that, in the case of further refinements of the model, would remain suitable for calculations. Here the coefficients appearing in this function must be recalculated. The approximating function must contain a small number of parameters and correspond to the largest possible range of flight altitudes.

It is interesting to note that various atmospheric models found by several authors at different times have a general character. In the altitude range from 130 (satellites cannot exist below this altitude) to 400-500 km, all the curves $\ln \rho(h)$ have their highest curvature in the area of 150 km; the curves gradually straighten /155 out with increase in altitude and by 400-500 km their slope remains nearly unchanged. This makes it possible to select as the approximating function for $\ln \rho(h)$ the quadratic parabola with vertex in the region of low altitudes:

$$\ln \rho = \bar{a}_0 - \bar{\varkappa}\sqrt{h - \bar{h}_0}, \qquad (3.112)$$

where h is the altitude of the level of the world ocean, and $\bar{a}_0$, $\bar{\kappa}$, $\bar{h}_0$ are the constant coefficients for the given atmospheric model.

Calculations show that this regularity is conserved for both the period of the maximum and the period of the minimum solar activity, in particular, for the standard atmospheric model of year 1964, GOST [State Standard] 4401-64.

Table 3.2 gives the values of coefficients $\bar{a}_0$, $\bar{\kappa}$, and $\bar{h}_0$ for different atmospheric models, as well as the deviations $\Delta\rho = \rho_{mod} - \rho_{appr}$ (where ρ_{mod} and ρ_{appr} are the densities of the selected model and approximating function, respectively).

We can see that the error in the approximation of ρ does not exceed 5-6 percent. The M-3 model is an exception. For example, at the altitude 140 km the deviation is 14 percent, but the approximation is suitable to altitudes of 700 km.

Thus, it is possible by using function (3.112) to represent with high accuracy $\ln \rho$ in the entire altitude range where principally satellite deceleration occurs (from 140 to 500 km).

TABLE 3.2

Model M-1	Alt., h, km	$\Delta\varrho$ %	VSA-60 Model, M-2	Alt., h, km	$\Delta\varrho$ %	ARDC-59 Model, M-3	Alt., h, km	$\Delta\varrho$ %
$\bar{a}_0=-20{,}051$	130	−3,5	$\bar{a}_0=-17{,}961$	140	−5,5	$\bar{a}_0=-19{,}023$	140	−14
$\bar{h}_0=125700$	150	+4,5	$\bar{h}_0=103030$	155	+3	$\bar{h}_0=104000$	150	0
$\bar{\varkappa}=0{,}01449$	200	+3,5	$\bar{\varkappa}=0{,}018844$	180	+1	$\bar{\varkappa}=0{,}01594$	200	+4,5
	250	+4		200	−1		250	+4
	300	+5					300	−3
	350	−1,5					350	−0,5
	400	+0,5					400	+2,5
							500	+6,5
							700	+5

We will assume that further refinements of the atmospheric model will not lead to an appreciable change in the nature of the function, enabling us to use the quadratic parabola. Slight deviations in the model of ρ, like fluctuations, if their laws will be found, will subsequently be allowed for by introducing the appropriate corrections. /156

The literature contains several approximations for ρ or $\ln \rho$. The exponential law

$$\varrho=\varrho_0 e^{-\frac{h-h_0}{H}}, \tag{3.113}$$

is the most common,
where ρ_0 is the density at some reference altitude h_0

H is the altitude of the homogeneous atmosphere ($H = kT/mg$)
T is temperature in °K
m is molecular weight, and
k is Boltzmann's constant.

On the other hand, H is the altitude to which it is necessary to ascend relative to h_0 in order for the density to be reduced by

e times. The constancy of H in this altitude range corresponds to constancy of temperature for uniform molecular composition of air. Hence we have the name "homogeneous atmosphere."

Actually, with variation in altitude both temperature and molecular composition of air change. Therefore H does not remain constant.

From Eq. (3.113) it follows that H can be considered as the derivative, that is,

$$H=\frac{-dh}{d\ln\varrho}.$$

On the other hand, based on Eq. (3.112) the derivative

$$\frac{dh}{d\ln\varrho}=-\frac{2}{\varkappa}\sqrt{h-\bar{h}_0},$$

whence

$$H=\frac{2}{\varkappa}\sqrt{h-\bar{h}_0}. \qquad (3.114)$$

In the altitude range 140-400 km H increases from 18 to 72 km for the M-1 model. In the following we will adopt it as the principal model. The function is very abrupt and nonlinear. So the approximation of the density by function (3.113) with constant H cannot show the requisite accuracy.

At the same time, to obtain qualitative characteristics of the orbital elements as functions of air drag and a preliminary estimate of the accuracy of determining density by measured changes in orbital elements, the exponential law has wholly justified itself [70].

Among the other approximations we should note the function /157

$$\varrho=\varrho_1\frac{\varkappa}{\left(1+\frac{y-y_0}{d}\right)^k}, \qquad (3.115)$$

which was used in [47].

Use of this function made it possible even before the launch of the first satellite to develop for the first time the theory

of determining the lifetime of an AES and to calculate on an electronic computer a network of curves from which the lifetime of a satellite can be easily determined if its ballistic coefficient and the initial apogee and perigee altitudes are known. By using the Mitra atmospheric model[3], which as shown by subsequent satellite launches, gives greatly overstated density values at low altitudes and understated density values at altitudes above 240 km, in determining lifetimes from this network very approximate results were obtained.

As for the actual function (3.115), it is more complex than (3.112) and, as noted by the authors, gives much larger approximation errors (to 15 percent). This latter comment can also be made of the functions used in [70, 27] when they were employed for large altitude ranges.

Integration of Equations of Motion Within a Single Revolution

To obtain functions of changes in orbital elements over prolonged time intervals, it is convenient to use the technique of separate integration of the equations of motion proposed in [61].

First integration is carried out within a single revolution. Then the increments in orbital elements obtained are assumed to be derivatives of these elements with respect to a new variable -- the number of revolutions. This replacement of increments by derivatives has proven quite warranted. However, as shown by calculations, in later revolutions the errors under this method increased to the extent that it is necessary to resort to ordinary methods of integrating the equations of motion.

We will adopt as the initial equations the following two equations in osculating elements -- for the orbital parameter and eccentricity:

$$\left.\begin{aligned} \frac{dp}{d\vartheta} &= \frac{2\gamma_1}{fM} r^3 T; \\ \frac{de}{d\vartheta} &= \frac{r^2\gamma_1}{fM}\left[S\sin\vartheta + \cos\vartheta\left(1+\frac{r}{p}\right)T + e\frac{r}{p}T\right]. \end{aligned}\right\} \qquad (3.116)$$

[3] S. K. Mitra, Verkhnyaya atmosfera [The Upper Atmosphere], Foreign Literature Publishing House, 1955.

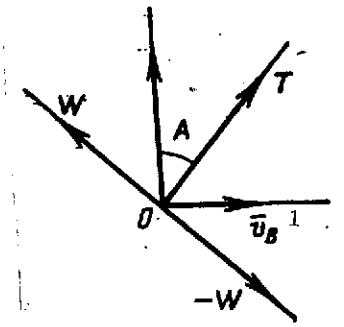

Fig. 3.5. Velocity of atmosphere rotating with the Earth in the AES-bound coordinate system
Key: 1. $\bar{v}_a$

In these equations the components of the perturbing air drag T and S are of the form [61] /158

$$S = -\frac{1}{2} b\varrho v_{\text{rel}} v_r; \qquad (3.117)$$

$$T = -\frac{1}{2} b\varrho v_{\text{rel}} (v_n - \Omega r \cos i), \qquad (3.118)$$

where b is the deceleration factor related to satellite mass (ballistic coefficient), that is,

$$b = \frac{c_x S_M}{m};$$

v_{rel} is the satellite velocity relative to the atmosphere rotating together with the Earth, and
Ω is the angular velocity of rotation of the Earth.

These formulas are not difficult to obtain if we consider the motion of a satellite relative to the atmosphere in the horizontal plane (Fig. 3.5).

The velocity of air v_a at latitude ϕ for the satellites considered

$$v_a = \Omega r \cos\varphi$$

is easterly in direction and is subtracted vectorially from the satellite velocity (absolute). As a result, we get the desired relative velocity

$$\bar{v}_{\text{rel}} = \bar{v} - \bar{v}_a.$$

By projecting the velocity v_{rel} onto the orbital axes, we get

$$v_{\text{rel}\,S} = v_r,$$
$$v_{\text{rel}\,T} = v_n - v_a \sin A,$$
$$v_{\text{rel}\,W} = v_a \cos A,$$

where A is the azimuth of the direction of the absolute velocity, and
v_r and v_n are the components of the absolute velocity in the directions of the satellite radius-vector and the transversal, respectively.

From spherical trigonometry we know that cos ϕ sin A = cos i, and cos ϕ cos A = sin i cos u. By replacing sin A and cos A in the expressions for $v_{rel\ T}$ and $v_{rel\ W}$, we get $v_{rel\ T} = v_n - \Omega r \cos i$ and $v_{rel\ W} = \Omega r \sin i \cos u$.

By projecting the component air drag forces - $1/2\ b\rho v^2_{rel}$ /159 onto the orbital axes, we arrive at the expressions (3.17) and (3.18) written for S and T. In addition, we have

$$W = -\frac{b}{2} \varrho v_{\text{rel}} \Omega r \sin i \cos u. \tag{3.119}$$

In contrast to the component T, the lateral component W is periodic. Its effect on satellite motion is very slight. The influence of atmospheric rotation on the component T is much more appreciable, being nearly constant in nature.

Actually, the transversal component depends only on cos i, which remains virtually unchanged, and on the radius-vector r. If in all cases we assume $r = r_\pi$, the errors in determining the component T when the satellite is moving in an elliptical orbit will be negligibly small. This arises from the rapid decrease in density ρ (and, therefore, in T) with increase in flight altitude. Over the sections of an orbit with altitude of only 100 km above the perigee altitude, air density is less than 10 percent of the density at the perigee. And since the actual influence of the atmospheric rotation does not exceed 5 percent of the influence of total air drag, the air will not be more than 0.5 percent. Obviously, this error can be neglected and in all cases we can allow for the rotation of the Earth by an appropriate change in the ballistic coefficient in Eq. (3.118):

$$T = -\frac{1}{2} b' \varrho v_{\text{rel}} v_n, \tag{3.120}$$

where

$$b' = b\left(1 - \frac{\omega_3 r_\pi}{v} \cos i\right);$$

v_n is the normal velocity component, and

r_π and v_n are assumed to be equal to their perigee values.

The relative velocity can also be expressed in terms of the absolute velocity, multiplied by some constant coefficient. Obviously, in this case we have have

$$v_{rel}^2 = v_r^2 + (v_n - \Omega r \cos i)^2 + \Omega^2 r^2 \sin^2 i \cos^2 u \qquad (3.121)$$

or

$$v_{rel}^2 = v^2 - 2v_n \Omega r \cos i + \Omega^2 r^2 \cos^2 i + \Omega^2 r^2 \sin^2 i \cos^2 u =$$
$$= v^2 - 2\sqrt{v^2 - v_r^2}\,\Omega r \cos i + \Omega^2 r^2 \cos^2 i + \Omega^2 r^2 \sin^2 i \cos^2 u.$$

Along with the summand $\Omega r \cos i$ for satellites, the vertical component of the absolute velocity v_r is a small quantity, particularly in the vicinity of the perigee. Therefore let us expand $\sqrt{v^2 - v_r^2}$ in a series, limiting outselves to the first term of the expansion. We get /160

$$v_{rel}^2 = v^2 \left[\left(1 - \frac{\Omega r \cos i}{v}\right)^2 + \frac{v_r^2}{v^2} \cdot \frac{\Omega r \cos i}{v} + \frac{\Omega^2 r^2}{v^2} \sin^2 i \cos^2 u \right].$$

We can neglect the last term in the square brackets, since it is less than $0.25 \cdot 10^{-4}$ in magnitude. To estimate the second term, let us make use of the expression

$$v_r = \sqrt{\frac{\mu}{p}}\, e \sin \vartheta.$$

Hence it is clear that v_r is $\frac{1}{e \sin \vartheta}$ times smaller than the characteristic satellite velocity $\sqrt{\frac{\mu}{p}}$. For both of the last terms to have the same order of smallness, we assume

$$\frac{v_r}{v} \leqslant \left(\frac{\Omega r}{v}\right)^{1/2},$$

that is, we must have $v_r/v < 0.2$.

Only when e > 0.2 do large values of the vertical velocity component appear and do so with separation from the perigee by

and altitudes exceeding the perigee by more than 1000 km.

By discarding both terms and replacing r and v by r_π and v_n, we find

$$v_{rel} = v\left(1 - \frac{\Omega r_\pi}{v_n}\cos i\right). \tag{3.122}$$

Finally, we have for the projections of the air drag S and T:

$$S = -\frac{1}{2} b' \varrho v v_r; \tag{3.123}$$

$$T = -\frac{1}{2} \bar{b} \varrho v v_n. \tag{3.124}$$

Here,

$$\bar{b} = b'\left(1 - \frac{\Omega r_\pi}{v_n}\cos i\right) = b\left(1 - \frac{\Omega r_\pi}{v_n}\cos i\right)^2.$$

As we can see, the ballistic coefficients b' and $\bar{b}$ for the components S and T differ by the multiplier $\left(1 - \frac{\Omega r_\pi}{v_n}\cos i\right)$. However, this difference is not appreciable since, as was explained, /161 S << T. Therefore in the following let us limit ourselves just to the value of the ballistic coefficient $\bar{b}$.

Let us return to the problem of integrating Eqs. (3.116). By substituting the values S and T we have found, we get

$$\left.\begin{aligned} \frac{dp}{d\vartheta} &= -\bar{b}\frac{r^3}{\mu}\varrho v v_n; \\ \frac{de}{d\vartheta} &= -\bar{b}\frac{r^2 \varrho v}{2\mu}\left[v_r \sin\vartheta + \cos\vartheta\left(1 + \frac{r}{p}\right)v_n + e\frac{r}{p}v_n\right]. \end{aligned}\right\} \tag{3.125}$$

Here we do not consider the multiplier γ_1.

As was shown in Section 3.1, the effect of multiplier γ_1 on satellite motion is negligibly small for elliptical orbits. For

near-circular orbits, this multiplier also need not be considered when we are solving the problem, in the first approximation.

Substituting into Eqs. (3.125)

$$\left.\begin{aligned} v &= \sqrt{\frac{\mu}{p}}\sqrt{1+2e\cos\vartheta+e^2};\\ v_r &= \sqrt{\frac{\mu}{p}}\,e\sin\vartheta;\\ v_n &= \sqrt{\frac{\mu}{p}}\,(1+e\cos\vartheta);\\ r &= \frac{p}{1+e\cos\vartheta}, \end{aligned}\right\} \tag{3.126}$$

we get

$$\frac{dp}{d\vartheta} = -\bar{b}_Q p^2\sqrt{1+2e\cos\vartheta+e^2}\;\frac{1}{(1+e\cos\vartheta)^2}; \tag{3.127}$$

$$\begin{aligned}\frac{de}{d\vartheta} &= -\bar{b}_Q\,\frac{p}{2}\sqrt{\frac{1+2e\cos\vartheta+e^2}{(1+e\cos\vartheta)^2}}\left\{e\sin^2\vartheta+\right.\\ &\left.+\left[\cos\vartheta\left(1+\frac{1}{1+e\cos\vartheta}\right)+\frac{e}{1+e\cos\vartheta}\right](1+e\cos\vartheta)\right\}=\\ &= -\bar{b}_Q p\sqrt{\frac{1+2e\cos\vartheta+e^2}{(1+e\cos\vartheta)^2}}(e+\cos\vartheta). \end{aligned} \tag{3.128}$$

Let us convert to the variable E (eccentric anomaly). From the equality

$$r=\frac{a(1-e^2)}{1+e\cos\vartheta}=a(1-e\cos E)$$

we can readily find /162

$$\cos\vartheta=\frac{\cos E-e}{1-e\cos E}$$

and

$$d\vartheta=\frac{\sqrt{1-e}}{1-e\cos E}\,dE.$$

Substituting the values cos and d and omitting the stroke at the coefficient b in Eq. (3.128), we find:

$$\frac{dp}{dE} = -bp^2\varrho\,\frac{(1+2e\cos\vartheta+e^2)^{1/2}}{(1+e\cos\vartheta)^2}\cdot\frac{\sqrt{1-e^2}}{1-e\cos E} =$$

$$= -ba^2\varrho(1-e^2)^{1/2}\left[\frac{2(1-e^2)}{1-e\cos E}-(1-e^2)\right]^{1/2}(1-e\cos E) =$$

$$= -ba^2(1-e^2)\varrho(1-e^2\cos^2 E)^{1/2},$$

or

$$\frac{dp}{dE} = -bpa\varrho(1-e^2\cos^2 E)^{1/2}. \tag{3.129}$$

Using similar transformations, we get

$$\frac{de}{dE} = -bp\varrho\left(\frac{1+e\cos E}{1-e\cos E}\right)^{1/2}\cos E. \tag{3.130}$$

We can find the density ρ, in accordance with Eqs. (3.112) and (3.129), from the expression

$$\varrho = Ae^{-\bar{x}\sqrt{a(1-e\cos E)-R-\bar{h}_0}}, \tag{3.131}$$

where $A = \bar{e}^{\bar{a}_0}$ is the density at the reference altitude $\bar{h}_0$, and

R is the Earth's radius for a point with latitude equal to the geographical latitude of the satellite at the given moment of time ($R = \bar{a}(1 - \bar{a}\sin^2\phi) = \bar{a}(1 - a\sin^2 i\sin^2 u)$).

Here

$$u = \omega + \vartheta;\quad \operatorname{tg}\frac{\vartheta}{2} = \sqrt{\frac{1+e}{1-e}}\operatorname{tg}\frac{E}{2}\Big).$$

Eqs. (3.129) and (3.130) cannot be directly integrated in their final form. Therefore it is best to use an expansion in powers of eccentricity e:

$$\left.\begin{aligned}\frac{dp}{dE} &= -bpa\varrho\left(1-\frac{1}{2}e^2\cos^2 E-\frac{1}{8}e^4\cos^4 E-\ldots\right);\\ \frac{de}{dE} &= -bp\varrho\Big(\cos E+e\cos^2 E+\frac{e^2}{2}\cos^2 E+\\ &\quad+\frac{e^3}{2}\cos^4 E+\frac{3}{8}e^4\cos^5 E+\ldots\Big).\end{aligned}\right\} \tag{3.132}$$

Similarly, for ω, Ω, and i we get /163

$$e\frac{d\omega}{dE}=-bp\varrho\left(1-e\cos E+e^2\cos^2 E\right)\sin E-e\frac{d\Omega}{dE}\cos i;$$

$$\frac{d\Omega}{dE}=-\frac{bp^{5/2}\varrho_3}{2\sqrt{\mu}}\varrho\left[\left(-e\cos E+\frac{1}{2}\cos 2E\right)\sin 2\omega+\right.$$

$$\left.+\left(-e\sin E+\frac{1}{2}\sin 2E\right)\cos 2\omega\right];$$

$$\frac{di}{dE}=-\frac{bp^{5/2}\varrho_3}{2\sqrt{\mu}}\sin i\cdot\varrho\left[\frac{1}{2}-e\cos E+\left(-e\cos E+\frac{1}{2}\cos 2E\right)\times\right.$$

$$\left.\times\cos 2\omega+\left(e\sin E-\frac{1}{2}\sin 2E\right)\sin 2\omega\right].$$

Let us write the expression for density ρ as

$$\varrho=Ae^{-c\sqrt{1-z\cos E}}, \qquad (3.133)$$

where

$$c=\varkappa\sqrt{a-R-\bar{h}_0};$$

$$z=\frac{ae}{a-R-\bar{h}_0}.$$

One feature of the function ρ is its rapid and very uneven variation with change in angle E. In the vicinity of the perigee the exponent $c\sqrt{1-z}$ is very large and Taylor or Fourier series for $e^{-c\sqrt{1-z\cos E}}$ converge very slowly. So it is best to single out the principal part of this function as a separate multiplier, by using an expansion in series for the rest.

For this purpose, first let us expand $\sqrt{1-z\cos E}$ by Newton's formula for the binomial:

$$f(E)=\sqrt{1-z\cos E}=1-\frac{z}{2}\cos E-\sum_{n=2}^{\infty}\frac{1\cdot 3\ldots(2n-3)}{2^n n!}z^n\cos^n E.$$

Since for any orbit [z cos E] < 1, the power series always converges.

Using the expansion in the Fourier series, for the same function f (E) we have /164

$$f(E)=\sqrt{1-z\cos E}=\frac{a_0}{2}+\sum_{k=1}^{\infty}a_k\cos kE,$$

where

$$a_k=\frac{2}{\pi}\int_0^{\pi}\sqrt{1-z\cos E}\cos kE\,dE=\frac{2}{\pi}\int_0^{\pi}\left[1-\frac{z}{2}\cos E-\right.$$
$$\left.-\sum_{n=2}^{\infty}\frac{1\cdot3\ldots(2n-3)}{\cdot\,2^n n!}z^n\cos^n E\right]\cos kE\,dE.$$

The Fourier series when expanded in cosines has a property of optimal convergence [38]. So it is best used for our case of a poorly converging series in the most important region, where E = 0 (vicinity of perigee).

By successively computing the coefficients of the Fourier series, we get

$$\frac{a_0}{2}=1-\frac{1}{2}\sum_{n=2}^{\infty}\frac{\prod_{\nu=2}^{n}(2\nu-3)}{n!\,2^{2n-1}}\binom{n}{\frac{n}{2}}z^n; \tag{3.134}$$

$$a_1=-\frac{z}{2}-\sum_{n=2}^{\infty}\frac{\prod_{\nu=2}^{n}(2\nu-3)}{n!\,2^{2n-1}}\binom{n}{\frac{n-1}{2}}z^n; \tag{3.135}$$

. . . . . .

$$a_k=-\sum_{n=2}^{\infty}\frac{\prod_{\nu=2}^{n}(2\nu-3)}{n!\,2^{2n-1}}\binom{n}{\frac{n-k}{2}}z^n. \tag{3.136}$$

The resulting series in expanded form are as follows for the first coefficients:

$$\left.\begin{aligned}\frac{a_0}{2}&=1-\frac{z^2}{2^4}-\frac{1\cdot3\cdot5}{2^{10}}z^4-\frac{1\cdot3\cdot5\cdot7}{2^{14}}z^6-\ldots;\\ a_1&=-\frac{z}{2}\left[1+\frac{3}{2^5}z^2+\frac{1\cdot5\cdot7}{2^{10}}z^4+\frac{1\cdot3\cdot5\cdot7\cdot11}{2^{16}}z^6+\ldots\right];\end{aligned}\right\} \tag{3.137}$$

$$a_2 = -\frac{z^2}{24}\left[1+\frac{5}{24}z^2+\frac{5\cdot7\cdot9}{2^{11}}z^4+\frac{3\cdot7\cdot11\cdot13}{2^{15}}z^6+\ldots\right];$$
$$a_3 = -\frac{z^3}{2^6}\left[1+\frac{5\cdot7}{2^6}z^2+\frac{7\cdot9\cdot11}{2^{11}}z^4+\frac{7\cdot11\cdot13\cdot15}{2^{16}}z^6+\ldots\right];$$
$$a_4 = -\frac{z^4}{2^{10}}\left[5+\frac{7\cdot9}{24}z^2+\frac{3\cdot7\cdot11\cdot13}{2^{10}}z^4+\frac{3\cdot5\cdot11\cdot13\cdot17}{2^{14}}z^6+\ldots\right]. \quad (3.137)\ \text{cont.}$$

Let us show that z cannot be more than unity, that is, /165

$$z=\frac{ae}{a-R-\bar{h}_0}=\frac{h_a-h_\pi}{h_a+h_\pi-2\bar{h}_0}\leqslant 1.$$

With increase in apogee altitude, $z \to 1$, and also for any assigned apogee, but with decrease in h_π down to $\bar{h}_0$ (the maximum admissible case) $z \to 1$.

For z = 1, we can easily obtain the majorant series, which can prove useful for any kind of estimate:

$$a_{k\,maj} = -\frac{\sqrt{2}}{\pi}\left[\frac{\cos\left(\frac{1}{2}-k\right)E}{\frac{1}{2}-k}+\frac{\cos\left(\frac{1}{2}+k\right)E}{\frac{1}{2}+k}\right]_0^\pi = \frac{4\sqrt{2}}{\pi(1-4k^2)}. \quad (3.138)$$

In accordance with these formulas, now air density can be represented thusly:

$$\varrho = A\,e^{-c\sqrt{1-z\cos E}} = A\exp\left(-\frac{ca_0}{2}\right)\exp(-ca_1\cos E)\times$$
$$\times\exp\left(-c\sum_{k=2}^{\infty}a_k\cos kE\right). \quad (3.139)$$

It is best to write the last exponent as a trigonometric series. To do this, let us first expand the function $\Phi(E)=\exp\left(-c\sum_{k=2}^{\infty}a_k\cos kE\right)$ in a Taylor series, which enables us to find the coefficients of the Fourier series in the simplest way:

$$\Phi(E)=\exp\left(-c\sum_{k=2}^{\infty}a_k\cos kE\right)=1-c\sum_{k=2}^{\infty}a_k\cos kE+$$
$$+\frac{c^2}{2}\left(\sum_{k=2}^{\infty}a_k\cos kE\right)^2-\ldots+(-1)^n\frac{c^n}{n!}\left(\sum_{k=2}^{\infty}a_k\cos kE\right)^n+\ldots=$$
$$=1-c\sum_{k=2}^{\infty}a_k\cos kE+\frac{c^2}{2!}\sum_{i,j=2}^{\infty}a_ia_j\cos iE\cos iE+\ldots$$
$$\ldots+(-1)^n\frac{c^n}{n!}\sum_{i,j,\ldots,n=2}^{\infty}a_ia_j\ldots a_n\cos iE\cos jE\ldots\cos nE+\ldots$$

Let us replace the products of the cosines by sums, utilizing the relations /166

$$\cos\alpha_0\cos\alpha_1\ldots\cos\alpha_n=\frac{1}{2^n}[\cos(\alpha_0-\alpha_1-\ldots-\alpha_n)+$$
$$+\cos(\alpha_0-\alpha_1-\ldots+\alpha_n)+\cos(\alpha_0-\alpha_1-\ldots+\alpha_{n-1}-\alpha_n)\ldots$$
$$\ldots+\cos(\alpha_0+\alpha_1-\ldots-\alpha_n)+\cos(\alpha_0-\alpha_1-\ldots+\alpha_{n-1}+\alpha_n)+\ldots$$
$$\ldots+\cos(\alpha_0+\alpha_1+\ldots+\alpha_{n-1}-\alpha_n)+$$
$$+\cos(\alpha_0+\alpha_1+\ldots+\alpha_{n-1}+\alpha_n)]. \qquad (3.140)$$

Here α_0 = iE, α_1 = jE, ..., and α_n = nE.

As we can see from Eq. (3.140), any combination of signs of α affecting the value of the cosine is encountered once. Therefore, by introducing i = k_1, j = k_2, ..., and k_n, we have

$$\Phi(E)=1-c\sum_{k_1=2}^{\infty}a_{k1}\cos k_1E+\frac{c^2}{2!}\sum_{k_1,k_2=2}^{\infty}a_{k_1}a_{k_2}\cos k_1E\cos k_2E+\ldots$$
$$\ldots+(-1)^n\frac{c^n}{n!}\sum_{k_1,k_2,\ldots,k_n=2}^{\infty}a_{k_1}a_{k_2}\ldots a_{k_n}\cos k_1E\cos k_2E\ldots\cos k_nE+$$
$$+\ldots=1-c\sum_{k_1=2}^{\infty}a_{k_1}\cos k_1E+$$

$$+\frac{c^2}{2\cdot 2!}\sum_{k_1,k_2=2}^{\infty} a_{k_1}a_{k_2}[\cos(k_2-k_1)E+\cos(k_2+k_1)E]+\ldots$$

$$\ldots+(-1)^n\frac{c^n}{2^{n-1}n!}\sum_{k_1,k_2,\ldots,k_n=2}^{\infty} a_{k_1k_2}\ldots a_{k_n}[\cos(k_1-k_2-\ldots-k_n)E+$$

$$+\cos(k_1-k_2-\ldots+k_n)E+\cos(k_1-k_2-\ldots+k_{n-1}-k_n)E+\ldots$$

$$\ldots+\cos(k_1+k_2+\ldots+k_{n-1}-k_n)E+$$

$$+\cos(k_1+k_2+\ldots+k_{n-1}+k_n)E]+\ldots=\frac{b_0}{2}+\sum_{i=1}^{\infty} b_i\cos iE.$$

The coefficients of the Fourier series b_i can be found from the formulas

$$b_i=\frac{2}{\pi}\int_0^{\pi}\Phi(E)\cos iE\,dE.$$

In integration it is important to remember that the integral /167

$$\int_0^{\pi}\cos(k_1\mp k_2\mp\ldots\mp k_n)\cos i\,E\,dE=0,$$

if

$$k_1\mp k_2\mp\ldots\mp k_n\neq i,$$

and it is equal to $\pi/2$ if

$$k_1\mp k_2\mp\ldots\mp k_n=i.$$

Here the different signs in front of the summands denote all possible nonrepeating combinations of the signs "+" and "-" in the sums of indexes k_j (j = 1, 2, ..., n) appearing under the sign of the cosine.

The general form of the first coefficients b_i is:

$$\frac{b_0}{2}=1+\frac{c^2}{2\cdot 2!}\sum_{k_1=2}^{\infty}a_{k_1}^2-\frac{c^3}{2^2\cdot 3!}\sum_{k_1,k_2,k_3=2}^{\infty}a_{k_1}a_{k_2}a_{k_3}+\ldots$$
$$\ldots+(-1)^n\frac{c^n}{2^n n!}\sum_{k_1,k_2,\ldots,k_n=2}^{\infty}a_{k_1}a_{k_2}\ldots a_{k_n}+\ldots. \qquad (3.141)$$

Part of the summands will be equal to zero. For the terms of the series not equal to zero, in accordance with the foregoing the following conditions are satisfied:

for the third summand:

$$\left.\begin{aligned} &1)\ k_1-k_2-k_3=0;\\ &2)\ k_1-k_2+k_3=0;\\ &3)\ k_1+k_2-k_3=0; \end{aligned}\right\} \qquad (3.142)$$

for the n-th term:

$$\left.\begin{aligned} &1)\qquad k_1-k_2-\ldots-k_n=0;\\ &2)\qquad k_1-k_2-\ldots+k_n=0;\\ &\ldots\ldots\ldots\ldots\ldots\\ &2^{n-1}-1)\ k_1+k_2+\ldots-k_n=0. \end{aligned}\right\} \qquad (3.142')$$

For the series coefficient b_1 we have

$$b_1=\frac{c^2}{2\cdot 2!}\sum_{k_1,k_2=2}^{\infty}a_{k_1}a_{k_2}-\frac{c^3}{2^2\cdot 3!}\sum_{k_1,k_2,k_3=2}^{\infty}a_{k_1}a_{k_2}a_{k_3}+\ldots$$
$$\ldots+(-1)^n\frac{c^n}{2^{n-1}n!}\sum_{k_1,k_2,\ldots,k_n=2}^{\infty}a_{k_1}a_{k_2}\ldots a_{k_n}+\ldots. \qquad (3.143)$$

The conditions for b_1 are /168

$$\left.\begin{aligned} &1)\ |k_1-k_2|=1;\\ &2)\ |k_1-k_2-k_3|=1;\\ &\quad |k_1-k_2+k_3|=1;\\ &\quad |k_1+k_2-k_3|=1;\\ &\ldots\ldots\ldots\ldots\\ &n-1)|k_1-k_2-\ldots-k_n|=1;\\ &\quad \ldots\ldots\ldots\\ &\quad |k_1+k_2+\ldots-k_n|=1. \end{aligned}\right\} \qquad (3.144)$$

The coefficients b_2 and b_3 were also computed by Eqs. (3.142), but the conditions in the right-hand parts contain the numbers 2 and 3, respectively.

The coefficient b_4 was similarly computed, but to the first conditions is added one more:

$$k_1 + k_2 = 4.$$

The following conditions will be added for the subsequent coefficients b_i:

$$k_1 + k_2 + \ldots + k_p = i,$$

where $2 \leq p \leq E(i/2)$, and p takes on all possible values that lie within these limits.

Let us write out the first coefficients b_i obtained by using conditions (3.142) and (3.144):

$$\left.\begin{aligned}
&\frac{b_0}{2} = 1 + \frac{c^2}{2\cdot 2!}(a_2^2 + a_3^2 + \ldots) - \frac{c^3}{2^2\cdot 3!}(3a_2^2a_4 + 6a_2a_3a_5 + \\
&\quad + 3a_3^2a_6 + 6a_2a_4a_6 + \ldots) + \frac{c^4}{2^3\cdot 4!}(3a_2^4 + \ldots) + \ldots; \\
&b_1 = \frac{c^2}{2\cdot 2!}(2a_2a_3 + 2a_3a_4 + \ldots) - \\
&\qquad - \frac{c^3}{2^2\cdot 3!}(3a_2^2a_3 + 6a_2a_3a_4 + \ldots) + \ldots \\
&\ldots\ldots\ldots\ldots\ldots\ldots\ldots\ldots
\end{aligned}\right\} \qquad (3.145)$$

Thus, the expression we seek for the atmospheric density becomes:

$$\varrho = Ae^{-c\sqrt{1-z\cos E}} = A_1 e^{a_1\cos E}\left(\frac{b_0}{2} + \sum_{i=1}^{\infty} b_i \cos iE\right).$$

Here

$$A_1 = A\exp\left(-\frac{ca_0}{2}\right);\ a_1 = -ca_1.$$

Specific values of the coefficients b_i were calculated based /169 on the formulas (3.145) presented. Depending on the required accuracy, a given number of terms can be retained. The more elongated the orbit, that is, the larger the c and z, the more terms are required. As an example coefficients b_i suitable for orbits having $c \leqslant 15$, which corresponds to $h_\alpha \leqslant 2000$ km, were found. It was found necessary to retain terms containing c^3.

The required number of coefficients b_i is 6-7. Here the last coefficients b_6 and b_7 represent only 1-2 percent of the principal term of the expansion of the density function.

The resulting coefficients b_i were:

$$\begin{aligned}
\frac{b_0}{2} &= 1 + c^2\frac{z^4}{2^{10}}\left(1+\frac{11}{24}z^2+\frac{61}{27}z^4\right)+5c^3\frac{z^8}{2^{21}}\left(1+\frac{1}{10}c\right);\\
b_1 &= c^2\frac{z^5}{2^{11}}\left(1+\frac{15}{24}z^2+\frac{85}{27}z^4\right)+c^3\frac{z^7}{2^{17}}\left(1+\frac{75}{26}z^2\right);\\
b_2 &= c\frac{z^2}{2^4}\left(1+\frac{5}{24}z^2+\frac{79}{29}z^4\right)+c^2\frac{z^6}{2^{15}}(5+c)\left(1+\frac{9}{8}z^2\right);\\
b_3 &= c\frac{z^3}{2^6}\left(1+\frac{35}{26}z^2+\frac{87}{26}z^4\right)+c^3\frac{z^7}{2^{16}}\left(1+\frac{75}{26}z^2\right);\\
b_4 &= 5c\frac{z^4}{2^{10}}\left(1+\frac{7}{9}z^2\right)+c^3\frac{z^4}{2^{10}}\left(1+\frac{5}{23}z^2\right)+5c^3\frac{z^8}{2^{20}};\\
b_5 &= 7c\frac{z^5}{2^{12}}(1+z^2)+c^3\frac{z^5}{2^{11}}\left(1+\frac{55}{26}z^2+\frac{85}{27}z^4\right);\\
b_6 &= c\frac{z^6}{2^{15}}(1+z^2)\left(21+7c+\frac{1}{3}c^2\right);\\
b_7 &= 3c^2\frac{z^7}{2^{15}}\left(1+\frac{4}{3}z^2\right)+c^3\frac{z^7}{2^{17}}\left(1+\frac{75}{26}z^2\right).
\end{aligned} \tag{3.147}$$

Now it remains to substitute Eq. (3.146) for density ρ into the equations of motion (3.132) and to integrate the latter within a single revolution:

$$\begin{aligned}
\frac{dp}{dE} &= -bpaA_1e^{a_1\cos E}\left(\frac{b_0}{2}+\sum_{i=1}^{\infty}b_i\cos iE\right)\times\\
&\times\left(1-\frac{1}{2}e^2\cos^2E-\frac{1}{8}e^4\cos^4E-\ldots\right);\\
\frac{de}{dE} &= -bpA_1e^{a_1\cos E}\left(\frac{b_0}{2}+\sum_{i=1}^{\infty}b_i\cos iE\right)\times\\
&\times\left(\cos E+e\cos^2E+\frac{e^2}{2}\cos^3E+\frac{e^3}{2}\cos^4E+\frac{3}{8}e^4\cos^5E+\ldots\right).
\end{aligned} \tag{3.148}$$

After multiplying the series and replacing the products and powers of the cosines by the cosines of the multiples of the angles, we get /170

$$\left.\begin{aligned}\frac{dp}{dE} &= -bpaA_1 e^{a_1\cos E}(B_0+B_1\cos E+B_2\cos 2E+\\ &\quad +B_3\cos 3E+\ldots);\\ \frac{de}{dE} &= -bpA_1 e^{a_1\cos E}(D_0+D_1\cos E+D_2\cos 2E+\\ &\quad +D_3\cos 3E+\ldots),\end{aligned}\right\} \qquad (3.149)$$

where

$$B_0=\frac{1}{2}\left[\left(1-\frac{e^2}{4}-\ldots\right)b_0-\left(\frac{e^2}{4}+\ldots\right)b_2-\ldots\right];$$

$$B_1=\frac{1}{2}\left[2\left(1-\frac{e^2}{4}-\ldots\right)b_1-\left(\frac{e^2}{4}+\ldots\right)b_1-\left(\frac{e^2}{4}+\ldots\right)b_3-\ldots\right];$$

$$B_2=\frac{1}{2}\left[2\left(1-\frac{e^2}{4}-\ldots\right)b_2-\left(\frac{e^2}{4}+\ldots\right)b_0-\left(\frac{e^2}{4}+\ldots\right)b_4-\ldots\right];$$

$$B_3=\frac{1}{2}\left[2\left(1-\frac{e^2}{4}-\ldots\right)b_3-\left(\frac{e^2}{4}+\ldots\right)b_1-\left(\frac{e^2}{4}+\ldots\right)b_5-\ldots\right];$$

$$B_4=\frac{1}{2}\left[2\left(1-\frac{e^2}{4}-\ldots\right)b_4-\left(\frac{e^2}{4}+\ldots\right)b_2-\left(\frac{e^2}{4}+\ldots\right)b_6-\ldots\right];$$

$$B_5=\frac{1}{2}\left[2\left(1-\frac{e^2}{4}-\ldots\right)b_5-\left(\frac{e^2}{4}+\ldots\right)b_3-\left(\frac{e^2}{4}+\ldots\right)b_7-\ldots\right];$$

. . . . . .

$$D_0=\frac{1}{2}\left[\left(1+\frac{3}{8}e^2+\ldots\right)b_1+\left(\frac{e}{2}+\frac{3e^3}{16}+\ldots\right)b_0+\right.$$
$$\left.+\left(\frac{e}{2}+\frac{e^3}{4}+\ldots\right)b_2+\left(\frac{e^2}{8}+\ldots\right)b_3+\left(\frac{e^3}{16}+\ldots\right)b_4+\ldots\right];$$

$$D_1=\frac{1}{2}\left[\left(1+\frac{3}{8}e^2+\ldots\right)b_0+\left(1+\frac{1}{2}e^2\ldots\right)b_2+\right.$$
$$\left.+\left(\frac{3}{2}e+\frac{5}{8}e^3+\ldots\right)b_1+\left(\frac{e}{2}+\frac{5}{16}e^3+\ldots\right)b_3+\left(\frac{e^2}{8}+\ldots\right)b_4+\ldots\right];$$

$$D_2=\frac{1}{2}\left[\left(1+\frac{3}{8}e^2+\ldots\right)b_3+\left(1+\frac{1}{2}e^2+\ldots\right)b_1+\right.$$
$$+\left(e+\frac{7}{16}e^3+\ldots\right)b_2+\left(\frac{e}{2}+\frac{e^3}{4}+\ldots\right)b_0+\left(\frac{e}{2}+\frac{e^3}{4}+\ldots\right)b_4+$$
$$\left.+\left(\frac{e^2}{8}+\ldots\right)b_5+\ldots\right]; \qquad /171$$

$$D_3=\frac{1}{2}\left[\left(1+\frac{3}{8}e^2+\ldots\right)b_4+\left(1+\frac{3}{8}e^2+\ldots\right)b_2+\right.$$
$$\left.+\left(e+\frac{3}{8}e^3+\ldots\right)b_3+\left(\frac{e}{2}+\frac{e^3}{4}+\ldots\right)b_5+\left(\frac{e^2}{8}+\ldots\right)b_0+\right.$$

$$+\left(\frac{e}{2}+\frac{5e^3}{16}+\ldots\right)b_1+\left(\frac{e^2}{8}+\ldots\right)b_6+\ldots\Big];$$

$$D_4=\frac{1}{2}\Big[\left(1+\frac{3}{8}e^2+\ldots\right)b_5+\left(1+\frac{3}{8}e^2+\ldots\right)b_3+$$
$$+\left(\frac{e}{2}+\ldots\right)b_2+\left(\frac{e}{2}+\ldots\right)b_4+\left(\frac{e}{2}+\ldots\right)b_6+\left(\frac{e^2}{8}+\ldots\right)b_1+$$
$$+\left(\frac{e^2}{8}+\ldots\right)b_7+\ldots\Big];$$

$$D_5=\frac{1}{2}\Big[\left(1+\frac{3}{8}e^2+\ldots\right)b_6+\left(1+\frac{3}{8}e^2+\ldots\right)b_4+$$
$$+\left(\frac{e}{2}+\ldots\right)b_3+\left(\frac{e}{2}+\ldots\right)b_5+\left(\frac{e}{2}+\ldots\right)b_7+\left(\frac{e^2}{8}+\ldots\right)b_2+\ldots\Big];$$

$$D_6=\frac{1}{2}\Big[\left(1+\frac{3}{8}e^2+\ldots\right)b_7+\left(1+\frac{3}{8}e^2+\ldots\right)b_5+$$
$$+\left(\frac{e}{2}+\ldots\right)b_4+\left(\frac{e}{2}+\ldots\right)b_6+\left(\frac{e^2}{8}+\ldots\right)b_3+\ldots\Big];$$

. . . . . .

Thus, the differential equations have been reduced to a form that enables them to be integrated if we use the integral representation of the Bessel functions of an imaginary argument

$$I_n(x)=\frac{1}{\pi}\int_0^{\pi}e^{x\cos\varphi}\cos n\varphi d\varphi.$$

Integrating these equations from 0 to 2π, that is, in a single satellite revolution around the Earth (relative to the perigee), we get expressions for the increments in the orbital parameter and eccentricity that can be taken as derivatives of the orbital elements p and e in terms of the number of revolutions n:

$$\Delta p=\frac{dp}{dn}=-2\pi bA_1pa\,[B_0I_0(\alpha_1)+B_1I_1(\alpha_1)+$$
$$+B_2I_2(\alpha_1)+B_3I_3(\alpha_1)+\ldots]^4; \qquad (3.150)$$

$$\Delta e=\frac{de}{dn}=-2\pi bA_1p\,[D_0I_0(\alpha_1)+D_1I_1(\alpha_1)+$$
$$+D_2I_2(\alpha_1)+D_3I_3(\alpha_1)+\ldots]. \qquad (3.151)$$

---

[4] Here and in the following in this chapter (α_1) is the functional dependence of I on α_1.

The increments of the other orbital elements dependent only on p and e can be readily determined from the familiar formulas in elliptical theory. For example, the increments (or derivatives in n) of the semi-major axis a, period T, and also the perigee and apogee altitudes can be calculated by the formulas: /172

$$\Delta a=\frac{p}{1-e^2}\left(\frac{\Delta p}{p}+\frac{2e}{1-e^2}\Delta e\right); \tag{3.152}$$

$$\Delta T=\frac{3\pi}{\sqrt{\mu}}a^{1/2}\Delta a=\frac{3\pi}{\sqrt{\mu}}\frac{p^{3/2}}{(1-e^2)^{3/2}}\left(\frac{\Delta p}{p}+\frac{2e}{(1-e^2)}\Delta e\right); \tag{3.153}$$

$$\Delta r_{\pi}=\frac{p}{1+e}\left(\frac{\Delta p}{p}-\frac{\Delta e}{1+e}\right); \tag{3.154}$$

$$\Delta r_{a}=\frac{p}{1-e}\left(\frac{\Delta p}{p}+\frac{\Delta e}{1-e}\right). \tag{3.155}$$

Based on Eqs. (3.150) and (3.151) the quantities Δp and Δe can be calculated for orbits with any eccentricities. However, for large eccentricities (practically speaking, when e > 0.5), the number of expansion terms that have to be retained when calculating the coefficients B_i and D_i (and the number of the coefficients as such) becomes too large. We can significantly improve the convergence of the series for large e if we use a procedure employed in [69]. Under this procedure, let us replace Eqs. (3.150) and (3.151) with their equivalent expressions:

$$\left.\begin{aligned}
\frac{dp}{dn}&=-2\pi bA_1pa\{(B_0+B_1+B_2+\ldots)I_0(\alpha_1)+\\
&\quad+B_1[I_1(\alpha_1)-I_0(\alpha_1)]+B_2[I_2(\alpha_1)-I_0(\alpha_1)]+\\
&\quad+B_3[I_3(\alpha_1)-I_0(\alpha_1)]+\ldots\};\\
\frac{de}{dn}&=-2\pi bA_1p\{(D_0+D_1+D_2+\ldots)I_0(\alpha_1)+\\
&\quad+D_1[I_1(\alpha_1)-I_0(\alpha_1)]+D_2[I_2(\alpha_1)-I_0(\alpha_1)]+\\
&\quad+D_3[I_3(\alpha_1)-I_0(\alpha_1)]+\ldots\}.
\end{aligned}\right\} \tag{3.156}$$

The sums of the coefficients appearing $I_0(\alpha_1)$ multiplied by A_1 are none other than the density of air at the perigee (ρ_{π}) related to $e^{\alpha 1}$ and multiplied for the first equation by $(1-e^2)^{1/2}$, and for the second -- by $\left(\frac{1+e}{1-e}\right)^{1/2}$ (see Eqs. (3.148), (3.129), and (3.130)). Let us introduce these quantities into the resulting equations:

$$\frac{dp}{dn} = -2\pi b p a \{\varrho_n e^{-\alpha_1}(1-e^2)^{1/2} I_0 + A_1 [B_1 (I_1 - I_0) + \ldots]\}; \quad (3.157)$$

$$\frac{de}{dn} = -2\pi b p \left\{p_\pi e^{-\alpha_1}\left(\frac{1+e}{1-e}\right)^{1/2} I_0 + A_1 [D_1 (I_1 - I_0) + \ldots]\right\}. \quad (3.158)$$

The values of the derivatives dp/dn and de/dn are determined mainly by the first term of the series. The remaining terms decrease compared to the corresponding terms in Eqs. (3.150) and (3.151) in proportion to the ratio /173

$$\left|\frac{I_i(\alpha_1) - I_0(\alpha_1)}{I_0(\alpha_1)}\right|.$$

The Bessel functions of a purely imaginary argument $I_i(\alpha_1)$ with an increase in the argument tend to the same quantity $\frac{e^{\alpha_1}}{\sqrt{2\pi\alpha_1}}$. So the difference between them decreases quite rapidly.

For circular orbits the formulas take on a form coinciding with the formulas derived under the assumption that the altitude of the homogeneous atmosphere is constant [69]:

$$\Delta p = \frac{dp}{dn} = -2\pi b a^2 \varrho_\pi = \Delta a; \quad (3.159)$$

$$\Delta e = \frac{de}{dn} = 0;$$

$$\Delta T = \frac{dT}{dn} = -\frac{6\pi^2}{\sqrt{\mu}} b a^{5/2} \varrho_\pi. \quad (3.160)$$

If we limit ourselves to the first power of the eccentricity, Eqs. (3.150) and (3.151) can be written in a form more suitable for computations:

$$\left.\begin{aligned}
\frac{dp}{dn} &= -2\pi b A_1 p^2 \left[\frac{b_0}{2} I_0(\alpha_1) + \sum_{i=1}^{7} b_i I_i(\alpha_1)\right]; \\
\frac{de}{dn} &= -2\pi b A_1 p \left\{\left[\frac{b_0}{2} I_1(\alpha_1) + \sum_{i=1}^{7} \frac{b_i}{2}(I_{i-1}(\alpha_1) + I_{i+1}(\alpha_1))\right] + \right. \\
&\quad + \frac{e}{2}\left[\frac{b_0}{2}(I_0(\alpha_1) + I_2(\alpha_1)) + \sum_{i=1}^{7} \frac{b_i}{2}(I_{|i-2|}(\alpha_1) + \right. \\
&\quad \left.\left. + 2I_i(\alpha_1) + I_{i+2}(\alpha_1))\right]\}.
\end{aligned}\right\} \quad (3.161)$$

Eqs. (3.161) can be used for computing the variation in orbital parameters due to air drag if the eccentricity is not more than 0.1-0.15. Here the error compared to the results of integrating the exact equations of motion as a rule does not exceed 2-3 percent.

To refine the developed theory and also to simplify its application in exact calculations, it is best to consider the influence of a variation in flight altitude on the deceleration of an AES in the atmosphere due to compression of the terrestrial ellipsoid. /174

The expression for the air density (3.112) can be represented as

$$\varrho = Ae^{-\bar{\varkappa}\sqrt{r+\Delta r-\bar{a}+\Delta\bar{a}-\bar{h}_0}},$$

where $r = a(1 - e\cos E)$ is the radius-vector of the AES relative to the Earth's center in accordance with elliptical theory

Δr is the increment in r at the instant of time t(E) caused by the influence of the oblateness of the Earth

$\bar{a}$ is the semi-major axis of the terrestrial ellipsoid

$\Delta\bar{a} = \bar{a}\,\bar{\alpha}\sin^2 i \sin^2 u$ is the increment in $\bar{a}$ in order to obtain the distance R from the Earth's center to the subsatellite point [satellite track] on the surface of a general terrestrial ellipsoid ($R = a - \Delta\bar{a}$), and

the algebraic sum $r + \Delta r - \bar{a} + \Delta\bar{a}$ is the flight altitude of the AES (the correction $(\Delta r + \Delta\bar{a})$ is not more than 10-15 km). Let us expand the exponent in a series, limiting ourselves to the linear term of the expansion

$$\varrho = Ae^{-\bar{\varkappa}\sqrt{r-\bar{a}-\bar{h}_0}}\cdot e^{-\frac{\bar{\varkappa}}{2}\cdot\frac{\Delta r+\Delta\bar{a}}{\sqrt{r-\bar{a}-\bar{h}_0}}}. \qquad (3.162)$$

Let us estimate the exponent of the corrective multiplier. When $\bar{\kappa} = 0.014\ m^{-1/2}$ and $\bar{h}_0 = 120{,}000$ m for an orbit with altitude $\approx$ 200 km, its maximum value is 0.3. On the average, this quantity will be much smaller. By an additional expansion in a power series, we get

$$e^{-\frac{\bar{\varkappa}}{2}\frac{\Delta r+\Delta\bar{a}}{\sqrt{r-\bar{a}-\bar{h}_0}}} = 1 - \frac{\bar{\varkappa}}{2}\frac{\Delta r + \Delta a}{\sqrt{r-\bar{a}-\bar{h}_0}}. \qquad (3.163)$$

The maximum error in density that can be realized at some point in a revolution due to the discarded quadratic term must not exceed 1.5 percent, which is acceptable.

Since density falls off very rapidly with altitude, it is sufficient to consider the layer in the area of a perigee with altitude ~ 100 km.

Considering higher layers in the corrective term would be tantamount to introducing quantities of the second order of smallness. This change in altitude changes the root by 40 percent. And the correction is reduced by one order of magnitude. At the perigee it is 90 percent of its value when $r = r_{\pi} + 100$ km. We will assume $r = r_{\pi}$ in computing the correction. We get

$$\rho=\bar{\rho}+\Delta\rho=Ae^{-\bar{\varkappa}\sqrt{r-\bar{a}-\bar{h}_0}}-A\frac{\bar{\varkappa}(\Delta r+\Delta\bar{a})}{2\sqrt{r_{\pi}-\bar{a}-\bar{h}_0}}e^{-\bar{\varkappa}\sqrt{r-\bar{a}-\bar{h}_0}}. \tag{3.164}$$

Based on Section 3.2 for orbits with small eccentricities /175

$$\Delta r+\Delta\bar{a}=\Delta p-p\Delta e\cos\vartheta-pe\Delta\omega\sin\vartheta+\bar{a}\bar{\alpha}\sin^2 i\sin^2 u, \tag{3.165}$$

where Δp, Δe, and $\Delta\omega$ are the changes in the orbital element with respect to some reference orbit that allows for the effect of the oblateness of the Earth on the orbit of the AES.

For the mean orbit proposed in Section 3.2, we have

$$\left.\begin{aligned}
&\Delta p=\frac{\varepsilon k}{\mu p}\cos 2u+\Delta_1;\\
&\Delta e=\frac{\varepsilon}{\mu p^2}\left[\left(1-\frac{5}{4}k\right)\cos\omega\cos u+\left(1-\frac{7}{4}k\right)\sin\omega\sin u+\right.\\
&\qquad\left.+\frac{7}{12}\bar{k}\cos(3u-\omega)\right]+\Delta_2;\\
&e\Delta\omega=\frac{\varepsilon}{\mu p^2}\left[-\left(1-\frac{5}{4}k\right)\sin\omega\cos u+\left(1-\frac{7}{4}k\right)\cos\omega\sin u+\right.\\
&\qquad\left.+\frac{7}{12}k\sin(3u-\omega)+e\left(2-\frac{5}{2}k\right)u\right]+\Delta_3.
\end{aligned}\right\} \tag{3.166}$$

Here $k = \sin^2 i$. The terms containing e to the first power and higher (except for the secular term in $\Delta\omega$) are discarded. The effect of eccentricity in accordance with the comment made on the role of variation in flight altitude is allowed for by the constant additions [augmentations]

$$\left.\begin{aligned}\Delta_1&=\frac{4\varepsilon k}{3\mu p}\,e\cos 2\omega;\\ \Delta_2&=\frac{\varepsilon}{2\mu p^2}\,e\left(1-\frac{3}{2}\,k+\frac{13}{4}\,k\cos 2\omega\right),\\ \Delta_3&=-\frac{\varepsilon}{2\mu p^2}\,e\left(1-\frac{13}{4}\,k\right)\sin 2\omega.\end{aligned}\right\}\qquad(3.167)$$

Substituting Δp, $e\Delta\omega$, and Δe into Eq. (3.165), after uncomplicated transformations we get

$$\Delta\varrho=-\bar{\varrho}\,\frac{\bar{\varkappa}}{2\sqrt{r_\pi-\bar{a}-\bar{h}_0}}\,(g_1+g_2\cos 2u-g_3 u\sin\vartheta),\qquad(3.168)$$

where

$$\left.\begin{aligned}g_1&=-\frac{\varepsilon}{\mu p}\left(1-\frac{3}{2}\,k\right)\left(1+\frac{e}{2}\right)-\frac{7}{24}\,\frac{\varepsilon k}{\mu p}\,e\cos 2\omega+\frac{1}{2}\,\bar{a}\bar{a}k;\\ g_2&=\left(\frac{\varepsilon}{6\mu p}-\frac{1}{2}\,\bar{a}\bar{a}\right)k;\\ g_3&=\frac{\varepsilon}{\mu p}\left(2-\frac{5}{2}\,k\right)e.\end{aligned}\right.$$

Referring to Eq. (3.146), we will have /176

$$\Delta\varrho=-A_2 e^{\alpha_1\cos E}\left(\frac{b_0}{2}+\sum_{i=1}^{\infty}b_i\cos iE\right)\times$$
$$\times(g_1+g_2\cos 2u-g_3 u\sin\vartheta),\qquad(3.169)$$

where

$$A_2=A_1\,\frac{\bar{\varkappa}}{2\sqrt{r_\pi-\bar{a}-\bar{h}_0}}.$$

Let us reduce the expression for $\Delta\rho$ to a single argument -- -- the eccentric anomaly E. Since the problem is to find a small correction for orbits with small eccentricities ($e < 0.1$-0.15), let us discard summands of the order of e in the periodic terms, and of the order of e^2 in the long-periodic terms. Here $\vartheta\approx E$.

Since

$$\cos 2u \approx \cos 2\omega \cos 2E - \sin 2\omega \sin 2E,$$
$$u = \omega + \vartheta \approx \omega + E,$$

we get

$$\Delta\varrho = -A_2 e^{\alpha_1 \cos E}\left\{\frac{b_0}{2}[g_1 + g_2 \cos 2(\omega+E) - g_3(\omega+E)\sin E] + \right.$$
$$\left. + \sum_{i=1}^{4} b_i \cos iE\,[g_1 + g_2 \cos 2(\omega+E) - g_3(\omega+E)\sin E]\right\}. \qquad (3.170)$$

Here the coefficients b_i coincide with the coefficients of (3.147). Analysis shows that it is sufficient to retain terms with coefficients to b_4 inclusively.

Let us proceed to integrating the equations of AES motion to Δp_{ob} and Δe_{ob}, that allow for the effect of the oblateness of the Earth.

Let us consider the products

1) $b_i e^{\alpha_1 \cos E} \cos iE \cos(2\omega + 2E)$ and 2) $b_i e^{\alpha_1 \cos E} \cos iE \cdot (\omega + E)\sin E.$

In case 1) we have

$$e^{\alpha_1 \cos E} \cos iE \cos(2\omega + 2E) = \frac{1}{2} e^{\alpha_1 \cos E}\{[\cos(i-2)E + $$
$$+ \cos(i+2)E]\cos 2\omega + [\sin(i-2)E - \sin(i+2)E]\sin 2\omega\}.$$

As was shown,

$$\int_0^{\pi} e^{\alpha_1 \cos E} \cos(i \pm 2)E\,dE = \pi I_{i\pm 2}(\alpha_1). \qquad (3.171)$$

The second integral $\int e^{\alpha_1 \cos E} \sin(i \pm 2)E\,dE$ is equal to zero when integrated within the limits 0 to 2π.

In case 2), the integrals for i = 0, 1, 2, and 3 are /177

$$
\begin{aligned}
&\int_0^{2\pi} e^{\alpha_1 \cos E}(\omega+E)\sin E dE = -\frac{2\pi}{\alpha_1}\left(e^{\alpha_1}-I_0\right);\\
&\int_0^{2\pi} e^{\alpha_1 \cos E}(\omega+E)\cos E \sin E dE = -\frac{2\pi}{\alpha_1}\left[\left(1-\frac{1}{\alpha_1}\right)\times\right.\\
&\qquad\left.\times e^{\alpha_1} - I_1 + \frac{1}{\alpha_1} I_0\right];\\
&\int_0^{2\pi} e^{\alpha_1 \cos E}(\omega+E)\cos 2E \sin E dE = -\frac{2\pi}{\alpha_1}\left[\left(1-\frac{4}{\alpha_1}+\frac{4}{\alpha_1^2}\right)e^{\alpha_1} - \right.\\
&\qquad\left. - I_2 + \frac{4}{\alpha_1} I_1 - \frac{4}{\alpha_1^2} I_0\right];\\
&\int_0^{2\pi} e^{\alpha_1 \cos E}(\omega+E)\cos 3E \sin E dE = -\frac{2\pi}{\alpha_1}\left[\left(1-\frac{9}{\alpha_1}+\frac{24}{\alpha_1^2} - \right.\right.\\
&\qquad\left.\left. - \frac{24}{\alpha_1^3}\right)e^{\alpha_1} - I_3 + \frac{6}{\alpha_1} I_2 - \frac{24}{\alpha_1^2} I_1 + \left(\frac{3}{\alpha_1}+\frac{24}{\alpha_1^3}\right) I_0\right].
\end{aligned}
\tag{3.172}
$$

Referring to these integrals when integrating the equations for p and e, we will have

$$
\Delta p_n(2\pi) = 2\pi b A_1 r a \left(\frac{\Delta B_0}{2} I_0 + \sum_{i=1}^{6} \Delta B_i I_i + c_1\right), \tag{3.173}
$$

where

$$
\begin{aligned}
\Delta B_0 &= \frac{A_2}{A_1}\left[\frac{b_0}{2} g_1 + \frac{b_2}{2} g_2 \cos 2\omega + \frac{g_3}{\alpha_1}\left(-\frac{b_0}{2} + \frac{b_1+3b_3}{\alpha_1} - \frac{4b_2}{\alpha_1^2} + \frac{24 b_3}{\alpha_1^3}\right)\right];\\
\Delta B_1 &= \frac{A_2}{A_1}\left[b_1 g_1 + \frac{b_1+b_3}{2} g_2 \cos 2\omega + \frac{g_3}{\alpha_1}\left(-b_1 + \frac{4}{\alpha_1} b_2 - \frac{24}{\alpha_1^2} b_3\right)\right];\\
\Delta B_2 &= \frac{A_2}{A_1}\left[b_2 g_1 + \frac{b_0+b_4}{2} g_2 \cos 2\omega + \frac{g_3}{\alpha_1}(-b_2 + 6b_3)\right];\\
\Delta B_3 &= \frac{A_2}{A_1}\left[b_3 g_1 + \frac{b_1}{2} g_2 \cos 2\omega - \frac{g_3}{\alpha_1} b_3\right];\\
\Delta B_4 &= \frac{A_1}{A_1}\left[b_4 g_1 + \frac{b_2}{2} g_2 \cos 2\omega\right];\\
\Delta B_5 &= \frac{A_2}{A_1} \cdot \frac{b_3}{2} g_2 \cos 2\omega;\\
\Delta B_6 &= \frac{A_2}{A_1} \cdot \frac{b_4}{2} g_2 \cos 2\omega;
\end{aligned}
$$

$$c_1=\frac{A_2}{A_1}\cdot\frac{g_3}{\alpha_1}e^{\alpha_1}\left[\frac{b_0}{2}+b_1\left(1-\frac{1}{\alpha_1}\right)+b_2\left(1-\frac{4}{\alpha_1}+\frac{4}{\alpha_1^2}\right)+\right.$$
$$\left.+b_3\left(1-\frac{9}{\alpha_1}+\frac{24}{\alpha_1^2}-\frac{24}{\alpha_1^3}\right)\right].$$

/178

Combining the correction $\Delta p_{ob}(2\pi)$ with the principal formula for Δp, we get

$$\Delta p=\frac{dp}{dn}=-2\pi bA_1pa\left[(B_0'+B_1'+B_2'+\ldots)\cdot I_0+B_1'(I_1-I_0)+\right.$$
$$\left.+B_2'(I_2-I_0)+\ldots-c_1\right], \qquad (3.174)$$

where

$$B_0'=B_0-\Delta B_0;$$
$$B_1'=B_1-\Delta B_1;$$
$$\ldots\ldots$$

A similar function for the change in eccentricity is of the form:

$$\Delta e=\frac{de}{dn}=-2\pi bA_1p\left[(D_0'+D_1'+D_2'+\ldots)I_0+D_1'(I_1-I_0)+\right.$$
$$\left.+D_2'(I_2-I_0)+\ldots-c_2\right], \qquad (3.175)$$

where

$$D_0'=D_0-\Delta D_0;$$
$$D_1'=D_1-\Delta D_1;$$
$$\ldots\ldots\ldots$$
$$\Delta D_0=\frac{A_2}{A_1}(\alpha_0'+\beta_0\cos 2\omega);$$
$$\Delta D_1=\frac{A_2}{A_1}(\alpha_1'+\beta_1\cos 2\omega);$$
$$\Delta D_2=\frac{A_2}{A_1}(\alpha_2'+\beta_2\cos 2\omega);$$
$$\Delta D_3=\frac{A_2}{A_1}(\alpha_3'+\beta_3\cos 2\omega);$$

$$c_2=\frac{A_2}{2A_1}\cdot\frac{g_3}{\alpha_1}\,e^{\alpha_1}\left[(b_0+b_2)\left(1-\frac{1}{\alpha_1}\right)+2b_1\left(1-\frac{2}{\alpha_1}+\frac{2}{\alpha_1^2}\right)+\right.$$
$$\left.+b_2\left(1-\frac{9}{\alpha_1}+\frac{24}{\alpha_1^2}-\frac{24}{\alpha_1^3}\right)\right];$$

/179

$$\alpha_0'=\frac{g_1}{2}\left(b_0\frac{e}{2}+b_1+b_2\frac{e}{2}\right)+\frac{g_3}{\alpha_1}\left(-\frac{b_1}{2}+\frac{b_0}{2\alpha_1}+\frac{2b_2}{\alpha_1}-\frac{2b_1}{\alpha_1^2}+\frac{12b_2}{\alpha_1^3}\right);$$

$$\alpha_1'=\frac{g_1}{2}\left(b_0+b_1e+b_2+b_3\frac{e}{2}\right)+\frac{g_3}{\alpha_1}\left(-\frac{b_0}{2}-\frac{b_2}{2}+\frac{2b_1}{\alpha_1}-\frac{12b_2}{\alpha_1^2}\right);$$

$$\alpha_2'=\frac{g_1}{2}\left(b_0\frac{e}{2}+b_1+b_2e+b_3+b_4\frac{e}{2}\right)+\frac{g_3}{\alpha_1}\left(-\frac{b_1}{2}+\frac{3b_2}{\alpha_1}\right);$$

$$\alpha_3'=\frac{g_1}{2}\left(b_1\frac{e}{2}+b_2+b_3e+b_4\right)-\frac{g_3b_2}{2\alpha_1};$$

$$\alpha_4'=\frac{g_1}{2}\left(b_2\frac{e}{2}+b_3+b_4e\right);$$

$$\alpha_5'=\frac{g_1}{2}\left(b_3\frac{e}{2}+b_4\right);\quad \alpha_6'=0;\quad \alpha_7'=0;$$

$$\beta_0=\frac{g_2}{4}\left(b_0\frac{e}{2}+b_1+b_2e+b_3+b_4\frac{e}{2}\right);$$

$$\beta_1=\frac{g_2}{4}\left(b_0+2b_1e+2b_2+\frac{3}{2}b_3e+b_4\right);$$

$$\beta_2=\frac{g_2}{4}\left(b_0e+2b_1+\frac{3}{2}b_2e+b_3+b_4e\right);$$

$$\beta_3=\frac{g_2}{4}\left(b_0+\frac{3}{2}b_1e+b_2+b_3e+b_4\right);$$

$$\beta_4=\frac{g_2}{4}\left(b_0\frac{e}{2}+b_1+b_2e+b_3+b_4e\right);$$

$$\beta_5=\frac{g_2}{2}\left(b_1\frac{e}{2}+b_2+b_3e+b_4\right);\quad \beta_6=\frac{g_2}{4}b_3;\quad \beta_7=\frac{g_2}{4}b_4.$$

Eqs. (3.175) and (3.176) were obtained for determining the changes in the orbital parameter Δp and in eccentricity Δe due to the influence of atmospheric drag, with reference to the oblateness of the Earth. They enable us to calculate these changes for an entire revolution based on the coefficients b_i (see (3.147)).

The results of deceleration over numerous revolutions is obtained by revolution-by-revolution summation or numerical integration with respect to the number of revolutions n.

For the M-1 atmospheric model, based on Eqs. (3.161) the lifetime of satellites with orbits having apogee altitude and

perigee altitude in the 155-515 km range and orbital inclination 65° was calculated. The coefficients b_i according to (3.147) and the ballistic coefficient 0.034 [5] were used in the calculations.

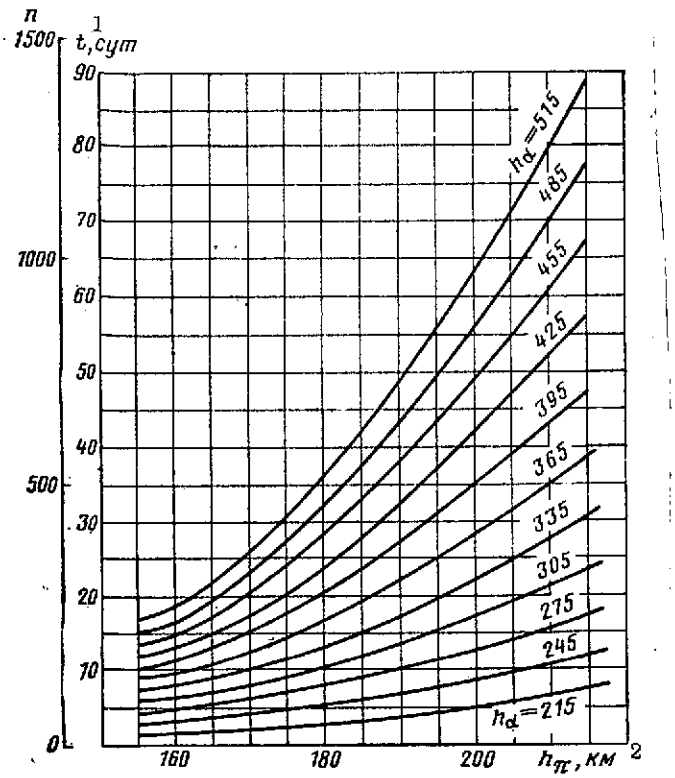

Fig. 3.6. Dependence of number of revolutions n and lifetime t of AES on apogee altitude h_α and perigee altitude h_π (b = = 0.034; i = 65°, and ω = 83°)
Key: 1. days
2. km

The Bessel functions /180 were computed by means of series. The following asymptotic expansions [52] were used for $\alpha_1 > 2$:

$$I_n(\alpha_1)=\frac{e^{\alpha_1}}{\sqrt{2\pi\alpha_1}}\left(1-\frac{4n^2-1}{8\alpha_1}-\frac{(4n^2-1)(4n^2-9)}{2!(8\alpha_1)^2}-\ldots\right). \quad (3.176)$$

The results of calculating the number of revolutions and the lifetime of satellites were plotted in the form of a grid of curves in Fig. 3.6 in the coordinates h_α (apogee altitude) and h_π (perigee altitude). Comparison with the exact method of numerical integration used for several orbits shows that the errors prove to be somewhat larger than would be expected, and reach 5-7 percent.

When the grids were used for satellites with ballistic coefficient b differing from the calculated value, it was necessary to modify the values of n or t_{da} [da = day] (calculated as ΣnT_{av} over individual sections of the orbit) taken from the graphs as inversely proportional to the ratio of this coefficient to 0.034.

[5] Here allowance was made for the change in the radius of the Earth under the perigee in accordance with the secular shift of the perigee (see Eq. (3.41)).

The calculations were made on an electronic computer. The machine-/181
time savings proved to be hundreds of times greater compared to the direct integration of the equations of motion, and tens of times greater compared to the method outlined in [39].

To verify the suitability of the M-1 atmospheric model (see Table 3.2) for calculating the descent of a satellite and its lifetime for flights lasting several years, the lifetime of the third Soviet satellite was calculated. The results showed good agreement between the calculated lifetime and the actual lifetime. A figure of 11,400 revolutions was obtained instead of 10,037 (a 13 percent overstatement). Therefore, the adopted atmospheric model is wholly suitable for calculating the changes in orbital elements over prolonged time intervals (at the period of the maximum 11-year cycle of solar activity).

Calculation of Parameters of AES Motion for an Arbitrary Point Within a Revolution ($e < 0.2$)

The above-presented method does not permit calculating the parameters of AES motion (p, e, ω, Ω, and i) within a revolution. However, this problem is often encountered, especially when one determines an orbit from measurements (see Chapter Four). Let us look at one of the possible methods of obtaining intermediate values of the changes in the orbital elements based on the expression of the derivatives dp/dE and de/dE in the form of trigonometric polynomials. Let us adopt as the initial equations Eqs. (3.148) with reference to the correction (3.170)

$$\left.\begin{aligned}
\frac{dp}{dE} &= -bpaA_1 e^{\alpha_1 \cos E}\left[\frac{b_0}{2}+\sum_{i=1}^{7} b_i \cos iE\right)\times \\
&\times\left\{1-\frac{A_2}{A_1}\left[g_1+ g_2\cos(2\omega+2E)\right]\right\}; \\
\frac{de}{dE} &= -bpA_1 e^{\alpha_1 \cos E}\left(\frac{b_0}{2}+\sum_{i=1}^{7} b_i \cos iE\right)\times \\
&\times\left\{1-\frac{A_2}{A_1}\left[g_1+ g_2\cos(2\omega+2E)\right]\right\}(e+\cos E).
\end{aligned}\right\| \qquad (3.177)$$

In Eqs. (3.177) the terms proportional to e^2 are discarded. In the second equation, e is used instead of $e\cos^2 E$; also discarded is a term proportional to $g_3(\omega + E)\sin E$, which corresponds to an error of the order of 1 percent.

Let us denote the right-hand members in Eq. (3.177) by f_1 and f_2, respectively. Then in accordance with the rule of

representing functions as a trigonometric polynomial, after integration we get /182

$$\Delta p = -bpaA_1\left[\frac{a'_{01}}{2}E + \sum_{m=1}^{n}\frac{a'_{m1}}{m}\sin mE - \sum_{m=1}^{n}\frac{b'_{m1}}{m}\cos mE - c'_1\right],$$
$$\Delta e = -bpA_1\left[\frac{a'_{02}}{2}E + \sum_{m=1}^{n}\frac{a'_{m2}}{m}\sin mE - \sum_{m=1}^{n}\frac{b'_{m2}}{m}\cos mE - c'_2\right], \qquad (3.178)$$

where

$$a'_{m1,2} = \frac{1}{\pi}\int_0^{\pi}[f_{1,2}(E) + f_{1,2}(-E)]\cos mE\,dE;$$
$$b'_{m1,2} = \frac{1}{\pi}\int_0^{\pi}[f_{1,2}(E) - f_{1,2}(-F)]\sin mE\,dE; \qquad (3.179)$$

c'_1 and c'_2 are the constants of integration calculated based on the initial value of the eccentric anomaly E_0.

Let us determine the coefficients a'_{m1} and b'_{m1}:

$$f_1(E) + f_1(-E) = 2e^{\alpha_1\cos E}\left(\frac{b_0}{2} + \sum_{i=1}^{7} b_i\cos iE\right)\times$$
$$\times\left[1 - \frac{A_2}{A_1}\left(g_1 + g_2\cos 2\omega\cos 2E\right)\right];$$
$$f_1(E) - f_1(-E) = 2e^{\alpha_1\cos E}\left(\frac{b_0}{2} + \sum_{i=1}^{7} b_i\cos iE\right)\times$$
$$\times\frac{A_2}{A_1}g_2\sin 2\omega\sin 2E;$$

$$a'_{m1} = \frac{2}{\pi}\int_0^{\pi} e^{\alpha_1\cos E}\left(\frac{b_0}{2} + \sum_{i=1}^{7} b_i\cos iE\right)\times$$
$$\times\left[1 - \frac{A_2}{A_1}\left(g_1 + g_2\cos 2\omega\cos 2E\right)\right]\cos mE\,dE;$$

or

$$a'_{m1}=\left(1-\frac{A_2}{A_1}g_1\right)\left[b_0 I_m(\alpha_1)+\sum_{l=1}^{7} b_l\left(I_{|l-m|}(\alpha_1)+I_{l+m}(\alpha_1)\right)\right]-$$
$$-\frac{A_2 g_2}{2A_1}\cos 2\omega\left[b_0\left(I_{|m-2|}(\alpha_1)+I_{m+2}(\alpha_1)\right)+\right.$$
$$\left.+\sum_{l=1}^{7} b_l\left(I_{|l-m+2|}(\alpha_1)+I_{|l+m-2|}(\alpha_1)+I_{|l-m-2|}(\alpha_1)+I_{l+m+2}(\alpha_1)\right)\right]. \quad (3.180)$$

The coefficient is

$$b'_{m1}=\frac{2}{\pi}\int_0^{\pi} e^{\alpha_1\cos E}\left(\frac{b_0}{2}+\sum_{l=1}^{7} b_l\cos lE\right)\times$$
$$\times\frac{A_2}{A_1}g_2\sin 2\omega\sin 2E\sin mE\,dE$$

or, after integration,

$$b'_{m1}=\frac{A_2 g_2}{2A_1}\sin 2\omega\left[b_0\left(I_{|m-2|}(\alpha_1)-I_{m+2}(\alpha_1)\right)+\right.$$
$$\left.+\sum_{l=1}^{7} b_l\left(I_{|l-m+2|}(\alpha_1)+I_{|l+m-2|}(\alpha_1)-I_{|l-m-2|}(\alpha_1)-I_{l+m+2}(\alpha_1)\right)\right]. \quad (3.181)$$

For the second equation, we have

$$a'_{m2}=ea'_{m1}+\frac{1}{\pi}\int_0^{\pi}\left[f_1(E)+f_1(-E)\right]\cos E\cos mE\,dE.$$

After integration, we get

$$a'_{m2}=a'_m e+\frac{1}{2}\left(1-\frac{A_2}{A_1}g_1\right)\left[b_0\left(I_{m-1}(\alpha_1)+I_{m+1}(\alpha_1)\right)+\right.$$
$$\left.+\sum_{l=1}^{7} b_l\left(I_{|l-m+1|}(\alpha_1)+I_{|l+m-1|}(\alpha_1)+I_{l-m-1}(\alpha_1)+I_{l+m+1}(\alpha_1)\right)\right]-\frac{A_2 g_2}{4A_1}\times \quad (3.182)$$
$$\times\cos 2\omega\left[b_0\left(I_{|m-3|}(\alpha_1)+I_{m+1}(\alpha_1)+I_{m-1}(\alpha_1)+I_{m+3}(\alpha_1)\right)+\right.$$
$$\left.+\sum_{l=1}^{7} b_l\left(I_{|l-m+3|}(\alpha_1)+I_{|l+m-3|}(\alpha_1)+I_{|l-m-1|}(\alpha_1)+\right.\right.$$
$$\left.\left.+I_{l+m+1}(\alpha_1)+I_{|l-m+1|}(\alpha_1)+I_{l+m-1}(\alpha_1)+I_{|l-m-3|}(\alpha_1)+I_{l+m+3}(\alpha_1)\right)\right].$$

Similarly, for the coefficient b'_{m2} we will have /184

$$b'_{m2}=b'_{m1}e+\frac{A_2g_2}{4A_1}\sin 2\omega\,[b_0(I_{|m-3|}(\alpha_1)-I_{m+1}(\alpha_1)+$$
$$+I_{m-1}(\alpha_1)-I_{m+3}(\alpha_1))+\sum_{i=1}^{7}b_i(I_{|i-m+3|}(\alpha_1)+I_{|i+m-3|}(\alpha_1)-$$
$$-I_{|i-m-1|}(\alpha_1)-I_{i+m+1}(\alpha_1)+I_{|i-m+1|}(\alpha_1)+I_{i+m-1}(\alpha_1)-$$
$$-I_{|i-m-3|}(\alpha_1)-I_{i+m+3}(\alpha_1))]. \qquad (3.183)$$

Calculation of the coefficients of the polynomials was made based on Eqs. (3.176) in the case when $\alpha_1 > 2$, and for small eccentricities ($\alpha_1 < 2$), using the formulas:

$$I_n(x)=\frac{\left(\frac{x}{2}\right)^n}{\Gamma(n+1)}+\frac{\left(\frac{x}{2}\right)^{n+2}}{1!\Gamma(n+2)}+\frac{\left(\frac{x}{2}\right)^{n+4}}{2!\Gamma(n+3)}+\cdots \qquad (3.184)$$

with reference to the rule of action with Bessel functions of a purely imaginary argument.

Calculating Flight Time ($e < 0.2$)

To the first approximation, we can write

$$\Delta t_2=\int_{u_0}^{u}\left(\frac{3r^2}{2p\sqrt{\mu p}}\Delta p-\frac{2r^3}{p\sqrt{\mu p}}\cos\vartheta\Delta e\right)du. \qquad (3.185)$$

Here Δt_2 is the variation in the flight time corresponding to a change in the parameter Δp and in eccentricity Δe over the section from u_0 to u due to air drag. The discarded terms, proportional to $\Delta\omega$ and W_s are very small (they yield a correction less than 1 percent).

After converting to the variable E and uncomplicated transformations, we get

$$\Delta t_2=\frac{a^{3/2}}{(1-e^2)\sqrt{\mu}}\int_{E_0}^{E}\left[\frac{3}{2a}(1-e\cos E)\Delta p+\right.$$
$$\left.+(3e-2(1+e^2)\cos E+e\cos 2E)\Delta e\right]dE. \qquad (3.186)$$

Let us use Eqs. (3.178) for Δp and Δe. After substituting them into (3.186) and several transformations we will have

$$\Delta t_2 = -\frac{bA_1 a^{5/2}}{\sqrt{\mu}} \int_{E_0}^{E} \left[\frac{3}{2}\left(\frac{a'_{01}}{2} + a'_{02} e\right) E + \sum_{m=1}^{n} \frac{3}{m}\left(\frac{1}{2} a'_{m1} + e a'_{m2}\right) \times \right.$$

$$\times \sin mE - \sum_{m=1}^{n} \frac{3}{m}\left(\frac{1}{2} b'_{m1} + e b'_{m2}\right) \cos mE - \frac{3}{2} c'_1 - 3ec'_2 -$$

$$-\left(\frac{3}{4} e a'_{01} + (1+e^2) a'_{02}\right) E \cos E - \sum_{m=1}^{n} \frac{1}{m}\left(\frac{3}{4} e a'_{m1} + \right.$$

$$+ (1+e^2) a'_{m2}) (\sin (m-1) E + \sin (m+1) E) +$$

$$+ \sum_{m=1}^{n} \frac{1}{m}\left(\frac{3}{4} e b'_{m1} + (1+e^2) b'_{m2}\right) (\cos (m-1) E +$$

$$+ \cos (m+1) E) + \left(\frac{3}{2} e c'_1 + 2(1+e^2) c'_2\right) \cos E +$$

$$+ e \frac{a'_{02}}{2} E \cos 2E + e \sum_{m=1}^{n} \frac{a'_{m2}}{2m} (\sin (m-2) E + \sin (m+2) E) -$$

$$\left. - e \sum_{m=1}^{n} \frac{b'_{m2}}{2m} (\cos (m-2) E + \cos (m+2) E) - e c'_2 \cos 2E \right] dE.$$

/185

After integration, we get

$$\Delta t_2 = -\frac{bA_1 a^{5/2}}{\sqrt{\mu}} \left[\frac{3}{4}\left(\frac{a'_{01}}{2} + a'_{02} e\right) E^2 - \left(\frac{3}{2} c'_1 + 3ec'_2 - \bar{b}_0\right) E - \right.$$

$$-\left(\frac{3}{4} e a'_{01} + (1+e^2) a'_{02}\right) E \sin E + \frac{1}{4} e a'_{02} E \sin 2E +$$

$$\left. + \sum_{m=1}^{n} \bar{a}_m \cos mE + \sum_{m=1}^{n} \bar{b}_m \sin mE \right]_{E_0}^{E}, \qquad (3.187)$$

where

$$\bar{a}_1 = -3\left(\frac{a'_{11}}{2} + a'_{12} e\right) - \frac{3}{4} a'_{01} e - (1+e^2) a'_{02} + \frac{1}{2}\left(\frac{3}{4} a'_{21} e + \right.$$

$$\left. + (1+e^2) a'_{22}\right) + \frac{1}{2} e a'_{12} - \frac{1}{6} e a'_{32};$$

$$\bar{a}_2 = -\frac{3}{4}\left(\frac{a'_{21}}{2} + e a'_{22}\right) + \frac{1}{6}\left(\frac{3}{4} a'_{31} e + (1+e^2) a'_{32}\right) + \frac{1}{2}\left(\frac{3}{4} a'_{11} e + \right.$$

$$\left. + (1+e^2) a'_{12}\right) + \frac{1}{8} e a'_{02} - \frac{1}{16} e a'_{42};$$

$$\bar{a}_3 = -\frac{1}{3}\left(\frac{a'_{31}}{2} + ea'_{32}\right) + \frac{1}{12}\left(\frac{3}{4}a'_{41}e + (1+e^2)a'_{42}\right) + \\ + \frac{1}{6}\left(\frac{3}{4}a'_{21}e + (1+e^2)a'_{22}\right) - \frac{1}{30}ea'_{52} - \frac{1}{6}ea'_{12};$$

/186

$$\bar{a}_4 = -\frac{3}{16}\left(\frac{a'_{41}}{2} + ea'_{42}\right) + \frac{1}{20}\left(\frac{3}{4}a'_{51}e + (1+e^2)a'_{52}\right) + \frac{1}{12}\left(\frac{3}{4}a'_{31}e + \right. \\ \left. + (1+e^2)a'_{32}\right) - \frac{1}{48}ea'_{62} - \frac{1}{16}ea'_{22};$$

$$\bar{a}_5 = -\frac{3}{25}\left(\frac{a'_{51}}{2} + ea'_{52}\right) + \frac{1}{30}\left(\frac{3}{4}a'_{61}e + (1+e^2)a'_{62}\right) + \frac{1}{20}\left(\frac{3}{4}a'_{41}e + \right. \\ \left. + (1+e^2)a'_{42}\right) - \frac{1}{70}ea'_{72} - \frac{1}{30}ea'_{32}; \qquad (3.188)$$

. . . . . .

$$\bar{b}_0 = \frac{3}{4}eb'_{11} + (1+e^2)b'_{12} - \frac{1}{4}eb'_{22};$$

$$\bar{b}_1 = -3\left(\frac{b'_{11}}{2} + eb'_{12}\right) + \frac{1}{2}\left(\frac{3}{4}b'_{21}e + (1+e^2)b'_{22}\right) + \frac{3}{2}c'_1e + \\ + 2(1+e^2)c'_2 - \frac{1}{6}eb'_{32} - \frac{1}{2}eb'_{12};$$

$$\bar{b}_2 = -\frac{3}{4}\left(\frac{b'_{21}}{2} + eb'_{22}\right) + \frac{1}{6}\left(\frac{3}{4}b'_{31}e + (1+e^2)b'_{32}\right) + \\ + \frac{1}{2}\left(\frac{3}{4}b'_{11}e + (1+e^2)b'_{12}\right) - \frac{1}{16}eb'_{42} - \frac{1}{2}ec'_2;$$

$$\bar{b}_3 = -\frac{1}{3}\left(\frac{b'_{31}}{2} + eb'_{32}\right) + \frac{1}{12}\left(\frac{3}{4}b'_{41}e + (1+e^2)b'_{42}\right) + \frac{1}{6}\left(\frac{3}{4}b'_{21}e + \right. \\ \left. + (1+e^2)b'_{22}\right) - \frac{1}{30}eb'_{52} - \frac{1}{6}eb'_{12};$$

$$\bar{b}_4 = -\frac{3}{16}\left(\frac{b'_{41}}{2} + eb'_{42}\right) + \frac{1}{20}\left(\frac{3}{4}b'_{51}e + (1+e^2)b'_{52}\right) + \frac{1}{12}\left(\frac{3}{4}b'_{31}e + \right. \\ \left. + (1+e^2)b'_{32}\right) - \frac{1}{48}eb'_{62} - \frac{1}{16}eb'_{22};$$

$$\bar{b}_5 = -\frac{3}{25}\left(\frac{b'_{51}}{2} + eb'_{52}\right) + \frac{1}{30}\left(\frac{3}{4}b'_{61}e + (1+e^2)b'_{62}\right) + \frac{1}{20}\left(\frac{3}{4}b'_{41}e + \right. \\ \left. + (1+e^2)b'_{42}\right) - \frac{1}{70}eb'_{72} - \frac{1}{30}eb'_{32};$$

. . . . . .

From Eq. (3.187) we can see that the change (decrease) in flight time Δt_2 due to atmospheric drag is generally proportional to the square of the eccentric anomaly E (approximately proportional to the square of the flight time), however a linear term, long-periodic terms, and periodic terms are present.

In one revolution of a satellite around the Earth, that is, when the eccentric anomaly varies within the limits 0-2π, the flight time will change by the amount /187

$$\Delta t_2(2\pi) = \frac{-\pi b A_1 a^{5/2}}{\sqrt{\mu}} \left[3\pi \left(\frac{a'_{01}}{2} + a'_{02} e \right) + 2 \left(\bar{b}_0 - \frac{3}{4} c'_1 - 3 e c'_2 \right) \right]. \quad (3.189)$$

Hence it follows that a change in the flight time of an AES due to air drag is proportional to the ballistic coefficient b, density of air at the reference altitude $\bar{h}_0$, the semi-axis of orbit a to the power 5/2, and the value of the Bessel function $I_0(\alpha_1)$, which reflects principally the effect of eccentricity.

The total flight time over the interval E_0 - E can be written in the form

$$t - t_0 = [(E) - (e)\sin(E) - (E_0) + (e)\sin(E_0)] \frac{(a)^{3/2}}{\sqrt{\mu}} + \Delta t_1 + \Delta t_2. \quad (3.190)$$

Here the elements (a), (e), and also the eccentric anomaly correspond to some mean undisturbed orbit determined by the method proposed above (see text page 117 [translation page]); Δt_1 is the correction that allows for the influence of the noncentrality of the force field (second harmonic) calculated from the elements of the undisturbed orbit, and Δt_2 is the change in flight time due to air drag. When the flight time is computed over n revolutions, it is expedient to use the method of revolution-by-revolution summation.

Second-Approximation Orbit

The Eqs. (3.178) obtained for calculating changes in orbital elements p and e within a revolution can be similarly augmented by the final expressions for changes in the remaining orbital elements due to the influence of atmospheric drag. We have

$$\Delta\Omega = -\frac{ba^3 A_1}{2\sqrt{\mu p}} Q_3 \left[\frac{a'_{03}}{2} E + \sum_{m=1}^{n} \frac{a'_{m3}}{m} \sin mE - \right. \quad (3.191)$$

$$-\sum_{m=1}^{n}\frac{b'_{m3}}{m}\cos mE-c_3\Big];$$

$$\Delta i=-\frac{ba^3A_1\sin i}{2\sqrt{\mu p}}\Omega_8\Big[\frac{a'_{04}}{2}E+\sum_{m=1}^{n}\frac{a'_{m4}}{m}\sin mE-$$

$$-\sum_{m=1}^{n}\frac{b'_{m4}}{m}\cos mE-c_4\Big];$$

$$e\Delta\omega=\frac{b}{2}pA_1\Big[\sum_{m=1}^{n}\frac{b'_{m5}}{m}\cos mE+c_5\Big]-\Delta\Omega\cos i,$$

(3.191) cont.

where

/188

$$a'_{m3}=\frac{1}{4}\sin 2\omega\{b_0[I_{m-2}+I_{m+2}-2e(I_{m-1}+I_{m+1})]+$$

$$+\sum_{l=1}^{n}b_l[I_{m-2-l}+I_{m-2+l}+I_{m+2-l}+I_{m+2+l}-$$

$$-2e(I_{m-1-l}+I_{m-1+l}+I_{m+1-l}+I_{m+1+l})]\};$$

$$b'_{m3}=\frac{1}{4}\cos 2\omega\{b_0[I_{m-2}-I_{m+2}-2e(I_{m-1}-I_{m+1})]+$$

$$+\sum_{l=1}^{n}b_l[I_{m-2-l}+I_{m-2+l}-I_{m+2-l}-I_{m+2+l}-$$

$$-2e(I_{m-1-l}+I_{m-1+l}-I_{m+1-l}-I_{m+1+l})]\};$$

$$a'_{m4}=\sum_{l=1}^{n}\frac{b_l}{2}\Big[I_{m-l}+I_{m+l}+\frac{1}{2}\cos 2\omega(I_{m-2-l}+I_{m-2+l}+$$

$$+I_{m+2-l}+I_{m+2+l})-2e\cos^2\omega(I_{m-1-l}+I_{m-1+l}+I_{m+1-l}+I_{m+1+l})\Big]+$$

$$+\frac{b_0}{2}\Big[I_k+\frac{1}{2}\cos 2\omega(I_{k-2}+I_{k+2})-2e\cos^2\omega(I_{k-1}+I_{k+1})\Big];$$

$$b'_{m4}=\frac{1}{4}\sin 2\omega\Big\{\sum_{l=1}^{n}b_l[-I_{m-2-l}-I_{m-2+l}+I_{m+2-l}+I_{m+2+l}+$$

$$+2e(I_{m-1-l}+I_{m-1+l}-I_{m+1-l}-I_{m+1+l})]+$$

$$+b_0[-I_{k-2}+I_{k+2}+2e(I_{k-1}-I_{k+1})]\Big\};$$

$$b'_{m5}=b_0\Big[I_{m-1}-I_{m+1}-\frac{e}{2}(I_{m-2}-I_{m+2})\Big]+$$

$$+\sum_{l=1}^{n}b_l[I_{m-1-l}+I_{m-1+l}-I_{m+1-l}-I_{m+1+l}-$$

$$-\frac{e}{2}(I_{m-2-l}+I_{m-2+l}-I_{m+2-l}-I_{m+2+l})].$$

Eqs. (3.178) and (3.191) determine the second-approximation orbit, with reference to the effect of air drag. It remains to find the revised changes in the osculating elements due to the influence of the Earth's oblateness (and flight time). To an accuracy up to the square of the compression of the terrestrial ellipsoid, they can be written as

1. $$\Delta\Omega=[A_{00}+A_{01}\cos\vartheta+A_{02}\cos(u+\omega)+A_{03}\cos(3u-\omega)]u+ \qquad \text{/189}$$
$$+\sum_{r=1}^{6}\sum_{s=-2}^{2}A_{rs}\sin(ru+s\omega), \qquad (3.192$$

where

$$A_{00}=-k_1\cos i\left[1+\frac{k_1}{2}\left(-1+\frac{5}{3}k+\frac{e^2}{3}+\frac{5}{12}e^2k+\right.\right.$$
$$\left.\left.+\frac{7}{6}e^2\cos 2\omega-\frac{5}{2}e^2k\cos 2\omega\right)\right];$$
$$A_{01}=-S_0ek_1^2\cos i; \quad A_{02}=\frac{1}{2}A_{01}; \quad A_{03}=-\frac{1}{6}A_{01};$$
$$A_{20}=-k_1\cos i\left[-\frac{1}{2}+\frac{k_1}{2}\left(1-\frac{13}{6}k+\frac{e^2}{6}-\frac{7}{6}e^2k\right)\right];$$
$$A_{40}=-\frac{k_1^2}{2}\cos i\left(-\frac{1}{4}+\frac{2}{3}k-\frac{e^2}{6}+\frac{23}{48}e^2k\right);$$
$$A_{1,-1}=-k_1\cos i\left[1+\frac{k_1}{2}\left(-9+\frac{329}{24}k\right)\right]e;$$
$$A_{11}=-k_1\cos i\left[-\frac{1}{2}+\frac{k_1}{2}\left(1-\frac{23}{4}k\right)\right]e;$$
$$A_{2,-2}=-\frac{k_1^2}{2}\cos i\left(-\frac{4}{3}+\frac{5}{8}k\right)e^2;$$
$$A_{22}=-\frac{5}{32}k_1^2\cos ike^2;$$
$$A_{3,-1}=-k_1\cos i\left[-\frac{1}{6}+\frac{k_1}{2}\left(\frac{11}{9}-\frac{13}{6}k\right)\right]e;$$
$$A_{31}=-\frac{k_1^2}{2}\cos i\left(-\frac{1}{4}+\frac{7}{6}k\right)e;$$
$$A_{4,-2}=-\frac{k_1^2}{2}\cos i\left(\frac{11}{24}-\frac{5}{8}k\right)e^2;$$
$$A_{5,-1}=-\frac{k_1^2}{2}\cos i\left(-\frac{1}{4}+\frac{13}{24}k\right)e;$$
$$A_{6,-2}=-\frac{k_1^2}{2}\cos i\left(-\frac{1}{18}+\frac{5}{48}k\right)e^2;$$
$$k=\sin^2 i; \quad k_1=\frac{\varepsilon}{\mu p^2}; \quad S_0=2-\frac{5}{2}k.$$

The remaining $A_{rs} = 0$.

2. $$\Delta i=[B_{00}+B_{01}\sin\vartheta+B_{02}\sin(u+\omega)+B_{03}\sin(3u-\omega)]u+\sum_{r=1}^{5}\sum_{s=-2}^{2}B_{rs}\cos(ru+s\omega), \qquad (3.193)$$

where

$$B_{00}=\frac{1}{4}k_2\left(\frac{7}{6}-\frac{5}{4}k\right)k_1^2e^2\sin 2\omega;$$

$$B_{02}=-\frac{1}{4}S_0k_2k_1^2e;$$

$$B_{03}=-\frac{1}{3}B_{02};$$

$$B_{1,-1}=-\frac{1}{4}k_2\left(\frac{1}{6}+\frac{11}{24}k\right)k_1^2e;$$

$$B_{11}=\frac{1}{4}k_2\left[k_1+\left(-\frac{7}{2}+\frac{15}{4}k\right)k_1^2\right]e;$$

$$B_{20}=\frac{1}{4}k_2\left[k_1-\left(\frac{1}{2}k-\frac{1}{2}e^2+\frac{3}{4}e^2k\right)k_1^2\right];$$

$$B_{22}=\frac{1}{4}k_2\left(\frac{1}{16}-\frac{1}{16}k+\frac{1}{8}e^2+\frac{7}{16}e^2k\right)k_1^2;$$

$$B_{3,-1}=\frac{1}{4}k_2\left[\frac{1}{3}k_1-\left(\frac{5}{18}+\frac{7}{36}k\right)k_1^2\right]e;$$

$$B_{31}=-\frac{5}{48}k_2kk_1^2e;$$

$$B_{4,-2}=\frac{1}{4}k_2\left(-\frac{7}{24}+\frac{5}{16}k\right)k_1^2e^2;$$

$$B_{40}=\frac{1}{4}k_2\left(\frac{3}{8}-\frac{13}{24}k+\frac{1}{6}e^2-\frac{13}{48}e^2k\right)k_1^2;$$

$$B_{5,-1}=\frac{1}{4}k_2\left(\frac{1}{6}-\frac{7}{24}k\right)k_1^2e.$$

The remaining $B_{rs} = 0$; $k_2 = \sin 2i$.

3. $$\frac{\Delta p}{p}=[C_{00}+C_{01}\sin\vartheta+C_{02}\sin(u+\omega)+C_{03}\sin(3u-\omega)]u+\sum_{r=1}^{5}\sum_{s=-2}^{2}C_{rs}\cos(ru+s\omega), \qquad (3.194)$$

where

$$C_{00}=\left(\frac{7}{6}k-\frac{5}{4}k^2\right)k_1^2e^2\sin 2\omega;$$

$$C_{02}=-S_0kk_1^2e,\quad C_{03}=-\frac{1}{3}C_{02};$$

$$C_{1,-1}=\left(\frac{1}{6}k-\frac{11}{24}k^2\right)k_1^2e;$$

$$C_{11}=ekk_1+\left(-\frac{7}{2}+\frac{15}{4}k\right)kk_1^2e;$$

$$C_{2,-2}=\frac{1}{12}e^2k^2k_1^2;$$

$$C_{20}=kk_1+\left(-\frac{1}{2}k+\frac{1}{2}e^2-\frac{3}{4}e^2k\right)kk_1^2;$$

$$C_{22}=\left(\frac{1}{16}-\frac{1}{16}k+\frac{1}{4}e^2+\frac{7}{16}e^2k\right)kk_1^2;$$

$$C_{3,-1}=\frac{1}{3}ekk_1-\left(\frac{5}{18}+\frac{7}{36}k\right)kk_1^2e;$$

$$C_{31}=\left(\frac{1}{4}-\frac{5}{12}k\right)kk_1^2e;$$

$$C_{4,-2}=\left(-\frac{7}{24}+\frac{5}{16}k\right)kk_1^2e^2;$$

$$C_{5,-1}=\left(\frac{1}{4}-\frac{7}{24}k\right)kk_1^2e;$$

$$C_{40}=\left(\frac{1}{2}k-\frac{13}{24}k^2+\frac{1}{3}e^2k-\frac{13}{48}e^2k^2\right)k_1^2.$$

The remaining coefficients are equal to zero.

4.
$$\Delta e=[D_{00}+D_{01}\sin\vartheta+D_{02}\sin(u+\omega)+D_{03}\sin(3u-\omega)+$$
$$+D_{04}\sin 2u+D_{05}\sin 2\vartheta+D_{06}\sin(4u-2\omega)+D_{07}\sin 3\vartheta+$$
$$+D_{08}\sin(u-3\omega)+D_{09}\sin(5u-3\omega)]u+\sum_{r=1}^{7}\sum_{s=-6}^{3}D_{rs}\cos(ru+s\omega),\quad(3.195)$$

where

$$D_{00}=\left(-\frac{23}{48}+\frac{5}{2}k+\frac{35}{24}e^2-\frac{5}{8}e^2k\right)ekk_1^2\sin 2\omega;$$

$$D_{01}=-S_0\left(\frac{3}{2}k-1+\frac{3}{8}e^2k-\frac{1}{4}e^2\right)k_1^2;$$

$$D_{02}=-S_0\left(\frac{1}{4}+\frac{11}{16}e^2\right)kk_1^2;$$

$$D_{03}=S_0\left(\frac{7}{12}+\frac{17}{48}e^2\right)kk_1^2;$$

$$D_{05}=-S_0\left(\frac{3}{2}k-1\right)ek_1^2,\qquad D_{06}=\frac{3}{4}S_0ekk_1^2,$$

$$D_{07}=-S_0\left(\frac{9}{24}k-\frac{1}{4}\right)e^2k_1^2;$$

$$D_{08}=\frac{3}{16}S_0e^2kk_1^2,\quad D_{09}=\frac{3}{16}S_0e^2kk_1^2;$$

$$D_{1,-3}=\frac{1}{16}e^2kk_1+\left(-\frac{1}{16}k+\frac{3}{32}k^2-\frac{5}{16}e^2+\right.$$
$$\left.+\frac{661}{192}e^2k+\frac{11}{384}e^2k^2\right)k_1^2;$$

$$D_{1,-1}=\left(1-\frac{3}{2}k+\frac{1}{4}e^2-\frac{3}{8}e^2k\right)k_1+$$
$$+\left(\frac{9}{4}-\frac{29}{4}k+\frac{1}{4}e^2-\frac{23}{6}e^2k+\frac{125}{192}k^2+\frac{751}{384}e^2k^2\right)k_1^2;$$

$$D_{11}=\left(\frac{1}{4}+\frac{11}{16}e^2\right)kk_1+\left(-\frac{1}{4}+\frac{33}{16}k-\frac{77}{32}k^2-\right.$$
$$\left.-\frac{7}{48}e^2-\frac{517}{192}e^2k+\frac{353}{384}e^2k^2\right)k_1^2;$$

$$D_{2,-4}=\left(\frac{29}{96}k+\frac{1}{16}k^2-\frac{1}{16}e^2+\frac{389}{384}e^2k+\frac{7}{128}e^2k^2\right)ek_1^2;$$

$$D_{2,-2}=\left(\frac{1}{2}-\frac{3}{4}k\right)ek_1+\left(\frac{37}{24}e-\frac{33}{16}ek-\frac{25}{64}ek^2+\right.$$
$$\left.+\frac{31}{61}e^3-\frac{43}{48}e^3k-\frac{3\,23}{1535}e^3k^2-\frac{1}{4e}+\frac{3}{4}\frac{k}{e}-\frac{61}{96}\frac{k^2}{e}\right)k_1^2;$$

$$D_{20}=\frac{5}{4}ekk_1+\left(\frac{5}{12}\frac{k}{e}-\frac{5}{8}\frac{k^2}{e}+\frac{1}{6}e+\frac{1}{24}e^3-\right.$$
$$\left.-\frac{67}{96}ek-\frac{7}{32}ek^2+\frac{31}{96}e^3k-\frac{39}{64}e^3k^2\right)k_1^2;$$

$$D_{22}=\left(-\frac{1}{64}\frac{k^2}{e}+\frac{1}{16}ek-\frac{13}{96}ek^2+\frac{1}{6}e^3k-\frac{493}{3072}e^3k^2\right)k_1^2;$$

$$D_{3,-3}=\left(\frac{1}{12}-\frac{1}{8}k\right)e^2k_1+\left(-\frac{1}{4}+\frac{3}{4}k-\frac{39}{64}k^2-\right.$$
$$\left.-\frac{29}{48}e^2+\frac{7}{4}e^2k-\frac{439}{768}e^2k^2-\frac{19}{18}ek^2-\frac{1}{3}e^3k^2\right)k_1^2;$$

$$D_{3,-1}=\left(\frac{7}{12}+\frac{17}{48}e^2\right)kk_1+\left(-\frac{1}{6}-\frac{11}{18}k-\frac{1}{8}e^2-\right.$$
$$\left.-\frac{463}{288}e^2k+\frac{5}{144}k^2+\frac{1}{144}e^2k^2\right)k_1^2;$$

$$D_{31}=\left(\frac{1}{16}-\frac{1}{96}k+\frac{51}{64}e^2-\frac{901}{768}e^2k\right)kk_1^2;$$

$$D_{4,-6}=-\left(\frac{31}{192}+\frac{1}{64}k\right)e^3kk_1^2;$$

$$D_{4,-4}=-\frac{1}{4}\left(\frac{2}{3}-2k+\frac{77}{48}k^3+\frac{37}{48}e^2-\frac{13}{6}e^2k+\frac{125}{96}e^2k^2\right)ek_1^2;$$

$$D_{4,-2}=\frac{3}{8}ekk_1+\left(-\frac{7}{24}\frac{k}{e}+\frac{7}{16}\frac{k^2}{e}+\frac{1}{3}e-\frac{263}{192}ek+\right.$$

$$\left.+\frac{9}{8}ek^2+\frac{1}{12}e^3+\frac{35}{1024}e^3k+\frac{87}{256}e^3k^2\right)k_1^2;$$

$$D_{40}=\left(\frac{7}{96}\frac{k^2}{e}+\frac{13}{12}ek-\frac{1679}{1024}ek^2+\frac{5}{1536}e^3k-\frac{159}{512}e^3k^2\right)k_1^2;$$

$$D_{5,-5}=-\frac{1}{5}\left(-\frac{61}{48}+\frac{27}{16}k+\frac{75}{256}k^2\right)e^2k_1^2;$$

$$D_{5,-3}=\frac{1}{16}e^2kk_1+\left(-\frac{37}{96}k+\frac{13}{40}k^2+\frac{7}{48}e^2-\right.$$

$$\left.-\frac{181}{480}e^2k+\frac{151}{160}e^2k^2\right)k_1^2;$$

$$D_{5,-1}=\left(\frac{7}{16}k-\frac{619}{960}k^2+\frac{163}{192}e^2k-\frac{4357}{3840}e^2k^2\right)k_1^2;$$

$$D_{6,-6}=-\frac{1}{6}\left(-\frac{7}{32}+\frac{5}{16}k+\frac{9}{216}k^2\right)e^3k_1^2;$$

$$D_{6,-4}=-\frac{1}{6}\left(-\frac{323}{256}ek^2-\frac{17}{24}ek-\frac{1}{8}e^3+\frac{1571}{768}e^3k-\frac{85}{64}e^3k^2\right)k_1^2;$$

$$D_{6,-2}=\left(-\frac{49}{576}\frac{k^2}{e}+\frac{175}{288}ek-\frac{485}{1536}ek^2+\frac{1}{6}e^3k-\frac{289}{4608}e^3k^2\right)k_1^2;$$

$$D_{7,-5}=\left(-\frac{13}{16}+\frac{21}{64}k\right)e^2kk_1^2.$$

The remaining coefficients are equal to zero.

5.

$$\Delta\omega=[E_{00}+E_{01}\cos\vartheta+E_{02}\cos(u+\omega)+E_{03}\cos(3u-\omega)+$$
$$+E_{04}\cos 2u+E_{05}\cos 2\vartheta+E_{06}\cos(4u-2\omega)+E_{07}\cos 3\vartheta+$$
$$+E_{08}\cos(u-3\omega)+E_{09}\cos(5u-3\omega)]u+\sum_{r=1}^{7}\sum_{s=-6}^{3}E_{rs}\sin(ru+s\omega), \qquad (3.196)$$

where

$$E_{00}=S_0k_1+\left(\frac{1}{2e}-\frac{3}{2}\frac{k}{e}+\frac{9}{8}\frac{k^2}{e}-\frac{1}{2}+\frac{133}{24}k-\frac{607}{192}k^2+\frac{7}{12}e^2-\right.$$

$$\left.-\frac{1}{64}e^2k+\frac{519}{256}e^2k\right)k_1^2+\left(-\frac{1}{2e}+2\frac{k}{e}-\frac{15}{8}\frac{k^2}{e}+\frac{3}{4}-\frac{29}{6}k+\right.$$

$$+\frac{9}{2}k^2+\frac{2}{3}e^2+\frac{1207}{192}e^2k+\frac{253}{128}e^2k^2\Big)k_1^2\cos 2v+$$

$$+\Big(-\frac{1}{64}+\frac{1}{32}k\Big)e^2kk_1^2\cos 4v;$$

$$E_{01}=\Big(\frac{1}{e}S_0-2e+\frac{9}{2}ek-\frac{5}{2}ek^2\Big)k_1^2;$$

$$E_{02}=\Big(\frac{1}{e}S_0-e+\frac{9}{4}ek-\frac{5}{4}ek^2\Big)k_1^2;$$

$$E_{03}=\Big(\frac{1}{3e}S_0+\frac{1}{3}e-\frac{3}{4}ek+\frac{5}{12}ek^2\Big)k_1^2;$$

$$E_{05}=\frac{1}{2e}S_0k_1^2;$$

$$E_{06}=\frac{1}{2}E_{05};\ E_{07}=\frac{2}{3}E_{05};\ E_{08}=2E_{05};\ E_{09}=\frac{2}{5}E_{05};$$

$$E_{1,-3}=\frac{1}{16}ekk_1+\Big(-\frac{1}{4}\frac{k}{e^2}+\frac{3}{8}\frac{k^2}{e^2}+\frac{21}{8}\frac{k}{e}-\frac{2}{e}-\frac{3}{16}\frac{k^2}{e}+\frac{1}{2}+$$

$$+\frac{27}{16}k-\frac{45}{32}k^2+\frac{3}{16}e-\frac{69}{32}ek+\frac{37}{16}ek^2\Big)k_1^2;$$

$$E_{1,-1}=\frac{1}{e}\Big(1-\frac{3}{2}k+\frac{7}{4}e^2-\frac{17}{8}e^2k\Big)k_1+\Big(\frac{1}{e^2}-3\frac{k}{e^2}+\frac{9}{4}\frac{k^2}{e^2}-$$

$$-\frac{3}{e}+6\frac{k}{e}-\frac{53}{16}\frac{k^2}{e}+\frac{11}{6}-5k+\frac{27}{8}k^2-\frac{9}{8}e+$$

$$+\frac{811}{96}ek-\frac{317}{64}ek^2\Big)k_1^2;$$

$$E_{11}=\Big(-\frac{1}{4}\frac{k}{e}-\frac{1}{2}e+\frac{15}{16}ek\Big)k_1+\Big(\frac{1}{12}\frac{k}{e^2}-\frac{33}{16}\frac{k^2}{e^2}-\frac{7}{4e}+$$

$$+\frac{29}{16}\frac{k}{e}+\frac{29}{16}\frac{k^2}{e}-\frac{1}{6}+\frac{53}{16}e-\frac{659}{48}ek-\frac{417}{32}ek^2+\frac{17}{24}k-\frac{11}{16}k^2\Big)k_1^2;$$

$$E_{2,-2}=\Big(\frac{1}{2}-\frac{3}{4}k\Big)k_1+\Big(-\frac{1}{2e^2}+\frac{3}{2}\frac{k}{e^2}-\frac{1}{2e}-\frac{131}{96}\frac{k^2}{e^2}+\frac{5}{8}\frac{k}{e}-$$

$$-\frac{7}{8}+\frac{145}{96}k-\frac{673}{256}k^2-\frac{13}{32}e^2+\frac{283}{192}e^2k-\frac{3761}{3072}e^2k^2\Big)k_1^2;$$

$$E_{20}=\frac{1}{2}\Big(\frac{5}{2}k-1\Big)k_1+\frac{1}{2}\Big(\frac{1}{8}\frac{k^2}{e^2}-\frac{1}{12}\frac{k}{e^2}+\frac{8}{3}-\frac{665}{48}k+\frac{1189}{96}k^2+$$

$$+\frac{617}{768}e^2-\frac{309}{256}e^2k+\frac{1043}{256}e^2k^2\Big)k_1^2;$$

$$E_{22}=\Big(-\frac{3}{32}+\frac{29}{96}k-\frac{47}{192}e^2+\frac{1}{96}e^2k+\frac{1}{32}\frac{k}{e^2}\Big)kk_1^2;$$

/195

$$E_{3,-1}=\left(\frac{7}{12}\frac{k}{e}-\frac{1}{6}e+\frac{19}{48}ek\right)k_1+\left(-\frac{1}{12}\frac{k}{e^2}-\frac{1}{8}\frac{k^2}{e^2}-\frac{23}{36}\frac{k}{e}+\right.$$
$$\left.+\frac{1}{36e}+\frac{1}{6}+\frac{173}{144}e-\frac{1435}{288}ek+\frac{647}{288}ek^2-\frac{13}{24}k+\frac{7}{16}k^2\right)k_1^2;$$

$$E_{3,-3}=\left(\frac{1}{12}-\frac{1}{8}k\right)ek_1+\left(-\frac{1}{3e^2}+\frac{k}{e^2}-\frac{3}{4}\frac{k^2}{e^2}-\frac{7}{12}+\frac{19}{12}k-\right.$$
$$\left.-\frac{51}{48}k^2-\frac{7}{18e}+\frac{47}{72}\frac{k}{e}-\frac{11}{32}\frac{k^2}{e}-\frac{1}{8}e-\frac{5}{24}ek+\frac{35}{64}ek^2\right)k_1^2;$$

$$E_{31}=\left(-\frac{1}{16}\frac{k}{e}+\frac{1}{6}\frac{k^2}{e}-\frac{1}{8}e+\frac{203}{192}ek-\frac{61}{32}ek^2\right)k_1^2;$$

$$E_{4,-4}=\left(-\frac{1}{8e}+\frac{3}{8}\frac{k}{e}-\frac{9}{32}\frac{k^2}{e}-\frac{1}{12}+\frac{35}{128}k-\frac{211}{768}k^2-\frac{3}{16}e^2+\right.$$
$$\left.+\frac{49}{96}e^2k-\frac{193}{3072}e^2k^2\right)k_1^2;$$

$$E_{4,-2}=\frac{3}{8}kk_1+\left(-\frac{773}{384}k+\frac{5657}{3072}k^2+\frac{5}{24}+\frac{65}{64}e^2-\frac{2935}{3072}e^2k+\right.$$
$$\left.+\frac{1}{12}e^2k^2-\frac{1}{8e}+\frac{5}{32}\frac{k}{e}\right)k_1^2;$$

$$E_{40}=\left(-\frac{1}{8}+\frac{29}{32}k-\frac{6437}{3072}k^2-\frac{11}{96}e^2+\frac{107}{192}e^2k-\frac{2027}{3072}e^2k^2\right)k_1^2;$$

$$E_{5,-3}=\frac{1}{16}ekk_1+\left(-\frac{7}{60}\frac{k}{e^2}+\frac{7}{40}\frac{k^2}{e^2}+\frac{39}{20}\frac{k}{e}+\frac{33}{40}\frac{k^2}{e}+\frac{1}{30}+\right.$$
$$\left.+\frac{9}{80}e-\frac{31}{240}k+\frac{19}{160}k^2-\frac{143}{120}ek+\frac{431}{320}ek^2-\frac{2}{e}\right)k_1^2;$$

$$E_{5,-1}=\left(\frac{7}{16}\frac{k}{e}-\frac{17}{16}\frac{k^2}{e}-\frac{1}{8}e+\frac{503}{480}ek-\frac{215}{128}ek^2\right)k_1^2;$$

$$E_{6,-4}=\left(-\frac{1}{16}\frac{k}{e}+\frac{3}{32}\frac{k^2}{e}-\frac{17}{72}k+\frac{185}{512}k^3+\frac{1}{48}e^2-\frac{13}{64}e^2k+\frac{185}{512}e^2k^2\right)k_1^2;$$

$$E_{6,-2}=\left(\frac{25}{48}-\frac{215}{128}k^2-\frac{1}{36}e^2+\frac{187}{1152}e^2k-\frac{1159}{4608}e^2k^2\right)k_1^2;$$

$$E_{7,-3}=\left(-\frac{7}{32}\frac{k^2}{e}+\frac{13}{64}ek-\frac{653}{1792}ek^2\right)k_1^2.$$

The remaining coefficients are equal to zero.

By assigning the subscript "1" to the increments in the osculating elements $\Delta\Omega$, Δi, Δp, Δe, $\Delta\omega$ of the second approximation that allow for the effect of the noncentrality of the Earth's gravitational field (second harmonic), and the subscript "2" to the increments of these same elements due to air drag, we get the overall perturbations /196

$$\left.\begin{aligned}\Delta\Omega &= \Delta\Omega_1 + \Delta\Omega_2;\\ \Delta i &= \Delta i_1 + \Delta i_2;\\ \Delta p &= \Delta p_1 + \Delta p_2;\\ \Delta e &= \Delta e_1 + \Delta e_2;\\ \Delta\omega &= \Delta\omega_1 + \Delta\omega_2.\end{aligned}\right\} \qquad (3.197)$$

These expressions were obtained for a given argument of latitude u of a disturbed [perturbed] orbit.

To obtain the flight time in the second approximation to an accuracy up to the square of the compression, the initial equation for dt/du can be represented as

$$\frac{dt}{du} = F_c + \frac{\partial F}{\partial p}\Delta p + \frac{\partial F}{\partial e}\Delta e + \frac{\partial F}{\partial \omega}\Delta\omega + \frac{r^2}{\sqrt{\mu p}}\cos i\frac{d\Omega}{du} + \\ + \frac{1}{2}d^2F + d\left(\frac{r^2}{\sqrt{\mu p}}\cos i\frac{d\Omega}{du}\right), \qquad (3.198)$$

where d^2F is the second differential of function F, and we obtain the derivative $d\Omega/du$ by differentiating Eq. (3.192) in u.

By substituting into (3.198) the values of the increments of the oscillating element in the second approximation found above (3.192) - (3.196), after integration we get (to an accuracy of up to e, $e > \bar{\alpha}$)

$$\delta t(k_1^2) = \frac{p^{3/2}}{\sqrt{\mu}}k_1^2\left\{\left[-\frac{1}{e} + 3\frac{k}{e} - \frac{9}{4}\frac{k^2}{e} + \frac{35}{8} - \frac{35}{4}k + \frac{75}{8}k^2 + \right.\right. \\ \left. + \left(-\frac{k}{3e} + \frac{27}{16}\frac{k^2}{e} + 4 - \frac{87}{16}k - \frac{13}{16}k^2\right)\cos 2\omega\right]u + \\ + \left[-\frac{7}{4}k + \frac{9}{4}k^2 + \left(-1 + 4k - \frac{15}{4}k^2\right)\cos 2\omega\right]\times \\ \times u\cos\vartheta + \frac{1}{8}S_0u^2\cdot\sin 2\omega + \\ + S_0u\left[\left(\frac{5}{6} - \frac{3}{4}k\right)\cos 2\vartheta + \left(\frac{1}{3} - \frac{1}{6}k\right)\cos 2u + \right. \\ + \frac{1}{2}\cos(2u - 4\omega) + \frac{1}{6}\cos 3\vartheta + \left(\frac{1}{30} + \frac{7}{48}k\right)\cos(4u - 2\omega) - \\ - S_0eu\sin\vartheta + (-6 + 7k)e\cos\vartheta - \left(1 + \frac{1}{2}k\right)e\cos(u + \omega) + \\ \left.\left. + \left(\frac{1}{3} + \frac{1}{6}k\right)e\cos(3u - \omega)\right]\right\}_{u_0}^{u}. \qquad (3.199)$$

/197

The total flight time can be calculated by the formula

$$t=\bar{t}+\Delta t_1+\Delta t_2 \qquad (3.200)$$

based on the elements of the undisturbed orbit. Here $\Delta t_1 = \overline{\delta t} + \delta t(k_1^2)$; $\overline{\delta t}$ can be calculated by Eq. (3.45). The inverse problem -- -- determining perturbations for assigned t -- is solved by the method of iterations.

The method of calculating orbital elements presented above does not make allowance for dynamic changes in atmospheric density. The effect of this factor (with the exception of slight displacements of the AES within a revolution) for extended predictions of motion (for more than two-three days) of a satellite is best compensated by introducing new atmospheric parameters $\bar{a}_0$, $\bar{\kappa}$, and $\bar{h}_0$ when converting to a new two- and three-day section of the flight. The values of these parameters when the orbital measurements are absent can be obtained by approximation of ρ with respect to h of the standard atmosphere for the appropriate value of the solar activity index, modified by corrections for the "swelling" of the atmosphere. The latter corrections can be obtained from the results of [37], utilizing orbital prediction data.

In periodic orbital measurements the parameters $\bar{a}_0$, $\bar{\kappa}$, and $\bar{h}_0$ are calculated as shown in Chapter Four.

Derivation of Finite Formulas for Determining Satellite Lifetime

Eqs. (3.157) and (3.158) or (3.161) enable us to quite simply calculate on an electronic computer changes in the principal orbital elements due to the effect of air drag. However, a drawback of all computer methods lies in the difficulty of performing qualitative analysis with them. Finite formulas permit this analysis to be conducted optimally. Moreover, to revise data on the density of the Earth's atmosphere, preliminary information on satellite motion can be more readily obtained by calculation using simple formulas than on a computer.

The direct integration of equations for the orbital elements p and e does not appear possible in view of their complexity.

Additional simplifications are needed. Let us divide the entier range of possible orbits into two groups. The first group /198

includes orbits with large eccentricities (e > 0.02) and the second --
-- with small eccentricities (e < 0.02).

Orbits with e > 0.02

Let us use the principle indicated at the outset of this section that for sufficiently elongated orbits satellite deceleration occurs principally in the area of the perigee, and let us expand in series cos E in Eqs. (3.129) and (3.130).

Substituting Eq. (3.133) into these equations, we get

$$\left.\begin{aligned}\frac{dp}{dE}&=-bpaAe^{-c\sqrt{1-z\left(1-\frac{1}{2}E^2\right)}}(1-e^2)^{1/2};\\ \frac{de}{dE}&=-bpAe^{-c\sqrt{1-z\left(1-\frac{1}{2}E^2\right)}}\left(\frac{1+e}{1-e}\right)^{1/2}\left(1-\frac{1}{2}E^2\right).\end{aligned}\right\}\qquad(3.201)$$

In the expansion we will leave only the term containing E^2. The residual term of the series $R_{res} < 1/24\ E^4$ then does not exceed 0.16 even when E = 80°. At the orbital point with e = 0.02 that has the eccentric anomaly E = 80°, flight altitude exceeds the perigee altitude by 107 km. The air density is roughly one order of magnitude smaller. For large eccentricities much smaller E values are required for the expansion error to have only a slight effect.

For example, when e = 0.1 (third Soviet AES) it was sufficient to take E equal to 35° for the density to be reduced by more than 10 times. This makes it possible to replace the expression 1 $\pm$ e cos E $\approx$ 1 $\pm$ e.

Now expanding $\sqrt{1-z\left(1-\frac{1}{2}E^2\right)}$ in a series and singling out the variable part, we get

$$\left.\begin{aligned}\frac{dp}{dE}&=-bpaAe^{-c\sqrt{1-z}}e^{-\frac{1}{2}cE^2}(1-e^2)^{1/2};\\ \frac{de}{dE}&=-bpAe^{-c\sqrt{1-z}}e^{-\frac{1}{2}cE^2}\left(\frac{1+e}{1-e}\right)^{1/2}\left(1-\frac{1}{2}E^2\right).\end{aligned}\right\}\qquad(3.202)$$

where

$$\gamma=\frac{cz}{4\sqrt{1-z}}. \qquad (3.203)$$

By integrating each equation within the limits from zero to E, /199 and here assuming the orbital parameters to be invariant, we find

$$\left.\begin{aligned}\Delta p&=-\frac{\sqrt{\pi}bA}{2\sqrt{\gamma}}\,pa\mathrm{e}^{-c\sqrt{1-z}}(1-e^2)^{1/2}\Phi\left(\sqrt{\gamma}E\right);\\ \Delta e&=-\frac{\sqrt{\pi}bA}{2\sqrt{\gamma}}\,p\mathrm{e}^{-c\sqrt{1-z}}\left(\frac{1+e}{1-e}\right)^{1/2}\left[\Phi\left(\sqrt{\gamma}E\right)-\frac{1}{4\gamma}\Phi\left(\sqrt{\gamma}E\right)+\right.\\ &\left.+\frac{1}{2\sqrt{\pi\gamma}}E\mathrm{e}^{-\gamma E^2}\right].\end{aligned}\right\} \qquad (3.204)$$

The system of equations obtained by integration is suitable for orbits with relatively large eccentricities.

By passing to the limit as $E \to \infty$, which to some extent allows for the deceleration over the orbital sections with large E, and by doubling the result, we finally get

$$\left.\begin{aligned}\frac{dp}{dn}&=-\frac{\sqrt{\pi}bA}{\sqrt{\gamma}}\,pa\mathrm{e}^{-c\sqrt{1-z}}(1-e^2)^{1/2};\\ \frac{de}{dn}&=-\frac{\sqrt{\pi}bA}{\sqrt{\gamma}}\,p\mathrm{e}^{-c\sqrt{1-z}}\left(\frac{1+e}{1-e}\right)^{1/2}\left(1-\frac{1}{4\gamma}\right).\end{aligned}\right\} \qquad (3.204')$$

By dividing the first equation by the second, we will have

$$\frac{dp}{de}=a(1-e)\frac{1}{1-\frac{1}{4\gamma}}.$$

By substituting into this equation $\gamma=\frac{cz}{4\sqrt{1-z}}$, where $c=\bar{\varkappa}\sqrt{a-R'}$; $z=\frac{ae}{a-R'}$; and $R'=R+\bar{h}_0$, and by denoting y = a (1 - e) - R', after simple transformations we arrive ar the equation

$$\frac{dp}{de}=(y+R')\frac{1}{1-\frac{\sqrt{y}}{\bar{\varkappa}ae}}. \qquad (3.205)$$

Since $$p=r_{\pi}(1+e)=(y+R')(1+e)$$

and $$dp=(1+e)dy+(y+R')de,$$

then, by replacing dp in Eq. (3.205) we get

$$(1+e)\frac{dy}{de}=(y+R')\left(\frac{1}{1-\frac{\sqrt{y}}{\bar{\varkappa}ae}}-1\right). \tag{3.205'}$$

The ratio $\frac{\sqrt{y}}{\bar{\varkappa}ae}$ (where y is the excess of the perigee over the reference altitude $\bar{h}_0$; ae is half the difference between the apogee altitude and the perigee altitude, and $\bar{\kappa}$ is one of the three atmospheric coefficients), when e > 0.02, this ratio is not more than 0.15. Therefore, the term $\left(1-\frac{\sqrt{y}}{\bar{\varkappa}ae}\right)^{-1}$ can be expanded in a series in Newton's binomial, by discarding the terms of degree greater than one. The error due to canceling out the residual term of the series is not more than 3 percent. As a result, we get /200

$$(1+e)\frac{dy}{de}=(y+R')\frac{\sqrt{y}}{\bar{\varkappa}ae}.$$

By replacing $ae=\frac{y+R'}{1-e}$, we have

$$(1+e)\frac{dy}{de}=\frac{1-e}{\bar{\varkappa}e}\sqrt{y} \tag{3.206}$$

or

$$\frac{\bar{\varkappa}dy}{\sqrt{y}}=\frac{1-e}{(1+e)e}de. \tag{3.206'}$$

After integration of Eq. (3.206'), we have

$$\bar{\varkappa}\sqrt{y}=\bar{\varkappa}\sqrt{y_0}-\ln\frac{e_0^{1/2}(1+e)}{e^{1/2}(1+e_0)}. \tag{3.207}$$

Bearing in mind that $\bar{\varkappa}\sqrt{\bar{y}}=c\sqrt{1-z}$, let us substitute the resulting expression for $\bar{\varkappa}\sqrt{\bar{y}}$ into the second equation (3.204'). By replacing simultaneously γ by its value equal to $\frac{cz}{4\sqrt{1-z}}$, we find

$$\frac{de}{dn}=-\frac{\sqrt{\pi}bA}{\sqrt{\bar{\gamma}}}\,pe^{-c\sqrt{1-z}}\left(\frac{1+e}{1-e}\right)^{1/2}\left(1-\frac{1}{4\gamma}\right)=$$

$$=-\frac{2\sqrt{\pi}bA\sqrt{r_\pi}\sqrt[4]{\bar{y}}\,e^{-\bar{\varkappa}\sqrt{\bar{y}_0}}e_0^{1/2}}{\sqrt{\bar{\varkappa}}(1+e_0)}\cdot\frac{(1+e)^{5/2}}{e}\left(1-\frac{\sqrt{\bar{y}}}{\bar{\varkappa}r_\pi}\cdot\frac{1-e}{e}\right).$$

Considering that the perigee radius $r_\pi = a\,(1-e)$ and $\sqrt[4]{\bar{y}}$ are very slowly varying quantities, in integration we can assume them to be constant and equal to their initial values (more exactly, to some mean values).

Let us denote /201

$$M=\frac{\sqrt{\bar{\varkappa}}(1+e_0)\,e^{\bar{\varkappa}\sqrt{\bar{y}_0}}}{2\sqrt{\pi}bA\sqrt{r_\pi}\sqrt[4]{\bar{y}}\,e_0^{1/2}},$$

then

$$\frac{dn}{de}=-M\frac{e}{(1+e)^{5/2}}\left(1+\frac{\sqrt{\bar{y}}}{\bar{\varkappa}r_\pi}\cdot\frac{1-e}{e}\right), \qquad (3.208)$$

where the expansion in Newton's binomial was used for the correctional term $\left(1-\frac{\sqrt{\bar{y}}}{\bar{\varkappa}r_\pi}\cdot\frac{1-e}{e}\right)^{-1}$. Here the error for $e > 0.02$ does not exceed 3 percent.

By integrating Eq. (3.208) when we average $\sqrt{y}$ in the corrective term, we finally get

$$n=M\left\{\frac{2}{(1+e)^{1/2}}\left[\left(1-\frac{1}{3(1+e)}\right)-\frac{\sqrt{\bar{y}}}{\bar{\varkappa}r_\pi}\left(1-\frac{2}{3(1+e)}\right)\right]\right\}_{e_0}^{e}. \qquad (3.209)$$

Knowing the initial values of orbital eccentricity e_0 and perigee altitude and assigning the finite value of e, by Eq. (3.209) we can calculate the corresponding number of revolutions n. Thereafter finding the flight time is not difficult.

Example. Let us calculate based on the initial data e_0 = = 0.111; e = 0.02; y_0 = 100,000 m; $\sqrt{y_0}$ = 316; $\bar{\kappa}$ = 0.0145 $m^{1/2}$; $\sqrt{\bar{\kappa}}$ = 0.122; $r_п$ = 6,575,000 m; A = $2 \cdot 10^{-9}$ is the lifetime (number of revolutions) of the third Soviet artificial Earth satellite.

Solution.

1. The third satellite has a cone (d = 1.73 m, l = 3.57 m) and weighs G_{III} = 1327 kg. Therefore its ballistic coefficient is

$$b_{III} = \frac{c_x S}{4G_{III}} g = \frac{2{,}1 \cdot 3{,}14 \cdot 0{,}865\,(3{,}57 + 0{,}865)\,9{,}81}{4 \cdot 1327} = 0{,}047 \text{ m}^3/\text{kg} \cdot \text{sec}^2,$$

where c_x is the coefficient of the aerodynamic drag on the sphere, and

S is the surface area of the satellite.

(For other satellites with weight G, we can assume approximately $b = 0.047 \sqrt[3]{\frac{G_{III}}{G}}$).

2. The calculation of the coefficient M is

$$M = \frac{\sqrt{\bar{\varkappa}}\,(1 + e_0)\,e^{\bar{\varkappa}\sqrt{L_0}}}{2\sqrt{\pi b A}\,\sqrt{r_п}\,\sqrt[4]{y}\,e_0^{1/2}} =$$

$$= \frac{0{,}122 \cdot 1{,}111 \cdot e^{4{,}58}}{3{,}54 \cdot 0{,}047 \cdot 2 \cdot 10^{-9} \cdot 2560 \cdot 17{,}7 \cdot 0{,}111^{1/2}} \approx 2608 \cdot 10^3.$$

3. Calculation of the number of revolutions by Eq. (3.209): /202

$$n = 2608 \cdot 10^3 \left\{ \frac{2}{1{,}02^{1/2}} \left[1 - \frac{1}{3 \cdot 1{,}02} - 0{,}33 \cdot 10^{-2} \left(1 - \frac{2}{3 \cdot 1{,}02} \right) \right] - \right.$$

$$\left. - \frac{2}{1{,}111^{1/2}} \left[1 - \frac{1}{3 \cdot 1{,}111} - 0{,}33 \cdot 10^{-2} \left(1 - \frac{2}{3 \cdot 1{,}111} \right) \right] \right\} = 13\,040.$$

This calculation compared with the results of the numerical integration of Eqs. (3.161) on a computer gives a 14 percent overstatement, which must be assumed to be good agreement for the approximate formula.

Orbits with e < 0.02

Eq. (3.209) becomes unsuitable when $e \lesssim 0.02$, that is, for orbits with small ellipticity and for circular orbits. Based on Eqs. (3.157) and (3.158) or (3.161), we can derive formulas suitable for this range of orbits.

By discarding all terms except the first (also assuming $e^2 = 0$) in Eq. (3.157), we get

$$\frac{dp}{dn} = -2\pi b p a \varrho_\pi e^{-\alpha_1} I_0(\alpha_1). \tag{3.210}$$

To estimate the error, let us compute the ratio of the largest of the discarded terms $A_1B_2(I_2 - I_0)$ to the principal term:

$$\frac{A_1B_2(I_2-I_0)}{\varrho_\pi e^{-\alpha_1} I_0} \approx \frac{A_1B_2(I_2-I_0)}{A_1 e^{\alpha_1}(B_0+B_1+B_2+\ldots)e^{-\alpha_1}I_0} \approx$$

$$\approx \frac{B_2}{B_0+B_2}\left(\frac{I_2}{I_0}-1\right) < \frac{B_2}{B_0+B_2} \approx \frac{\frac{cz^2}{24}}{1+\frac{cz^2}{24}} = \frac{1}{1+\frac{16}{cz^2}} < f.$$

From the condition $\frac{1}{1+\frac{16}{cz^2}} < f$, let us find the allowable value

$$cz^2 = \frac{\bar{\varkappa} a^2 e^2}{(a-R')^{3/2}} = \frac{\bar{\varkappa}(r_a-r_\pi)^2}{\sqrt{2}(r_a+r_\pi-2R')^{3/2}} < 2. \tag{3.211}$$

Hence we can determine the apogee radius r_α if the radius of the perigee r_π is known. Assuming f = 9 (the discarded term must be one order smaller than the remaining term), for h_π = 200-300 km we get eccentricity e = 0.01-0.02.

The division of orbits by eccentricity is somewhat arbitrary, since the second parameter a also influences cz^2.

By integrating Eq. (3.210) and replacing in it $c_*=A_1e^{\alpha_1}$ /203

and $A_1=Ae^{-c\frac{a_0}{2}}\approx Ae^{-c}$, since the fraction $a_0/2$ for small e is very close to unity, we get

$$\frac{dp}{dn}=-2\pi bp^2Ae^{-c}I_0(\alpha_1).$$

Let us convert to the variable $c=\bar{\varkappa}\sqrt{a-R'}$, then we have

$$dc=\frac{\bar{\varkappa}}{2\sqrt{a-R'}}da=\frac{\bar{\varkappa}}{2\sqrt{p-R'}}dp=\frac{\bar{\varkappa}^2}{2c}dp$$

when we neglect the term of the order of 2e. Further,

$$p^2=\left(\frac{c^2}{\bar{\varkappa}^2}+R'\right)^2$$

and the differential equation becomes

$$\frac{dn}{dc}=-\frac{ce^c}{\pi bA\bar{\varkappa}^2I_0(\alpha_1)\left(\frac{c^2}{\bar{\varkappa}^2}+R'\right)^2}=-\frac{ce^c}{\pi bA\bar{\varkappa}^2R'^2\left(1+\frac{c^2}{\bar{\varkappa}^2R'}\right)^2},$$

whence we have

$$dn=-\frac{c}{\pi bA\bar{\varkappa}^2R'^2I_0(\alpha_1)}\left(1-\frac{2}{\bar{\varkappa}^2R'}c^2\right)e^c\,dc.$$

with an error of the order of $3\frac{c^4}{\bar{\varkappa}^4R'^2}<0{,}01$. Integration gives us

$$n=\frac{1}{\pi bA\bar{\varkappa}^2R'^2I_0(\alpha_1)}\left\{e^c\left[c-1-\frac{2}{\bar{\varkappa}^2R'}((c-1)^3+3c-5)\right]\right\}_c^{c_0}. \qquad (3.212)$$

Here $I_0(\alpha_1)$ is assumed constant and equal to the initial value of this function. For orbits with small eccentricities, $I_0(\alpha_1)$ is close to unity. Some increase in $I_0(\alpha_1)$ with increase in e_0 compensates for the effect of the discarded terms.

Example. Based on the initial data h_α = 237 km; h_π = 180 km; b = 0.031; $\bar{\kappa}$ = 0.0145; A = $2 \cdot 10^{-9}$; and $\bar{h}_0$ = 125,700 m, let us determine the number of revolutions and the lifetime of the Vostok-2 satellite when it descends by means of natural aerodynamic deceleration.

Solution.

1. Calculation of orbital elements a and e:

$$e = \frac{h_\alpha - h_\pi}{h_\alpha + h_\pi + 2R} = \frac{57}{417 + 12\,740} = 0{,}00434;$$

$$a = \frac{1}{2}(h_\alpha + h_\pi) + R = 6580 \cdot 10^3 \text{ m}.$$

2. Calculation of c_0, z_0, α_1, and $I_0(\alpha_1)$: /204

$$c_0 = \bar{\kappa}\sqrt{a - R'} = 0{,}0145\sqrt{6580 \cdot 10^3 - 6370 \cdot 10^3 - 125\,700} = 4{,}22;$$

$$z_0 = \frac{ae}{a - R'} = \frac{6580 \cdot 10^3 \cdot 0{,}00434}{85\,000} = 0{,}336;$$

$$\alpha_1 = c_0 \frac{z_0}{2}\left(1 + 0{,}1 z_0^2\right) = 4{,}22 \frac{0{,}336}{2}(1 + 0{,}1 \cdot 0{,}336^2) = 0{,}78;$$

$$I_0(\alpha_1) = I_0(0{,}78) = 1{,}158.$$

3. Verification of the suitability of Eq. (3.212). For verification, let us use the condition (3.211)

$$c_0 z_0^2 = 4{,}22 \cdot 0{,}336^2 = 0{,}476 < 2,$$

according to which the formula is applicable.

Before we calculate the number of revolutions by Eq. (3.212), we must set the lower limit of integration c. We find c from the condition that semi-axis a, prior to the descent of the Vostok-2 satellite, must be larger than R' by at least 10-15 km. This corresponds approximately to the flight altitude of 135 km. Actually, exact calculations show that below 135-140 km the satellite passes into the descent trajectory in two or three revolutions. Hence for c we obtain the condition

$$c = \bar{\kappa}\sqrt{a - R'} = 0{,}0145\sqrt{15\,000} \approx 2.$$

4. Calculation of the number of revolutions by Eq. (3.212):

$$n = \frac{1}{3\cdot 14\cdot 0{,}031\cdot 2\cdot 10^{-9}\cdot 0{,}21\cdot 10^{-3}\cdot 6496^2\cdot 10^6\cdot 1{,}158}\times$$
$$\times\left\{e^{4{,}22}\left[4\cdot 22-1-\frac{2}{0{,}21\cdot 10^{-3}\cdot 6496\cdot 10^3}((4{,}22-1)^3+3\cdot 4{,}22-5)\right]-\right.$$
$$\left.-7{,}39\left[2-1-\frac{2}{0{,}21\cdot 10^{-3}\cdot 6496\cdot 10^3}((2-1)^3+3\cdot 2-5)\right]\right\}=106,$$

or n = 106 revolutions.

5. Calculation of satellite lifetime. The period of revolution of the Vostok-2 satellite around the Earth was 88 min. Therefore its lifetime in orbit in the case of aerodynamic deceleration is

$$t_{lif} = 106\cdot\frac{88}{1440} = 6.5 \text{ days},$$

which is very close to the results obtained by numerical integration of the exact equations of motion for the same initial data.

3.6. Effect of Sunlight Pressure

The light field of the Sun has a force influence on cosmic bodies. P. N. Lebedev [17] discovered this phenomenon and concluded that the forces of the Sun's gravitational field and its light field are equivalent. He established that the resultant force F with which the Sun attracts a given body is equal to the difference between the Newtonian force of attraction G and the force of light pressure H. In fractions of the Newtonian force, the resultant force can be expressed thusly: /205

$$F=\frac{G-H}{G}=1-\frac{3p_c}{4Qr_T\varrho_T}, \qquad (3.213)$$

where p_c is the force of sunlight pressure per unit area perpendicular to the direction of the sunlight, at a distance of one astronomical unit from the Sun[6] ($p_c = 0.6\cdot 10^{-6}$ kg/m^2 for the absorbing surface with blackbody factor $A_S = 0.72$)

Q is the acceleration due to solar gravity at a distance of one astronomical unit ($Q = 0.6\cdot 10^{-2}$ m/sec^2)

r_T is the radius of the spherical body, and

ρ_T is the mass density of the body.

[6] An astronomic unit is the mean distance from Earth to Sun.

For a given cosmic body (satellite), the ratio of the pressure force to the gravitational force H/G is a characteristic constant, independent of the distance to the Sun, since p_c and Q_T depend equally on this distance (inversely proportional to its square).

Replacing p_c and Q_T by their numerical values, we get

$$F=1-\frac{0{,}75\cdot 10^{-4}}{r_T\varrho_T}, \qquad (3.214)$$

that is, the repelling force of sunlight $\left(\frac{0{,}75\cdot 10^{-4}}{r_T\varrho_T}\right)$ at a specific distance from the Sun is inversely proportional to the product of the radius of the body by its density.

For Earth satellites, Eq. (3.213) can be taken as a working formula enabling us to allow for the effect of solar gravity and the pressure of sunlight.

Let us write Eq. (3.213) in a more general form as follows [8, 35]:

$$F=1-\frac{\chi}{fMM_\odot}=\frac{f_1}{f}, \qquad (3.215)$$

where M is the mass of the spacecraft
$M_\odot$ is the solar mass
f_1 is a new constant:

$$f_1=f-\frac{\chi}{MM_\odot} \qquad (3.216)$$

(the constant κ is determined from the condition $H = \kappa/R^2$), and
R is the distance from spacecraft to Sun.

The resultant force of attraction of the craft by the Sun will be

$$G_1=G-H=\frac{f_1MM_\odot}{R^2}. \qquad (3.217)$$

Eq. (3.217) is of the same form (which was indicated by Tsander) as the Newtonian formula for the law of universal gravity. /206

So light pressure can be allowed for (after calculating f_1 for a given spacecraft) based on the equations in Section 3.4, by replacing the constant f in the expression for the disturbing function by the constant f_1.

When calculating the force of light pressure H for a given spacecraft using the formula

$$H=\frac{3p_cG}{4Qr_T\varrho_T}=\frac{\Delta M_\odot M}{R^2} \tag{3.218}$$

we must consider that as a rule the spacecraft is not a spherical body. To the first approximation t_T can be calculated (for an oriented craft) as the radius of a circle whose area is equal to the area of the projection of the craft onto a plane normal to the direction of the sunlight. For a wholly unoriented spacecraft we must begin from the mean-probable area of this projection (a problem analogous to the problem of determining the average greatest cross section for calculating air drag). Here also to the first approximation the value of r_T can be determined as the radius of the sphere having a surface equal to the total surface area of the spacecraft. The exact calculation of the solar pressure force is very difficult to carry out, since pressure depends on the condition of the body surface.

Depending on the blackbody factor and other factors, not only does the magnitude, but also the direction of the force change when there is invariant inclination of the particular surface element to the direction of sunlight.

It is meaningful to allow for the pressure of sunlight for orbits with perigee altitude above 400-450 km, since even at the altitude 400 km the fraction of solar light pressure with respect to air drag is of the order of 7-10 percent. At an altitude of about 550 km, both forces become equal in magnitude.

The effect of the force of solar light pressure for light satellites moving at high altitudes is particularly manifest. For example, for the American Echo satellite (sphere with diameter 30 m, weight 70.4 kg, and launched 12 August 1960) with a near-circular orbit with perigee altitude 1500 km and apogee 1700 km, and lifetime calculated without allowing for solar light pressure, 20 years, and with allowance for pressure -- 1-2 years [34]. In 60 days the sunlight pressure reduced the perigee altitude by 350 km. The orbit became elongated and gradually the perigee descended into the dense atmospheric layers where due to air drag the satellite began to rapidly descent.

In this chapter we gave only a general background on allowing for solar light pressure. More detailed theoretical considerations on this question can be found in the study [52].

CHAPTER IV

/207

DETERMINATION OF ORBITS FROM NAVIGATIONAL MEASUREMENTS

4.1. Main Concepts. Measured and Determined Parameters. Measurement Errors

To control a spacecraft (SC), for tie-in to the time of scientific observations made onboard the spacecraft, for guidance of antennas of ground measuring, command, and communication radio facilities, we must know the parameters of the orbit in which the SC is moving. To uniquely determine the instantaneous parameters of SC motion, it is sufficient to note six parameters of motion at the initial instant of time and the forces acting on the SC during flight. Instead of the initial values of the parameters of motion, we can assign any six other independent parameters uniquely determining the orbit (for example, the values of the osculating orbital elements for any moment of time, for the value of the radius-vector of the SC positions at different moments of time, and so on).

The independent parameters of motion selected, uniquely determining the trajectory, we will call the main parameters of the trajectory and we will designate them by a_i ($i = 1, 2, \ldots, 6$).

Thus, the determination of the true trajectory of a SC is equivalent to determining the true values of the main parameters a_i.

It may be that in the system of forces determining the flights of SC some forces are known inadequately well and these forces (or certain parameters determining them) are best revised, for example, the parameters of the atmosphere, the coefficients of expansion of the gravity field, the coordinates of the measuring stations, the time tie-ins, and so on. These quantities can also be related to the main parameters to be determined for the unique characterization of SC motion.

For generality, we will assume that the SC trajectory is determined uniquely if we know the values of m main parameters a_i ($i = 1, 2, \ldots, m$). We will call the vector column

$$a = \|a_1\ a_2\ \ldots\ a_m\|^T \quad [1] \qquad (4.1)$$

[1] The superscript "T" will denote the operation of transposition of vectors and matrices.

the vector of the main trajectory parameters. Thus, any trajectory parameter η is determined by the formula /208

$$\eta=\eta(\boldsymbol{a}, t), \tag{4.2}$$

where t is time.

Functions of the type (4.2) that quite accurately describe the motion of an SC are assigned usually by differential equations in which the effect of all the main forces is allowed for (see Chapter One).

The system of the principal forces that must be considered in exact calculations of the trajectory of an SC flight is usually quite complex (it includes the assumed model of the Earth's gravity field, allowing for its noncentrality, the force of attraction by Moon, Sun, and other planets, as well as the aerodynamic forces of the action on the SC of the Earth's upper atmosphere). So exact calculations of the values of the trajectory of parameters we are interested in are usually based on numerical integration of the differential equations of motion for known values of the main trajectory parameters.

To determine the main trajectory parameters, navigational measurements must be taken during the flight. The main parameters most often cannot be measured directly, so to determine them we have to measure several trajectory parameters functionally associated with them.

We will call the trajectory parameters measured by navigation instruments the measured or navigational parameters and we will denote them by γ in contrast to the trajectory parameters calculated with expressions of the (4.2) type. Obviously, for γ we can write relations analogous to (4.2):

$$\gamma = \gamma(a, t). \tag{4.3}$$

We will call the flight-time interval $t_H - t_k$ during which navigational measurements can be made the navigational interval, and we will call the corresponding orbital section the navigational section.

At present, instruments of two types are used in making navigational measurements: onboard navigational measuring instruments and ground navigational measuring instruments.

Onboard navigational instruments include various types of optical instruments measuring the angles between different directions (for example, sextants), onboard altimeters of the radio frequency or laser types, and so on.

The navigational parameters involved when these instruments are used are as follows:

the angular altitudes of celestial bodies above the Earth's horizon

the angles between celestial bodies and landmarks on the Earth's surface

the angles between celestial bodies and the local vertical to the Earth's surface, and /209

flight altitude, and so on.

Among the ground navigational instruments are various types of radars, optical astronomical devices of the telescope type, laser locators, and so on. The following are the navigational parameters for these devices:

the ranges from the measuring instrument to the SC

the angles determining in space the direction to the SC

the rates of change in distances to the SC (radial rates), and

the angular rates of variation in direction to the SC in space.

The navigational measurements are always accompanied by errors. The main causes of these errors are as follows:

errors of the measuring instruments caused by imprecisions in their manufacture and functioning

errors in the tie-in of the measurements to astronomical time

errors in a knowledge of the coordinates of the ground measuring facilities, and

inaccuracy in knowledge of various astronomical and astrophysical constants used in measurement procedures (velocity of propagation of radio waves, dimensions of the Earth and celestial bodies, unevenness of visible surfaces of Earth and celestial bodies, and so on).

The actual laws of the distribution of measurement errors as a rule are not known. However, as experience has shown, a better approach to the actual distribution is ensured if one allows for the overall errors of the navigational measurements obeying the normal multidimensional distribution law.

Let us make the following assumptions.

Assumption 1. The errors of the vector of navigational measurements are distributed according to a multidimensional normal law with matrix of the second moments B and with zero mathematical expectations[2]. As a rule, here we call the vector-column composed of all navigational measurements used in determining the vector a the vector of navigational measurements γ.

Assumption 2. The navigational measurements are made instantaneously. Assumption 2 is used only when investigating the conditions for the optimality of the distributions of the navigational measurements along the trajectory. This assumption enables us to significantly simplify the relation and is justified /210 by the fact that generally the time of one navigational measurement is so short that one can neglect the effect of variation during this time in the parameters of motion on the estimate of accuracy.

The matrix of the second moments of the measurement errors B is an n x n matrix (n is the total number of measurements). We will denote the matrix elements by β_{ij}. The coefficient of correlation between the various measurements can be expressed by the following familiar formula:

$$k_{ij}=\frac{\beta_{ij}}{\sqrt{|\beta_{ii}||\beta_{jj}|}}. \qquad (4.4)$$

Depending on the modulus of the coefficient of correlation, we will distinguish the following types of measurement errors:

independent measurement errors if $|k_{ij}| = 1$ when $i = j$ and $|k_{ij}| = 0$ when $i \neq j$ (i, j are the measurement numbers)

systematic errors if $|k_{ij}| = 1$ for all i and j, and

correlation errors, if $|k_{ij}| = 1$ when $i = j$ and $0 < |k_{ij}| < 1$ when $i \neq j$.

Matrix B for errors of the first type is diagonal in form and its rank is always equal to the number of measurements n. In the following matrix B for independent errors will be denoted by B_0.

---

[2] The assumption that the mathematical expectations are zero does not detract from generality, since the earlier-known displacements of the mathematical expectations can always be allowed for in processing and can be canceled out of the errors.

A positively determined matrix B for errors of the second type, as we can readily see, always has an error equal to unity, and it can be written as follows:

$$B_{sys} = \mathbf{b}^T\mathbf{b}, \tag{4.5}$$

where **b** is some vector-row. It can be assumed that the vector **b** is made up of those values of the systematic error function b(t) that it takes on at the moments of measurement t_i.

The rank of matrix B for errors of the third type can be found in the range $2 \leq r \leq n$.

By using the representation of the systematic errors in the form (4.5), we can transform matrix B as follows. Let us select the diagonal matrix B_0 so that the matrix

$$\Delta B = B - B_0 \tag{4.6}$$

would be nonnegatively determined[3]. Obviously, ΔB is a symmetric matrix. The following relation obtains:

$$\Delta B = I^T \Delta B_{0r} I, \tag{4.7}$$

where ΔB_{0r} is a diagonal matrix made up of the eigenvalues of matrix ΔB

I is an orthogonal matrix composed of eigenvectors of matrix ΔB. Since the rank of ΔB is r, the number of diagonal terms ΔB_{0r}, nonzero (and being positive), is r. We denote /211

$$B_{rn} = \Delta B_{0r}^{1/2} I. \tag{4.8}$$

Obviously, matrix B_{rn} has r rows and n columns. By substituting (4.8) into (4.7) and using (4.6), we get

$$B = B_0 + B_{rn}^T B_{rn}. \tag{4.9}$$

---

[3] The quadratic form corresponding to ΔB can take on only nonnegative values.

Matrix B_{rn} can be called the matrix of systematic errors. Actually, if we denote the vector-row of matrix B_{rn} by $\mathbf{b}_j$ ($j = 1, 2, \ldots, r$, $r \leq n$), expressions (4.9) can be brought to the following form:

$$B = B_0 + \sum_{j=1}^{r} \mathbf{b}_j^T \mathbf{b}_j. \qquad (4.10)$$

Matrix B written in the form (4.9) or (4.10) will be often used in the following treatment. From Eq. (4.10) it is clear that the correlation matrix of the general type can always be represented as a sum of matrices of the second moments of independent and systematic errors. The form in which matrix B is represented (4.10) therefore is convenient in its practical computations.

To determine the vector of the principal trajectory parameters with dimension m, from all the measurements made, generally speaking it is adequate to select m measurements that enable us to set up a system of m equations of the (4.13') type, from which we can determine the value of the vector **a**. However, the random measurement errors under this definition of vector **a** usually leads to large errors. Therefore, to lower the effect of random errors of measurements on the accuracy of the determination of vector **a**, generally an excess number of navigational measurements is used, that is, $n > m$, and some statistical method is employed to define vector **a**.

The method of maximum likelihood is a method of statistical treatment of measurements that has been time-tested. A particular case of this method is the method of least squares. Therefore we adopt one more assumption.

Assumption 3. To process measurements and to estimate the values of the main trajectory parameters, let us use the method of maximum likelihood. A fairly complete exposition of this method can be found in numerous studies, for example, in [41, 67]. Below we present only a brief presentation of the concept of the method and its main relations used frequently in the sections to follows.

4.2. Method of Maximum Likelihood /212

Suppose that to determine the orbit of an SC over some section of the orbit $n > m$ measurements are made:

$$\boldsymbol{\gamma}^T = \| \gamma_1 \gamma_2 \ldots \gamma_n \|. \qquad (4.11)$$

The actual value of the measured parameter γ_i is determined by the function

$$\tilde{\gamma}_i = \tilde{\gamma}_i(a, t), \tag{4.12}$$

and the actually measured value is distorted by measurement errors, therefore

$$\gamma = \tilde{\gamma}(a) + \delta\gamma, \tag{4.13}$$

where $\delta\gamma$ is a vector-column composed of measurement errors.

The vector a is unknown and can be determined based on the relation

$$\gamma - \tilde{\gamma}(\hat{a}) = \Delta\gamma, \tag{4.13'}$$

where $\hat{a}$ is the vector of the main parameters, here this vector is taken as the true vector, and

$\Delta\gamma$ is the so-called mismatch vector made up of the measurement errors and the errors of calculating $\tilde{\gamma}(\hat{a})$ due to the difference of $\hat{a}$ from its true value.

The random vector of measurements according to assumption 1 is distributed according to a multidimensional normal law. Since to each a substituded into (4.13') there corresponds a specific $\Delta\gamma$, then to it there corresponds a specific value of the probability density of vector γ.

Let $p(\gamma/a)$ denote the probability density of γ under the condition that the value of the vector of the main trajectory parameters is a. According to equality (4.13') we can write

$$p(\gamma/a) = p(\Delta\gamma) = p[\gamma - \tilde{\gamma}(a)]. \tag{4.14}$$

The conditional probability $p(\gamma/a)$ is called the function of likelihood for vector a and is denoted by

$$p(\gamma/a) = f(\gamma, a). \tag{4.15}$$

According to the method of maximum likelihood, it is assumed that the most probable true value of a satisfying condition (4.13') is the value that corresponds to the maximum of the likelihood function (4.15).

For the multidimensional normal law of distribution of probability density we have /213

$$f(\gamma, a)=\frac{1}{\sqrt{(2\pi)^n |B|}}\exp\{[\gamma-\tilde{\gamma}(a)]^T B^{-1}[\gamma-\tilde{\gamma}(a)]\}, \quad (4.16)$$

where B is the matrix of the second moments of the measurement errors.

The method of maximum likelihood in this case reduces to minimization of the function

$$\Phi=[\gamma-\tilde{\gamma}(a)]^T B^{-1}[\gamma-\tilde{\gamma}(a)].$$

The necessary condition for a minimum of function Φ, from which the corresponding vector a can be determined, leads to the following matrical equation, which is called the equation of likelihood:

$$W(a)B^{-1}[\gamma-\tilde{\gamma}(a)]=0, \quad (4.17)$$

where

$$W(a)=\begin{Vmatrix} \frac{\partial\gamma_1}{\partial a_1} & \frac{\partial\gamma_2}{\partial a_1} & \cdots & \frac{\partial\gamma_n}{\partial a_1} \\ \frac{\partial\gamma_1}{\partial a_2} & \frac{\partial\gamma_2}{\partial a_2} & \cdots & \frac{\partial\gamma_n}{\partial a_2} \\ \cdots & \cdots & \cdots & \cdots \\ \frac{\partial\gamma_1}{\partial a_m} & \frac{\partial\gamma_2}{\partial a_m} & \cdots & \frac{\partial\gamma_n}{\partial a_m} \end{Vmatrix} \quad (4.18)$$

If the measurement errors are independent, that is, if B is the diagonal matrix, Eq. (4.17) converts into a relation in the classical method of least squares. Sometimes Eq. (4.17) for an arbitrary form of matrix B (valid for the normal law of error distribution) is called the relation of the generalized method of least squares. Thus, all formulas deriving from the general form of Eq. (4.17) are called formulas of the generalized method of least squares.

The actual matrix B of the second moments of measurement errors usually proves to be unknown. Therefore, as a rule we use as B an approximated matrix obtained by some method, adopting various additional assumptions relative to the kind of navigation measurement errors. A question of a rational selection of the approximate matrix B will be discussed in Section 4.3.

Sometimes to determine the main orbital parameters we use along with navigational measurements some apriori information, for example, we assume that the values of all or some of the main parameters a_i are known with some errors. This apriori information can be allowed for in processing the measurements.

Let us denote the vector of the apriori-known parameters with $\mathbf{a}^*$; the errors of vector $\mathbf{a}^*$ are characterized by the matrix of the second moments B^*. In this case the known values of $\mathbf{a}^*$ can be estimated as the results of measurements of these quantities and included as part of a sampling used for determining the vector of the main parameters a. This augmented sampling of measurements will be of the form /214

$$\gamma_{tot} = \left\| \begin{matrix} \gamma \\ a^* \end{matrix} \right\|, \tag{4.19}$$

and the matrix of the second moments of the errors of vector γ_{tot} can be written as:

$$B_{tot} = \left\| \begin{matrix} B & 0 \\ 0 & B^* \end{matrix} \right\|. \tag{4.20}$$

Further processing of sampling γ_{tot} does not differ in any way from what has been just considered.

The equation of likelihood (4.17) in the general case is nonlinear, since both vector $\tilde{\gamma}$ and the derivatives $\frac{\partial \gamma_i}{\partial a_j}$ depend nonlinearly on the main orbital parameters a_j. The solution of Eq. (4.17) represents certain difficulties, however there are several methods for the numerical solution of this equation (see, for example, [6, 10]). We will not consider methods of solving this equation here. We will note only that iterative processes underlie most of the methods. Some value of the vector $\mathbf{a}_0$ is taken as the initial approximation. Then we seek the increment $\Delta\mathbf{a}$ by some method and verify the degree to which the vector $\mathbf{a} = \mathbf{a}_0 + \Delta\mathbf{a}$ satisfied Eq. (4.17), and so on.

The solution of the problem of finding the vector a from the results of navigational measurements is always carried out with certain errors caused by measurement errors, errors in the knowledge of the constants appearing in Eqs. (4.17), and also errors arising due to the use of particular assumptions and simplifications.

Analysis of errors is made most often in a linear approximation, that is, on the assumption of the smallness of the errors such as to admit the linearization of the main relations relative to the resulting solution. This method is used below.

Let us denote the vector of the main parameters of an actual orbit by ã. The measurements made with errors can be written in the form (4.13). Suppose that by solving the equations of likelihood we obtain some value of vector a, which we can represent in the following form:

$$\boldsymbol{a}=\boldsymbol{a}(\tilde{\boldsymbol{a}},\ \delta\boldsymbol{\gamma}).$$

The vector of the errors in the determination of the main parameters is /215

$$\delta\boldsymbol{a}=\boldsymbol{a}-\tilde{\boldsymbol{a}}.$$

Let us expand the functions $\gamma(a)$ and $W(a)$ in the neighborhood of ã in a Taylor series:

$$\left.\begin{aligned}\boldsymbol{\gamma}(\tilde{\boldsymbol{a}}+\delta\boldsymbol{a})&=\boldsymbol{\gamma}(\tilde{\boldsymbol{a}})+W^{\mathrm{T}}(\tilde{\boldsymbol{a}})\delta\boldsymbol{a}+\ldots;\\ W(\boldsymbol{a})&=W(\tilde{\boldsymbol{a}})+\ldots,\end{aligned}\right\}\qquad(4.21)$$

where $W(\tilde{a})$ is matrix (4.18) when $a = \tilde{a}$.

By substituting (4.21) into (4.17) and retaining only terms not higher than the first order of smallness, we get

$$W(\tilde{\boldsymbol{a}})B^{-1}W^{\mathrm{T}}(\tilde{\boldsymbol{a}})\delta\boldsymbol{a}=W^{\mathrm{T}}(\tilde{\boldsymbol{a}})B^{-1}\delta\boldsymbol{\gamma};$$

whence

$$\delta\boldsymbol{a}=H\delta\boldsymbol{\gamma},\qquad(4.22)$$

where

$$H=[W(\tilde{\boldsymbol{a}})B^{-1}W^{\mathrm{T}}(\tilde{\boldsymbol{a}})]^{-1}W(\tilde{\boldsymbol{a}})B^{-1}.\qquad(4.23)$$

Eq. (4.22) is the solution of the likelihood equation in the linear approximation.

Using this solution for the successive refinement of the reference value of vector $\tilde{a}$ (that is, the value relative to which linearization is carried out), we can construct an iterative process of the numerical solution of the nonlinear system of likelihood equations. In the following we will often call the matrix H defined by Eq. (4.23) the likelihood matrix.

Since vector δa in the linear approximation was obtained from the vector $\delta\gamma$ by means of a linear transformation, as follows from theory [41], the mathematical expectation δa is zero, and the matrix of the second moments of its errors is determined by the formula

$$K=HBH^{\tau}. \tag{4.24}$$

By substituting (4.23) into (4.24), we get

$$K=(WB^{-1}W^{\tau})^{-1}. \tag{4.25}$$

If for vector a some other orbital parameter $\eta(a)$ is found, in the linear approximation the following equality obtains

$$\delta\eta=l_{\eta}^{\tau}\delta a, \tag{4.26}$$

where

$$l_{\eta}^{\tau}=\left\| \frac{\partial\eta}{\partial a_1}\ \frac{\partial\eta}{\partial a_2}\ \ldots\ \frac{\partial\eta}{\partial a_m} \right\|. \tag{4.27}$$

So the dispersion of the errors in determining parameter η is determined by the formula /216

$$D_{\eta}=l_{\eta}^{\tau}Kl_{\eta}. \tag{4.28}$$

Since the true matrix B is usually not known, some approximate (estimational) matrix B_{es} is used in computing matrix H. This same matrix is often used even for computing matrix K. In this case we get

$$K=K^{*}=H_{es}B_{es}H_{es}^{\tau}=(WB_{es}^{-1}W^{\tau})^{-1}, \tag{4.29}$$

which does not correspond to the characteristics of the actual errors δa obtained when B_{es} is used in H.

Actually, when the matrix B_{es} is used for H, the true value of matrix K is determined by the formula

$$K = K_H = H_{es} B H_{es}^T, \tag{4.30}$$

Thus, a methodological error ΔK_M in the computation of matrix K arises:

$$\Delta K_M = K^* - K_H = H_{es} (B_{es} - B) H_{es}^T. \tag{4.31}$$

The matrix of the second moments of measurement errors can always be represented as (see Eq. (4.10))

$$B = B_0 + B_{rn}^T B_{rn} = B_0 + \sum_{i=1}^{r} b_i^T b_i, \ (r \leqslant n). \tag{4.32}$$

On the basis of analysis, let us assume that in the real matrix B we were able to find the characteristics of the random errors and $k \leq r$ systematic errors, that is, to determine the matrix B_0 and k functions of systematic errors $b_i(t)$ (i = 1, 2, ..., k). The remaining r - k systematic errors remained undetermined. The matrix

$$B_{es} = B_0 + \sum_{i=1}^{k} b_i^T b_i = B_0 + B_{kn}^T B_{kn} \tag{4.33}$$

is taken as the real matrix and used both for constructing matrix H as well as for finding matrix (4.29).

The real matrix can be represented in the following form:

$$B = B_{es} + \sum_{i=k}^{r} b_i^T b_i = B_{es} + B_{ln}^T B_{ln}, \tag{4.34}$$

where l = r - k. With reference to (4.34), the formula for ΔK_M (4.31) can be transformed as follows:

$$\Delta K_M = H_{es} B_{ln}^T B_{ln} H_{es}^T \tag{4.35}$$

If it is possible to determine virtually all systematic errors, then obviously $\Delta K_M = 0$ and matrix K will be determined /217

by Eq. (4.25). In this case we denote

$$K = K_y = (WB^{-1}W^T)^{-1}. \tag{4.36}$$

Matrix K_y corresponds to the case when in the statistical treatment all the types of errors accompanying navigational measurements are taken into account, and matrix K_H corresponds to the case when only part of these errors are allowed for. By using the representation of matrix B in the form (4.34), let us transform Eqs. (4.30) and (4.36). For these transformations let us use the following formula to invert the sum of the matrices. If A = B + + CDF, then

$$A^{-1} = B^{-1} - B^{-1}CS^{-1}FB^{-1}, \tag{4.37}$$

where A, B are matrices of dimension $n_1 \times n_1$, where $|B| \neq 0$

C is a matrix of dimension $n_1 \times n_2$

D is a matrix of dimension $n_2 \times n_2$, where $n_2 \leq n_1$, $|D| \neq 0$, and

F is a matrix of dimension $n_2 \times n_1$

$$S = D^{-1} + FB^{-1}C.$$

This formula can be quite simply verified by using the formula $AA^{-1} = E$.

Actually,

$$(B+CDF)(B^{-1}-B^{-1}CS^{-1}FB^{-1}) = (E+CDFB^{-1})(E- \\ -CS^{-1}FB^{-1}) = E+CDFB^{-1}-CD(E+FB^{-1}CD)^{-1}FB^{-1}- \\ -CDFB^{-1}CD(E+FB^{-1}CD)^{-1}FB^{-1} = E+CD[E-(E+ \\ +FB^{-1}CD)(E+FB^{-1}CD)^{-1}]FB^{-1} = E.$$

Let us use Eq. (4.37) to invert matrix B written in the form (4.34). By substituting the expression obtained into (4.30) and (4.36) and applying once again Eq. (4.37), we get

$$K_y = (WB^{-1}W^T)^{-1} = (WB_{es}^{-1}W^T)^{-1} + CS^{-1}C^T; \tag{4.38}$$

$$K_H = H_{es}BH_{es}^T = (WB_{es}^{-1}W^T)^{-1} + CC^T. \tag{4.39}$$

Here

$$C=HB_{ln}^{\tau}=(WB_{es}^{-1}W^{\tau})^{-1}WB_{es}^{-1}B_{ln}^{\tau};$$
$$S=E+B_{ln}^{\tau}B_{es}^{-1/2}QB_{es}^{-1/2}B_{ln};$$
$$Q=E-B_{es}^{-1/2}W^{\tau}(WB_{es}^{-1}W^{\tau})^{-1}WB_{es}^{-1/2}. \qquad (4.40)$$

We note that in Eqs. (4.38) and (4.39) the first terms characterize the matrix components K_y and K_H that correspond to random and systematic measurement errors allowed for in matrix B_{es}, while the second terms correspond to error not allowed for in matrix B_{es}. /218

Naturally, we must have

$$K_y \leqslant K_H. \qquad (4.41)$$ [4]

Actually, we can show that the following inequality always obtains:

$$S \geqslant E. \qquad (4.42)$$

Using this inequality, by employing Eqs. (4.38) and (4.39) we can readily see that Eq. (4.41) is valid. The proof of inequality (4.42) can be found by the reader in [6, 10].

The enlargement of matrix K due to the nonconsideration in the statistical treatment of some of the systematic errors is determined by the formula

$$\Delta K_y=K_H-K_y=C(E-S^{-1})C^{\tau}. \qquad (4.43)$$

Remark. Let us recall that ΔK_M and ΔK_y characterize different errors. Thus, ΔK_M characterizes the errors arising because we had to use Eq. (4.29) instead of the more correct Eq. (4.30) in computing K with known B_{es} and unknown actual matrix B. But the value of ΔK_y characterizes the error of computing K due to nonconsideration of several systematic errors in the calculations (or in other words, in matrix B_{es}).

---

[4] Here and in the following, if A < B, the value of the quadratic form corresponding to A is smaller than the form corresponding to B.

From Eqs. (4.38) and (4.39) it is not difficult to find similar expressions for the particular case when only independent random errors are taken into account in the statistical treatment, that is, for the case when

$$B_{es} = B_0,$$

where B_0 is a diagonal matrix.

4.3. Estimates of Errors in Determining Orbital Parameters

But if the actual matrix B of the second moments of measurement errors was known, the characteristics of the errors in determining the vector of the main trajectory parameters a -- matrix K -- could have been computed by Eq. (4.25), and the dispersion of errors of any parameter $\eta(a)$ -- by Eq. (4.28). However, nearly always the real matrix B cannot be determined and therefore for practical computations it is replaced by some other B_{es} obtained from various approximate estimates of measurement errors. Often, for example, it is assumed that measurement errors are independent, that the dispersions of these errors are estimated, and on the basis of these estimates, the diagonal matrix $B_{es} = B_0$ is set up.

Matrix B_{es} is used both in the likelihood equation (4.17) or (4.22), as well as in computing the matrix of the second moments K of vector a. By employing B_{es} instead of B in the likelihood equations, generally speaking the errors in determining vector a increase (or at best, remain unchanged), but by using B_{es} in computing matrix K we get an incorrect result. /219

The increase in the errors of determining vector a (and thus, in any parameter $\eta(a)$) in the first case occur because in replacing the real matrix B with any other matrix, for example, B_{es} the likelihood matrix H becomes nonoptimal with respect to the criterion of the method of maximum likelihood. The reader can find in [6, 10] the proof that the errors in determining vector a when the real matrix B is replaced by B_{es} are not reduced, that is,

$$\Delta K_{ob} = K_{ob} - K \geq 0, \qquad (4.44)$$

where

$$K_{ob} \; H_{es} B H_{es}^{T}; \quad K = (W B^{-1} W^{T})^{-1};$$
$$H_{es} = (W B_{es}^{-1} W^{T})^{-1} W B_{es}^{-1},$$

The error in computing matrix K (and therefore, D_η) when B_{es} is used in place of B arises because, when matrix B is unknown, one must use instead of the relation

$$K_{ob} = H_{es} B H_{es}^T,$$

the relation

$$K_{es} = H_{es} B_{es} H_{es}^T = (W B_{es}^{-1} W^T)^{-1}.$$

Naturally, in the general case we have

$$K_{es} \neq K_{ob}$$

and the following methodological errors arise:

$$\Delta K_M = K_{es} - K_{ob}; \tag{4.45}$$

$$(\Delta D_\eta)_M = l_\eta^T \Delta K_M l_\eta. \tag{4.46}$$

As shown by analysis, ΔK_M can be both determined (positively or negatively), as well as undetermined, and the error $(\Delta D_\eta)_M$ can be both positive or negative.

The most dangerous methodological errors are those that lead to the understating of the dispersions in the determination of the orbital parameters, that is, $(\Delta D_\eta)_M < 0$. The danger of understating D_η lies in the fact that in this case, when designing navigational facilities and planning measurements, facilities and measurement conditions can be selected that cause much greater errors in orbital determination compared to those assumed, that is, they are responsible for poorer accuracy of navigation than is required.

In order not to allow understatements of possible errors in determining the trajectory parameters, in the following the estimate of the dispersion of errors in the determination of parameter $\eta(a)$ obtained so that the following relation always holds /220

$$(\Delta D_\eta)_M \geqslant 0. \tag{4.47}$$

is used as the characteristic of the accuracy of the determination

of this parameter [η(a)]. We will denote this estimate of dispersion by Dη. If the estimate Dη can be calculated by a formula of the form

$$D\eta = l_\eta^T A l_\eta, \tag{4.48}$$

where A is the symmetric, positively determined matrix of dimension (m x m), identical for any parameter η(a), so we will call matrix A the estimational matrix of the second moments of the errors of vector a. In the following we will denote the estimational matrix by $\overline{K}$ in contrast to the actual matrix of the second moments K of vector a.

At present there are several methods of finding estimates of dispersions of errors in determining the parameter η(a). The main methods are discussed in [10]. Below these methods are described.

All the estimates of dispersions of parameters determined, examined below, are divided into two classes. Let us introduce, for the determination of which class an estimate belongs to, the concept of the delimiting set of matrices of the second moments of the measurement errors and the concept of the replacement matrix.

Suppose that from the analysis of the means and processes of measurements some minimum set of symmetric, positively determined matrices is determined, among which there is also the actual matrix B of the second moments of measurement errors. We will call this set the delimiting set and denote it by g.

We will call the matrix $\overline{B}_\eta$ that has the following property the replacement matrix for the delimiting set g and for the determined parameter η: the property that the dispersion of the errors in the determination of parameter η, calculated on the assumption that the matrix of the second moments of the measurement errors is $\overline{B}_\eta$ is not smaller than the dispersion of the errors in the determination of the same parameter η calculated for arbitrary $B \in g$. Here it is assumed that the matrix of likelihood H_{li} [li = likelihood] is the single matrix for all the parameters determined and is constructed by using some estimational matrix B_{li} that in the general case differs from $\overline{B}_\eta$. Thus,

$$H_{li} = (W B_{li}^{-1} W^T)^{-1} W B_{li}^{-1}; \tag{4.49}$$

$$\sigma_\eta = l_\eta^T H_{li} \overline{B}_\eta H_{li}^T l_\eta. \tag{4.50}$$

All the methods of finding the estimates of the dispersions $D\eta$ differ by the techniques of finding the delimiting sets. We make the above-noted subdivision of estimate types into two classes in the following. But now let us formulate two requirements that the replacement matrix $\overline{B}$ must satisfy. /221

Let B_i be the arbitrary matrix of set g and let $K_i = H_{li} B_i H_{li}^T$.

And thus, $\overline{K} = H_{li} \overline{B} H_{li}^T$.

Requirement 1. The magnitude of the methodological error ΔK_M must satisfy the condition

$$\Delta K_M = \overline{K} - K_i = H_{li} (\overline{B} - B_i) H_{li}^T \geqslant 0, \tag{4.51}$$

where

$$\overline{K} = H_{li} \overline{B} H_{li}^T.$$

The following consequence derives from Eq. (4.51):

$$B \geqslant B_i.$$

Eq. (4.51) means that using the replacement matrix in the estimates of errors in the determination of vector a is tantamount to overstating the measurement errors. So it is best to select a matrix $\overline{B}$ utilizing (4.51), with which the overstatement of the measurement errors will be at a minimum. This condition can be regarded as the second requirement on the replacement matrix. It can be formulated more clearly as follows.

Requirement 2. The replacement matrix $\overline{B}$ must be such that if instead of it we take another matrix $B' < \overline{B}$, then in the set g we can always find B_i for which condition (4.51) is not satisfied.

1. The first class of estimates includes estimates obtained through use of delimiting set g such that for these sets the replacement matrices $\overline{B}_\eta$ do not depend on parameters η but depend only on the set g itself, that is,

$$\overline{B}_\eta = \overline{B} \neq \overline{B}(\eta).$$

The estimational matrix $\overline{K}$ exists for this estimate class, so that the estimate of the dispersion of any parameter can be calculated by Eq. (4.48).

Let us look at the types of estimates of dispersions of errors in the determination of parameter $\eta(a)$ of the first class.

1. Suppose that we know the delimiting set g and the replacement matrix $\overline{B}$ corresponding to it, which is unique for all trajectory parameters. The matrix $\overline{B}$ is used for setting up the likelihood matrix.

The estimate $D\eta$ of the first type is defined by the relation

$$D\eta = D_1\eta = l_\eta^T K_1 l_\eta, \tag{4.52}$$

where

$$K_1 = H_1 \overline{B} H_1^T = (W B^{-1} W^T)^{-1}; \tag{4.53}$$

$$H_1 = (W \overline{B}^{-1} W^T)^{-1} W \overline{B}^{-1}. \tag{4.54}$$

Let us look at the particular case when matrix $\overline{B}$ is a diagonal matrix, that is /222

$$\overline{B} = B_0. \tag{4.55}$$

In this case we denote the estimates by $K_1^{(0)}$ and $D_1^0\eta$, respectively:

$$K_1^{(0)} = (W B_0^{-1} W^T)^{-1}; \quad D_1^0\eta = l_\eta^T K_1^{(0)} l_\eta. \tag{4.56}$$

We note that K_1 can be computed also by Eq. (4.38) if $\overline{B}$ is given in the form (4.9).

The case when the entire set g consists of a single matrix -- -- the matrix of the actual errors of measurements B -- is a trivial case of estimates (4.52). Clearly, Eq. (4.52) is suitable for calculating the characteristics of the errors in the determination of trajectory parameters even in this case.

2. Suppose that we know the delimiting set and the replacement matrix $\overline{B}$. However, to simplify the computational process or for other reasons when the measurements are statistically treated, their systematic errors either are not at all allowed for or else are allowed for in part. The matrix B_{1i} is computed by means of the following formula:

$$B_{1i} = \overline{B} - B_{r-1,n}^T B_{r-1,n}, \tag{4.57}$$

where $B_{r-l,n}=\|b_i\|$, $i=r-l, r-l+1, \ldots, r$;

$b_i(t)$ is a function of the i-th systematic error not allowed for in B_{li}

r is the number of systematic errors in $\overline{B}$, and

ℓ is the number of systematic errors not allowed for in B_{li}.

Obviously, if not all the systematic errors are not allowed for,

$$B_{li} = B_0, \tag{4.58}$$

where B_0 is the diagonal matrix.

In this case we denote the estimational matrix of the second moments of the errors of vector a by K_2, and the estimate of dispersion -- by $D_{2\eta}$. We have:

$$K_2=H_{li}\overline{B}H_{li}^{\tau}=(WB_{li}^{-1}W^{\tau})^{-1}+H_{li}B_{r-l,n}^{\tau}B_{r-l,n}H_{li}^{\tau}=K_{li}+\Delta K_M \tag{4.59}$$

where

$$H_{li}=(WB_{li}^{-1}W_{\tau})^{-1}WB_{li}^{-1};$$

ΔK_M is the increase of the estimational matrix due to the nonconsideration in B_{li} of ℓ systematic errors

$$D_2\eta=l_\eta^{\tau}K_2l_\eta. \tag{4.60}$$

Let us single out in this type of estimates the particular case when the replacement matrix consists of a matrix with only one systematic error, that is, /223

$$\overline{B}=B_0+b^{\tau}b. \tag{4.61}$$

Here the following

$$B_{li} = B_0 \tag{4.62}$$

is used in the likelihood matrix. This particular kind of the type of estimate we are considering we denote by $K_2^{(0)}$ and $D_2^0\eta$, respectively. Obviously,

$$K_2^{(0)} = H_{1i}\overline{B}H_{1i}^{\tau}; \tag{4.63}$$

$$\mathcal{E}_2^0\eta = l_\eta^{\tau}K_2^{(0)}l_\eta. \tag{4.64}$$

When one of the estimates of the first class was used as the characteristic of the accuracy of the determination of the orbit from navigational measurements, there exists an optimal matrix B_{1i} that is unique for all parameters $\eta(a)$, and used for constructing the likelihood matrix. The overall error of the computation of matrix K is determined by the quantity

$$\Delta K_\Sigma = \Delta K_{1i} + \Delta K_M,$$

where ΔK_{1i} is determined by Eq. (4.44), and
ΔK_M is determined by Eq. (4.45).

With optimal selection of B_{1i}, $\Delta K\Sigma$ must take on a minimum value if the following condition is satisfied

$$\Delta K_\Sigma \geqslant 0. \tag{4.65}$$

The condition of optimality B_{1i} is determined by the following theorem.

Theorem 1. The minimum value of error $\Delta K\Sigma$ in the computation of matrix K satisfying condition (4.65) is attained if it is assumed that

$$B_{1i} = \overline{B}. \tag{4.66}$$

Proof. We have

$$\Delta K_\Sigma = \Delta K_{1i} + \Delta K_M = H_{1i}BH_{1i}^{\tau} - (WB^{-1}W^{\tau})^{-1} +$$
$$+ H_{1i}(\overline{B} - B)H_{1i}^{\tau} = H_{1i}\overline{B}H_{1i}^{\tau} - (WB^{-1}W^{\tau})^{-1}.$$

By virtue of the definition of $\overline{B}$, the following obtains for any B_{1i}:

$$H_{1i}\overline{B}H_{1i}^{\tau} \geqslant (WB^{-1}W^{\tau})^{-1},$$

that is

$$\Delta K_\Sigma \geqslant 0.$$

Still, according to (4.44) the quantity /224

$$H_{1i}\overline{B}H_{1i}^{T}=(WB_{1i}^{-1}W^{T})^{-1}WB_{1i}^{-1}\overline{B}B_{1i}^{-1}W^{T}(WB_{1i}^{-1}W^{T})^{-1}$$

has its smallest value only when

$$B_{1i} = B_{1i}^{opt} = \overline{B}.$$

Obviously, here the matrix $\Delta K\Sigma$ will also be a minimum. Since $\overline{B}$ is the same for all parameters $\eta(a)$, B_{1i}^{opt} will also be unique for all $\eta(a)$, which is what was to be proved.

A practical method of finding replacement matrices B is indicated by the result obtained in [6]. Below this result is formulated as a theorem.

Theorem 2. If any matrix B_i belonging to a delimiting set g is defined by the relation

$$B_i=B_0+C^{T}\Pi_i^{T}\Pi_iC, \tag{4.67}$$

where B_0 is a diagonal matrix with positive elements
C is some known matrix of dimension k x n, and
Π_i is a matrix of dimension p x k (where $k \geq p$) such that the moduli of the eigenvalues of the matrix $\Pi_i^{T}\tilde{\Pi}_i$ do not exceed unity, then for this set g there exists a replacement matrix defined by the relation

$$\overline{B}=B_0+C^{T}C. \tag{4.68}$$

We present a fairly general example of a possible method of using theorem 2 for computing the replacement matrix.

Example I. Suppose that from an analysis of the measurements it is found that the errors in measurements using navigation facilities examined in any specific case are characterized by random independent components with dispersions $\sigma_{\gamma l}^2$ (l_i is the number of the measured parameter) and systematic components. From the dispersions at the moments of measurement let us set up a diagonal matrix B_0 along whose diagonal the following can be successively arranged:

$$\sigma^2_{\gamma 1}(t_{11}),\ \sigma^2_{\gamma 1}(t_{12}),\ \ldots,\ \sigma^2_{\gamma 1}(t_{1n_1}),\ \sigma^2_{\gamma 2}(t_{21}),\ \ldots,\ \sigma^2_{\gamma 2}(t_{2n_2}),\ \ldots,\ \sigma^2_{\gamma s}(t_{s1}),\ \ldots,$$
$$\ldots,\ \sigma^2_{\gamma s}(t_{sn_s}).$$

Here $\gamma_1, \gamma_2, \ldots, \gamma_s$ are the parameters measured, and
$n_1, n_2, \ldots, n_s$ are the numbers of measurements of the corresponding parameters.

Systematic components of measurement errors are caused by an inexact knowledge of the law of variation with time of any parameters c_j. Most often the following are included in the category /225
of errors Δc_j in space navigation practice:

the root-mean-square errors of the geodetic tie-in of measuring stations;

root-mean-square errors of various astronomic constants;

root-mean-square errors in the coefficients of the expansion in series of potentials of the gravitational fields of celestial bodies; and

systematic errors of navigation measurements, and so on.

All these errors can be viewed as random and independent in estimates of the corresponding constants, but in the course of measurements they remain invariant and therefore lead to systematic measurement errors. In the linear approximation the effect of Δc_j on measurement errors can be characterized by the formula

$$b_j(t) = \frac{\partial \gamma_l(t)}{\partial c_j} \Delta c_j,$$

where l is the number of the navigation measurement measured. We will call the functions $b_j(t)$ functions of systematic measurement errors owing to the j-th systematic error. Let us set up by means of $b_j(t)$ the vector of the j-th systematic error:

$$\boldsymbol{b}_j = \| b_{1j}(t_{11}) \ldots b_{1j}(t_{1n_1}) \ldots b_{sj}(t_{s1}) \ldots b_{sj}(t_{sn_s}) \|,$$

where s is the number of parameters measured, and
$n_1, \ldots, n_s$ is the number of measurements in the corresponding parameters.

If $\Delta c_j < \Delta c_{j\,max}$, where $\Delta c_{j\,max}$ is some limiting estimate, the vector b_j corresponding to $\Delta c_{j\,max}$ we will denote by $b_{j\,max}$. We will assume Δc_j to be independent of each other.

Let us set up a matrix of the maximum systematic errors

$$B_{rn} = \left\| \begin{matrix} b_{1\max} \\ b_{2\max} \\ \vdots \\ b_{r\max} \end{matrix} \right\|.$$

from the vectors $b_{j\,max}$ (j = 1, 2, ..., r).

The matrix of the real values of the systematic measurement errors could have been derived as follows:

$$B^{\partial}_{rn} = \Pi B_{rn},$$

however, matrix Π is unknown. But from the definition of B_{rn} it follows that matrix Π is diagonal and its elements do not exceed unity with respect to the values of their moduli, since

$$|\Delta c_j|_{real} \leqslant \Delta c_{j\max} \quad \text{and} \quad |b^{\partial}_j(t_i)| \leqslant |b_{j\max}(t_i)|.$$

In this case the moduli of the eigenvalues of matrix $\Pi\Pi^T$ also do not exceed unity and under theorem 2, the replacement matrix can be determined by the relation /226

$$\overline{B} = B_0 + B^{T}_{rn} B_{rn}. \tag{4.69}$$

II. The second class of estimates includes estimates of dispersions of errors made in the determination of the trajectory parameters η obtained in those cases when for the delimiting set found either there is no replacement matrix unique for all parameters η, or else its use is unreasonable owing to the resulting extreme overstatement of the measurement errors and, thus, of the estimates $D\eta$. Typical of estimates in the second class is the fact that each parameter η has its own replacement matrix. Of all the possible estimates of the second class, below we examine only one type of estimate and several important particular cases. Let us derive the general formula for estimates of this type.

Suppose that s groups of measurements of n_i measurements each are made. The following data are known about the errors of these measurements:

the dispersions of the errors for any moments of measurements can be expressed by formulas of the type $\sigma^2_{\gamma\ell}(t)$ (ℓ is the number of the parameter);

the modulus of the coefficient of correlation between the measurement errors within the ℓ-th group ($\ell = 1, 2, \ldots, s$) does not exceed some known value $\hat{k}'_\ell$; and

the correlations between the measurements of different types of groups are nonexistent.

A set of all possible diagonally cellular matrices of n-th degree (n is the total number of measurements) in which each ℓ-th diagonal cell is a positively determined symmetric matrix with the following elements is the delimiting matrix for the actual matrix of the second moments of the measurement errors if the information indicated above is available:

$$b^l_{ij} = \sigma^2_{\gamma l}(t_i) \quad (i = 1, 2, \ldots, n_l) \tag{4.70}$$

and with the diagonal elements delimited by the following inequalities

$$b^l_{ij} \leqslant \hat{k}_l \sqrt{\sigma^2_{\gamma l}(t_i)\sigma^2_{\gamma l}(t_j)}, \tag{4.71}$$

where $\sigma^2_{\gamma\ell}(t_i)$ is the dispersion of the error of the ℓ-th group of measurements at moment t_i; and

$\hat{K}_\ell$ is a known limiting value of the modulus of the coefficient of correction [sic, perhaps should be correlation] of the errors of the ℓ-th group.

The remaining elements of the matrix are equal to zero.

The diagonal matrix B_0 made up of dispersions of the measurement errors is used as the likelihood matrix, in accordance with known information on the measurement errors.

The estimate of the dispersion of the determination of parameter η when the above data are available is constructed as follows. /227
For each parameter η, a replacement matrix is selected so that its values of the nondiagonal terms bounded by inequalities of the type (4.71) correspond to the maximum dispersion of the errors made in

determining parameter η. The estimate of the dispersion of the errors in parameter η is calculated in accordance with this replacement matrix.

We will denote this estimate of the dispersion of the errors made in the determination of parameter η by $D_3\eta$. In [10] this estimate is investigated in detail and a theorem determining the rules of its computation[5] is proven.

Theorem 3. Estimate $D_3\eta$ is defined by the relation

$$D_3\eta = \sum_{l=1}^{s} D\eta(\hat{k}_l), \tag{4.72}$$

where

$$D\eta(\hat{k}_l) = (1-\hat{k}_l)[D\eta(0)]_l + \hat{k}_l[D\eta(1)]_l; \tag{4.73}$$

$$[D\eta(0)]_l = \sum_{j=1}^{nl} p_{lj}^2; \tag{4.74}$$

$$[D\eta(1)]_l = \left(\sum_{j=1}^{nl} |p_{lj}|\right)^2, \tag{4.75}$$

$p_{\ell j}$ ($j = 1, 2, \ldots, n$) are the components of vectors p_ℓ, and

p_ℓ ($\ell = 1, 2, \ldots, s$) are the vector-rows into which the vector $\ell_\eta^T H_0 = ||p_1 p_2 \ldots p_\ell \ldots p_s||$ corresponding to s cells is decomposed (the dimension of vector p_ℓ is equal to $1 \times n_\ell$, where n_ℓ is the number of measurements in the ℓ-th group);

$$H_0 = (WB_0^{-1}W^T)^{-1}WB_0^{-1}.$$

If the measurements are not divided into groups, that is, if $s = 1$, $D_3\eta = D\eta(\hat{k})$. Further, if the limiting values of the coefficient of correlation $\hat{k} = 0$, that is, the measurements are independent, we have

$$D\eta(\hat{k}) = D\eta(0) = D_1^0\eta. \tag{4.76}$$

---

[5] In this study the estimate of this type of error is denoted by $D_2\eta$.

The case when s = 1 is very often encountered in practice. Therefore the estimate corresponding to this case is best given an independent notation. In the following we will denote this estimate by /228

$$D_4\eta = D\eta(\hat{k}) = D_3\eta_{s=1}. \tag{4.77}$$

A particular case of this estimate when $\hat{k} = 1$, that is, when the total (but apriori unknown) correlation of the measurement errors is possible, is denoted by $D_4^0\eta$. From Eq. (4.73) we find

$$D_4^0\eta = D\eta(1) = \left(\sum_{i=1}^{n} |p_i| \sigma_{\eta i}\right)^2. \tag{4.78}$$

If the number of measurements is at a minimum, that is, n = m, we will denote this estimate for this case by

$$D_4^0\eta_m = D_4^0\eta_{n=m}. \tag{4.79}$$

Thus, we can write

$$D_4\eta = (1-\hat{k})\, D_1^0\eta + \hat{k} D_4^0\eta. \tag{4.80}$$

From theorem 3 there follows the following corrolary.

Corrolary. Estimate $D_4\eta$ with variation in $\hat{k}$ within the limits $0 \leq \hat{k} < 1$ varies linearly within the limits

$$D_1^0\eta \leqslant D_4\eta \leqslant D_4^0\eta. \tag{4.81}$$

In concluding our examination of estimates in the second class, let us dwell on the calculation of the maximum modulus of the coefficient of correlation $\hat{k}$. We will illustrate one of the possible methods of computing $\hat{k}$ by the following examples.

Example 2. Suppose we know that navigational measurements are accompanied by two types of errors:

by random errors with known dispersions $\sigma_1^2(t)$; and

by correlation errors whose dispersions $\sigma_2^2(t)$ are known, and whose coefficients of correlation are unknown, but satisfy the inequality

$$|\hat{k}_{ij}| \leqslant \hat{k}.$$

In this case, only the diagonal matrix B_0 can be used in defining the orbit:

$$B_0 = \begin{Vmatrix} \sigma_1^2(t_1)+\sigma_2^2(t_1) & 0 \ldots & 0 \\ 0 & \sigma_1^2(t_2)+\sigma_2^2(t_2) \ldots & 0 \\ \ldots & \ldots & \ldots \\ 0 & 0 & \sigma_1^2(t_n)+\sigma_2^2(t_n) \end{Vmatrix}.$$

To characterize the accuracy of orbital determination, we can employ estimate $D_4\eta$, and to construct it we take the quantity k. /229

Example 3. Estimate $D_4\eta$ can be used also under the conditions of example 1. Suppose, as in example 1, we know the dispersions of the random independent measurement errors characterizing the matrix B_0, and the vectors of the maximum systematic errors of measurements b_j (j = 1, 2, ..., r). Since we must know the total dispersions of the measurement errors and the largest modulus of the possible coefficients of correlation in constructing the estimates of the second class, to determine these quantities we are justified in starting from the formula

$$B = B_0 + \sum_{j=1}^{r} b_j^T b_j. \qquad (4.82)$$

To reduce the notation, we will denote the elements of the diagonal matrix B_0 by σ_i^2, and the elements of vectors b_j of systematic errors by b_{ji}. The elements of matrix B are referred to by β_{ik}.

From Eq. (4.82) we find that the total dispersion of errors of the i-th measurement is defined by the formula

$$\beta_{ll}=\sigma_{\Sigma l}^2=\sigma_l^2+\sum_{j=1}^{r} b_{jl}^2. \tag{4.83}$$

The nondiagonal elements of matrix B can be determined by a formula, which is also not difficult to derive from Eq. (4.82):

$$\beta_{lk}=\sum_{j=1}^{r} b_{jl}b_{jk}. \tag{4.84}$$

The limiting value of the modulus of the coefficient of correlation $\hat{k}$ over this navigation interval is defined by the relation

$$\hat{k}=\max_{lk=\text{var}}\left\{\frac{|\beta_{lk}|}{\sqrt{\sigma_{\Sigma l}^2\sigma_{\Sigma k}^2}}\right\}. \tag{4.85}$$

Based on Eqs. (4.85) with reference to (4.84), the following simpler estimational expression can be obtained:

$$\hat{k}\leqslant\max_{l=\text{var}}\left\{\frac{1}{\sigma_{\Sigma l}^2}\sum_{j=1}^{r} b_{jl}^2\right\}. \tag{4.86}$$

Let us denote the expression appearing in the parentheses of Eq. (4.86) by $f(t_i)$, where t_i is the moment of measurement. With reference to this, we can write /230

$$\hat{k}\leqslant f(t)|_{\max},\ (t_{\text{H}}\leqslant t\leqslant t_{\text{K}}), \tag{4.87}$$

where t_H and t_K are the times of the beginning and ending of the navigation interval; and
$f(t)|_{max}$ is the maximum value of function f(t) on the navigation interval.

Eq. (4.87) then enables us to estimate the magnitude of $\hat{k}$ on the navigation interval, while Eq. (4.83) gives us the total dispersions of the measurement errors necessary in setting up the estimates of the second class.

In several practical cases there arises the problem of estimating the accuracy of determining simultaneously a group of

trajectory parameters η_i (i = 1, 2, ..., q). We denote the vector-column constructed of these parameters by η. In the general case, the parameters η_i can relate to different instants of time t_i (i = 1, 2, ..., q).

Let us denote the vector of the derivatives of parameter $\eta_i(t_i)$ with respect to the main trajectory parameters a_j (j = 1, 2, ..., m) by $\ell_{\eta i}(t_i)$. We denote the matrix of derivatives constructed of vectors ℓ_η by L_η:

$$L_\eta = \| l_{\eta 1} l_{\eta 2} \ldots l_{\eta q} \|. \tag{4.88}$$

For each of the parameters η_i of this group, by one of the methods indicated above we can find the corresponding estimate of the dispersion of the errors in its determination.

To construct the estimates of the first class according to the definition, the replacement matrix $\overline{B}$ unique for all parameters $\eta = \eta(a, t)$ can be used. Here, since in the linear approximation

$$\Delta\eta = L_\eta \Delta a,$$

and since matrix (4.58) corresponds to the estimate of the second moments of the errors in the determination of vector a, the matrix of the second moments of vector η can be estimated thusly:

$$K_{1\eta} = L_\eta^T K_1 L_\eta. \tag{4.89}$$

All the remaining estimates of the first class considered, being particular cases of estimate K_1, can also be obtained by means of an expression of the type (4.89), in which the corresponding estimational matrices $K_1^{(0)}$, K_2, and so on are substituted in place of estimational matrix K_1.

If for the estimates of the dispersions in determining each parameter η_i of this group we use some estimate of the second class, for the entire group of parameters η no unique replacement matrix $\overline{B}$ exists. By virtue of the definition of the estimates of the second class, the nondiagonal terms $\overline{B}_{\eta i}$ are selected within the limits of the constraints (4.71) so that /231

$$D_{\eta_i} = D_{\eta_i \max},$$

that is, the dispersions of the estimates of all parameters η_i of the components η will be estimated on the basis of the assumption that there is the worst correlation of errors for each parameter η_i over the entire time interval of the measurement of this parameters.

Since the actual matrix B does not depend on the composition of the parameters to be determined, use of estimates of the second class or the group of parameters to be determined generally speaking leads to large overstatements of the estimates of the dispersions of errors in determining the group of parameters η.

4.4. Space of Trajectory Parameters

Definition of space G. In analyzing the accuracy of the determination of the flight trajectory in the linear formulation, as follows from the preceding sections, often we have to deal with vectors whose components are partial derivatives of some trajectory parameter $\eta(a)$ with respect to the main parameters a_i, for example, of the following type:

$$l_\eta = \left\| \frac{\partial \eta}{\partial a_1} \frac{\partial \eta}{\partial a_2} \dots \frac{\partial \eta}{\partial a_m} \right\|^T. \tag{4.90}$$

Vector l_η in the linear approximation uniquely characterizes the variation in parameter η during measurements of vector a:

$$\Delta\eta = l_\eta^T \Delta a.$$

In this chapter dealing mainly with an analysis of the accuracy with which the flight trajectory of an SC is determined and problems of optimal planning of navigation measurements, the investigation is conducted in the linear approximation. So vectors of the type (4.90) in the following will often be called vectors of one-dimensional trajectory parameters[6], or simply vectors of trajectory parameters.

---

[6] Multidimensional parameters to be determined are characterized by the matrices (4.88).

Employing concepts of vectors of the (4.90) type makes it possible to carry out graphical geometrical interpretations of the main relations in the theory of measurement errors.

Let us look at a set of all possible trajectory parameters and let us bring into correspondence to this set a set of vectors of the type (4.90). Let us divide all the trajectory parameters into two groups:

trajectory parameters whose values can be measured by the navigation facilities employed; and

trajectory parameters whose values cannot be measured directly /232 but are determined indirectly from measurements of other parameters.

Accordingly, the vectors of the parameters in the first group we will refer to by

$$w = w(a, t) \tag{4.91}$$

and we will call them navigational vectors. The vectors of the second-group parameters we will refer to by

$$l_\eta = l_\eta(a, t). \tag{4.92}$$

and call them vectors of parameters to be determined. The dispersion of the errors in navigational measurements we designate by

$$D_{\gamma l}(t) = \sigma^2_{\gamma l}(t). \tag{4.93}$$

We will designate the dispersions of the errors in determining the parameters ℓ_η from navigation measurements thus by

$$D_\eta(t) = \sigma^2_\eta(t). \tag{4.94}$$

Let us bring into consideration the vectors of the navigational parameters of trajectories related to the root-mean-sqaure errors of the corresponding parameters:

$$w_{Hl} = \sigma^{-1}_{\gamma l} w_l(a, t); \; l_{\eta H} = \sigma^{-1}_\eta l_\eta(a, t). \tag{4.95}$$

Let us introduce into the set of these vectors of all possible types the operation of vector addition and vector multiplication by the numbers corresponding to the formulas:

$$w_{H1} + w_{H2} = \left\| \sigma^{-1}_{\gamma 1} \frac{\partial \gamma_1}{\partial a_1} + \sigma^{-1}_{\gamma 2} \frac{\partial \gamma_2}{\partial a_1} \ldots \sigma^{-1}_{\gamma 1} \frac{\partial \gamma_1}{\partial a_n} + \sigma^{-1}_{\gamma 2} \frac{\partial \gamma_2}{\partial a_n} \right\|^\tau,$$

$$\mu w_H = \left\| \mu \sigma^{-1}_\gamma \frac{\partial \gamma}{\partial a_1} \ldots \mu \sigma^{-1}_\gamma \frac{\partial \gamma}{\partial a_n} \right\|^\tau.$$

The set of all possible vectors (4.95) with introduced operations of vector addition and vector multiplication by a number constitutes a linear space. In the following we will refer to this space as the space of the trajectory parameters and denote it by G. The dimension of space G obviously is equal to the dimension of the vector of the main trajectory parameters a.

If the navigational measurements of parameter γ_i can be made over some flight time interval $[t_H, t_K]$, the navigational vector $w_{H\,i}(a, t)$ corresponding to γ_i over this interval will take on a series of successive values, and its end will describe the hodograph curve. If over this flight section measurements of several parameters γ_i are possible ($i = 1, 2, \ldots, s$), the vectors corresponding to them will describe s hodographs.

In several cases, it is convenient for the investigation to adopt as the argument of the navigational vector-functions not the flight time, but some quantity, to each value of which only one vector would correspond even for simultaneous measurements of several parameters. Sometimes the variable τ associated as follows with time is adopted as this argument in the space G. Let $t_{H\,i}$ and $t_{K\,i}$ be the beginning and endpoint of the time interval over which measurements of the navigational parameter γ_i are possible. Let us call the quantity defined by the relation /233

$$\Delta\tau_{\text{н}}=\sum_{l=1}^{s}(t_{\text{к}l}-t_{\text{н}l})=\sum_{l=1}^{s}\Delta t_l, \tag{4.96}$$

where s is the number of motion parameters determined, the total navigational interval.

We define the variable τ according to the equality

$$\tau=t_{\text{н}1}+\Delta\tau, \tag{4.97}$$

where $\Delta\tau$ takes on successively all values from 0 to $\Delta\tau_{\text{п}}$. We will assume that over the interval from $\tau_H = t_{H\,1}$ to $\tau_H + \Delta t_1$ measurements of only the first navigational parameter are possible, and over the interval $[\tau_H + \Delta t_1, \tau_H + \Delta t_1 + \Delta t_2]$ -- measurements of only the second parameter, over the interval $\left[\tau_{\text{н}}+\sum_{j=1}^{l-1}\Delta t_j, \tau_{\text{н}}+\sum_{j=1}^{l}\Delta t_j\right]$ --

-- the measurements of only the i-th parameter, and so on. Under this definition of the variable τ, to each value of τ there is brought into unique correspondence a specific instant of flight time and the number of the parameter being measured that uniquely define the navigational vector $w_{H\,i}(t)$. We note that the relation between τ and t depends on the composition of the parameters being measured.

Convex covering of navigational vector-function. As noted above, the vector-function $w_H(\tau)$, when τ is varied over the entire navigational interval (4.96), describes in the space G a hodograph. In the general case this hodograph is discontinuous and it consists of a finite number of cusps of continuous lines. In addition to the hodograph of $w_H(\tau)$, we will consider the hodograph of the negative vector-function $-w_H(\tau)$. Obviously, hodographs of positive and negative vector-functions exhibit a central symmetry relative to the origin of coordinates. We will form about these hodographs a convex covering, to be defined thusly.

We will refer to as a convex covering of the navigation vector-function in m-dimensional space G a surface of minimum convex figure containing hodographs of the vector-functions $\pm w_H(\tau)$ over the entire interval of their definition. This covering is formed, for example, by the evolution of hodographs with hyperplane $\mathcal{L}$ with dimension m - 1 (Fig. 4.1). We will call the hyperplane $\mathcal{L}$ the reference hyperplane. In fact, it obviously then is also the tangential plane to the convex covering. /234

In being evolved, hyperplane $\mathcal{L}$ can be tangent to hodographs simultaneously at one, two, and some finite set of points. Finally, if the entire hodograph of some vector-function or a section of it lies in a plane with dimension less than m (but greater than zero), simultaneous tangency of the hodograph to hyperplane $\mathcal{L}$ can occur at an infinitely large number of points.

The set of points of a convex covering falling within the hyperplane $\mathcal{L}$ for each of its fixed positions we will refer to as the face of the covering and denote it by Λ. Under this definition the number of faces of the convex covering can be infinitely large. The dimension of face Λ of a convex covering can lie within the limits

$$0 \leqslant m_f \leqslant m-1.$$

The dimension $m_f = 0$ [f = face] obtains when there is tangency between plane $\mathcal{L}$ and the convex covering at a single point. The

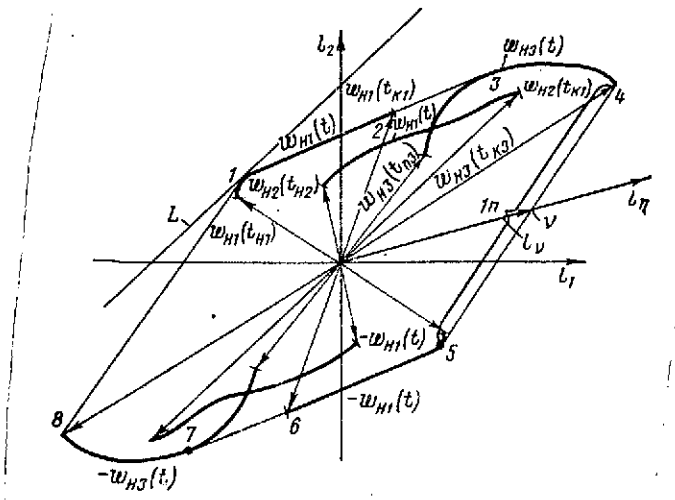

Fig. 4.1. Scheme of formation of convex covering in two-dimensional space G:
1, 2, ..., 8 -- Convex covering of navigational vector-functions $w_{H1}(t)$, $w_{H2}(t)$, and $w_{H3}(t)$

dimension $m_f = 1$ obtains when there is tangency between the plane $\mathcal{L}$ and the convex covering over the segment of a line, and so on. Faces that have the dimension $m_f = 0$ we will refer to as the vertices of the convex covering.

The set of vertices of the navigational vectors situated in each face of the convex covering we will call the reference set and denote it by $\mathcal{M}$. Obviously, $\mathcal{M}$ is always a part of (or coincides with) the set Λ. The set of instants of time corresponding to the set of reference vectors we will call the set of reference instants and denote it by T. /235

The vector of the trajectory parameter being determined $l_{\eta H}$ (or it's extension) intersect the convex covering at some point, which we designate by ν_η. Let us denote the vector colinear with l_η whose apex is the point ν_η, by l_ν. The face of the convex covering containing the point ν_η we denote by Λ_η (in the general case the number of these faces can be more than 1, in particular, if l_η extends through the apex of the covering). The part of the reference set $\mathcal{M}$, that is part of face Λ_η we denote by $\mathcal{M}_\eta$, and the part of the set T that enters into face Λ_η we denote by T_η.

Let us set up the matrix

$$F = \sum_{i=1}^{s} \int_{t_H}^{t_K} w_{Hi}(t)\, w_{Hi}^{T}(t)\, dt, \qquad (4.98)$$

where $w_{H\,i}(t)$ are the vectors of the parameters $\gamma_i(t)$ measured, and s is the number of parameters measured.

In order that among the measurements possible over the interval $[t_H, t_K]$ we can always find such $n \geq m$ measurements that would determine the finite value of the estimate of the vector of the main parameters a, the following condition must be satisfied

$$\det F \neq 0. \tag{4.99}$$

4.5. Several Geometrical Interpretations in the Space G

Above all the vectors in space G were divided into two groups:

vectors of (navigational) parameters measured, and

vectors of parameters determined from measurements. Since the dispersions of the errors in making the navigational measurements can always be estimated by some method, the navigational vectors in the space G can assume to be known.

The vectors of the parameters $\ell_{\eta H}$ determined are known in direction, since derivatives that are components of vector ℓ_η can always be computed. The dispersion of the errors in the determination of the parameter η is estimated from the value of the vectors $w_{H\,i}$. The methods of these estimates are examined in Section 3 of this chapter.

Thus, various methods of estimating the dispersions of errors in making the determination of parameter η from navigation measurements in space G can be interpreted as various geometrical constructions with which we find the vector $\ell_{\eta H}$ from the vectors $w_{\eta H\,i}$. Let us examine a specific interpretation of several types of estimates.

Interpretation of estimates in the first class. All estimates in the first class are based on finding the replacement matrix of the second moments of the errors in making the measurements $\overline{B}$. /236 After $\overline{B}$ was found, one seeks the matrix of the estimates of the second moments of the errors in determining the vector of the main trajectory parameters K_I and the estimate of the dispersion $D_{1\eta}$ from Eqs. (4.52) and (4.53). Let us rewrite the formula for $D_{1\eta}$ with reference to (4.95) in the following form:

$$l_{\eta H}^{T} K_I l_{\eta H} = 1. \tag{4.100}$$

For the arbitrary vectors $\ell_{\eta H}$, Eq. (4.100) define the surface of an ellipsoid. If the direction of the vector $\ell_{\eta H}$ is given, Eq. (4.100) defines $\ell_{\eta H}$ as the distance from the origin of coordinates to the surface of the ellipsoid measured in the direction of the vector $\ell_{\eta H}$.

Thus, the estimates of the dispersions in the first class, (that is, $D_1\eta$, $D_1^0\eta$, $D_2\eta$, and $D_2^0\eta$) reduce to constructing in the space G some ellipsoid defined by the replacement matrix of the errors in making the measurements $\overline{B}$ and computing the distance from the origin of coordinates to the ellipsoid along some direction of vector $\ell_{\eta H}$. Different types of estimates of the first class are characterized by various forms of the ellipsoids (4.100) used for determining the vector $\ell_{\eta H}$.

Transformation of formulas for the estimates $D_1^0\eta$ and $D_4^0\eta_M$. The formula for calculating these estimates was obtained above (see Eq. (4.78)) and is of the form

$$D_4^0\eta=\left(\sum_{i=1}^{n}\sigma_{\eta i}|p_i|\right)^2, \tag{4.101}$$

where p_i (i = 1, 2, ..., n) are the components of vector p;

$$p=l_\eta^T H_0;\quad H_0=(WB_0^{-1}W^T)^{-1}WB_0^{-1};$$

B_0 is the diagonal matrix of the measurement errors, and

$\sigma^2_{\gamma\ell}$ are the elements of matrix B_0.

Let us introduce the notation

$$W_H=WB_0^{-1/2};\quad b_H=\|\operatorname{sign} p_1 \operatorname{sign} p_2 \ldots \operatorname{sign} p_n\|.$$

The vector-column $w_{H\,i}$ (i = 1, 2, ..., n) of matrix W_H are the vectors of the linear space G.

With reference to this notation, let us bring Eq. (4.101) to the form

$$(D_4^0\eta)^{1/2}=l_\eta^T(W_HW_H^T)^{-1}W_Hb_H^T. \tag{4.102}$$

We will examine further the transformations of a somewhat more general formula

$$\Delta\eta = l_1^T (W_H W_H^T)^{-1} l_2. \qquad (4.103)$$

In particular, if $l_1 = l_\eta$, and $l_2 = W_H b_H^T$, then $\Delta\eta = (D_4^0 \eta)^{1/2}$; if $l_1 = l_2 = l_\eta$, then as we can easily see, $\Delta\eta = D_1^0 \eta$. The elements of matrix $K = W_H W_H^T)^{-1}$ we will denote by κ_{ij}, and the components of vectors l_1 and l_2, $\mu_{1\,i}$ and $\mu_{2\,i}$ ($i = 1, 2, \ldots, m$), respectively. The vectors $w_{H\,i}$ in which the j-th component is canceled out will be denoted by $w^j_{H\,i}$. Thus, the matrix made up of the vectors $w^j_{H\,i}$ is denoted by

$$W_{Hj} = \| w^j_{H1} w^j_{H2} \ldots w^j_{Hn} \|. \qquad (4.104)$$

With reference to the derived notation, we can rewrite Eq. (4.103) as follows:

$$\Delta\eta = \sum_{i=1}^{m} \sum_{j=1}^{m} \kappa_{ij} \mu_{1i} \mu_{2j}. \qquad (4.105)$$

The following equality obtains:

$$\kappa_{ij} = (-1)^{i+j} \det (W_{Hi} W_{Hj}^T) \det^{-1} (W_H W_H^T)^{-1}. \qquad (4.106)$$

Here $W_{H\,i}$ and $W_{H\,j}$ are the matrices obtained from W_H by canceling out the i-th and j-th rows, respectively. The notation of these matrices corresponds to (4.104).

Let us transform Eq. (4.106), by using the Binet-Cauchy formula [16]. According to this formula, the determinant of matrix A of dimension m x m is equal to the product of the rectangular matrix B of dimension m x n. ($m \leq n$) in the rectangular matrix C of dimension n x m is equal to the sum of the products of all possible minors of order m of matrix B by the corresponding minors of matrix C. We denote with b_i and c_i the m-dimensional vector-columns of matrices B and C^T, respectively, such that

$$B=\|b_1b_2\dots b_n\|;\quad C^{\mathrm{T}}=\|c_1c_2\dots c_n\|. \tag{4.107}$$

Then the Binet-Cauchy formula can be written thusly:

$$\det A=\det(BC)=$$
$$=\sum_{1\leqslant k_1<k_2<\dots<k_m\leqslant n}\det\|b_{k_1}b_{k_2}\dots b_{k_m}\|\cdot\det\|c_{k_1}c_{k_2}\dots c_{k_m}\|. \tag{4.108}$$

In the following, for brevity we will denote

$$\sum_m=\sum_{1\leqslant k_1<k_2<\dots<k_m\leqslant n}\quad\text{or}\quad\sum_{m-1}=\sum_{1\leqslant k_1<\dots<k_{m-1}\leqslant n}. \tag{4.109}$$

Using Eq. (4.108) for $\det(W_H W_H^{\mathrm{T}})$ and $\det(W_{H\,i}W_{H\,j}^{\mathrm{T}})$ in Eq. (4.106) and introducing into the numerator the sign of summation of all possible minors within the parentheses, and also by increasing the exponent (- 1) by an even number $2k_m$, with reference to the fact that /238

$$\sum_{l=1}^{m}\mu_l(-1)^{l+k_m}\det\|w^l_{Hk_1}\dots w^i_{Hk_{m-1}}\|=\det\|w_{Hk_1}\dots w_{Hk_{m-1}}l\|, \tag{4.110}$$

after transformations we get

$$\Delta\eta=\Big[\sum_{m-1}\det\|w_{Hk_1}\dots w_{Hk'_{m-1}}l_1\|\cdot\det\|w_{Hk_1}\dots w_{Hk_{n-1}}l_2\|\Big]\times$$
$$\times\Big[\sum_m\det^2\|w_{Hk_1}\dots w_{Hk_m}\|\Big]^{-1}. \tag{4.111}$$

Let us set $l_1 = l_\eta$ and $l_2 = W_H b_H^{\mathrm{T}}$ in (4.111). We can represent vector l_η as a linear combination of vectors appearing in the matrix $\|w_{Hk_1}\dots w_{Hk_m}\|$. We will denote the coefficients of the expansion of l_η in terms of this combination of vectors by $\mu_{k_i}(k_1, k_2, \dots, k_m)$. We can represent the vector l_2 in the following form:

$$W_{\mathrm{H}} b_{\mathrm{H}} = \sum_{i=1}^{n} \beta_i w_{\mathrm{H}i}. \tag{4.112}$$

Let us substitute Eq. (4.112) into Eq. (4.111):

$$\sqrt{D_4^0 \eta} = \left[\sum\nolimits_{m-1} \det \| w_{\mathrm{H}k_1} \ldots w_{\mathrm{H}k_{m-1}} l_\eta \| \sum_{k_m=1}^{n} \beta_{k_m} \det \| w_{\mathrm{H}k_1} \ldots \right.$$
$$\left. \ldots w_{\mathrm{H}k_m} \| \right] \left[\sum\nolimits_m \det^2 \| w_{\mathrm{H}k_1} \ldots w_{\mathrm{H}k_m} \| \right]^{-1}. \tag{4.113}$$

By substituting the expression for ℓ_η into Eq. (4.113), we get

$$\sqrt{D_4^0 \eta} = \left[\sum\nolimits_{m-1} \mu_{k_m}(k_1, \ldots, k_m) \det \| w_{\mathrm{H}k_1} \ldots w_{\mathrm{H}k_m} \| \times \right.$$
$$\left. \times \sum_{k_m=1}^{n} \beta_{k_m} \det \| w_{\mathrm{H}k_1} \ldots w_{\mathrm{H}k_m} \| \right] \left[\sum\nolimits_m \det^2 \| w_{\mathrm{H}k_1} \ldots w_{\mathrm{H}k_m} \| \right]^{-1}. \tag{4.114}$$

We note the following with respect to this resulting formula.

1. The number of summands defined by the sign Σ_{m-1} is larger than the summands defined by the sign Σ_m, since in the first case we are considering combinations of n vectors of m - 1 per combination, and in the second case, combinations of n vectors of m per combination.

2. The determinants in the sum determined by the sign $\sum_{k_m=1}^{n}{}'$, in whose composition we obtain identical vector-columns are equal to zero.

3. For a series of matrices $\| w_{\mathrm{H}k_1} \ldots w_{\mathrm{H}k_m} \|$, when combinations of vectors are varied according to the sign Σ_{m-1}, we also obtain identical vector-columns, so that their determinants are also equal to zero. /239

Noting these facts, Eq. (4.114) can be reduced to this form:

$$\sqrt{D_4^0 \eta} = \frac{\left[\sum\nolimits_m \det^2 \| w_{\mathrm{H}k_1} \ldots w_{\mathrm{H}k_m} \| \sum_{i=1}^{m} \mu_{k_i}(k_1, \ldots, k_m) \beta_{k_i} \right]}{\left[\sum\nolimits_m \det^2 \| w_{\mathrm{H}k_1} \ldots w_{\mathrm{H}k_m} \| \right]}. \tag{4.115}$$

If the total number of measurements is at a minimum, that is, n = m, the number of combinations of vectors defined by Σ_m is equal to unity, and as a result we get

$$\sqrt{D_4^0\eta_{n=m}} = \sqrt{D_4^0\eta_m}\sum_{i=1}^{m}\mu_i(1, 2, \ldots, m)\beta_i. \qquad (4.116)$$

From Eq. (4.113) we get one more form of the expression for $D_4^0\eta_m$. To do this, let us find that for n = m, we have

$$\sum_{m-1}\det\|w_{Hk_1}\ldots w_{Hk_{m-1}}l_\eta\|\sum_{k_m=1}^{n}\beta_{k_m}\det\|w_{Hk_1}\ldots w_{Hk_m}\| =$$

$$=\det\|w_{H1}\ldots w_{Hm}\|\sum_{l=1}^{m}\beta_l\det\|w_{H1}\ldots w_{Hl-1}l_\eta w_{Hl+1}\ldots w_{Hm}\|.$$

Substituting this into (4.113) and also multiplying and dividing the right-hand side of the equality by $|l_\nu| / |l_\eta|$ (where l_ν is some vector collinear to l_η), after transformations we get

$$\sqrt{D_4^0\eta_m} = \frac{|l_\eta|}{|l_\nu|}\frac{\sum_{l=1}^{m}\det\|w_{H1}\ldots w_{Hl-1}l_\nu w_{Hl+1}\ldots w_{Hm}\|\beta_l}{\det\|w_{H1}\ldots w_{Hm}\|}. \qquad (4.117)$$

Let us denote the estimate $D_4^0\eta_m$ obtained when defining the orbit by the vectors $w_{Hk_1}, w_{Hk_2}, \ldots, w_{Hk_m}$, by $D_4^0\eta(k_1, k_2, \ldots, k_m)$. Moreover, we denote

$$\alpha(k_1, k_2, \ldots, k_m) = \det^2\|w_{Hk_1}\ldots w_{Hk_m}\|\left[\sum_m\det^2\|w_{Hk_1}\ldots w_{Hk_m}\|\right]^{-1}, \qquad (4.118)$$

and it is obvious that $\sum_m\alpha(k_1, k_2, \ldots, k_m) = 1$.

With reference to all of the foregoing, we can finally bring /240 Eq. (4.115) to the following form:

$$\sqrt{D_4^0\eta} = \sum_m\alpha(k_1, k_2, \ldots, k_m)\sqrt{D_4^0\eta_m(k_1, k_2, \ldots, k_m)}. \qquad (4.119)$$

Let us show that Eq. (4.119) coincides with Eq. (4.117) if $n > m$ measurements from which the orbit is determined are made at m moments, with n_i homogeneous measurements in each moment, so that $\sum_{i=m}^{m} n_i = n$. In this case n_i homogeneous measurements will correspond to n_i identical navigational vectors $w_{H\,i}$. The determinants $\det \| w_{Hk_1} \ldots w_{Hk_m} \|$ corresponding to this, containing two or more identical vectors, will be equal to zero. The corresponding summands in Eq. (4.119) will also be equal to zero[7]. In all the remaining terms the quantities $D_4^0\eta_m(k_1, \ldots, k_m)$ will be identical, since they will depend on the same navigational vectors. Therefore,

$$\sqrt{D_4^0\eta} = \left[\frac{\sum_m \det^2 \| w_{Hk_1} \ldots w_{Hk_m} \|}{\sum_m \det^2 \| w_{Hk_1} \ldots w_{Hk_m} \|} \right] \sqrt{D_4^0\eta_m(1, 2, \ldots, m)} = \sqrt{D_4^0\eta_m}. \qquad (4.120)$$

Eq. (4.120) enables us to generalize the result obtained in [40]. According to this study, the minimum estimate $D_1^0\eta$ is attained if m measurements are made (where m is the dimension of the vector of the main parameters) at m moments selected optimally. Eq. (4.120) enables us to formulate the following generalizing theorem.

Theorem 1. When $n \geq m$ measurements are made to determine an orbit, the estimate of the dispersion $D_4^0\eta$ takes on a minimum value if all n measurements are made at m moment of time selected optimally, with n_i homogeneous measurements in each moment. The value of the estimate $D_4^0\eta$ in this case coincides with the estimate when one measurement each is made at these moments ($D_4^0\eta_m$).

The result of theorem 1 is important because in practice correlations can never attain the limiting values and the poorest

---

[7] When two identical vectors are present we have indeterminacy, since $\alpha(k_1, k_2, \ldots, k_i, k_i, k_{i+2}, \ldots, k_m) = 0$; $D_4^0\eta_m(k_1, k_2, \ldots, k_i, k_i, k_{i+2}, \ldots, k_m) = \infty$. It is not difficult to analyze this indeterminacy and to show that the quantity $\alpha(k_1, \ldots, k_m)$ in this case is proportional to an infinitesimal of second order (0^2) and $\sqrt{D_4^0\eta_m}$ is inversely proportional to an infinitesimal of first order (0^1), so that their product is proportional to an infinitesimal of first order (0^1).

combinations. So making measurements in the number n > m as a rule actually improves the accuracy of the determination of orbital parameters and therefore is optimal. Theorem 1 guarantees that here the results even in the extreme case, that is, for the poorest correlations, are not made poorer. /241

Geometrical interpretation of estimates $D_4^0\eta_m$ and $D_4^0 n$. Let us construct in space G navigational vectors corresponding to n measurements. Since we exclude the possibility of making several measurements of the same trajectory parameter at the same instant of time, in the general case the number of vectors differing from each other can be smaller than the number of measurements. We will select from n navigational vectors m vectors such that they satisfy a condition analogous to (4.98): $w_{Hk_1}, w_{Hk_2}, \ldots, w_{Hk_m}$.

Let us draw through the vertices of the m selected vectors a hyperplane $\mathcal{L}$ with dimension m - 1. Let the line of action of vector $\overrightarrow{\ell\eta}$ intersect this plane at point ν. We will denote the vector $O\nu$ (O is the orgin of coordinates) by ℓ_ν.

Let us construct on the navigational vectors an m-dimensional pyramid S. The volume of this pyramid is determined by the formula

$$u_{tot} = \frac{1}{m!}\det\|w_{Hk_1}w_{Hk_2}\ldots w_{Hk_m}\|, \tag{4.121}$$

where $\|w_{Hk_1}w_{Hk_2}\ldots w_{Hk_m}\|$ is a square matrix whose columns are selected navigational vectors.

Now let us replace in this group of navigational vectors the vector $w_{H\,ki}$ with the vector ℓ_ν and construct thereon the pyramid S_{k_i} analogous to the one considered above. The volume of this pyramid is determined by the formula

$$u_{k_l} = \frac{1}{m!}\det\|w_{Hk_1}\ldots w_{Hk_{l-1}}\ell_\nu w_{Hk_{l+1}}\ldots w_{Hk_m}\|. \tag{4.122}$$

We will call the relation

$$\bar{u}_{k_l} = \frac{u_{k_l}}{u_{tot}} = \frac{\det\|w_{Hk_1}\ldots w_{Hk_{l-1}}\ell_\nu w_{Hk_{l+1}}\ldots w_{Hk_m}\|}{\det\|w_{Hk_1}w_{Hk_2}\ldots w_{Hk_m}\|}. \tag{4.123}$$

the relative volume of pyramid S_{k_i}. Obviously, the number of pyramids S_{k_i} that can be constructed by utilizing m navigational vectors and the vector ℓ_ν is equal to m, and here

$$\sum_{i=1}^{m} \bar{u}_{k_i} = 1. \tag{4.124}$$

We can regard $\bar{u}_{k_i}$ as coordinates of the vector ℓ_ν in the basis formed by the vectors w_{Hk_1}, w_{Hk_2}, ..., w_{Hk_m}. Actually, by substituting into (4.123) the expression

$$l_\nu = \sum_{i=1}^{m} \mu_{\nu k_i} w_{H k_i}, \tag{4.124'}$$

we find

$$\bar{u}_{k_i} = \frac{\det \| w_{H k_1} \ldots w_{H k_{i-1}} (\mu_{\nu k_i} w_{H k_i}) w_{H k_{i+1}} \ldots w_{H k_m} \|}{\det \| w_{H k_1} w_{H k_2} \ldots w_{H k_m} \|} = \mu_{\nu k_i}. \tag{4.125}$$

In accordance with these formulas, let us make the substitutions into Eq. (4.117). As the result, we get

$$\sqrt{D_4^0 \eta_m} = \frac{|l_\eta|}{|l_\nu|} \sum_{i=1}^{m} \bar{u}_i \beta_i. \tag{4.126}$$

If when the vector ℓ_η is expanded in the vectors w_{Hk_i} of the (4.124') type, the result is that one or several coefficients μ_{k_i} (k_1, k_2, ..., k_m) are negative, so we will call ℓ_η external with respect to this group of vectors. But if all coefficients μ_{k_i} prove to be positive, ℓ_η is an internal vector. In space G vector ℓ_η can always be made an internal vector. To do this, it is sufficient to reverse the sign of those vectors w_{Hk_i} to which the negative coefficients μ_{k_i} correspond. Here the value of the estimate $D_4\eta$ remains unchanged.

If the vector ℓ_η is an internal vector, all the components of vector b_H, as we can prove without difficulty, are equal to 1, that is, $\beta_{k_i} = 1$. Accordingly, Eqs. (4.116) and (4.126) become simplified and take on the form

$$\sqrt{D_4^0\eta_m(k_1, k_2, \ldots, k_m)} = \sum_{l=1}^{m} \mu_{k_l}(k_1, k_2, \ldots, k_m) = \frac{|l_\eta|}{|l_*|} \quad [8] \qquad (4.127)$$

From the last formula we find that the desired length of vector $\ell_{\eta H}$ corresponding to the estimate $D_4^0\eta_m$ is determined by the formula

$$|l_{\eta H}| = |l_\eta| \left[D_4^0\eta(k_1, k_2, \ldots, k_m)\right]^{-1/2} = |l_*|. \qquad (4.128)$$

Thus, the length of vector $\ell_{\eta H}$ determined according to the estimate $D_4^0\eta_m$ in space G is equal to the distance measured along the known direction of vector $\ell_{\eta H}$ from the origin of coordinates to the hyperplane L drawn through the ends of the navigational vectors[9]. Here the navigational vectors, by change of their signs, as was indicated above, must ensure that vector ℓ_η is internal with respect to them. /243

According to theorem 1 of Section 4.5, Eq. (4.128) determines the length of vector $\ell_{\eta H}$ also for the estimate $D_4^0\eta$, if n measurements are made at m moments, with n_i monotypical measurements at each moment.

The geometrical interpretation of estimate $D_4^0\eta$ in the general case is quite complex.

Let us first transform Eq. (4.119) for one of the possible interpretations, by inserting into it the expression for $D_4^0\eta_m$ from Eq. (4.127), and we have:

---

[8] The latter formulas explain the physical significance of the condition of internal status of ℓ_η; the condition of internal status of ℓ_η with respect to the vectors $w_{Hk_1}, \ldots, w_{Hk_m}$ is equivalent to the condition of poorest correlation of the measurement errors adopted for the estimate $D_4^0\eta$.

[9] [Footnote appears on following page.]

$$|l_{\eta H}| = \frac{|l_\eta|}{\sqrt{D_{4\eta}^0}} = \left[\sum_m \frac{\alpha(k_1, k_2, \ldots, k_m)}{|l_\nu(k_1, k_2, \ldots, k_m)|}\right]^{-1}. \quad (4.129)$$

In this formula $l_\nu(k_1, \ldots, k_m)$ is the vector l_ν, constructed on a group of navigational vectors w_{Hk_1}, w_{Hk_2}, ..., w_{Hk_m}.

According to Eq. (4.129), we can give the definition of the length $l_{\eta H}$ in space G based on the estimate $D_{4\eta}^0$ in the following manner. Among the vectors corresponding to n measurements, all possible combinations of m navigation vectors each are singled out, differing by at least one vector. For each i-th group, by the above-described method the vectors $l_{\nu i}(k_1, k_2, \ldots, k_m)$ are found, which are estimates $l_{\eta H}$ in the determination of the orbit based on the vectors of this group. Next, the estimates $l_{\nu i}$ are weighted according to Eq. (4.129).

Note that the estimate $D_{4\eta}^0$ of general form is seldom used in practice owing to the great overstatement of the errors in the determination of parameter $\eta(a)$ resulting when it is employed (see [10] for more details).

4.6. Optimal Distribution of Measurements

Formulation of problem. In designing navigation systems of an SC, the question always arises: which measurements are best used for a given type of SC and how must they be best distributed along the trajectory. In the general case the answer to this question is ambiguous and depends on a number of additional conditions that must be determined.

First, we must stipulate from what point of view we consider the expediency of any particular composition of measurements, that is, we must adopt an optimality criterion. In this section, we take as the optimality criterion of the navigational measurements /244

[9] We have not defined the metric in space G. Ordinary lengths, that is, square roots of the sum of the squares of coordinates, are the referents for the terms "distance" and "vector length" as employed here.

the accuracy with which some selected, most important trajectory parameter $\eta = \eta(a)$ is determined based on them. Here we will characterize the accuracy of the determination of parameter $\eta(a)$ by $D_4\eta$, presupposing that we know how the dispersions $\sigma_\gamma^2(t)$ of the measurement errors depend on the time the measurements are taken, and also that we know the maximum value of the modulus of the coefficient of correlation of the measurement errors $\hat{k}$ for the sampling selected.

Further, we must know from which kinds of navigational measurements we must make the selection and over what section (or sections) of the trajectory the distribution of measurements is possible. Below these data are assumed to be known by us.

In this section we will also use assumption 2, given in Section 4.1 of this chapter. Under this assumption it is assumed that the navigational measurements can be made as often as desired.

The given possible types of navigational measurements, the flight time interval over which the measurements are possible, as well as the assigned maximum rate of measurements determine the set of all possible navigational measurements. We denote this set by Γ. Under the definition of set Γ a sample of any n measurements from it signifies the determination of the types of these measurements, the moments at which they are made, and also the dispersions and maximum coefficient of correlation of the errors in making these measurements.

Finally, we will assume that the last auxiliary condition assigning the maximum number of navigational measurements n which can be made for the determination of the SC orbit.

With reference to the foregoing, let us formulate the problem of optimally distributing the measurements, being solved in this section, as follows: among the set of possible measurements Γ it is required to find the measurements whose total number is not greater than the assigned n, that ensures the determination of the selected orbital parameter $\eta = \eta(a)$ with the smallest estimate of dispersion $D_4\eta$ of the errors in its determination.

Theorems on properties of optimal distribution of measurements. Let us prove a number of theorems determining the principal properties of the optimal distribution of measurements (in the above-indicated sense).

Lemma 1. The minimum values of the dispersion estimates for values of the limiting correlations $\hat{k} = 1$ (estimate $D_4^0\eta$) and $\hat{k} = 0$

(estimate[10] $D_1^0\eta$) are attained when $n \geq m$ measurements are distributed at m moments t_i with $n_{i\ opt}$ homogeneous measurements at each moment.

Here /245

$$n_{i\ opt} = n\bar{u}_i; \tag{4.130}$$

$$D_1^0\eta = \frac{1}{n}\frac{|l_\eta|^2}{|l_\nu|^2}; \tag{4.131}$$

$$D_4^0\eta = |l_\eta|^2/|l_\nu|^2. \tag{4.132}$$

Here $\bar{u}_i$ is the relative volume determined by Eq. (4.123), and l_ν is the vector defined by (4.124').

Proof. The optimality of the distribution of $n \geq m$ measurements at m moments for the estimate $D_1^0\eta$ was shown in [25]. Under theorem 1 (Section 4.5), the optimality of this distribution obtains also for the estimate $D_4^0\eta$. The formula for the value of estimate $D_4^0\eta$ in this sense is of the form (4.127) (if by suitable change in the signs of vectors $w_{H\ i}$ the internal situation of l_η with respect to them is provided), which confirms the soundness of Eq. (4.132). To prove Eq. (4.130) and (4.131) let us transform (4.56), by using Eq. (4.111) and by setting $l_1 = l_2 = l_\eta$ in it. Since according to the first part of the lemma the case in which n measurements are made at m moments, with n_i homogeneous measurements at each moment is considered, then n vectors $w_{H\ i}$ corresponding to these measurements are subdivided into m groups of n_i identical vectors in each group:

$$\left.\begin{array}{l} w_{H1},\ w_{H2}\ \ldots,\ w_{Hn_1}; \\ w_{H(n_1+1)},\ w_{H(n_1+2)},\ \ldots,\ w_{H(n_1+n_2)}; \\ \ldots\ldots\ldots\ldots\ldots\ldots\ldots\ldots\ldots \\ w_{H(n_1+n_2+\ldots+n_{m-1}+1)},\ w_{H(n_1+\ldots+n_{m-1}+2)},\ \ldots,\ w_{H(n_1+\ldots+n_m)}. \end{array}\right|$$

[10] The optimal distribution of measurements for the estimate $D_1^0\eta$ (that is, $\hat{k} = 0$) in the case when $m \leq 3$ was first obtained in [84].

Therefore we can draw a single hyperplane $\mathcal{L}$ of dimension m - 1 across the vertices of all n navigational vectors. Let the direction of vector $\ell_{\eta H}$ intersect $\mathcal{L}$ at point ν. We denote the vector $\overline{O\nu}$ (O is the origin of coordinates), as before, by ℓ_ν. With reference to the foregoing, Eq. (4.56) can be brought to the following form, without difficulty:

$$D_1^0\eta = \frac{|l_\eta|^2}{|l_\nu|^2}\sum_{m-1}\det^2\|w_{Hk_1}w_{Hk_2}\ldots w_{Hk_{m-1}}l_\nu\|\times \\ \times\left[\sum_m \det^2\|w_{Hk_1}\ldots w_{Hk_m}\|\right]^{-1}. \tag{4.133}$$

Among all possible determinants $\det\|w_{Hk_1}\ldots w_{Hk_m}\|$, only those that differ from zero whose vector-columns belong to different groups, and all these determinants are equal to each other. By suitably sorting the indices of the vectors constituting the determinants, we get /246

$$\sum_m \det^2\|w_{Hk_1}\ldots w_{Hk_m}\| = \det^2\|w_{H1}\ldots w_{Hm}\|\prod_{j=1}^m n_j, \tag{4.134}$$

where $\prod_{j=1}^m n_j = n_1\cdot n_2\cdot\ldots\cdot n_m$ (see Eq. (4.109) for the definition of the symbols $\sum_m$ and $\sum_{m-1}$). Similarly, we can get

$$\sum_{m-1}\det^2\|w_{Hk_1}\ldots w_{Hk_{m-1}}l_\nu\| = \sum_{i=1}^m\prod_{j=1}^m\frac{n_j}{n_i}\times \\ \times\det^2\|w_{H1}\ldots w_{Hi-1}l_\nu w_{Hi+1}\ldots w_{Hm}\|. \tag{4.135}$$

Substitute Eqs. (4.134) and (4.135) into Eq. (4.133). Referring to Eq. (4.123), we get

$$D_1^0\eta = \frac{|l_\eta|^2}{|l_\nu|^2}\sum_{i=1}^m\frac{\bar{a}_i^2}{n_i}. \tag{4.136}$$

It is not difficult to find that the minimum of $D_4^0\eta$, under the condition $\sum_{i=1}^m n_i = n$ with reference to (4.124), is attained for n_i measurements determined by the formula:

$$n_{i\ opt} = n\bar{u}_i.$$

We thus have proven the results of (4.130). Substituting (4.130) into Eq. (4.136), we get Eq. (4.131).

Thus, lemma 1 has been proven in full.

Remark 1. Since $\bar{u}_i$ can have nonintegral values, $n_{i\ opt}$ can also formally be obtained as a nonintegral value. In the actual distribution of the measurements, the values $n_{i\ opt}$ must be rounded to the nearest integer. By this rounding, $D_1^0\eta$ will differ from the optimal value. However, as shown by actual experience, this difference proves to be small. Under otherwise equal conditions, this difference is the smaller, the larger n/m. The method of estimating nonoptimality by rounding $n_{i\ opt}$ is determined by theorem 3 (see below).

Theorem 1. When n measurements are optimally distributed at m moments, the optimal placement of these moments along the navigational section of the trajectory does not depend on the limiting correlation of the measurement errors $\hat{k}$.

Proof. The estimate $D_4\eta$ is determined by Eq. (4.80). Substi- /247
tute Eqs. (4.131) and (4.132) that are valid when n measurements are optimally distributed over m moments into Eq. (4.80). We get

$$D_4\eta = \frac{1-\hat{k}+n\hat{k}}{n}\,\frac{|l_\eta|^2}{|l_\nu|^2}. \qquad (4.137)$$

From this formula we see that only l_ν depends on the ratio of the moments of measurements, and with variations in $\hat{k}$ l_ν remains unchanged. This then proves theorem 1.

Theorem 1 enables us to find the optimal moments for measurements for any selected value $\hat{k}$, for example $\hat{k} = 0$ or $\hat{k} = 1$. The moments of measurements thus selected will be optimal also for any other values of $\hat{k}$.

Suppose that in space G we have constructed navigational vector-functions corresponding to the given navigational interval and to the parameters being measured, and suppose that their convex covering has been constructed (see Section 4.4 of this chapter). Also suppose that the direction of vector $l_{\eta H}$ corresponding to parameter $\eta(a)$ has been given. The direction $l_{\eta H}$

will penetrate the convex covering at point ν belonging to face $\Lambda\eta$. The following lemma obtains.

Lemma 2. The minimum number of measurements $n_{\eta_{min}}$ needed to define parameter η whose vector (or its extension) passes through face $\Lambda\eta$ satisfies the inequality

$$n_{\eta_{min}} \leqslant m_f + 1, \tag{4.138}$$

where m_f is the dimension of face Λ_η.

Here

$$l_\eta = \sum_{i=1}^{m_f+1} \mu_{\eta i} w_{Hi}, \tag{4.138'}$$

and among the set of reference vectors of face Λ_{η_i} we could always find linearly independent vectors such that all the coefficients

$$\mu_{\eta i} \geqslant 0 \ (i = 1, 2, \ldots, m_f + 1), \tag{4.138"}$$

and at least one of them

$$\mu_{\eta k} > 0.$$

Proof. Since the point ν is situated on the face $\Lambda\eta$ and all the vertices of this face (in accordance with the adopted definition of a convex covering) rests on the vertices of the navigational vectors and their number is not less than $m_f + 1$, we can always find $m_f + 1$ vertices of the face such that the pyramid S' of dimension m_f constructed on these vertices will enclose point ν. We can /248 consider pyramid S' as the base of pyramid S with its vertex at the origin of coordinates and whose dimension is $m_f + 1$. The vector l_ν will be enclosed within pyramid S. The navigational vectors $w_{H\,i}$ ($i = 1, 2, \ldots, m_f + 1$) corresponding to the vertices of pyramid S' will serve as the edges of pyramid S. These vectors $w_{H\,i}$ uniquely determine the position in space G of the m_f-dimensional plane of face $\Lambda\eta$ and therefore are linearly independent. So all vectors whose vertices lie in $\Lambda\eta$, including l_ν, can be linearly expressed in terms of these vectors, which proves that (4.138) is valid.

Since ℓ_ν lies within pyramid S, all the coefficients of expansion ℓ_ν in vectors $w_{H\,i}$, being the edges of the pyramid, must be nonnegative, while at least one of them must be greater than zero, since $\ell_\eta = \alpha\ell_\nu$, where α is a positive number, and thus we have proven that Eqs. (4.138') and (4.138") are valid.

Lemma 2 enables us to determine the minimum number of measurements needed to determine the parameter $\eta(a)$, by using geometrical methods and investigating the dimension of the face of the convex covering through which vector $\ell_{\eta H}$ extends.

Theorem 2. The minimum value of the estimate $D_4\eta$ when the measurements are distributed over the measurement moments according to Eq. (4.130) is attained on the set of reference points $\mathcal{M}_\eta$ of face Λ_η.

Proof. For assigned n and $\hat{k}$, the minimum of estimate $D_4\eta$ according to (4.137) occurs when the modulus of vector ℓ_ν is at a maximum, and according to (4.127) vector ℓ_ν must be internal with respect to the vectors $w_{H1}, w_{H2}, \ldots, w_{Hm}$ used in the definition of the vector ℓ_η.

But the maximum $|l_\nu| = |l_\nu(w_{H1}, w_{H2}, \ldots, w_{Hm})|$ is attained on the reference set $\mathcal{M}_\eta$. Actually, from the condition of constructing the convex covering it follows that all the navigational vectors whose vertices are not part of the set of reference points are situated within the convex covering. Hence it follows that the replacement of any reference moment by the moment not part of the set $\mathcal{M}_\eta$ only diminishes ℓ_ν. Thus, the assertion of the theorem has been proven.

The property of optimality of the set of reference moments defined by theorem 2 enables us to elaborate a simple algorithm for finding the optimal moments of the measurements. This algorithm can be based on finding the face of the convex covering containing the point ν. Briefly, this algorithm will be considered below.

Suppose that to determine the trajectory of motion of the spacecraft at m moments n measurements of n_i monotypical measurements at each moment are made. A hyperplane $\mathcal{L}$ of dimension m - 1 is drawn through the vertices m of the navigational vectors $w_n(t_i)$.

We will call the vertices of the navigational vectors lying in the plane $\mathcal{L}$ the navigational points. To each navigational point there /249 corresponds n_i measurements. We will call the point whose position is defined by the vector

$$l_c = \frac{1}{n}\sum_{i=1}^{m} n_i w_{Hi}. \tag{4.139}$$

the center of gravity of the navigational point. The numbers n_i/n can be taken as the coordinates of vector l_c in the system of vectors $w_{H\,i}$. Let ν be the point of intersection of vector $l_{\eta H}$ (or its extension) with hyperplane $\mathcal{L}$. We denote

$$\Delta l = l_\nu - l_c. \tag{4.140}$$

We denote the estimate of the dispersion of the errors made in determining the trajectory vector corresponding to l_c by $D_4\eta_c$. The following theorem is valid for the system of navigational points.

Theorem 3. (Theorem on the center of gravity of navigational points.) If in defining the trajectory we use m navigational points, and in each of them n_i measurements are made, the estimate $D_4\eta$ can be expressed by the formula

$$D_4\eta = D_4\eta_c + \delta D_4\eta, \tag{4.141}$$

where

$$D_4\eta_c = \frac{|l_\eta|^2}{|l_\nu|^2}\left[(n-1)\hat{k}+1\right]; \tag{4.142}$$

$$\begin{aligned}\delta D_4\eta &= \frac{|l_\eta|^2}{|l_\nu|^2}\left[(n-1)\hat{k}+1\right]|\Delta l|\sum_{i=1}^{m}\frac{|\Delta l|M_{\Delta l_i}^2 + 2M_{ci}M_{\Delta l_i}}{\det^2\|w_{H1}w_{H2}\ldots w_{Hm}\|} = \\ &= \frac{|l_\eta|^2}{|l_\nu|^2}\left[(n-1)\hat{k}+1\right]\sum_{i=1}^{m}(\mu_{i\nu}-\mu_{ci}); \\ M_{\Delta l_i} &= \det\left\|w_{H1}\ldots w_{H\,i-1}\frac{\Delta l}{|\Delta l|}w_{H(i+1)}\ldots w_{Hm}\right\|; \\ M_{ci} &= \det\|w_{H1}\ldots w_{H(i-1)}l_c w_{H(i+1)}\ldots w_{Hm}\|;\end{aligned} \tag{4.143}$$

$\mu_{c\,i}$ and $\mu_{i\,\nu}$ are the coordinates of vectors ℓ_c and ℓ_ν, respectively, in the system of vectors $w_{H1}, w_{H2}, \ldots, w_{Hm}$.

Proof. Estimate $D_4\eta$ is defined by Eq. (4.80). Let us substitute into this formula the expression for $D_1^0\eta$ (4.136) and the expression for $D_4^0\eta$, Eq. (4.127). We get

$$D_4\eta = \frac{|l_\eta|^2}{|l_*|^2}\left[(n-1)\hat{k}+1\right]\sum_{i=1}^{m}\frac{\bar{u}_i^2}{n_i}. \qquad (4.144)$$

Here $\bar{u}_i$ is determined by Eq. (4.123). Let us represent the vector ℓ_ν in the form $\ell_\nu = \ell_c + \Delta\ell$, where ℓ_c is the vector defined by Eq. (4.139). Using this expression for ℓ_ν, we can write /250

$$\sum_{i=1}^{m}\frac{\bar{u}_i^2}{n_i} = \sum_{i=1}^{m}\frac{1}{n_i}\frac{M_{\nu i}^2}{M^2} = \sum_{i=1}^{m}\frac{1}{n_i}\frac{M_{ci}}{M^2} + \sum_{i=1}^{m}\frac{2M_{ci}M_{\Delta\ell_i}+M_{\Delta\ell_i}^2}{n_iM^2}, \qquad (4.145)$$

where M stands for $\det\|w_{H1}w_{H2}\ldots w_{Hm}\|$.

Let us examine the first sum. Let us substitute into $M_{c\,i}$ instead of ℓ_c, its expression (4.139) and let us expand $M_{c\,i}$ into a sum of m determinants. All these determinants with the exception of one will each contain two identical columns and therefore will be equal to zero. Accordingly, we have

$$\sum_{i=1}^{m}\frac{1}{n_i}\frac{M_{ci}^2}{M^2} = \sum_{i=1}^{m}\frac{\left(\frac{n_i}{n}\right)^2M^2}{n_iM^2} = \frac{1}{n}.$$

Let us examine the second sum. We remove the quantity $|\Delta\ell|$ from the sign of the determinant and the sign of the sum. By substituting $M_{\Delta\ell_i}$ and the expressions found for the sums into Eq. (4.144), we get Eq. (4.141) in which $\delta D_4\eta$ is of the form of the first part of Eq. (4.143).

Let us represent the vector ℓ_ν in the following form:

$$l_\nu = \sum_{i=1}^{m} \mu_{i\nu} w_{Hi},$$

Here $\sum \mu_{i\nu} = 1$. Substituting this ratio and Eq. (4.139) into Eq. (4.140), we get

$$\Delta l = l_\nu - l_c = \sum_{i=1}^{m} \left(\mu_{i\nu} - \frac{n_i}{n} \right) w_{Hi}.$$

By substituting this formula into the second sum of Eq. (4.145) and performing the transformations analogous to those done on the determinants of the first sum and also substituting the resultant into the formula for $D_4\eta$ (4.144), we get an expression in which $\delta D_4\eta$ is of the form of the second part of Eq. (4.143). The theorem is proven.

From theorem 3 there follow several important corrolaries.

Corrolary 1. If point ν coincides with the center of gravity of the navigational points, $D_4\eta$ has a minimum value and Eq. (4.141) coincides with Eq. (4.137):

$$D_4\eta = \frac{1}{n}\left[(n-1)\hat{k}+1\right]\frac{|l_\eta|^2}{|l_\nu|^2}. \qquad (4.146)$$

Actually, from Eq. (4.143) it always follows that /251

$$\delta D_4\eta \geqslant 0.$$

If point ν coincides with the center of gravity, $\Delta l = 0$. From Eq. (4.143) it follows that here $\delta D_4\eta = 0$ whence Eq. (4.146) must be valid.

Using Eq. (4.146) we can also simply estimate the utility of increasing the number of measurements in order to make the determination of the trajectory more accurate for different values of the limiting correlation k. (Recall that when $\hat{k} = 1$, $D_4\eta = D_4^0\eta$ and it does not depend on the number of measurements $n > m$.)

Corrolary 2. The optimal distribution of n measurements of m points each defined by lemma 1 (see Eq. (4.130)) corresponds to the coincidence of the center of gravity of a system of n navigational points with point ν.

Actually, from (4.143) it follows that $\delta D_4\eta = 0$ if the condition

$$\mu_{i\nu} - \frac{n_i}{n} = 0 \ (i = 1, 2, \ldots, m), \tag{4.147}$$

or

$$n_i = n\mu_{i\nu}. \tag{4.148}$$

are satisfied. According to (4.125), $\mu_i = \bar{u}_i$. Substituting this equality into (4.148), we get $n_i = n\bar{u}_i$. Since $\mu_{c\,i} = n_i/n$ are the coordinates of vector ℓ_c in the system of vectors w_{H1}, w_{H2}, ..., w_{Hm}, conditions (4.147) are equivalent to equality $\Delta\ell = 0$, which then proves the assertion of corrolary 2.

Corrolary 3. If the number of reference points of face Λ_η of an m-dimensional convex covering of the navigational vector-function is larger than m, among them the combinations of the reference points that ensure a minimum for the quantity $\delta D_4\eta$ for integral values of $n_{i\,opt}$ and the internal situation of ν with respect to them are optimal among these reference points.

Actually, by theorem 2 of this section the distribution of measurements over the elements of set $\mathcal{M}_\eta$ for the estimate $D_4\eta$ written in the form (4.137) is optimal. According to corrolary 2 this corresponds to the coincidence of the center of gravity of the navigational points with the point ν. When $n_{i\,opt}$ is rounded to integral numbers, this equivalence is violated and the difference vector $\Delta\ell = \ell_\nu - \ell_c$ arises, which according to Eq. (4.142) leads to the appearance of $\Delta D_4\eta > 0$. Clearly, if different combinations of the navigational vectors satisfying the condition of corrolary 3 are possible, then those of them that correspond to the optimal accuracy of the determination of $\eta(a)$ for which $|\Delta\ell|$ and therefore, also $\delta D_4\eta$ are at a minimum.

On the algorithm for the optimal planning of a sampling of measurements. Based on the results and geometrical interpretations obtained above, we can set up various algorithms for finding the sets of reference points and vectors. /252

One of the possible algorithms for finding the optimal distribution of measurements briefly amounts to the following.

1. Vectors of hodographs of navigational vector-functions $w_{H\,j}(t)$ $(j = 1, 2, \ldots, s)$ and the vector of the parameter ℓ_η to be determined are calculated for the navigational interval with a sufficiently small step.

2. By sliding the plane $\mathcal{L}$ of dimension m - 1 over the vectors $\pm w_{H\,j}(t_i)$ so that in any of its positions it does not intersect even one navigational vector $w_{H\,j}(t_j)$, one can find the position of this vector to which the minimum value of vector ℓ_ν corresponds. This corresponds to the plane $\mathcal{L}$ transiting through face Λ_η.

3. In defining the face Λ_η, one finds the largest number of linearly independent reference vectors n_{min} of this face, that is, the dimension of the face equal to

$$m_f = n_{min} - 1.$$

In the general case, as noted above, $m_f \leq m - 1$.

By lemma 2, the minimum number of measurements for the determination of the parameter $\eta(a)$ is

$$n_{\eta\,min} = m_f + 1.$$

If $n_{\eta\,min} < m$, this means that the parameter $\eta(a)$ depends not on all the main trajectory parameters a_i, but some of them, numbering $m - n_{\eta\,min}$, can be removed from the dependence $\eta(a)$.

4. Among all the reference vectors of face Λ_η those combinations of the vectors, $n_{\eta\,min}$ in each, are determined that ensure that ℓ_η is internally situated with respect to them.

5. Using Eqs. (4.130) or (4.148), the optimal distribution of the total given number of navigational measurements n is determined over the combinations of reference vectors found in subsection 4. Here the numbers n_i are rounded to the nearest whole number. Using Eqs. (4.142) or (4.143), the combination of reference vectors for which the increase in the estimate $\delta D_4\eta$ is at a minimum is determined by rounding the number of measurements to an integral number.

The reference vectors of face Λ_η found by this method define the kinds of optimal parameters to be measured and the moments of their measurements. These measured parameters and the optimal numbers of measurements determined in Section 5 comprise the optimal planning of measurement sampling.

CHAPTER V

/253

DEORBITING OF SATELLITE TO EARTH

Return to Earth is one of the most important stages of flight into space. Due to the high velocity (more than 8 km/sec) a flight vehicle returning to Earth will experience severe aerodynamic heating and high g-loads on moving in the atmosphere.

The protection of the craft from overheating and excessive g-loads is a basic condition for its safe return to Earth. We will call the stage of the flight of an AES or some part of it in its return to Earth the descent.

In order to begin deorbiting [descent from orbit] one must first reduce the satellite velocity. This is achieved by applying to it a jet impulse directed toward the side opposite to the motion of the satellite in orbit (or by using aerodynamic braking). After the impulse has been imparted, the craft begins to slow down and enters the dense atmospheric layers. Depending on the magnitude and direction of the impulse applied, two cases are possible:

1) the craft, before entering the dense atmospheric layers, makes several revolutions (orbits) around the Earth, gradually descending due to deceleration in the dense atmospheric layers, and

2) the craft, without performing additional revolutions around the Earth, enters the dense atmospheric layers.

The descent of the craft can be ballistic (without the use of lift) or gliding (using lift)[1].

Ballistic descent from the standpoint of the organization of propulsion is simpler, since when it is carried out nearly no flight control is required (except for the section of the jet deceleration for deorbiting).

However, the design g-loads and heating of the craft by this method prove to be quite high. By using special air brakes that permit deceleration to begin at high altitudes, the longitudinal g-loads can be appreciably reduced.

---

[1] Deceleration with jet action is not considered here.

In gliding descent, lower g-loads and lesser craft heating can be provided than in ballistic descent, since the lift exerts a much greater effect on the flight trajectory than the drag. Still, owing to the greater complexity of allowing for the lift, the trajectory of gliding descent can be calculated less exactly than the trajectory of ballistic descent. But in gliding descent the inaccuracies in calculating the trajectory are compensated by the considerably greater possibilities of flight control. /254

The simplicity of ballistic descent predetermined its application during the first launches of manned spacecraft and unmanned spacecraft (in particular, capsules returning to Earth scientific documentation from the satellite that was difficult to transmit by radio).

For a capsule moving in a ballistic curve during its descent, the problem of protecting it against heating is similar to the problem of heat protection of the nose cones of long-range rockets. However, one feature of the trajectories of capsules ejected from a satellite is the small reentry angles, where heating is significantly reduced since the capsule loses most of its velocity in the rarified atmospheric layers at small velocity heads[2].

The descent of manned craft is more complex, since in this case, besides protecting the craft against overheating, g-loads acceptable to man must be ensured.

Let us examine the trajectories of ballistic and gliding descents, as well as methods of evaluating trajectories from the standpoint of craft heating and axial g-loads. We will analyze the accuracy of the landing of a craft in ballistic descent and also the possibilities of control in gliding flight.

5.1. Ballistic Descent

The motion of a craft in ballistic descent in the coordinate system x, y, z bound to the rotating Earth with its origin at the Earth's center and with the Oz axis directed toward the north pole is described by the following differential equations:

$$\left.\begin{aligned}
\ddot{x} &= -\frac{\mu}{r^3}x+\frac{\varepsilon}{r^5}x\left(1-5\frac{z^2}{r^2}\right)-\frac{1}{2}g_0 Q v\dot{x}+x\Omega_3^2+2\Omega_3\dot{y}+p_x;\\
\ddot{y} &= -\frac{\mu}{r^3}y+\frac{\varepsilon}{r^5}y\left(1-5\frac{z^2}{r^2}\right)-\frac{1}{2}g_0 Q v\dot{y}+y\Omega_3^2-2\Omega_3\dot{x}+p_y;\\
\ddot{z} &= -\frac{\mu}{r^3}z+\frac{\varepsilon}{r^5}z\left(3-5\frac{z^2}{r^2}\right)-\frac{1}{2}g_0 Q v\dot{z}+p_z,
\end{aligned}\right\} \qquad (5.1)$$

[2] However, the overall heat fluxes (during the entire descent time) can rise appreciably.

where $\mu = fM$ is the product of the gravitational constant by the the Earth's mass /255

σ is the ballistic coefficient

ρ is the density of air

v is the velocity of the satellite relative to the selected coordinate system:

$$v=\sqrt{\dot{x}^2+\dot{y}^2+\dot{z}^2};\quad r=\sqrt{x^2+y^2+z^2};$$

p_x, p_y, p_z are the component accelerations of thrust along the x, y, and z axes, and

ε is a constant appearing in the terms that allow for the effect of the Earth's oblateness, and determined from the formula

$$\varepsilon=\mu\bar{a}^2\left(\alpha-\frac{m}{2}\right). \tag{5.2}$$

In Eq. (5.2):

$\bar{a}$ is the equatorial radius of the Earth

$\alpha=\frac{\bar{a}-\bar{b}}{\bar{a}}$ is the degree of distortion [compression] of the Earth ($\bar{b}$ is the polar radius);

$$m=\frac{\Omega_E^2\bar{a}}{g_e}; \tag{5.3}$$

g_e is the acceleration due to gravity at the equator, and

Ω_E is the angular velocity of rotation of the Earth.

For a nonrotating system of coordinates $\Omega_E = 0$, therefore the centrifugal and Coriolis forces in the equations of motion will be absent.

In view of the high complexity, it is best that the system of equations (5.1) be solved on a computer, since the use of elliptical theory [51] for approximate calculations is possible only at altitudes above 80-90 km where the effect of aerodynamic forces is low.

We will investigate trajectories in which the g-loads do not exceed values tolerable by the human organism and in which the craft heating does not exceed the allowable level. Also, these trajectories must ensure that it is possible to land in a given areally confined region. Under these conditions, in investigating

motion we must allow only for the principal forces acting on the craft -- the central field of the Earth's gravity and aerodynamic drag. Solutions of the differential equations of motion in ballistic descent obtained on a computer enable us to select trajectories that are optimal in terms of g-loads and their time of action. Analysis of the descent trajectories also enables us to estimate the craft heating with respect to characteristic equilibrium temperatures. This estimate makes it possible to find the optimal trajectories with allowance for craft heating.

Let us examine axial g-loads and their time of action as a function of these parameters.

G-Loads in Ballistic Descent /256

Axial g-loads in ballistic descent, like the other quantities characterizing the descent of an AES are determined by the motion parameters when the craft enters the dense atmospheric layers (v_0, θ_0, H_0), the coefficient of its aerodynamic drag c_x, and the load at the maximum cross section p_M (the ratio of craft weight to the area of its maximum cross section), where the coefficient of aerodynamic drag as well as the load on the maximum cross section can change during the flight.

The g-load due to the aerodynamic drag is

$$n_x = \frac{R_x}{G} = \sigma \frac{\rho v^2}{2}, \qquad (5.4)$$

where R_x is the aerodynamic drag

G is craft weight

σ is ballistic coefficient, or the coefficient of deceleration determined by the formula $\sigma = \frac{c_x F_M}{G}$, and

F_M is the area of the maximum craft cross section.

Since the trajectory of ballistic descent is determined by the initial parameters of motion and by the deceleration coefficient σ, g-loads are also determined by these same quantities. In the following we will assume that along each descent trajectory σ = const. This assumption is quite justified if we are considering the motion of bodies with virtually constant external shapes and mass at hypersonic velocities, since the c_x of these bodies is determined only by the coefficient of wave drag $c_{x\,w}$, which in the range of M numbers 5-25 changes little.

To find the overall trend of the dependence of g-loads on these factors, numerical calculations were made on a computer for system (5.1) simplified according to these assumptions, as the initial conditions of motion and the coefficient σ were varied over wide limits. The parameters of motion v_0 and θ_0 at the altitude 100 (or 80) km were assumed as the initial conditions, since the atmospheric density, as shown by calculations, begins to markedly affect descent trajectory only at these altitudes. The results of the calculations show that the nature of the variation in the axial g-loads n_x with respect to flight time are roughly the same for all trajectories of ballistic descent (there is one well-defined maximum on all the curves).

To illustrate this conclusion, in Figs. 5.1 and 5.2 are presented the curves of g-loads with respect to flight time and with respect to altitude on trajectories differing from each other by the angle of reentry into the atmosphere θ_0.

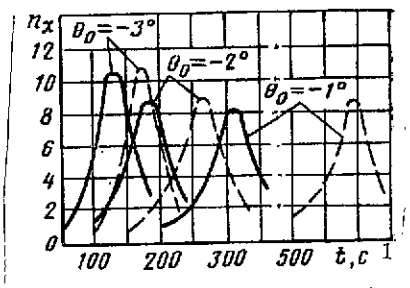

Fig. 5.1. G-load n_x as a function of flight time t for different reentry angles θ_0 and different ballistic coefficients σ:
———— σ = 0.01 m^2/kg
---------- σ = 0.001 m^2/kg
Key: 1. sec

The maximum g-load at a given trajectory and the time of action of high g-loads are the main parameters determining the effect of g-loads on man. /257

Figs. 5.3 and 5.4 present the calculated curves of the maximum g-loads $n_{x\ max}$ as functions of the initial parameters of motion θ_0 and v_0 and the deceleration coefficient σ, where for greater graphical clarity the plots are constructed in different coordinate systems. Fig. 5.5 shows the flight distances in ballistic descent x and the velocity of encounter with Earth v_{en} as a function of the coefficient $k_x = \sigma g$ and the entry angle θ_0. The calculations were made for the following initial descent parameters and coefficient σ:

$$7 \text{ km/sec} \leqslant v_0 \leqslant 9 \text{ km/sec};$$

$$-5° \leqslant \theta_0 \leqslant 0;$$

$$0.0005 \text{ m}^2/\text{kg} \leqslant \sigma \leqslant 0.01 \text{ m}^2/\text{kg}.$$

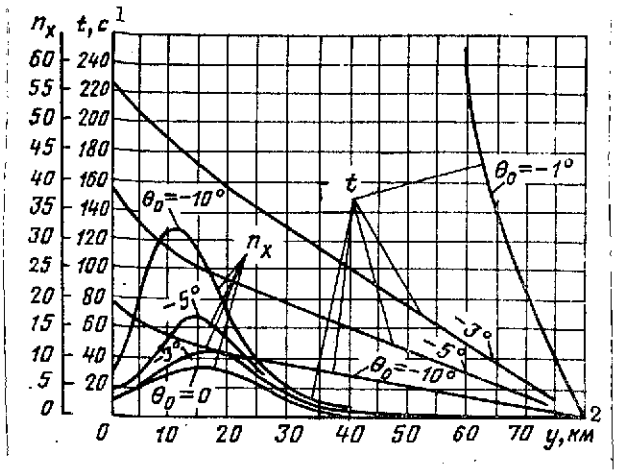

Fig. 5.2. Dependence of g-load n_x and flight time t on altitude y for different entry angles θ_0

Key: 1. sec
2. km

From Figs. 5.2-5.5 it is clear that the maximum g-load depends mostly on the angle of craft reentry into the atmosphere θ_0. When the modulus of entry angle is increased, the maximum g-loads /259 rise sharply and even at the angle $\theta_0 = -5°$ they reach values that are dangerous to man (see Fig. 5.4).

The maximum g-loads depend only slightly on the ballistic coefficient σ, but they are the smaller, the larger the σ.

The value of σ strongly influences the position of the g-load maximum on the trajectory (see Fig. 5.1).

Dependence of Craft Heating on the Parameters of Its Atmospheric Reentry

In calculations, the initial parameters of craft reentry into the atmosphere corresponded to the altitude H_0 = 100 km. The descent trajectory was described by differential equations (5.1) and the condition that $\Omega_E = 0$, and the Earth's field is a central field.

The trajectories were calculated on an electronic computer for the initial reentry parameters as below:

v_0 = 7750, 8000, 8500, and 9000 m/sec
θ_0 = 0, - 1, - 2, - 3, - 4, and - 5°
σ_0 = 0.0005, 0.001, 0.002, 0.0035, 0.005, 0.01, and 0.05 m^2/kg.

To estimate the heating of the craft hull over the calculated descent trajectories, the following criteria were used:

1) the hull temperature T_{max} that was a maximum along the trajectory, at the critical point of the heat-insulating spherical surface with a radius of 1 m, when the coefficient of surface radiation ε - 0.8, and

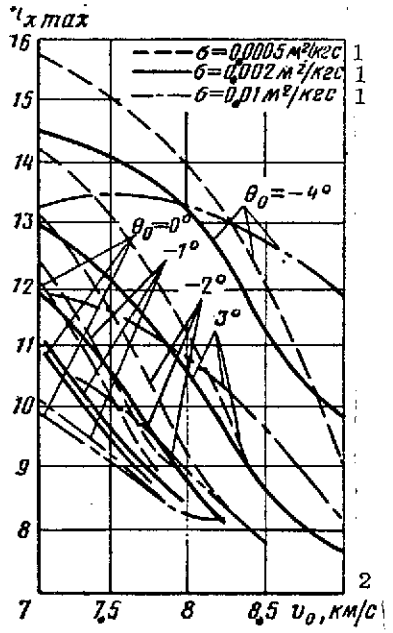

Fig. 5.3. G-load n_{max} as a function of atmospheric reentry velocity v_0 for different σ and θ_0

Key: 1. m^2/kg
2. km/sec

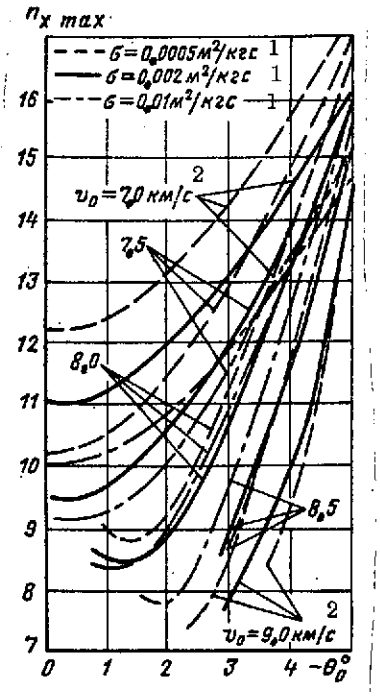

Fig. 5.4. G-load $n_{x\,max}$ on reentry angle θ_0 for various v_0 and σ

Key: 1. m^2/kg
2. km/sec

2) the hull heating time Δt with T_{max} > 1500° C (conditional temperature).

The heating of the craft hull as functions of initial craft reentry parameters were calculated for the turbulent flow regime.

Let us examine the effect of each of these initial reentry parameters on the craft heating conditions.

The reentry angle strongly affects T_{max} and the time of action Δt of high temperatures. Typically, with increase in the negative reentry angle an increase in maximum temperatures is observed, with a simultaneous decrease in the time of action of temperatures above 1500° C. Therefore, for normal operating conditions of the structure, when elevated temperatures act on it there can be some optimal angle θ_0 for certain values of the parameters v_0 and σ_0.

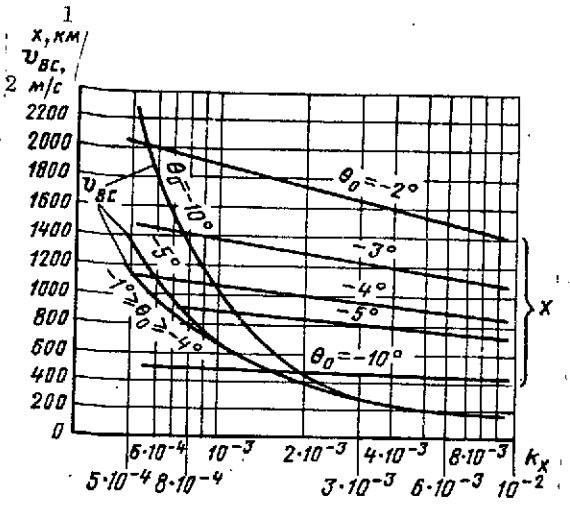

Fig. 5.5. v_{en} at which the AES encounters the Earth and the flight range x (for decrease in altitude y from 80 km to 0) as functions of the coefficient $k_x = \sigma g_0$ for different reentry angles θ_0

Key: 1. km
2. m/sec

The corresponding functions of T_{max} and Δt are shown in Figs. 5.6 and 5.7. For all the atmospheric reentry angles considered, with increase in parameter σ there is a decrease in T_{max} and in the time of action Δt of temperatures exceeding 1500° C. Here the greatest drop in T_{max} and Δt occurs in the range σ = 0.0005--0.05, since with further increase in σ the change in T_{max} and Δt becomes slight.

From the trend of these functions it follows that to reduce the heating of the craft structure it is desirable to have as large as possible σ, that is, high values of the drag c_x and low loading on the maximum cross section p_M. So it is best to design the craft in the form of a body of revolution of blunt shape with large maximum cross-sectional areas. /260

The effect of the initial reentry of velocity v_0 was examined in the range of reentry angles θ_0 from 0 to - 5° for three constant values of σ = 0.0005, 0.002, and 0.01 in the given range of variation in velocity 7750-9000 m/sec for the turbulent flow regime.

From analyzing the resulting function $\Delta t(v_0)$ it follows that with increase in velocity v_0 the time of action Δt of temperature increases over the entire range of reentry angles considered (see Fig. 5.7).

Interestingly, in the range of angles θ_0 from 0 to - 2°, beginning at velocity v_0 = 7750 m/sec, there is a decrease in the maximum temperatures T_{max} with increase in initial velocity (see Fig. 5.6). For the rest of the range of reentry angles, in contrast, one observes an increase in T_{max} with an increase in v_0, and the larger the ballistic coefficient σ_0, the smaller the change in T_{max}.

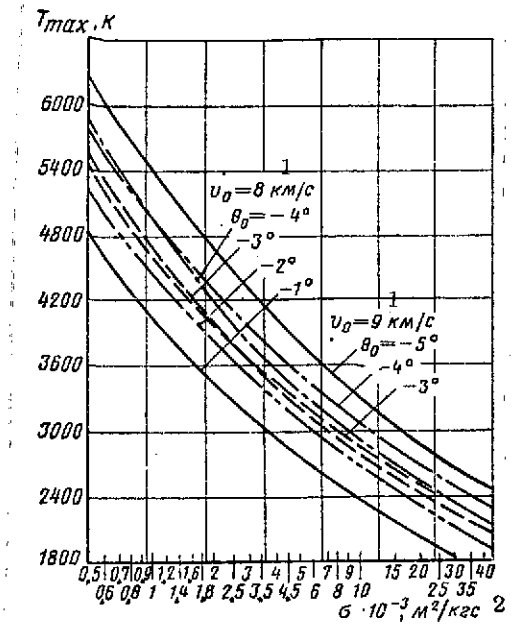

Fig. 5.6. T_{max} as a function of of ballistic parameter σ in turbulent flow regime
Key: 1. km/sec
2. m^2/kg

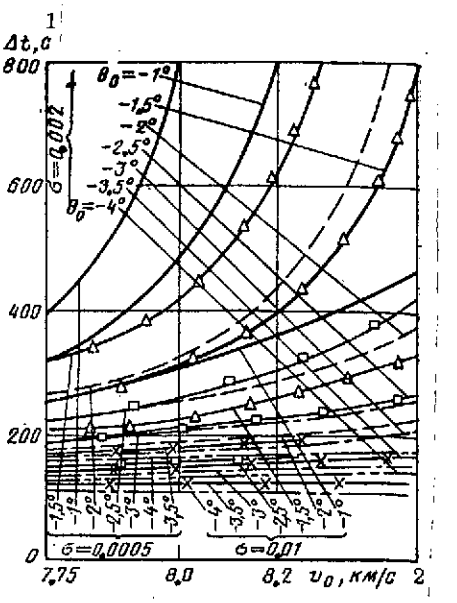

Fig. 5.7. Time of action Δt of elevated deceleration temperatures as a function of velocity v_0 of atmospheric reentry
Key: 1. sec
2. km/sec

Estimating Accuracy of Landing

/261

Let us first consider deviations from the designated landing point of a craft due to errors as the craft is given additional velocity by means of the retro-firing engine (RFE). The errors during the imparting of additional velocity we will characterize by the deviation Δu (the additional velocity u), the deviation Δα (the angle of direction of the vector of the additional velocity α), and the component of the velocity along the normal to the orbital plane v_z (Fig. 5.8). Here we will assume the orbit to be known exactly. These errors can cause deviations in the landing point from the projected point in the orbital plane ΔL and in the direction perpendicular to the orbital plane Δz. We will neglect the effect of the Earth's rotation on the landing accuracy, since this effect is insubstantial in this particular case. Moreover, when analyzing the effect of the errors Δu, Δα, and v_z on the deviations ΔL and Δz, we will neglect the effect of the atmosphere on the descent trajectory. The errors of the section of the flight in the dense atmospheric layers are examined separately (see text page 265 [translation page]).

284

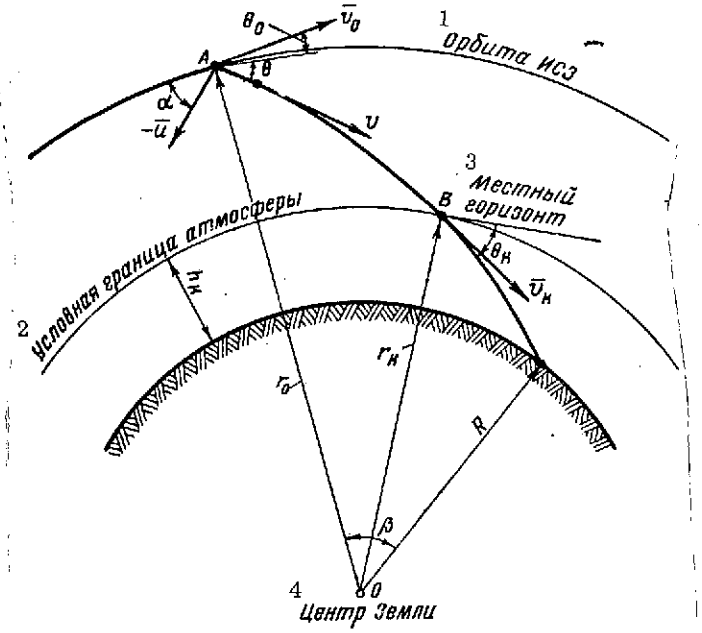

Fig. 5.8. Scheme of deorbiting of artificial Earth satellite
Key: 1. Orbit of AES
2. Conditional atmospheric boundary
3. Local horizon
4. Earth's center

The lateral deviation of the landing point is /262

$$\Delta z \cong \frac{v_z}{v_0} R \sin \beta, \quad (5.5)$$

where v_0 is the velocity in orbit
R is the Earth's radius, and
β is the angular range of descent.

When $v_0 = 8000$ m/sec, we get the estimate $\frac{\Delta z}{v_z} \leqslant 0{,}8 \frac{\text{km}}{\text{m/sec}}$.

Let us find the deviations ΔL due to the errors Δu and Δα.

Suppose that the satellite, at the moment the retro-engine is fired, has the velocity v_0 directed at the angle θ_0 to the local horizon. At this moment we designate the distance of the satellite from the Earth's center by r_0. If we assume that the imparting of the additional velocity to the satellite or to part of it is quite brief, its velocity v and its direction (angle θ) after the additional velocity has been imparted can be determined from the formulas

$$v^2 = v_0^2 \left[1 + \left(\frac{u}{v_0} \right)^2 + 2 \left(\frac{u}{v_0} \right) \cos \alpha \right]; \quad (5.6)$$

$$\theta = \theta_0 + \delta\theta; \quad (5.7)$$

$$\sin \delta\theta = \frac{u}{v} \sin \alpha. \quad (5.8)$$

Since the additional velocity must decelerate the craft in order to make its descent to Earth possible, in subsequent calculations we will assume

$$u < 0; \; 90^\circ \geqslant \alpha \geqslant 0.$$

Also note that we are considering only the case when the vector of the additional velocity is situated in the orbital plane of the satellite.

Let us find the angular range of the flight of the craft from the point at which it is given the additional velocity to the landing point by using the formula[3]

$$\operatorname{tg}\frac{\beta}{2}=\frac{1}{A}\cos\theta\left(\sin\theta+\sqrt{\sin^2\theta+\frac{r_0-R}{R}A}\right), \tag{5.9}$$

where

$$A=\frac{2}{k}-\cos^2\theta\,\frac{r_0+R}{R},\quad k=\frac{r_0v^2}{\mu}.$$

In addition, let us determine the angle θ_K at the end of the section of the descent trajectory as the craft enters the dense atmospheric layers, since the deviations from the calculated parameters over the section of the flight trajectory in the atmosphere depends strongly on this angle. We get this angle from /263 from the formula

$$\cos\theta_f=\frac{r_0v}{r_fv_f}\cos\theta, \tag{5.10}$$

G

where

$$v_f=\sqrt{v^2+2\mu\left(\frac{1}{r_f}-\frac{1}{r_0}\right)},\quad r_f=R+h_f;$$

and h_f is the altitude at which the angle is calculated.

Besides determining the range angle and the angle of reentry, we are interested in the derivatives with respect to range for the parameters characterizing the magnitude and direction of the additional velocity u. These derivatives can be calculated by the formulas

$$\frac{\partial L}{\partial\alpha}=\frac{\partial L}{\partial v}\frac{\partial v}{\partial\alpha}+\frac{\partial L}{\partial\theta}\frac{\partial\theta}{\partial\alpha}; \tag{5.11}$$

---

[3] A detailed analysis of the question of the angular range of the craft flight in a central force field is to be found in [51].

C-4

$$\frac{\partial L}{\partial u}=\frac{\partial L}{\partial v}\frac{\partial v}{\partial u}+\frac{\partial L}{\partial \theta}\frac{\partial \theta}{\partial u}, \tag{5.12}$$

where

$$\left.\begin{aligned}&\frac{\partial L}{\partial v}=\frac{2R}{B}\frac{1-\cos\beta}{v};\\&\frac{\partial L}{\partial \theta}=\frac{kR}{B}\left[\sin(\beta+2\theta)-\frac{r_0}{R}\sin 2\theta\right];\\&B=\sin\beta-k\sin(\beta+\theta)\cos\theta.\end{aligned}\right\} \tag{5.13}$$

The other derivatives appearing in Eqs. (5.11)-(5.13) can be obtained from Eqs. (5.6)-(5.8):

$$\left.\begin{aligned}&\frac{\partial v}{\partial \alpha}=-\frac{v_0}{v}u\sin\alpha;\quad \frac{\partial \theta}{\partial \alpha}=1-\frac{v_0}{v}\cos(\theta-\theta_0);\\&\frac{\partial v}{\partial u}=\frac{u}{v}+\frac{v_0}{v}\cos\alpha;\quad \frac{\partial \theta}{\partial u}=\frac{v_0}{v^2}\sin\alpha.\end{aligned}\right\} \tag{5.14}$$

The descent process was calculated for three circular orbits with altitudes 200, 300, and 400 km. In the calculations the angle α was varied over a wide range. The calculation results are shown in Figs. 5.9-5.11, where L_u and L_α are the derivatives of range L in u and α. The calculations are presented for three values of the additional velocity 0.3, 0.4, and 0.5 km/sec. The plots show that for all the orbits and all values of the additional velocity there are angles α at which the derivative $\partial L/\partial\alpha$ tends to zero. The derivative $\partial L/\partial u$ close to the value of angle α at which $\partial L/\partial\alpha = 0$ has a value that is near-minimum. Therefore, it is convenient to perform the descent at this angle α, since here the effect on the landing point of errors in satellite orientation is virtually limited. For the additional velocity and adopted orbits under consideration, the angle α at which the derivative /265 $\partial L/\partial\alpha$ tends to zero lies in the range 35-60°.

These cases do not allow for the possible orbital eccentricity. If the satellite orbit has some eccentricity, the parameters of the descent will depend on the point on the orbit at which the deceleration takes place. Here, as shown by calculations, for orbits with small eccentricities ($e \lesssim 0.03$), descent does not differ strongly from the cases shown in Figs. 5.9-5.11.

For preliminary conclusions, we will center on the circular orbit at the altitude 300 km (see Fig. 5.10). Fig. 5.12 shows the descent parameters as functions of the additional velocity

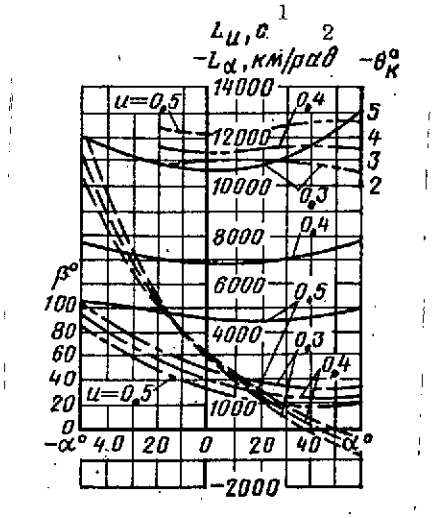

Fig. 5.9. Dependence of parameters determining the accuracy of landing on angle α for different u, km/sec (u < 0, and the falling altitude H = 200 km):
——— L_u —·—·—·— β
------- L_α —·—·—·— θ_f
Key: 1. sec
2. km/rad

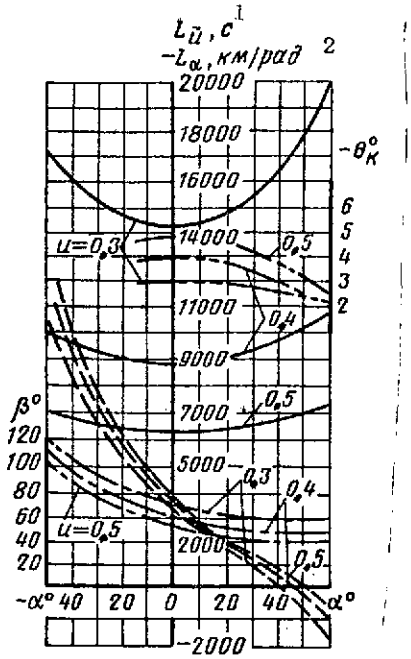

Fig. 5.10. Parameters determining landing accuracy as a function of angle α for different u, km/sec (u < 0, falling altitude H = 300 km)
——— L_u —·—·—·— β
------- L_α —·—·—·— θ_f
Key: 1. sec
2. km/rad

at values of the angle α ensuring that the condition $\partial L/\partial\alpha = 0$ is satisfied for an orbit at the altitude 300 km. The graph shows that as u is increase, the angular range β and the derivative $\partial L/\partial u$ decrease sharply. However, the deviation of the range corresponding to 1 percent of the error in additional velocity changes more weakly (see the quantity $\zeta = \frac{\Delta L}{1\%\ \Delta u/u}$). Based on this it can be assumed that if the error Δu is not determining, then it is best to increase the additional velocity u in order to reduce the effect of errors Δu down to 300-400 m/sec, since a further increase in the additional velocity does not lead to an appreciable reduction in the error $\frac{\Delta L}{1\%\ \Delta u/u}$.

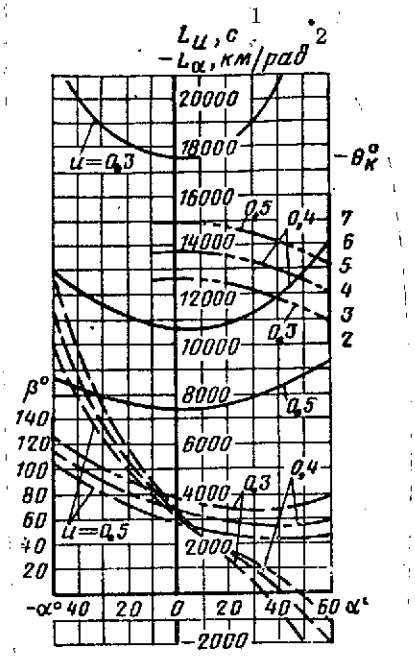

Fig. 5.11. Parameters determining landing accuracy as a function of angle α for different u, km/sec (u < 0, falling altitude H = 400 km):

——— L_u —·—·—·— β

------- L_α —··—··— θ_f

Key: 1. sec
2. km/rad

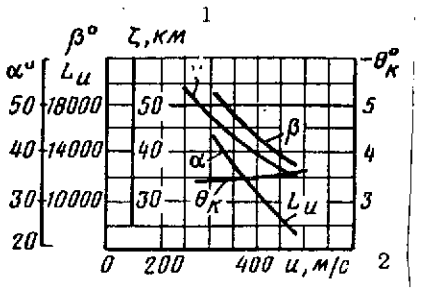

Fig. 5.12. $\zeta = \frac{\Delta L}{1\% \cdot \Delta u/u}$,

L_u, α, β, and θ_f as functions of u

Key: 1. km
2. m/sec

Let us look at the effect of errors on the section of flight within the atmosphere. These errors result from the possible error that appears when the air drag is being determined.

Air drag can differ from the calculated value due to errors in the determination of the following quantities:

the deceleration factor $k_x = c_x g/p_M = \sigma g$ (p_M is the load on the maximum cross section);

air density, ρ; and

random deviations in the parameters of motion from the calculated values during atmospheric reentry.

Below we examine the effect of errors in the determination of the coefficient k_x, density ρ, and reentry angle θ_0 on the scatter of range values during flight in the atmosphere. To

find the effect of these errors we used the above-presented results of the calculations of flight range x in ballistic descent for different reentry angles θ_0 and coefficient k_x (see Fig. 5.5). The calculations are presented under the assumption that the Earth does not rotate. It can be shown that this assumption does not lead to large errors. /266

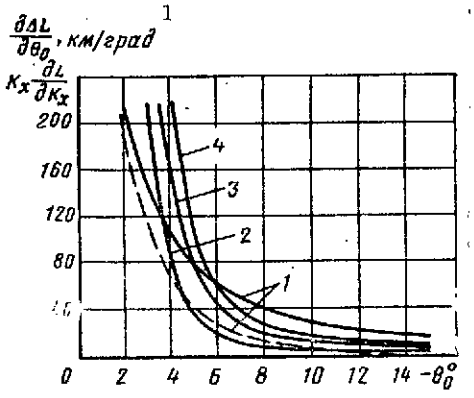

Fig. 5.13. $k_x \frac{\partial L}{\partial k_x}$, $\frac{\partial \Delta L}{\partial \theta_0}$ as functions of reentry angle θ_0 (solid lines refer to descent from 80 km down to zero, and the dashed line refers to descent from 80 to 15 km):

1 – $\frac{\partial L}{\partial k_x}$; 2 – $\frac{\partial \Delta L}{\partial \theta_0}$ when $k_x = 5 \cdot 10^{-4}$;

3 – $\frac{\partial \Delta L}{\partial \theta_0}$ when $k_x = 2{,}5 \cdot 10^{-3}$;

4 – $\frac{\partial \Delta L}{\partial \theta_0}$ when $k_x = 10^{-2}$

Key: 1. km/deg

By graphical differentiation of the function $x(k_x)$, the derivative $\partial x / \partial k_x$ was determined. It was found that $k_x \partial x / \partial k_x$ is nearly independent of k_x, that is, the effect of the relative error $\delta k_x / k_x$ on the scatter of range values is the same for all k_x in the interval under consideration.

Since only the product $k_x \rho$ appears in the equation of motion, obviously the effect of the relative errors $\delta k_x / k_x$ and $\delta \rho / \rho$ on the trajectory parameters is quite identical under the condition that the variation in the errors as such during the flight will also be identical (in the particular case, when $\delta k_x / k_x$ and $\delta \rho / \rho$ remain unchanged during the flight).

The curve characterizing the variation in $k_x \frac{\partial x}{\partial k_x}$ as a function of the reentry angle of the trajectory into the atmosphere θ_0 is shown in Fig. 5.13 (solid line).

From an inspection of this curve it follows that when high landing accuracy in the designated region is required, the angle of reentry into the atmosphere must not be less than 4-6°, since when $|\theta_0| \leq 4°$ to each variation of 10 percent in $\delta k_x / k_x$ there corresponds a deviation in range $\delta x \geq 10$ km. These figures also characterize the influence of the error $\delta \rho / \rho$.

It was of interest as to which of the altitudes in the atmosphere most strongly affect the deviations in range when the craft is in flight along trajectories with different reentry angles. For this purpose, calculations were made to determine

$k_x \frac{\partial x}{\partial k_x}$, corresponding to flight at altitudes y from 80 to 15 km.

The curve of variation of this quantity is shown in Fig. 5.13 (dashed line). It turns out that when $|\theta_0| > 4.5°$, the main scatter in range values arises at altitudes less than 15 km, while when $|\theta_0| > 10°$, the scatter is virtually absent at altitudes greater than 15 km. At reentry angles $|\theta_0| < 4.5°$, the greatest scatter is observed at altitudes exceeding 15 km. /267

Therefore, in calculations of motion along trajectories with angles of reentry into the atmosphere that are greater than 4.5° in absolute magnitude, the coefficient k_x and the density of air at altitudes less than 15 km must be determined with greater accuracy than for altitudes greater than 15 km. When $|\theta_0| < 4.5°$, in contrast, the coefficient of drag c_x and air density at altitudes above 15 km must be determined more accurately.

When there are random deviations in the angle of reentry θ_0, the flight range will change differently for different craft drag coefficients. But if $k_x = 0$, the variation in flight range would correspond to the elliptical theory. When $k_x \neq 0$, range variation occurs both due to change in the elliptical range as well as due to change in the time of action and air drag.

To determine the scatter of range values in this case, we calculated the differences Δx between range under the elliptical theory and range with reference to air drag for different θ_0. By graphical differentiation, we obtained the dependence of the derivative $\partial \Delta x / \partial \theta_0$ on the angle θ_0 for different coefficients k_x. This function is also shown in Fig. 5.13 (curves 2, 3, and 4).

From the figure it follows that the derivative $\partial \Delta x / \partial \theta_0$ rises sharply when $|\theta_0| < 4°$. When $|\theta_0| > 7°$, the derivative varies little and is small in magnitude. When $k_x \leqslant 0.01$, $\partial \Delta x / \partial \theta_0 \leqslant 30$ km/deg in this range of angles. When $\theta_0 \approx 3°$, the quantity $\partial \Delta x / \partial \theta_0$ is about 300-350 km/deg.

5.2. Coasting Descent

The main advantage of the coasting descent of manned craft over ballistic descent is that craft heating and the effective g-loads can be reduced by increasing flight altitude and by regulating the flight as a function of deviations in the heating levels and g-loads from the design values. Also important in coasting descent is the possibility of various maneuvers.

Below we examine, from the standpoint of providing lowest heating, one possible method of selecting and calculating the main trajectory section of flight in the dense atmospheric layers along which the greatest deceleration of velocity takes place. The section of the transition from the trajectory of reentry into the atmosphere to the trajectory section with greatest deceleration /268 is not examined here.

As we know, heat expended in heating a craft as it is moving in the atmosphere results from the work done by the air drag forces. To the first approximation it can be assumed that the ratio of energy expended in craft heating to the work done by the drag forces is a constant. In this case it is expedient to adopt as the design motion the motion in which the per-second rate of work done by the drag forces is constant along most of the trajectory. This is attained under the assumption that the heat reaching the craft is uniformly distributed along the entire trajectory.

The per-second work done by air drag forces can be expressed by this formula:

$$N_x = c_x F \frac{\varrho v^3}{2}, \tag{5.15}$$

where F is the area to which the drag force is related (in the following we will relate the aerodynamic forces to the area of the craft control surfaces).

The constancy of power during the action of the drag forces is equivalent to the condition

$$c_x \varrho v^3 = f(v, y) = \text{const}. \tag{5.16}$$

This condition determines the dependence of velocity on altitude, that is,

$$v = v(y).$$

In the general case the ratio of energy expended in heating the craft to the per-second work (power) of the drag forces is a function of altitude, velocity, and time. The condition that power is constant (5.16) can be replaced by any other condition and we can still obtain the function v(y).

If the function v(y) is given, then when calculating the trajectory at each point of the trajectory the angle between the velocity vector and the local horizon (trajectory inclination) is uniquely determined for given craft parameters. Here as earlier, the reentry angle is the negative angle between the velocity vector and the horizon at the beginning of the trajectory section under study. However, due to various errors the satellite can reenter the atmosphere along a trajectory that has an inclination greater than the calculated value. In addition, the aerodynamic characteristics of the craft and the law of variation of density with altitude are known always with errors which can also cause deviations in the trajectory of motion from the design value. These deviations of trajectory must be eliminated by the action of additional aerodynamic forces, otherwise the deviations in velocity from the design law will be quite large, and will occur in the increasing direction. This will cause an intolerable overheating of the craft.

Calculated Motion in the Atmospheric Trajectory of Descent /269

As stated above, we will start from the fact that we know the law of variation of velocity with flight altitude v(y).

The equations of motion of the mass center of a satellite are of the form (under the assumption that the gravity field is central and the Earth does not rotate) as follows:

$$\left.\begin{aligned} m\frac{dv}{dt} &= -c_x F\frac{\varrho v^2}{2} - mg\sin\theta;\\ mv\frac{d\theta}{dt} &= c_y F\frac{\varrho v^2}{2} + \left(\frac{mv^2}{R+y} - mg\right)\cos\theta;\\ \frac{dy}{dt} &= v\sin\theta;\\ \frac{dx}{dt} &= v\cos\theta, \end{aligned}\right\} \qquad (5.17)$$

where y is the altitude
x is the flight range measured from the origin of the section under study
t is the flight time from the moment that the trajectory section begins, and
m is the mass of the satellite.

We can assume the exponential law of variation with altitude

$$\varrho=\varrho_0 e^{-by}$$

for the density ρ (b, ρ_0 = constant coefficients).

In this case it is best to convert to the independent variable y. In this instance, Eqs. (5.17) become

$$\left.\begin{aligned}
&\frac{d(v^2)}{dy}\sin\theta=-k_x\varrho v^2-2g\sin\theta;\\
&\frac{d\theta}{dy}\sin\theta=\frac{1}{2}k_y\varrho-\frac{g}{v^2}\cos\theta+\frac{\cos\theta}{R+y};\\
&\frac{dt}{dy}=\frac{1}{v\sin\theta};\\
&\frac{dx}{dy}=\operatorname{ctg}\theta,
\end{aligned}\right\} \tag{5.18}$$

where

$$\left.\begin{aligned}
k_x&=\frac{c_xF}{m}=\frac{c_xg_0}{p_F};\\
k_y&=\frac{c_yF}{m}=\frac{c_yg_0}{p_F};
\end{aligned}\right\} \tag{5.19}$$

$$p_F=\frac{mg_0}{F}. \tag{5.20}$$

In the following, we will assume the acceleration due to gravity g along the trajectory to be constant and equal to some averaged value. From the first equation of system (5.18) let us determine sin θ: /270

$$\sin\theta=-\frac{k_x\varrho v^2}{2g+\frac{d(v^2)}{dy}}. \tag{5.21}$$

Since the function v(y) is known, this formula determines the angle θ as a function of y. Let us differentiate (5.21) in y:

$$\frac{d\theta}{dy}=\operatorname{tg}\theta\left[\frac{1}{\varrho}\frac{d\varrho}{dy}+\frac{1}{v^2}\frac{d(v^2)}{dy}-\frac{\frac{d^2(v^2)}{dy^2}}{2g+\frac{d(v^2)}{dy}}\right]. \tag{5.22}$$

Substituting $\frac{d\theta}{dy}$ from (5.22) into the second equation of system (5.18) and solving it for k_y, we get

$$k_y = \frac{2}{\varrho}\left\{\left[\frac{1}{\varrho}\cdot\frac{d\varrho}{dy}+\frac{1}{v^2}\cdot\frac{d(v^2)}{dy}-\frac{\frac{d^2(v^2)}{dy^2}}{2g+\frac{d(v^2)}{dy}}\right]\frac{\sin^2\theta}{\cos\theta}+\right. \tag{5.23}$$

$$\left.+\frac{g\cos\theta}{v^2}-\frac{\cos\theta}{R+y}\right\}.$$

Eq. (5.23) enables us to calculate the required values of the lift coefficients, and thus, the angles of attack at any point of the trajectory for a given F.

The flight time from the initial altitude y_{max} to any altitude is determined by the formula

$$t = \int_{y_{max}}^{y} \frac{dy}{v\sin\theta}. \tag{5.24}$$

The flight range from the beginning of the section under study to any point on the trajectory is

$$x = \int_{y_{max}}^{y} \operatorname{ctg}\theta\, dy. \tag{5.25}$$

Thus, the elements of the trajectory at any point on it are determined by Eqs. (5.21)-(5.25) for any assigned law v(y).

Depending on the choice of law v(y), we can obtain different descent ranges for the virtually identical heating and g-loads, that is, a range maneuver can be effected. /271

The high available lift-to-drag of coasting type craft permits maneuvering also in the side direction for several thousands of kilometers. In this case the number of "landing" orbits is appreciably increased, since the condition of the orbit transiting across the landing area is not mandatory.

Another important advantage of gliding type craft is the possibility of maneuvers associated with rotation of the orbital plane of the flight vehicles in near-Earth flight.

Let us examine the case of coasting descent at constant temperature of the craft hull skin. The equilibrium temperature of the heat-insulating surfaces obtained from the heat-balance equation, which is of the form

$$q_{em} = q_{conv} + q_{rad},$$

where q_{em}, q_{conv}, and q_{rad} represent, respectively, the emissive (radiational), convective, and radiative thermal flows per second.

As we know, to the first approximation the equilibrium temperature is determined by the function

$$T = A\varrho^m V^n, \tag{5.26}$$

where A, m, and n are constants.

Hence, at a constant equilibrium temperature we get the altitude (density) as a function of flight velocity more exactly than based on condition (5.16) with c_x = const. This enables us to entirely define the descent trajectory in this sense.

This analysis showed that the function

$$\varrho V^6 = \text{const} = C \tag{5.27}$$

ensures the approximate constancy of the equilibrium temperature, at least at the altitudes 40-90 km, both for the surface of a plate, as well as for the critical line of a swept wing and for a spherical face.

Using condition (5.27) and Eqs. (5.19), (5.21), and (5.23), we get (n = 6):

$$\sin\theta = -\frac{n}{2}\frac{\sigma_x g_0 \varrho V^2}{ng + bV^2}; \tag{5.28}$$

$$K_{\text{eff}} = -\frac{2}{\sigma_x g_0 \varrho}\left\{\frac{b}{n}\left(n - 2 + \frac{2bV^2}{ng + bV^2}\right)\frac{\sin^2\theta}{\cos\theta} + \left(\frac{1}{R+H} - \frac{g}{V^2}\right)\cos\theta\right\}. \tag{5.29}$$

The maximum effective lift-to-drag ratio K_{eff} required to satisfy condition (5.27), determined from Eq. (5.29), depends on the constant C for a fixed wing loading $P_F = G/F$. This value was selected so that the maximum required c_y did not exceed the maximum available value corresponding to the given angle of attack. /272

The constant C was determined thusly. For the trajectory section of this study, the inequality $ng << bV^2$ obtained. Also, θ had the maximum possible value of the order of several degrees, and therefore it can be assumed that $\sin\theta \approx \theta$ and $\cos\theta \approx 1$.

Then the function (5.29) will be appreciably simplified

$$K_{eff} = -\frac{n^2\sigma_x g_0}{2b}\varrho + \frac{2}{\sigma_x g_0 \varrho}\left(\frac{g}{V^2} - \frac{1}{R+H}\right). \tag{5.30}$$

Using the function (5.30) and the equation for the derivative $dK_{eff}/dH = 0$, we obtain equations for determining the altitude H and velocity V at which the maximum effective lift-to-drag ratio is attained,

$$H = \frac{\frac{4}{n-2}}{K_{eff}\sigma_x g_0 \varrho + \frac{(n-1)n^2\sigma_x^2 g_0^2 \varrho^2}{(n-2)b} + \frac{2n}{(n-2)b(R+H)^2}} - R; \tag{5.31}$$

$$V = \sqrt{\frac{2g}{K_{eff}\sigma_x g_0 \varrho + \frac{n^2\sigma_x^2 g_0^2 \varrho^2}{2b} + \frac{2}{R+H}}}, \tag{5.32}$$

and C can be found from the H and V found, by Eq. (5.27).

In accordance with Eqs. (5.28) and (5.29), the required lift-to-drag ratios K_{eff} were calculated for various values of coefficient C. The results of the calculations are presented in Fig. 5.14.

The values of the aerodynamic coefficients c_y and c_x as a function of the angle of attack α were calculated by the familiar Newton's polar for hypersonic velocities:

$$c_y = 2\sin^2\alpha\cos\alpha;$$
$$c_x = c_{x0} + 2\sin^3\alpha.$$

The angle of attack α ensuring a maximum value for $c_{y\ max}$ was adopted: $\alpha_{c_{y\ max}} \approx 55°$; $c_{y\ max} = 0.769$; and $c_x = 1.088$.

From Fig. 5.14 it is clear that as the coefficient C is increased, the section over which the program $\rho V^6 = C$ is satisfied is shifted toward the side of lower altitudes, and the K_{ava} [ava = /273 = available] required for the realization of this program is also reduced.

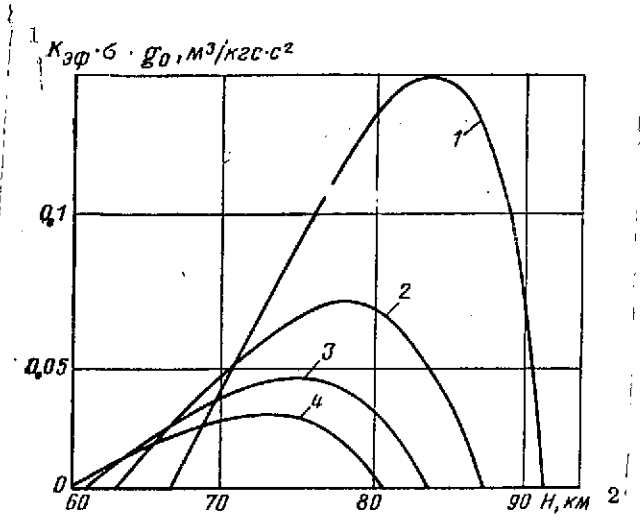

Fig. 5.14. Variation in lift-to-drag ratio as a function of flight altitude ensuring descent with C = const:

1. $C = 0.857 \cdot 10^{17}$ kg·m²/sec⁴. $p = 50$ kg/m²;
2. $C = 0.187 \cdot 10^{18}$ kg·m²/sec⁴, $p = 100$ kg/m²;
3. $C = 0.252 \cdot 10^{18}$ kg·m²/sec⁴, $p = 150$ kg/m²;
4. $C = 0.379 \cdot 10^{18}$ kg·m²/sec⁴, $p = 200$ kg/m².

Key: 1. $K_{eff} \cdot \sigma \cdot g_0$, m³/kg·sec²
2. km

There is a definite relation between K_{ava} and C for a fixed specific wing loading $p_F = G/F$. Since $c_{y\ max}$ is given, we will characterize the trajectory by the specific wing loading. To estimate the characteristics of craft heating, the heating temperatures of a plate moving in the descent trajectory under study were calculated. The temperatures we calculated for turbulent and laminar flow of air past the plate according to Eq. (5.26).

The results of calculating the temperature at the plate surface are in Fig. 5.15. From the figure we see that as the wing loading was varied, the constancy of altitude with height was disturbed, and as the loading was increased this nonuniformity rose, but however it did not attain an appreciable value even at a relatively high loading $p_F = 400$ kg/cm². Moreover, for low specific loadings ($p_F \leq 50$ kg/cm²), with increase in altitude a slight temperature drop was observed, while with increase in specific wing loading the temperature at the end of the trajectory section began to rise due to the transformation of the laminar regime into a

turbulent regime. Here as the wing loading was increased the transition to the turbulent regime occurred earlier.

These trajectories cannot be attained over the entire atmospheric section of the flight: at altitudes greater than 80-100 km it is necessary to ensure arrival at these trajectories from the transfer ellipse, while at low altitudes arrival from these trajectories is required owing to the constraint on g-loads. /274

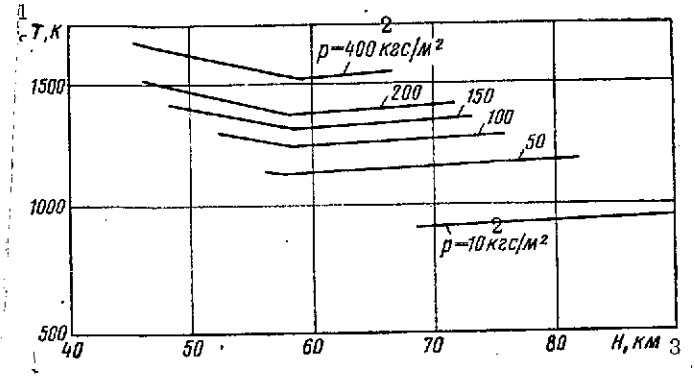

Fig. 5.15. Variation in temperature at surface of plate as a function of flight altitude

Key: 1. T, °K
2. kg/m^2
3. km

Figs. 5.16 and 5.17 present the curves of variation in the plate temperature and several other parameters of motion along several actual descent trajectories. The initial trajectory section strongly affects the integral thermal fluxes owing to its long duration. Therefore, the ensuring of minimum flight time will be the main requirement on this trajectory section.

Obviously, to achieve the shortest flight time along this trajectory section we must obtain the program of variation in the lift coefficient c_y that would ensure the greatest atmospheric reentry angle. If the angle of atmospheric reentry θ_{en} is not given, as shown above motion when $c_y = c_{y\,max}$ until the isothermal trajectory is attained is the optimal motion. The reentry angle here can be selected as maximum from all the possible angles for a given available $c_{y\,max}$, and as a result the arrival at trajectory $\rho V^6 = C$ will be characterized by minimum time. /275

To determine the reentry angle θ_{en} and the reentry velocity V_{en}, by varying the altitude at which the principal trajectory section begins H_{beg}, we must calculate a series of trajectories with $c_{y\,max}$, by integrating the system of equations of motion from H_{beg} to H_{en}. We get the function $V_{en}(\theta_{en})$. We can compute a similar function for a given orbit by varying the retro-impulse. The points of intersection of the curves of these functions give the required reentry parameters (Fig. 5.18).

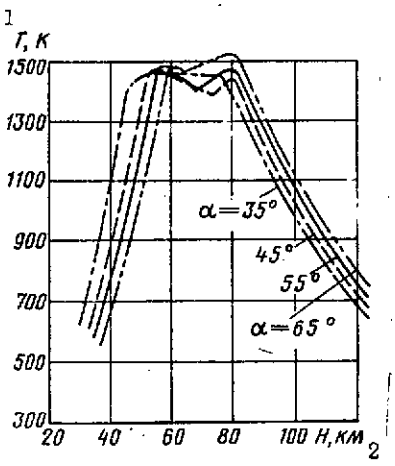

Fig. 5.16. Plate surface temperature as a function of trajectory ($p = 200$ kg/m^2)
Key: 1. T, °K
2. km

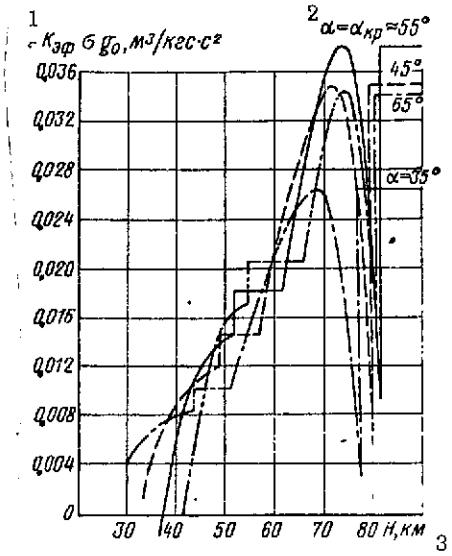

Fig. 5.17. Variation in lift-to-drag ratio for a number of trajectories ($p = 200$ kg/m^2)
Key: 1. $K_{eff} \cdot \sigma \cdot g_0$, $m^3/kg \cdot sec^2$
2. $\alpha = \alpha_w \approx 55°$ [w = wing]
3. km

Since there are constraints on the g-loads, we must introduce an iso-g-load section. Then in place of (5.27) we have the condition $\rho V^2 = C$; here we must set $n = 2$ in functions (5.28) and (5.29). The transitional section between the isothermal and the iso-g-load trajectory sections is determined in this case with a constant lift-to-drag ratio corresponding to the isothermal section. /276

Fig. 5.17 presents the lift-to-drag ratios as functions of altitude for $p_F = 200$ kg/m^2 and the angles of attack $\alpha = 35.45°$, and $\alpha_{cr} \approx 55.65°$. Fig. 5.19 shows the dependence of temperature T at the plate surface (at 1 meter from the leading edge) for these trajectories as a function of loading p_F.

5.3. Coasting Descent of a Satellite with Low Lift-to-Drag Ratio

In Section 5.2 we showed the advantages of the coasting descent of a craft from orbit [deorbiting] over the ballistic descent. However, coasting-design space satellites are more complicated to build than noncoasting satellites.

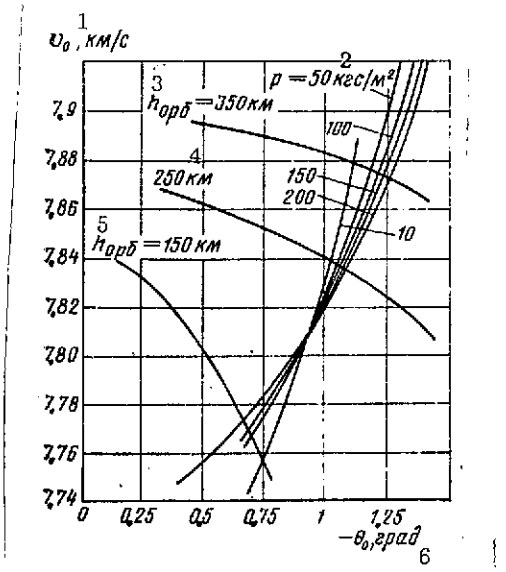

Fig. 5.18. For determination of parameters of spacecraft reentry into atmosphere (h_{orb} is orbital altitude)

Key: 1. km/sec
2. kg/m^2
3. h_{orb} = 350 km
4. km
5. h_{orb} = 150 km
6. deg

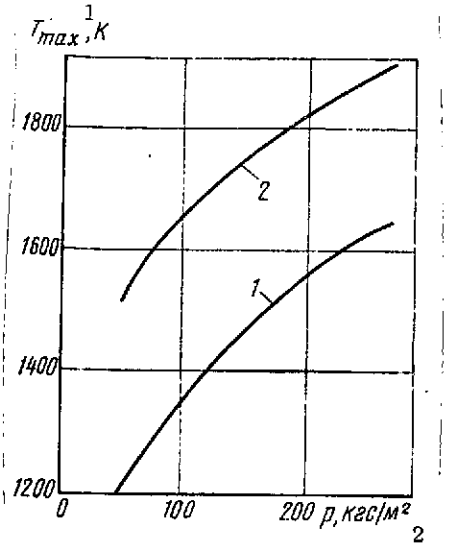

Fig. 5.19. Maximum temperature as a function of wing loading:
1. Temperature at wing surface at distance x = 1 m from leading edge
2. Temperature at critical point of spherical face d = 1 m

Key: 1. T_{max}, °K
2. p, kg/m^2

When developing craft with lift capabilities, use was made of experience in building ballistic type reentry vehicles (RV). In particular, efforts were made to find configurations with maximum drag (to reduce thermal flux) and configurations with significant aerodynamic lift (the lift-to-drag ratio of the RV). All this made it possible to build so-called skipping descent craft marked by high drag coefficient ($c_x > 1$) and high lift coefficient ($c_y > 0.3$-0.5), along with the highest lift-to-drag ratio ($K \simeq 0.2$-0.4).

Among the schemes of skip descent craft, the scheme of a segmented-conical shaped craft was of high interest, being a body of revolution with a segmented frontal surface of the RV and a conical rear. For symmetric flow past this kind of shape (when $\alpha = 0$), the lift will be absent, that is, the descent will be ballistic. In the case of nonsymmetric flow ($\alpha \neq 0$), a vertical component of the aerodynamic force -- lift ($K \neq 0$) -- appears.

The descent regime of an RV of this shape with $\alpha \neq 0$ can be provided by applying jet control forces producing a small angle of attack α along the descent trajectories -- control by means of variable angle of attack. However, this method involves large outlays of reaction mass for jet control, since the moments of inertia relative to the transverse axes of craft of the segmented-conical shapes are quite large. There is another approach. Let us shift the center of gravity of the RV upward from the symmetry axis. Then the descent [deorbiting] of this kind of craft will occur with some balancing angle of attack $\alpha = \alpha_b \neq 0$, so that they will appear a moment relative to the center of gravity from the drag which for the transition to the stable-flight regime will be equalized by the moment from the lift. No special jet control[4] will be required to retain the craft in flight at α_b. One important feature bears noting: the lift vector lies in the plane of symmetry of the craft extending through the center of gravity and the pressure center of the craft. Therefore when the craft is rotated by the angle γ relative to the axis connecting the center of gravity with the pressure center or the velocity axis O_1x (we call γ the roll angle) the projection of the lift $Y_b = c_y S \frac{\rho v^2}{2}$ onto the vertical plane of symmetry of the RV will change. The lift for flight at the balanced angle of attack $\alpha = \alpha_b$ and at the roll angle $\gamma = 0$ we will call Y_b. Then the vertical component Y_v [v = vertical] when $\gamma \neq 0$ is $Y_v = Y_b \cos \gamma$ and, thus, the horizontal component $Y_h = Y_b \sin \gamma$.

/277

Thus, it appears possible not only to achieve lift Y_v, but also to modify it during flight from $Y_v = Y_b$ to $Y = -Y_b$ by changing the angle of roll. Because the RV is virtually statically neutral as it rotates relative to the axis "center of gravity-pressure center," the reaction force for rotation and retaining the craft at some angle γ is very slight and the amount of reaction momentum is determined mainly by the possible moment of drag with coefficient m_{x_0} arising due to the technological asymmetry of the craft, the nonuniform entrainment of mass during ablation of the thermal shield, and so on. This is a very great advantage of RV that can be controlled by modifying the angle of roll.

---

[4] Jet control to stabilize $\alpha = \alpha_b$ is necessary for coping with various objections.

It should be noted that the deorbiting of skip type craft over the main trajectory section (at M numbers > 5-6) occurs with virtually constant spatial angle of attack α_b. So the assumption that the drag coefficient c_x, lift coefficient c_y, and thus the aerodynamic lift-to-drag ratio $K_b = \frac{c_y}{c_x}\Big|_{\alpha=\alpha_b}$ is quite sound.

Then it is convenient to characterize skip type craft with the ballistic parameter σ_x and the available lift-to-drag ratio K_{ava}, for which we take the value of the lift-to-drag ratio K_b for flight with angle of attack $\alpha = \alpha_b$: $K_{ava} = K_b$.

The vertical component of the aerodynamic lift-to-drag ratio, called the effective lift-to-drag ratio, like the lift, depends on the angle of roll γ: $K_{eff} = K_b \cos \gamma$. Accordingly, one speaks of control by means of varying the angle of roll or the "effective" lift-to-drag ratio.

From the foregoing it is clear that the landing of "skip" type craft must be effected by the same means as for ballistic type craft, for the small available aerodynamic lift-to-drag ratio does not permit a coasting descent. /278

Noncontrolled Coasting Descent [deorbiting]

The simplest kind of coasting descent is the so-called "uncontrolled" coasting descent during which only roll stabilization of the craft can be required.

Let us examine g-loads and their time of action on trajectories of an "uncontrolled" coasting craft over a wide range of variation of the parameters of atmospheric reentry under the following assumptions:

the Earth's gravity field is central

the Earth's rotation does not affect [craft] motion

the deceleration factor σ remains unchanged during the flight

the lift-to-drag ratio of the craft $K = c_y/c_x$ is constant, and

there are no craft vibrations.

Trajectories of coasting descent under these assumptions can be described by the following system of differential equations:

$$\left.\begin{aligned}
\dot{v} &= -\sigma g_0 \frac{\rho v^2}{2} - \frac{\mu}{r^2}\sin\theta;\\
\dot{\theta} &= \frac{k\sigma g_0}{v}\frac{\rho v^2}{2} + \frac{v}{r}\left(1 - \frac{1}{k_1}\right)\cos\theta;\\
\dot{h} &= v\sin\theta;\quad \dot{\Phi} = \frac{v}{r}\cos\theta,
\end{aligned}\right\} \qquad (5.33)$$

where

$$k_1 = \frac{v^2 r}{\mu};\quad r = R + h;$$

h, Φ are flight altitude and angular range

g_0 is the acceleration due to gravity at the Earth's surface, and

$\mu = 3986 \cdot 10^9$ m^3/sec^2 is the constant of the Earth's gravitational field.

The g-load due to the aerodynamic drag is

$$n_\Sigma = \sqrt{n_x^2 + n_y^2},\quad \text{or}\quad n_\Sigma = n_x\sqrt{1+K^2},$$

where

$$n_x = \frac{R_x}{G} = \sigma\frac{\rho v^2}{2};\quad n_y = \frac{R_y}{G} = \sigma K\frac{\rho v^2}{2}.$$

Since the coasting descent trajectory is determined by the initial motion parameters, the coefficient of deceleration, and the lift-to-drag ratio of the craft K, the g-loads are also determined by these quantities.

To find the general trend of the dependence of g-loads on these factors, a computer was used to arrive at the numerical solutions of system (5.33) as the initial conditions of motion, coefficient σ, and craft lift-to-drag ratio K were varied. The motion parameters v_0 and θ_0 at the altitude 100 km were adopted as the initial conditions. /279

The nature of the variation of the maximum g-loads from the calculation data, as a function of the initial motion parameters and the coefficient σ for K = 0.1, 0.25, 0.5, and 0.75 is illustrated by Figs. 5.20 and 5.21.

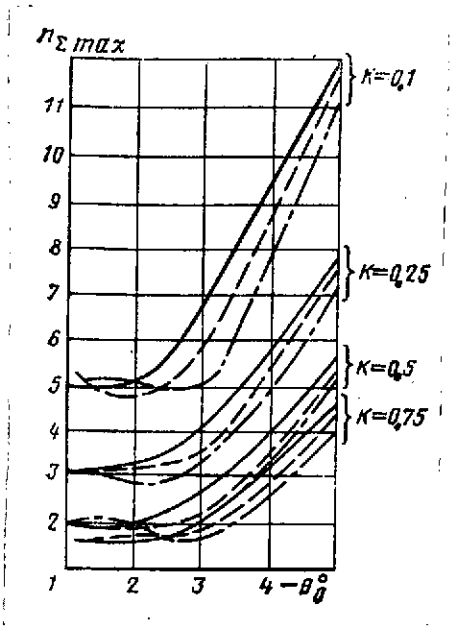

Fig. 5.20. G-load $n_{\Sigma\ max}$ as a function of the reentry angle θ_0 for the ballistic parameter $\sigma_0 = 0.001\ m^2/kg$ and the reentry velocity $v_0 = 7.8$ km/sec (——); $v_0 = 8$ km/sec (----); and $v_0 = 8.2$ km/sec (-·-·-)

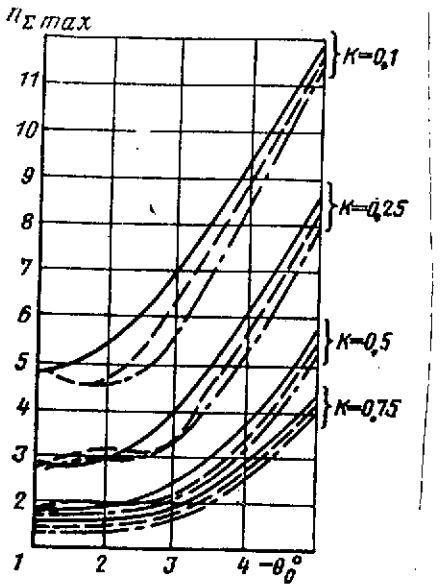

Fig. 5.21. $n_{\Sigma\ max}$ as a function of θ_0 when $\sigma = 0.005\ m^2/kg$ and $v_0 = 7.8$ km/sec (——); $v_0 = 8.0$ km/sec (-·--); and $v_0 = 8.2$ km/sec (-·-·-)

The calculations were made for the velocities $v_0 = 8.2$, 8.0, and 7.8 km/sec, and the initial reentry angles $-5° \leqslant \theta_0 \leqslant -1°$. The deceleration coefficient σ was varied over the range $0.001 \leqslant \sigma \leqslant 0.005\ m^2/kg$.

The curves in Figs. 5.20 and 5.21 characterizing the variation in maximum g-loads are similar, and the g-loads showed a slight dependence on velocity and almost no dependence on σ. At the reentry angles θ_0 from - 1° to - 3°, the maximum g-loads for the same K varied only slightly, just as in the variation of the initial reentry velocities, within the range 7.8-8.2 km/sec. When $\theta_0 < -3°$, the maximum g-loads will rise sharply and exceed the allowable limits, therefore the reentry angle must not be more than - 3°.

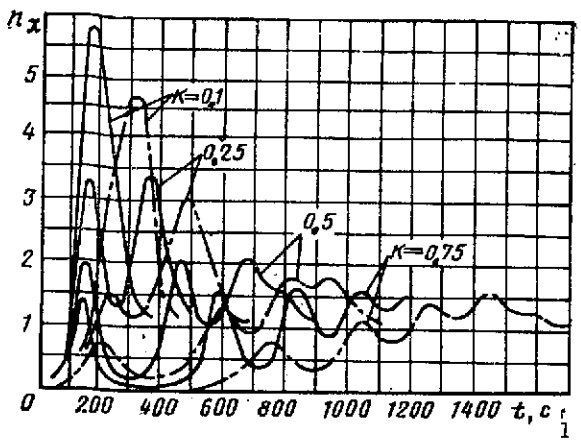

Fig. 5.22. n_x as a function of flight time t at v_0 = 8 km/sec and σ = 0.001 m^2/kg:

———— $\theta_0 = 3°$

-·-·-·- $\theta_0 = 2°$

Key: 1. t, sec

Considering that when the coefficient of deceleration is varied over the range 0.001 < < σ < 0.005 m^2/kg, the maximum g-loads show virtually no change, and so all the subsequent calculations were made for the single value σ = 0.001 m^2/kg. Calculation results show that when the lift-to-drag ration was varied over the range 0.1 < K < 0.75, the maximum g-loads decreased, and they did not exceed n_Σ = 4 when K = 0.25 for the reentry angles θ_0 from - 1° to - 3°. When K = 0.5 for the same reentry angles, n_Σ will not be more than 3 (Fig. 5.22). The human organism readily tolerates a g-load n = 4 in the chest-back direction for 4.5 min. Fig. 5.22 gives the variations in g-load along the trajectory for all adopted K values at the reentry angles θ_0 = - 2 and - 3° and at the reentry velocity v_0 = 8 km/sec. /280

Curves characterizing the variation in velocity, altitude, angle of inclination of velocity vector to the local horizon, and velocity heads q with time are shown in Figs. 5.23-5.26. These curves were calculated for v_0 = 8 km/sec, θ_0 = - 2° and - 3°, σ = 0.001 m^2/kg, and K = 0.1, 0.25, 0.5, and 0.75.

From an inspection of these curves it follows that when K is increased the descent time rises sharply. Descent occurs not along the smooth curve, but along the so-called fugoid. Motion along it is undesirable since the g-load and temperature peaks increase, the descent time becomes longer, therefore, craft heating is more intense. In order to reduce the descent time and the g-load and temperature peaks, one must reduce the lift-to-drag ratio down to K ≃ 0.25. For a rapid descent the angle θ_0 must also be reduced, but not below - 3°, since at smaller reentry angles g-loads will rise sharply.

Thus, as calculations have shown, when uncontrolled coasting descent is used the maximum g-loads for the appropriate selection of parameters of atmospheric reentry and lift-to-drag ratio will not exceed 3-4. /281

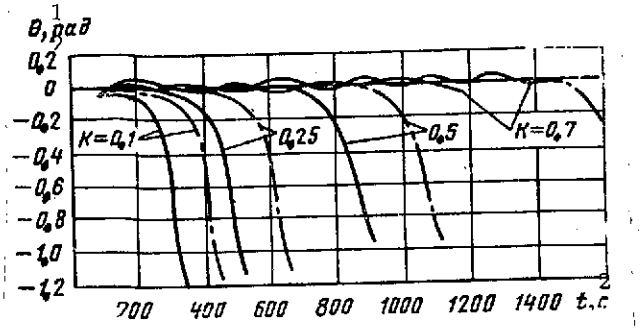

Fig. 5.23. Angle θ as a function of flight time when v_0 = 8 km/sec, σ = 0.001 m^2/kg, and θ_0 = 3 and 2°:

_____ θ_0 = 3°; ___.___ θ_0 = 2°

Key: 1. rad
2. t, sec

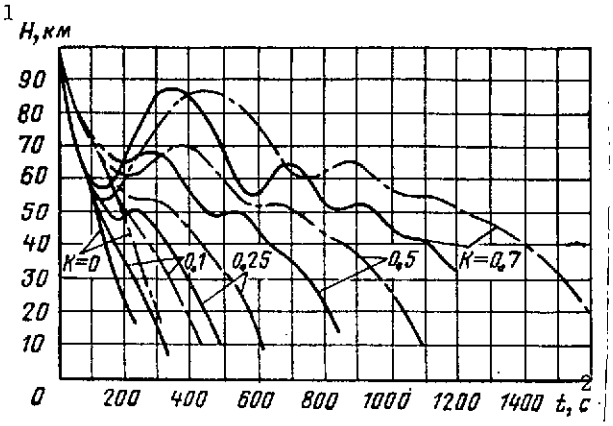

Fig. 5.24. Altitude H as a function of flight time t when v_0 = 8 km/sec, σ = 0.001 m^2/kg, and various θ_0 and K:

_____ θ_0 = 3°; ___.___ θ_0 = 2°

Key: 1. H, km
2. t, sec

The strongest effect on the g-loads, as in ballistic descent, comes from the angle of atmospheric reentry θ_0 (for uncontrolled coasting deorbiting [descent] of manned satellites, trajectories with atmospheric reentry angle θ_0 not less than - 3° are regarded as acceptable. Rapid descent is achieved at a reentry angle -3°.).

The effect of atmospheric reentry velocity on the maximum g-loads, just as in the case of ballistic descent, is small. Here an increase in the velocity at constant reentry angle leads to lower g-loads. A variation in the deceleration coefficient $0.001 \leq \sigma \leq 0.005$ has virtually no effect on g-loads. /282

Controlled Coasting Descent

The main disadvantage of uncontrolled coasting descent is the large scatter of satellite landing points due to the effect of all possible errors and perturbations. To eliminate this disadvantage, /283 a system for control of the lift-to-drag ratio is installed on a satellite. Control can be effected from the signals of sensitive elements responding to g-load changes during the flight.

Fig. 5.27 shows the dependence of the range of descent and overall heat flux for the reentry angle θ_0 = - 2° and velocity

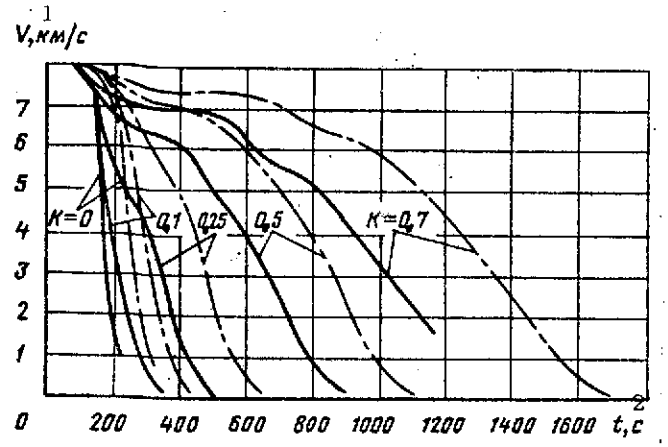

Fig. 5.25. Velocity v as a function of flight time t when σ = = 0.001 m^2/kg and various angles θ_0:

——— θ_0 = 3°; —·— θ_0 = 2°

Key: 1. km/sec
2. t, sec

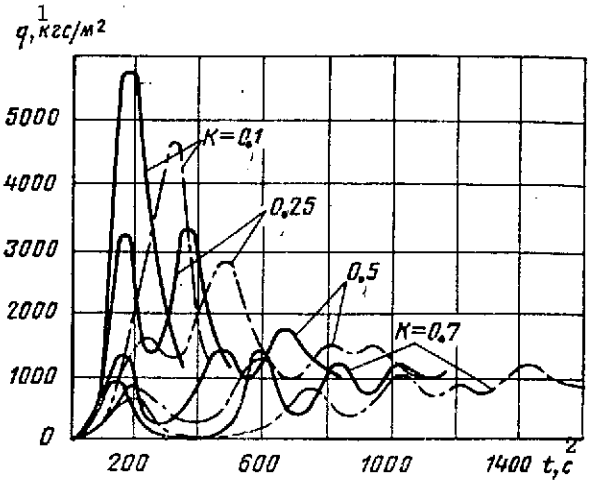

Fig. 5.26. Parameter q as a function of flight time t when v_0 = 8 km/sec, σ = 0.001 m^2/kg, and various angles θ_0:

——— θ_0 = 3°; —·— θ_0 = 2°

Key: 1. kg/m^2
2. t, sec

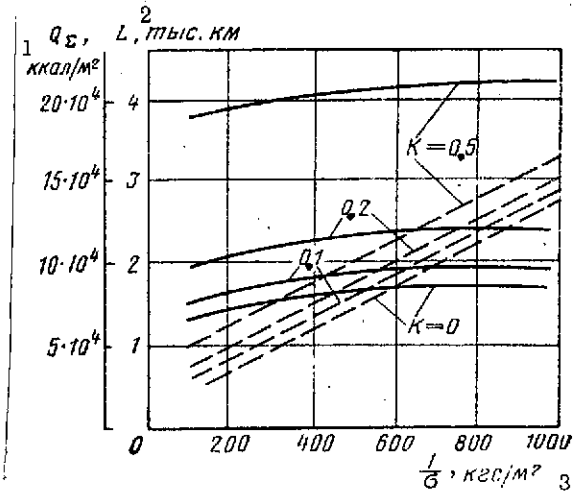

Fig. 5.27. Descent range in overall thermal flux as a function of ballistic parameter (v_0 = = 7.8 km/sec; θ_0 = - 2°):

——— L; ------ Q_Σ

Key: 1. $kcal/m^2$
2. thousands of km
3. kg/m^2

v_0 = 7.8 km/sec (with variation in lift-drag ratio from K = 0 to K - 0.5) on the reciprocal of the parameter σ. The curves give an idea of the size of scatter in range for uncontrolled descent.

The presence of lift permits controlling the descent in performing various missions, the principal being the goal of ensuring an exact landing in a designated area of the Earth with mandatory maintenance of g-load constraint:

$$n_\Sigma \leqslant n_{\max\,\text{al}}.$$

Here $n_{max\ al}$ is the maximum value of the allowable g-load, and

n_{Σ} is the instantaneous overall g-load along the descent trajectory.

In controlled descent some decrease in the required weight of the craft heat shield can also be achieved. Accordingly, in the following we will consider these aspects:

control of final flight range of the RV (control of final state of object), and

control of motion along a trajectory that is optimal (from the standpoint of minimum weight of heat shield) with mandatory satisfaction of the condition for the exact landing of the RV in a designated area and fulfilling of the constraints on g-loads. /284

Control of skipping type craft, as noted above, is best effected by varying the angle of roll. The variability of lift for rotation with respect to roll is ensured by selecting the aerodynamic configuration and centering. This approach is marked by adequate simplicity and minimum required outlays of reaction mass in RV stabilization. Programmed variation during a descent in the angle of roll (varying the vertical component of the lift) makes possible a descent along trajectories satisfying the conditions imposed.

The process of varying during flight the RV angle of roll in order to bring a craft to a given point in phase space or to maintain a specific optimal trajectory is carried out by the descent control system (DCS).

When performing various tasks, the most diverse requirements can be imposed on the DCS, depending on the purpose of the space object. In some cases the basic condition can be the requirement of building a minimum-weight DCS ensuring appropriate landing accuracy, while in another case it can be an exceptionally exact landing, and so on. There are quite numerous ways of building DCS at the present time. Each system has its own advantages and drawbacks with respect to the landing accuracy afforded, reliability, weight expenditures, required onboard and ground facilities, simplicity of implementation, and the like. Because of this, one has to give preference to a particular system in each specific case in relation to the tasks imposed and the available sources.

The first stage in building a DCS [54] is determining the nominal program of variation in the control parameter (nominal control ensuring the descent of the RV along a specific given (programmed) trajectory or a trajectory developed in the course of the flight). In the general case, the conditions posed can satisfied for motion along the most diverse trajectories. The

task of nominal control is to determine this family of trajectories and to ensure RV motion along them in nominal conditions (in the absence of perturbations).

The second stage in constructing a DCS is to find the law of variation of the control parameter ensuring the descent of the craft along the selected nominal trajectory (or, at least, along a near-nominal trajectory) in actual conditions -- when acted on by various kinds of perturbations.

One of the main features in building control systems for skip type craft is the necessity of control of the longitudinal and lateral flight ranges by means of one control parameter -- the angle of roll. In this case control of lateral range can be achieved only within the frame of reference of controlling the longitudinal range by rotating the RV "from side-to-side" at specific instants along the descent trajectory. The craft will move along a fluctuating curve relative to the given direction of motion. At the instants of rotation, the control system actually is disconnected and the condition of stability of longitudinal range control can be violated. /285

This factor materially hinders the building of DCS for skip type RV.

Using the angle of roll γ as the only control parameter, we must select it so as to ensure simultaneously longitudinal and lateral control. The general solution of this problem lies in separate use of the modulus and sign of the angle γ in one of two variants:

variation in the modulus of γ is subordinated to the requirements of longitudinal control, and variation in the sign of γ -- -- to requirements of lateral control, and

the reciprocal distribution of modulus and sign of γ.

Here control by means of variations in sign or sense [clockwise or counterclockwise] is discrete owing to which at the end of a trajectory there is an uncontrolled section along which some final miss with respect to the corresponding coordinate forms. The first variant is more convenient, more universal, and more exact, since in this case the more improved control (by modulus of angle γ) is employed to perform the most complex part of the mission -- forming and stabilizing the trajectory in the longitudinal plane, and more flexible control (by the sign of angle γ) -- to eliminate the relatively small lateral deviations.

Simple Systems of Continuous Action

The requirement of the exact landing of an RV in a designated area of the Earth at present is dominant. The descent control system must ensure that this requirement is satisfied while certain constraints are observed, above all, constraints on g-loads. This accounted for the end-goal direction in building DCS -- control of the final flight range, that is, control of the end state of the object.

We can consider the following ways of building DCS of continuous action:

1) using precalculated program functions;

2) with "prediction" of the landing point, and

3) mixed type, when the program function is selected from the results of the prediction.

DCS of the first type are the simplest. By simple DCS we mean systems which are built with the use of simple information readily accessible to measurement and that provide for processing this information (for the generation of the control signal) on the simplest computers (or simple analog devices). /286

At the present time it can be assumed that measurement of g-loads, integrals of g-loads, and flight time represent this kind of simple information. The DCS is made most simply if the g-loads are measured in axes rigidly coupled to the RV hull.

When designing continuous-action DCS, it is necessary to determine some function of the phase coordinates (control functional), which when maintained close to the design coordinates permits the necessary landing exactness to be achieved. We can consider as such a function the departure of the final landing point from the given landing point $\Delta L_f = L_f - L_{des}$, which must be equal to zero.

Considering that the perturbations acting on an RV are small, a deviation from the landing point (in the longitudinal plane of motion) can be written thusly:

$$\Delta L_f(t_i) = \frac{\partial L_f}{\partial x_i}\Delta x_i + \frac{\partial L_f}{\partial y_i}\Delta y_i + \frac{\partial L_f}{\partial V_{x_i}}\Delta V_{x_i} + \frac{\partial L_f}{\partial V_{y_i}}\Delta V_{y_i}, \qquad (5.34)$$

where $\frac{\partial L_f}{\partial x_i}, \ldots, \frac{\partial L_f}{\partial V_{y_i}}$ are partial derivatives of final flight range in terms of coordinates and velocity components taken at the instant t_i, and

Δx, Δy, ΔV_x, ΔV_y are the deviations of the coordinate and velocity components of the RV at the instant t_i from the given values.

By reducing to zero the expression for $\Delta L_f(t_i)$ at each moment of time by introducing the corresponding control action

$$\Delta L_f(t_i) = \xi \frac{\partial L_f}{\partial \gamma} \Delta\gamma = 0, \tag{5.35}$$

we can ensure the condition of landing in a designated area ($\frac{\partial L_f}{\partial \gamma}$ is the partial derivative of the final range in terms of angle of roll for the instant t_i; the coefficient $\xi \neq 0$ must be introduced to improve the dynamics of the control process).

To solve the selected functional, we must know the partial derivatives $\frac{\partial L_f}{\partial x}, \ldots, \frac{\partial L_f}{\partial \gamma}$, designed (programmed) values of the trajectory parameters x_{des}, y_{des}, $\ldots$, γ_{des}, and the instantaneous values of these same parameters that must be determined onboard the RV.

The partial derivatives can be determined either by the numerical integration of the equations of motion on an onboard digital computer with the input of deviations for the corresponding /287 parameters, and here the derivatives are defined thusly:

$$\frac{\partial L_f}{\partial x} = \lim_{\Delta x \to 0} \frac{\Delta L_f}{\Delta x}, \ldots, \frac{\partial L_f}{\partial \gamma} = \lim_{\Delta\gamma \to 0} \frac{\Delta L_f}{\Delta \gamma}, \tag{5.36}$$

or by integrating a system conjugate to the initial linearized system.

In many cases actually simple systems are used, employing minimum data and the simplest data processing. These systems include above all DCS utilizing information from one integrating accelerometer. The axis of this accelerometer is either rigidly coupled to the RV hull and permits the "bound" g-load to be obtained (n_{bo}) or else is positioned in a specific way in inertial space. The programmed dependence of variation in g-loads n_{bo} or or n_{in} is stored onboard the RV (n_{in} is the "inertial g-loads) as

a function of the argument used in the DCS. Generally, the apparent velocity V_S is used as the argument. The control signal $\Delta\gamma = \xi\Delta n$ is formed along the programmed and instantaneous trajectory from the magnitude of the mismatches of g-loads $\Delta n_{bo} = (n_{bo})_{ins} - (n_{bo})_{pr}$ or $\Delta n_{in} = (n_{in})_{ins} - (n_{in})_{pr}$. The coefficient ξ can be constant during the entire descent time or variable along the trajectory. This is determined mainly by the requirements imposed on the accuracy of RV landing. Let us also note that onboard the RV several program functions of n_{bo} or n_{in} in the actual flight can be recorded. Depending on the available initial conditions of RV reentry into the dense atmospheric layers, a particular program ensuring the best satisfaction of the conditions posed is selected. In some cases, in place of g-load mismatches, mismatches as to descent time along the instantaneous and program trajectories can be used.

Systems for Discrete Control of SC Flight Range

An algorithm for a discrete control system can be constructed by using the method of so-called hit trajectories. We will call the trajectories for which the flight of a craft leads to striking the given point hit trajectories, that is, ensures the attainment of the given range with mandatory satisfaction of the g-load constraints:

$$n_{max} \leqslant [n_{max}]_{add}.$$

Let us examine in brief one of the possible control approaches for the discrete correction of trajectory at its characteristic points by using the family of hit trajectories. In synthesizing the control system by this approach, we start from the fact that there are m points along the descent trajectory at which the magnitude of the control force can be changed (by introducing a correcting measurement) in such a way that the perturbations will be compensated. /288

The operating principle of the autonomous control system constructed by using this proposed method is as follows. At the moment the craft attains a fixed value of the system argument $p = p_0$ based on data obtained onboard, some constant angle of roll γ_0 with which the remaining flight is executed is determined. At the moment the argument of the value $p = p_1$ is attained from the results of comparing the value of some functional calculated from onboard measurement data with some precalculated value, a correction

to the initial angle $\gamma_1 = \gamma_0 + \Delta\gamma_1$ is made. At subsequent moments $p = p_2$, p_3, and p_m corrections are made by an analogous method to the values γ_1, γ_2, ..., γ_m, respectively, where the corrections are made so that at each stage transfer to the nearest hit trajectory is effected.

Thus, by selecting the angle γ_0 (at the instant $p = p_0$) the design trajectory to the first approximation is defined. When various kinds of perturbations are acting, the parameters of the actual trajectory will differ from the parameters of the design trajectory. Therefore in subsequent moments of the flight, based on onboard measurements that are continuing, corrections are made to the instantaneous values of the lift-drag ratio of the first, second, ..., and m-th approximations at several characteristic trajectory points (for assigned fixed values of the argument).

This method is called the method of hit trajectories, according to which a system is constructed under the assumption that at each flight stage (from correction to correction) the ship will fly along the nearest hit trajectory for their entire possible totality.

To determine onboard the components of the RV status vector, use is made of the following equation:

$$\ddot{\vec{r}} = \frac{\mu}{r^3}\vec{r} + \vec{a},$$

where $\vec{r}$ and r are the radius-vector of the RV and the vector modulus

$\vec{a}$ is the vector of accelerations due to the action of active forces, $\vec{a} = \frac{\vec{P}}{m}$ over the section along which the retro-engine is firing;

$$\vec{a} \simeq \frac{c_x g \rho}{2} V^* \left[-V^* + \frac{KV^*}{\sqrt{(V_1^*)^2 + (V_3^*)^2}} \left([\bar{h}_2 \times V^*] \cos\gamma + \right.\right.$$

$$\left.\left. + \frac{\sin\gamma}{V^*} [V^* \times [\bar{h}_2 \times V^*]] \right) \right]$$

along the section of aerodynamic deceleration of the RV.

In the last formula $\bar{V}^*$ and V^* are the craft velocity vector relative to the incident flow and the modulus of the relative velocity vector, respectively; and /289

V_1^*, V_2^*, V_3^* are the projections of vector V^* on the axes Oh_1, Oh_2, and Oh_3.

The axes of the inertial rectangular coordinate system coinciding with the sensitivity axes of the accelerometers have the following directions: Oh_1 -- from the Earth's center to the point of design firing of the retro-engine; Oh_3 -- in the orbital plane along the direction of motion; Oh_2 forms a right-handed system with the axes Oh_1 and Oh_3; and h_2 is the unit vector of the Oh_2 axis.

The vector $\overline{V}$ is calculated by the formula $\overline{V}^* = \overline{V} - [\Omega \times r]$ (V is the RV velocity vector).

To allow for the dynamics of motion around the mass center, to the basic system of equations is added the equation

$$J\gamma = M_{con} f(\sigma) \pm M_{drag},$$

where J is the RV moment of inertia
M_{con} is the moment of roll control
M_{drag} is the moment of aerodynamic drag

$$f(\sigma) = \begin{cases} 1 \text{ when } \sigma > \sigma^*; \\ 0 \text{ when } -\sigma^* \leqslant \sigma \leqslant \sigma^*; \\ 1 \text{ when } \sigma < -\sigma^*; \end{cases}$$

σ^* is the sensitivity zone

$$\sigma = T_\gamma(\gamma_{req} - \gamma_{ins}) + T_{\dot\gamma}\dot\gamma$$

(T_γ and $T_{\dot\gamma}$ are constant coefficients; γ_{ins} and γ_{req} are the instantaneous and required roll angles, respectively).

Before the beginning of the descent the coordinates of the required landing accuracy are specified. In the design case the required longitudinal range measured in the plane of a great circle of the Earth's surface is ensured by the design time of firing the retro-engine in orbit and by flight in an atmosphere with selected effective aerodynamic lift-drag ratio K_{eff}. The required departure of the landing point in the lateral direction from the longitudinal plane of motion is ensured by rotating the craft "from side to side" at a specific point along the trajectory (the roll angle changes sign).

The initial values of the status vector component are determined on Earth or onboard and are fed to the onboard digital computer. At the moment of retro-engine firing, the problem of determining the instantaneous status vector with reference to the operation of the retro-engine begins to be solved. The clocks used for obtaining additional data on the trajectory are activated independently of the actual instant of retro-engine firing. After completion of retro-engine burn along the second section of the descent -- in the rarified atmospheric layers -- the accelerometers are switched off and the assumed acceleration from the action of aerodynamic forces is calculated by using the values of the rate at atmospheric density, and thus the systematic and random acceleration errors will not be included in the calculation. But over this same section, with reference to the errors in the generation of the deceleration impulse, a new design value of the roll angle γ_0 is calculated, ensuring that the given longitudinal flight range is attained. /290

During reentry into the dense atmospheric layers (H ~ 100 km), the accelerators are again triggered and their readings are used in solving the first navigational problem. At the moment a small fixed g-load n_ϕ is attained from the readings of the onboard clocks, the true time is compared with the calculated time. The mismatch is the input data for making the first correction, whose goal is to compensate the specifying of the initial values of the status vector components and the perturbations accumulated during a flight in the rarified atmospheric layers.

After the correction is made, the roll angle is established:

$$\gamma_1 = \bar{\gamma}_0 + \Delta\gamma_0;$$

$$\Delta\gamma_0 = a_0(\Delta t - \Delta t_{\text{atm}});$$

$$\Delta t = t_{n_\phi} - \tilde{t}_{n_\phi};$$

$$\Delta t_{\text{atm}} = a_1(\sigma_x\xi - \sigma_{x\,\text{des}})^2 + a_2(\sigma_x\xi - \sigma_{x\,\text{des}});$$

$$a_0 = \left(\frac{\frac{\partial L}{\partial t}}{-\frac{\partial L}{\partial \gamma}} \right)_{n_\phi, \tilde{\gamma}_0},$$

where t_{n_ϕ}, $\tilde{t}_{n_\phi}$ are the flight time at the moment g-load n_ϕ is attained along the true trajectory from the onboard clock readings, and along the design trajectory with roll angle $\tilde{\gamma}_0$, respectively

Δt_{atm} is the time mismatch along the instantaneous and design trajectories caused by deviations in the

aerodynamic coefficients and atmospheric density from the design values

$\sigma_{x\ des}$ is the rated ballistic coefficient

$\xi = \rho/\rho_{des}$ is the ratio of the true density to the design density

a_1, a_2 are coefficients determined onboard, and

$\frac{\partial L}{\partial t}$, $\frac{\partial L}{\partial \gamma}$ are the derivatives of the finite longitudinal flight range with respect to time and roll angle, respectively.

In addition to the change in the roll angle, after the first the first correction to compensate the initial errors in the status vector, the design value of the final longitudinal flight range is changed: /291

$$L_{cal} = L_{f.des} + C(L_1 - L_{f.des}),$$

where $L_{f.des}$ is the rated final longitudinal flight velocity

L_1 is the predicted value of this range calculated for flight with roll angle γ_1, from the moment of the first correction, and

C is the empirical coefficient.

After the first correction is made with reference to the relatively low effectiveness of control in the upper, relatively rarified atmospheric layers, some time ΔT (to the altitude ~ 65 km) the RV flight occurs in the regime of roll angle γ_1 stabilization.

As the time ΔT passes, the periodic solution of the second navigation problem and the institution of corrections on the roll angle begin. The required roll angles are determined on the basis of a prediction of the further motion by numerical integration of the equations of motion.

Using the simple formulas presented below, onboard the aerodynamic lift-drag ratio of the RV and the product of the ballistic coefficient by the ratio of the actual density to the design density are periodically determined. These values are assumed to be constant in solving the prediction problem:

$$K = \frac{n_y}{n_x}; \quad \sigma_x \xi = \frac{2n_x}{\varrho_{des} V^2};$$

$$n_x = \frac{n_1 V_1 + n_2 V_2 + n_3 V_3}{V}; \quad n_y = \sqrt{n_\Sigma^2 - n_x^2};$$

$$n_\Sigma = \sqrt{n_1^2 + n_2^2 + n_3^2}; \quad V = \sqrt{V_1^2 + V_2^2 + V_3^2}.$$

Here n_j and V_j ($j = 1, 2, 3$) are the projections of the vectors of total g-load and of velocity onto the axes of the inertial coordinate system.

To reduce the requirements on the response of the onboard digital computer, the number of calculations of the lead trajectories permitted is limited at the initial stage of descent, increasing as the RV descends and with decrease in the predicted flight time. For a flight time smaller than some value t', only one calculation of the lead trajectories is permitted. The necessary change in the roll angle γ is determined here by using an approximation of the partial derivative $\partial L/\partial\gamma = bV^m$, where b, and are constants found in advance; and V is the flight velocity corresponding to the beginning of the section of the predicted motion. For the flight time $t' \leq t < t''$, a repeated calculation of the lead trajectories is allowed, and so on. This enhances the accuracy of the problem's solution. /292

The following method is used in compensating for the side deviation of the landing point from the calculated site. The lead trajectories are calculated in an accelerated time scale with the roll angle whose sign is opposite the actual value. Here the virtual nondependence of the longitudinal flight range to the landing site on the sign of the roll angle ($\Delta L < 2$ km) is used. The side deflection of the landing point is determined with the assumed change in the sign of the roll angle at the stage of the next correction. After the value of the predicted side deflection of a landing point falls within some allowable neighborhood of "insensitivity" with respect to the calculated point determined by the required landing accuracy, then follows the actual rotation of the RV "from side to side" (the roll angle changes sign). One can be limited to two such rotations in a trajectory.

The interval between the corrections can be either constant or variable and selected on the conditions that the required landing accuracy and the necessary operating speed of the onboard computer are provided.

When this control algorithm is used, a landing accuracy within the limits ~ 5 km can be ensured, when possible perturbations are in effect and with reference to the dynamics of motion with respect to roll and the existing instrumental errors. To achieve this algorithm requires an onboard computer with an operating speed totaling 10,000 simple operations per second (for a three-address command system) and a 17-bit network of operational memory (when numbers are recorded with floating decimal point). Fig. 5.28 shows the results of calculations of the potentialities of compensating side and longitudinal deviations of the landing site through controlling descent for various available lift-to-drag RV ratios. /293

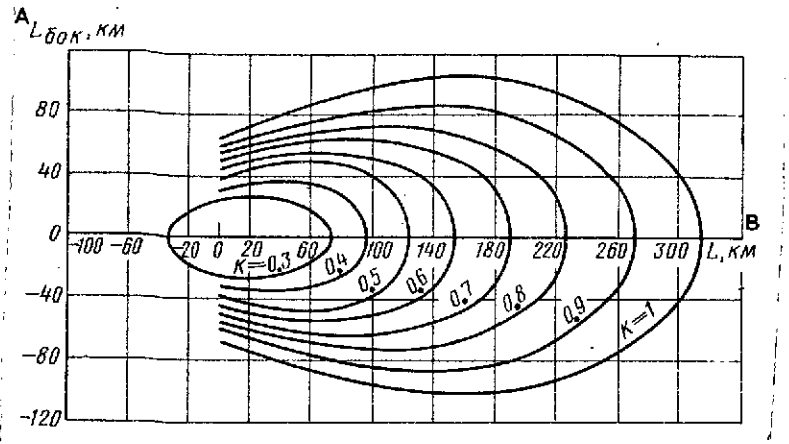

Fig. 5.28. Zone of craft maneuver from altitude H = 40 km
Key: A. L_{si}, km
B. km

5.4. Aerodynamic Method of Descent

In spite of the extremely small aerodynamic forces acting on an AES in flight, they determine the lifetime of the satellite and influence its orbital elements. Naturally the question arises of artificially changing the aerodynamic forces by using special controlling devices installed on the AES to modify its orbital element.

Control of flight and descent into a given region can be achieved by changing the drag P and the lift of the object.

In the case of aerodynamic control, P is artificially varied by changing the braking coefficient $S - c_x F_M/2m$, that is, by changing c_x or F_M, where F_M is the maximum cross-sectional area.

The change in c_x and F_M can be done by rotating the objects about its mass center or using special controlling devices, for example, inflatable balloons or surfaces (plates) that change in area. As an example of an inflatable balloon, we can mention the American relay satellite Echo. In its inflated state this is a sphere 30 m in diameter, and its shell weighs only 40 kg.

The lift can be achieved with special plates. Zenger estimated the lift effectiveness of plates [27, 62].

The ratio of lift to drag (lift-to-drag ratio) of the wing proves to be much less than unity. This indicates the low efficiency of the surface in conditions of free-molecular flow. The lift-to-drag ratio decreases with increase in the Mach number. Thus, maneuvering with the aid of lift is best conducted in the dense atmospheric layers followed by insertion into orbit using a jet impulse.

This section deals principally with landing in the event the retrofiring engine (RV) fails, utilizing aerodynamic control of the AES flight in orbit.

Concept of Aerodynamic Landing

The idea of a landing supported by calculations (the calculations were performed on an M-20 computer) based on the well-known equations of AES motion through numerical integration consists in its most general form of the following. By increasing the braking at the apogee (S_{max}) and by decreasing it at the perigee (S_{min}), an enhanced orbital ellipticity is preserved up to the last orbit. Here, in the event of adequate ellipticity the capture of the satellite by the atmosphere and landing occurs in the region of the lowest flight altitudes, where in fact the landing area must be chosen. /294

To increase the probability of landing in a selected region, during the last orbits the directly opposite regime of aerodynamic braking S_{max} is switched on at the perigee, and S_{min} at the apogee ("descent" regime). This braking program ensures at the end of the flight large velocity losses as the satellite passes through the low altitude region and increases the probability of AES capture in the perigee region.

When the orbit does not have sufficient ellipticity, before the "descent" regime the S_{min} regime is switched on, which enables the ship to be stopped in orbit down to the lowest altitudes, enhancing the effectiveness of the subsequent "descent" regime.

Selection of the orbit for landing occurring across a given region is carried out by means of selection of the duration of action of the various regimes (the mean braking coefficieng S_{av}, S_{max}, and S_{min}) that modify the satellite lifetime.

Programmed braking (change in S) can be used to displace the low altitude region relative to the given region of landing latitudes, which can ensure landing of the object precisely in these latitudes.

To effect this braking program using the orientation system (change in S), the satellite must have a different braking coefficient S when the angle of attack is being varied.

The coefficient $f = S_{max}/S_{min}$ varies within the limits 1, 2-6 for present-day spacecraft-satellites. By special devices ([gas] bottles, shields, and so on) this coefficient can be significantly increased.

Setting Up an Aerodynamic Braking Program

As an example, let us calculate aerodynamic control for an orbit with apogee altitude h_α = 217 km and perigee altitude h_π = = 180 km, T = 88.17 min, i = 65°, and for a lifetime of about four days.

The values of the coefficient S adopted in the calculation are given in Table 5.1.

TABLE 5.1

S_{av}	S_{max}	S_{min}	f
0.0132	0.0173	0.0107	1.62

The value S_{av} = 0.0132 corresponds approximately to the equiprobable orientation of an object in space.

Aerodynamic braking S_{max} must be carried out in a specific region of the apogee. To select this region descent trajectories were calculated on a computer, showing that the landing of the object during braking (S_{max}) in the range of true anomaly θ=120° to 240° ($\Delta\theta$= 120°) occurred within the latitudes of the USSR. The effect of changing the position of the deceleration region in the apogee area (θ= 160-280°) to the position of the apogee can be seen in Fig. 5.29 (T_{cr} is the minimum or critical period). /295

Calculations showed that in the variations (S_{max} regime at the apogee, S_{min} at the perigee) for f = 1.62, the eccentricity e was increased before the descent by about 10-12 percent.

A series of calculations were made for f = 6 (when S_{max} = = 0.0642 and S_{min} = 0.0107). The calculations showed that at this f value the orbital ellipticity can be increased in nearly to a descent, the perigee altitude B° can be strongly influenced (Fig. 5.29), and the lifetime can be markedly shortened (47 hr). This assists in confidently selecting the longitude of the landing region.

The variation in orbital parameters without artificial braking is shown in Fig. 5.30.

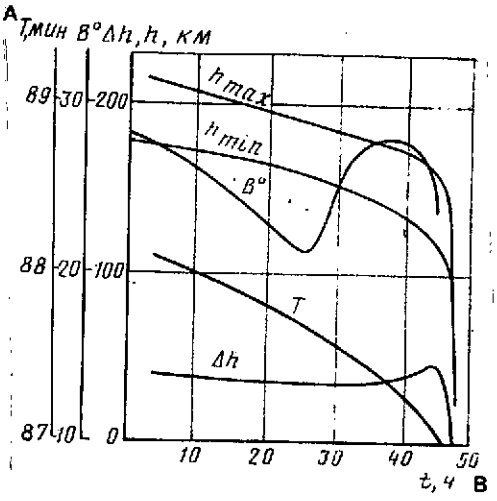

Fig. 5.29. Effect of artificial braking on orbit when f = 6 (braking was carried out at the angles $\theta = 160-280°$ after a day of flight with S_{av} over two days before the descent):
$t = 47^h, 0$
$B_{l.p} = 63°48'$
$L_{l.p} = 112°46'$
$T_{cr} = 86^m, 76$
Key: A. T, min B° Δh, h, km
B. t, hr

To clarify the distribution of the descent points, in the series of calculations for the selected orbit (when f = 1.62) relative to the position of the orbital apogee, a graph was plotted (Fig. 5.31). In it the latitude of the landing points were laid out along the X-axis.

From the graph it is clear that the descent of the AES does not occur at the apogee. Thus, the probability of the satellite entering the apogee region for orbits with the assumed ellipticity and greater, when aerodynamic control was used, is nearly zero.

In the case of landing by means of aerodynamic braking, it is very important to predict the lifetime in the last orbits. To investigate the possibility of determining from the period of revolution the lifetime for different S in the last orbits, calculations were performed on a computer. The results are in Fig. 5.32. In this graph the time remaining prior to descent /296 is plotted along the X-axis, and the period of revolution -- along the Y-axis.

These graphs show that the lifetime Δt depends nonlinearly on the period of revolution and also on the braking coefficient S and the preceding braking program. So by knowing the braking program and S, we can determine Δt from the period of revolution to an accuracy corresponding to the errors of the atmospheric density.

The errors in the atmospheric density and the coefficient in the last orbit, given the condition that experimental data were obtained on the descent of satellites, can be of the order of 15-20 percent, that is, for example, over five orbits before descent the prediction accuracy will be one orbit, which is quite sufficient when $f \geq 6$. When f = 1.62, this accuracy already markedly increases the probability of landing within the USSR (See Fig. 5.30).

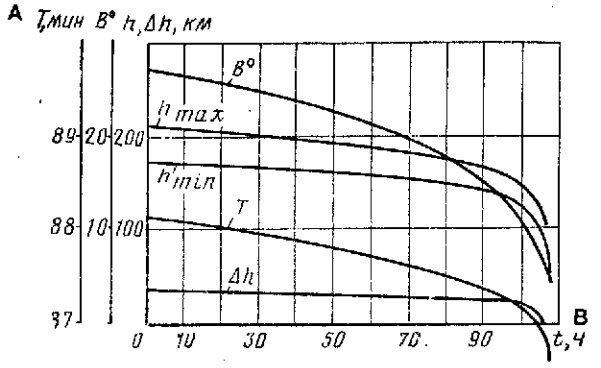

Fig. 5.30. Variation in nominal orbital parameters with respect to flight time (f = 1.62; S_{av} = = const up to descent; t = = 107^h57^m; $B_{l.p} = -34°34'$; $L_{l.p} \approx 176°38'$; and $T_{cr} = 86^m82$)
Key: A. T, min B° h, Δh, km
B. t, hr

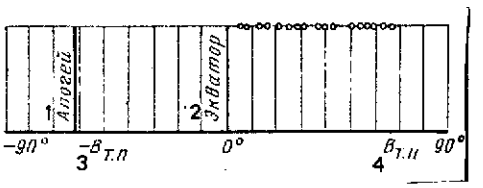

Fig. 5.31. Latitude of landing points when aerodynamic control was used (the points are indicated)
Key: 1. Apogee
2. Equator
3. $-B_{l.p}$
4. $B_{l.p}$

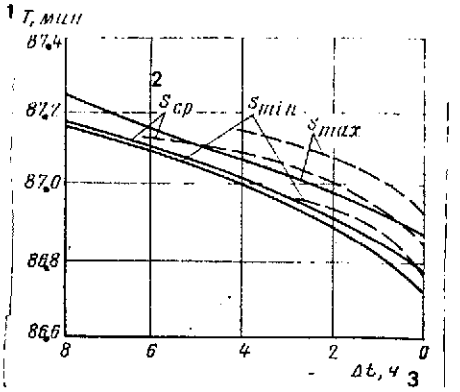

Fig. 5.32. Period of revolution T as a function of lifetime of satellite Δt prior to descent after a flight of three days with S_{av} [as indicated]:
- - - Flight with S_{max}, S_{av}, or S_{min}
——— Flight for 0.5 day with variations in S, further with S_{max}, S_{av}, or S_{min}
Key: 1. T, min
2. S_{av}
3. Δt, hr

/297

One of the variants of this program is shown in Table 5.2 (the time is indicated from the launch moment).

In setting up the program, it proved possible for the selected orbit (in view of the adequate preservation of ellipticity for S_{av}) not to resort to the S_{max} regime at the apogee and the S_{min} regime at the perigee. This cut down on the number of needed maneuvers.

Long-Life AES

It is useful for manned long-life AES to provide for a special craft configuration and braking device.

TABLE 5.2

Firing time			Remark
S_{av}	S_{max}	S_{min}	
0^h20^m			S_{av} regime
	71^h41^m		S_{max} regime
		92^h00^m	S_{min} regime
	99^h07^m	99^h35^m	
	100^h34^m	101^h02^m	Descent regime: S_{max} in ascending orbits in the latitude range 60° S. lat. to 60° N. lat.; S_{min} for the rest of the orbit
	102^h01^m		Region of landing point: latitude $B_{l.p}$ = 50° N. lat. longitude $L_{l.p}$ = 50° E. long.

The configuration of the above-considered satellite provides for minimum S for orbital flight with nozzle (or landing module) forward and a maximum braking coefficient for sideward flight.

The AES configuration must ensure for sideward and noseward-forward flight the coincidence of the mass center and the pressure center. This must prevent perturbing aerodynamic moments and materially facilitate operating the orientation system.

When there is a simultaneous breakdown of the orientation system and the RFE [retro-firing engine], it is not possible to achieve a landing using the above-presented program of aerodynamic braking employing a change in the object's orientation. To achieve landing even in this case within the USSR, use is made of the aerodynamic braking technique employing special [gas] braking bottles (spherical or some other shape), and also other braking devices (shields, special plates, and so on).

To brake a satellite with S_{av} = 0.0132, as shown by calculations, the diameter of the spherical type bottle must not be more than 10-20 m [sic], and the weight -- about 30 kg. /298

Braking for the purpose of landing is best carried out during ascending orbits, since they have the greatest extent over the territory of the USSR (for example, the first, second, and third orbit of each day).

The calculation of landing using braking spherical bottles was carried out as applied to the above-considered orbit for a satellite with a braking coefficient exceeding $S_{av} = 0.0132$ by 5, 10, 20, and 50 times.

The bottles are ejected over the geographical latitudes B_{ej} = 50° S. lat.; 0-30° N. lat. during the first, fifth, and tenth orbits before the descent, calculated without reference to the braking bottle.

The calculations showed that an increase in $S > S_{av}$ for the object and orbit considered is inexpedient.

For a prediction accuracy up to the first orbit, the ejection of bottles increasing the coefficient S^*_{av} 20 times entirely ensures landing within the latitudes of the USSR.

CHAPTER VI /299

SOME PROBLEMS IN SATELLITE ORIENTATION

To perform many functions with an artificial satellite, a definite orientation of its axes in space is necessary. The descent of a cosmonaut to Earth after a flight in orbit would be impossible without the appropriate orientation of the axis of the power plant during its firing time. Observation of the Earth's surface and establishing informative radio communication is also difficult without orientation toward the Earth of some axis associated with the spacecraft. Finally, passing to another given orbit, arrival in the vicinity of a satellite station, and docking are all functions that require orientation and stabilization of the AES which differ in accuracy and with respect to other characteristics.

Satellite orientation and stabilization systems can be divided into passive and active.

Methods of passive orientation and stabilization are of interest in that they are based on using several physical phenomena existing in space and do not require the consumption of [reaction] mass to sustain a stabilized attitude. These methods can be based on the moments induced due to change in a gravity field with altitude, and also the light pressure force or the aerodynamic force. The moments are very small and it is extremely complicated, in engineering terms, to achieve this stabilization.

Methods of active orientation are based on control moments produced by some control system. Here two of the three main functions of any satellite control system are most simply executed: rotating the craft about its mass center and sustaining the given orientation relative to any fixed or mobile axes [55].

K. E. Tsilkovskiy proposed two methods for rotation about the mass center: producing reaction thrust whose line of action does not pass through the mass center, and using flywheels inducing a reaction moment when they are deployed with a specific angular acceleration.

Gyroscopes (inertial system), photocells within whose field of view selected celestial bodies are kept (Sun, large stars, and so on), infrared detectors aimed at the Earth's horizon, and so on can be used as sensitive elements of active orientation systems. /300

6.1. General Equations of Motion About Mass Center

Let us assume that an arbitrary coordinate system $O'\xi\eta\zeta$ was chosen with its origin at the satellite mass center. Then the coordinates of any point in the principal reference system Oxyz can be represented in the form

$$\begin{aligned} x &= x_{0'} + a_{11}\xi + a_{12}\eta + a_{12}\zeta; \\ y &= y_{0'} + a_{21}\xi + a_{22}\eta + a_{23}\zeta; \\ z &= z_{0'} + a_{31}\xi + a_{32}\eta + a_{33}\zeta, \end{aligned}$$

where $x_{0'}, y_{0'}, z_{0'}$ are the coordinates of the satellite mass center in the principal system

ξ, η, ζ are the coordinates of the selected point in space in an auxiliary system (local) with its origin at the satellite mass center; and

a_{jk} $(j, k = 1, 2, 3)$ are the direction cosines of the axes of the auxiliary system relative to the principal system (the subscript "j" refers to the principal system, and "k" -- to the auxiliary system).

From mechanics we know that the position of a system of rectangular coordinates relative to another is wholly determined by the coordinates of the origin of the second system and by three angles of rotation, that is, when both origins are brought into coincidence at the same point any given position of the second system can be obtained by three rotations in three different planes.

It is most convenient to carry out these rotations in the Euler's scheme. The first rotation is effected about the axis Oz (counterclockwise, like the others). Here the Ox and Oy axes are rotated in the Oxy plane by the angle Ω (Fig. 6.1). The Ox axis will occupy the new position Ok, and the Oy axis -- the position Oy'. The second rotation is effected about the new axis Ok, resulting in the axes Oy' and Oz being deviated by the angle i. The Oz axis will occupy the position $O\zeta$, and the Oy' axis -- the position Oy".

The last, third, rotation is performed about the just-obtained $O\zeta$ axis. Here the Ok and Oy" axes will be displaced in a plane perpendicular to $O\zeta$, by the angle ϑ in the positions $O\xi$ and On, respectively. Thus, after three rotations of the coordinate axes Oxyz, a new coordinate system $O\xi\eta\zeta$ is obtained, whose position /301

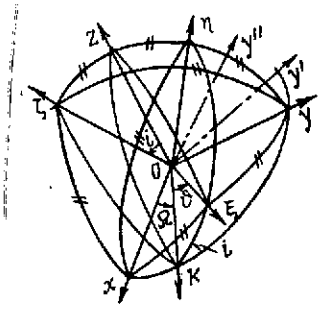

Fig. 6.1. For deriving the relationship between Euler's angles and the direction cosines

relative to the initial system is wholly determined by the three angles Ω, i, ϑ.

The angle Ω is called the angle of precession, the angle i -- the angle of nutation, and ϑ -- the angle of intrinsic rotation (Euler's angles).

According to the theorem on cosines the sides in a spherical triangle (the cosine of a side is equal to the product of the cosines of the two other sides plus the product of the sines of these sides by the cosine of the angle between them) of an expression for the direction cosines will be of the form:

$$
\left.
\begin{aligned}
a_{11} &= \cos\vartheta\cos\Omega + \sin\vartheta\sin\Omega\cos(180^\circ - i);\\
a_{21} &= \cos\vartheta\cos(90^\circ - \Omega) + \sin\vartheta\sin(90^\circ - \Omega)\cos i;\\
a_{31} &= \cos\vartheta\cos 90^\circ + \sin\vartheta\sin 90^\circ\cos(90^\circ - i);\\
a_{12} &= \cos(90^\circ + \vartheta)\cos\Omega + \sin(90^\circ + \vartheta)\sin\Omega\cos(180^\circ - i);\\
a_{22} &= \cos(90^\circ + \vartheta)\cos(90^\circ - \Omega) + \sin(90^\circ + \vartheta)\sin(90^\circ - \Omega)\cos i;\\
a_{32} &= \cos(90^\circ + \vartheta)\cos 90^\circ + \sin(90^\circ + \vartheta)\sin 90^\circ\cos(90^\circ - i);\\
a_{13} &= \cos 90^\circ\cos\Omega + \sin 90^\circ\sin\Omega\cos(90^\circ - i);\\
a_{23} &= \cos 90^\circ\cos(90^\circ - \Omega) + \sin 90^\circ\sin(90^\circ - \Omega)\cos(90^\circ + i);\\
a_{33} &= \cos 90^\circ\cos 90^\circ + \sin 90^\circ\sin 90^\circ\cos i.
\end{aligned}
\right\}
$$

After obvious simplifications we get

$$
\left.
\begin{aligned}
a_{11} &= \cos\vartheta\cos\Omega - \sin\vartheta\sin\Omega\cos i;\\
a_{21} &= \cos\vartheta\sin\Omega + \sin\vartheta\cos\Omega\cos i;\\
a_{31} &= \sin\vartheta\sin i;\\
a_{12} &= -\sin\vartheta\cos\Omega - \cos\vartheta\sin\Omega\cos i;\\
a_{22} &= -\sin\vartheta\sin\Omega + \cos\vartheta\cos\Omega\cos i;\\
a_{32} &= \cos\vartheta\sin i; \quad a_{13} = \sin\Omega\sin i;\\
a_{23} &= -\cos\Omega\sin i; \quad a_{33} = \cos i.
\end{aligned}
\right\} \qquad (6.1)
$$

We can formulate the following rule to set up system (6.1): a direction cosine a_{jk} is found by using Table 6.1 as the product of the cosine of the angle of intrinsic rotation ϑ (for k = 1) or 90° + ϑ (for k = 2) or the angle 90° (for k = 3) by the

cosine of the angle of precession Ω (for j = 1) or 90° - Ω (for j = 2), or 90° (for j = 3) plus the product of the sines of the same angles by the cosine of the angle of nutation i minus 180°, or simply i, or i - 90°. The angles associated with ϑ, are taken from the k column at the j and k rows of the column with respect to the numerical value of the subscript k, while the angles associated with Ω and i are taken from the corresponding j column in the j and k rows of the column with respect to the numerical value of the subscript j.

TABLE 6.1

/302

j, k	k	j	j
0	1	2	3
1 2 3	ϑ $90°+\vartheta$ 90°	Ω $90°-\Omega$ 90°	$i-180°$ i $i-90°$

Remark. When k = 3, add the angle 90° to the third column. Thus, to obtain, for example, the direction cosine a_{12} (j = = 1, k = 2), let us take for k = 2 the angle $90°+\vartheta$, from the second row of the first column, for j = 1 -- the angle Ω from the first row of the second column, and from the first row of the third column let us take the angle i - 180°. Then, by using the cosine theorem we get

$$a_{12}=\cos(90°+\vartheta)\cos\Omega+\sin(90°+\vartheta)\sin\Omega\cos(i-180°)=-\sin\vartheta\cos\Omega-\cos\vartheta\sin\Omega\cos i,$$

which wholly coincides with Eq. (6.1).

If the direction cosine has the subscript k = 3, then we act in accordance with the remark to Table 6.1. For example, for a_{23}, from the third row of the first column we take the angle + 90°, from the second row of the second column 90° - Ω, and from the second row of the third column i + 90° (with reference to the addition of the angle 90°). Using the theorem of cosines, we get

$$a_{23}=\cos 90°\cos(90°-\Omega)+\sin 90°\sin(90°-\Omega)\cos(i+90°)=-\cos\Omega\sin i.$$

Thus, this mnemonic rule enables us, without resorting to mathematical derivation, to determine with the aid of Table 6.1 the direction cosines expressed in terms of Euler's angles.

The position of the axes of the coordinate system $O'\xi\eta\zeta$ relative to the principal system Oxyz can be assigned not mandtorily by Euler's angles. However, any three angles can be readily replaced with Euler's angles.

Often the table of direction cosines is written in matrical form. Then the expression for transforming from the coordinate system $O'\xi\eta\zeta$ to the system Oxyz proves to be the following:

$$\begin{bmatrix} x-x_{0'} \\ y-y_{0'} \\ z-z_{0'} \end{bmatrix} = [a_{jk}] \begin{bmatrix} \xi \\ \eta \\ \zeta \end{bmatrix},$$

where the matrix is

$$[a_{jk}] = \begin{bmatrix} a_{11}a_{12}a_{13} \\ a_{21}a_{22}a_{23} \\ a_{31}a_{32}a_{33} \end{bmatrix}.$$

This abridged expression shows that to obtain, for example, the increment $y - y_{0'}$, we must take the coefficients a_{2k} $(k = 1, 2, 3)$, /303
multiply them successively by ξ, η, and ζ, and add the results, that is,

$$y - y_{0'} = a_{21}\xi + a_{22}\eta + a_{23}\zeta.$$

If it is necessary, in contrast, to express the coordinates ξ, η, and ζ in terms of $(x - x_{0'})$, $(y - y_{0'})$, and $(z - z_{0'})$, then we write

$$\begin{bmatrix} \xi \\ \eta \\ \zeta \end{bmatrix} = [a_{kj}] \begin{bmatrix} x-x_{0'} \\ y-y_{0'} \\ z-z_{0'} \end{bmatrix},$$

where $[a_{kj}]$ is the matrix transposed with respect to $[a_{jk}]$:

$$[a_{kj}] \begin{bmatrix} a_{11}a_{21}a_{31} \\ a_{12}a_{22}a_{32} \\ a_{13}a_{23}a_{33} \end{bmatrix}.$$

Now let us look at the motion of a satellite about the mass center when acted on by moments from small forces operative during the orbit. As was explained, up to altitudes 500-600 km aerodynamic forces are the small forces. At greater altitudes moments from the gravitational force and the light pressure force basically begin to take effect.

As we know, the motion of a solid about the mass center can be described by these equations:

$$\left.\begin{aligned} A\dot{p} + (C - B)qr &= M_x; \\ B\dot{q} + (A - C)rp &= M_y; \\ C\dot{r} + (B - A)pq &= M_z. \end{aligned}\right\} \qquad (6.2)$$

where A, B, C are the principal central moments of inertia
p, q, r are the projections of the instantaneous angular velocity onto the axes Ox, Oy, and Oz (the coordinate system is a bound system, the axes Ox, Oy, and Oz are directed along the principal central axes of inertia of the satellite); and
M_x, M_y, M_z are the projections of the perturbing moment onto the axes Ox, Oy, and Oz.

The equations of motion about the mass center (Euler's equations) are derived on the basis of the familiar theorem from mechanics dealing with kinetic moment:

$$\frac{d\overline{K}}{dt} = \overline{M},$$

where $\overline{K}$ is the vector of the kinetic moment, and
$\overline{M}$ is the vector of the principal moment of the external forces.

Depending on which forces we are examining, the right-hand sides of the equations (of system (6.2)) will differ. The appearance of the left-hand sides depends on the design features /304

of the satellite. Thus, when the two equatorial moments of inertia (A = B) are equal, characteristic of most satellites (dynamic symmetry), the equations become

$$A\dot{p}+(C-A)qr=M_x;$$
$$A\dot{q}+(A-C)pr=M_y;$$
$$C\dot{r}=M_z.$$

The system of equations of satellite motion about the mass center can be solved only in several particular cases in which the forces are assigned. However, if the effective forces are small, we can use the methods of perturbation theory [13, 14]. Both systems are integrated to completion if the motion is unperturbed, that is, if there are zeros in the right-hand sides (Euler's case). By using the method of variations of constants of integration (similar to how we derived the equations for osculating elements), we can obtain quite simple and exact expressions for describing the principal properties of perturbed motion.

The following principal conclusion was obtained in [13].

If a satellite is moving under the influence of aerodynamic and gravitational perturbing forces, its motion can be decomposed into unperturbed motion about the vector of the kinetic moment (regular precession for the satellite with dynamic symmetry) and secular motion of the kinetic moment vector as such. This secular motion occurs about a time-varying (due to the displacement of the orbital plane -- the precession of the nodes) direction that is close to the direction of the tangent to the orbit at the perigee if the influence of the aerodynamic forces is greater than the influence of the gravitational forces, that is, for low orbits, and in a direction close to the direction of the normal to the orbital plane if gravitational forces predominate.

Motion relative to the precessing orbit differs little from motion relative to a fixed orbit.

At high altitudes (above 500 km) the moments appearing due to the gradient of the Earth's gravity field as a function of satellite design features can be greater or lesser than the moments arising from light pressure forces. So both kinds of forces must be examined jointly, as was done in [17].

6.2. Active Stabilization of AES Using Flywheels

For oriented satellites revolving about the Earth for a more or less prolonged time, the problem of mass flow of reaction mass in control is fundamental. Accordingly, let us look at the principle of control using flywheels. The use of flywheels for /305
an extended time cannot entirely obviate the necessity of consuming [reaction] mass, since given the continually acting external moments the angular rate of flywheel rotation will steadily rise. However this mass flow (through the jet nozzles), whose purpose is to reduce to zero the accumulating angular rate of the flywheels, will be many times smaller than when just nozzles are used (by several orders of magnitude).

We will assume[1] that n statically and dynamically balanced reaction flywheels have been installed in the spacecraft hull with arbitrarily oriented suspension axes relative to some fixed rectangular coordinate system Oxyz with its origin at the satellite mass center.

Let us introduce the notation:

a_{ix}, a_{iy}, a_{iz} are the direction cosines of the suspension axes (with the positive direction of each of the axes determined in advance)

$\bar{\omega}_i$ is the vector of the angular rate of the i-th flywheel, and

$\omega_i a_{ix}, \omega_i a_{iy}, \omega_i a_{iz}$ are the projections of the vector onto the axes Ox, Oy, and Oz.

The kinetic moment of the system in relative motion reduced to the point O will be

$$\bar{K} = \int [\bar{r} \times \bar{v}]\, dm,$$

where $\bar{v}$ is the vector of the velocity of mass element dm relative to the inertial axes of the coordinates, and
$\bar{r}$ is the radius-vector of mass dm (integration is carried out over the entire system S).

The vector $\bar{K}$ can be represented as the sum of the kinetic moment obtained from rotation of the spacecraft hull together

---

[1] The theory of control using flywheels was formulated by B. V. Raushenbakh and Ye. N. Tokar' in the article [55].

with the flywheels assumed to be fixed (translational velocity) and the intrinsic rotation of the flywheels relative to the axes Oxzy:

$$\bar{K}=\int_{s'}[\bar{r}\times\bar{v}]\,dm+\sum_{i=1}^{n}\int_{\mu_i}[\bar{r}\times\bar{v}_{\text{tr}}]\,dm+\sum_{i=1}^{n}\int_{\mu_i}[\bar{r}\times\bar{v}_{\text{rel}}]\,dm=$$

$$=\int_{s}[\bar{r}\times[\bar{\omega}\times\bar{r}]]\,dm+\sum_{i=1}^{n}\int_{\mu_i}[\bar{r}\times\bar{v}_{\text{rel}}]\,dm.$$

In this expression, the velocities of hull points and the translational velocities of the flywheels were replaced according to Euler's formula $\bar{v}=\bar{\omega}\times\bar{r}$.

Taking as the centers of reduction for the flywheels their mass centers, we can write /306

$$\bar{K}_{\text{rel } i}=\omega_i I_i,$$

where I_i are the axial moments of inertia of the flywheels ($i = 1, 2, \ldots, n$).

Since the velocities of the flywheel mass centers relative to the system Oxyz are zero, their kinetic moments do not depend on the center of reduction. So by adopting the point O as the center of reduction we will have

$$\bar{K}=\int_{s}[\bar{r}\times[\bar{\omega}\times\bar{r}]]\,dm+\sum_{i=1}^{n}\bar{\omega}_i I_i.$$

Obviously, the first term will be the kinetic moment of the satellite when the flywheels are halted.

Let us orient the axes Ox, Oy, and Oz along the principal central axes of inertia of the imaginary solid body thus obtained. The moments of inertia of this body about these axes we will denote by A, B, and C, respectively. Then we get for the first term

$$\int_{i}[\bar{r}\times[\bar{\omega}\times\bar{r}]]\,dm=Ap\bar{e}_x+Bq\bar{e}_y+Cr\bar{e}_z,$$

where $\bar{e}_x$, $\bar{e}_y$, $\bar{e}_z$ are the unit vectors along the axes, and
p, q, r are the projections of the angular rate of the system onto the same axes.

The second term can be written as

$$\sum_{i=1}^{n} \bar{\omega}_i I_i = \bar{e}_x \sum_{i=1}^{n} \omega_i a_{ix} I_i + \bar{e}_y \sum_{i=1}^{n} \omega_i a_{iy} I_i + \bar{e}_z \sum_{i=1}^{n} \omega_i a_{iz} I_i.$$

Referring to these expressions, we get

$$\begin{aligned} \bar{K} = &\left(Ap + \sum_{i=1}^{n} \omega_i a_{ix} I_i \right) \bar{e}_x + \left(Bq + \sum_{i=1}^{n} \omega_i a_{iy} I_i \right) \bar{e}_y + \\ &+ \left(C\bar{r} + \sum_{i=1}^{n} \omega_i a_{iz} I_i \right) \bar{e}_z \end{aligned} \qquad (6.3)$$

Applying the theorem of the kinetic moment of the system $\bar{M} = d\bar{k}/dt$ and converting to projections, we get the following equations of motion about the mass center of the flywheel system: /307

$$\left.\begin{aligned} &A\dot{p} + \sum_{i=1}^{n} \dot{\omega}_i a_{ix} I_i + q\left(Cr + \sum_{i=1}^{n} \omega_i a_{iz} I_i \right) - \\ &- r\left(Bq + \sum \omega_i a_{iy} I_i \right) = M_{px} + M_{rx}; \\ &B\dot{q} + \sum_{i=1}^{n} \dot{\omega}_i a_{iy} I_i + r\left(Ap + \sum_{i=1}^{n} \omega_i a_{ix} I_i \right) - \\ &- p\left(Cr + \sum_{i=1}^{n} \omega_i a_{iz} I_i \right) = M_{py} + M_{ry}; \\ &C\dot{r} + \sum_{i=1}^{n} \dot{\omega}_i a_{iz} I_i + p\left(Bq + \sum_{i=1}^{n} \omega_i a_{iy} I_i \right) - \\ &- q\left(Ap + \sum_{i=1}^{h} \omega_i a_{ix} I_i \right) = M_{pz} + M_{rz}, \end{aligned}\right\} \qquad (6.4)$$

where $M_{p\,x}$, $M_{p\,y}$, $M_{p\,z}$ are the projections of the perturbing moment onto the axes Ox, Oy, and Oz, and $M_{r\,x}$, $M_{r\,y}$, $M_{r\,z}$ are the projections of the reaction moments from the nozzles (we neglect the mass flow of the gas).

Let us transform this system as follows (we omit the subscript of summation i from 1 to n):

$$A\dot{p}-\sum a_{ix}(a_{ix}\dot{p}+a_{iy}\dot{q}+a_{iz}\dot{r})I_i+\sum a_{ix}(\dot{\omega}_i+a_{ix}\dot{p}+$$
$$+a_{iy}\dot{q}+a_{iz}\dot{r})I_i+qr(C-B)=M_{px}+M_{rx}-q\sum\omega_i a_{iz}I_i+$$
$$+r\sum\omega_i a_{iy}I_i;$$
$$B\dot{q}-\sum a_{iy}(a_{ix}\dot{p}+a_{iy}\dot{q}+a_{iz}\dot{r})I_i+\sum a_{iy}(\dot{\omega}_i+a_{ix}\dot{p}+a_{iy}\dot{q}+$$
$$+a_{iz}\dot{r})I_i+rp(A-C)=M_{py}+M_{ry}-r\sum\omega_i a_{ix}I_i+p\sum\omega_i a_{iz}I_i;$$
$$C\dot{r}-\sum a_{iz}(a_{ix}\dot{p}+a_{iy}\dot{q}+a_{iz}\dot{r})I_i+\sum a_{iz}(\dot{\omega}_i+a_{ix}\dot{p}+a_{iy}\dot{q}+$$
$$+a_{iz}\dot{r})I_i+pq(B-A)=M_{pz}+M_{rz}-p\sum\omega_i a_{iy}I_i+$$
$$+q\sum\omega_i a_{ix}I_i.$$

The third terms in the left-hand sides of the resulting equations are the sums of the projections onto the axes Ox, Oy, and Oz of the derivatives with respect to the projections of the total angular rate of the flywheels onto their suspension axes, multiplied by the moment of inertia I_i. /308

By applying Euler's dynamic equations individually to the flywheels, the summands in the left-hand side can be transformed thusly:

$$\sum a_{ix}(\dot{\omega}_i+a_{ix}\dot{p}+a_{iy}\dot{q}+a_{iz}\dot{r})I_i=\sum a_{ix}(M'_{ai}+M'_{ci})=$$
$$=-\sum a_{ix}(M_{ai}+M_{ci}),$$ and so on ,

where

M'_{ai} is the active moment of the engine rotating the flywheel

M_{ai} is the opposite moment applied to the hull

M'_{ci} is the moment of drag on the flywheel shaft

M_{ci} is the opposite moment applied to the hull, and

M'_{ai}, M_{ai}, M'_{ci}, M_{ci} are the algebraic quantities calculated with reference to the positive direction from the flywheel.

By converting to the quantities M_{ai} and M_{ci}, we finally get

$$\left.\begin{aligned}
&A\dot{p}-\sum a_{ix}(a_{ix}\dot{p}+a_{iy}\dot{q}+a_{iz}\dot{r})\,I_i+qr(C-B)=M_{px}+\\
&+M_{rx}+\sum a_{ix}(M_{ai}+M_{ci})-q\sum\omega_i a_{iz}I_i+r\sum\omega_i a_{iy}I_i;\\
&B\dot{q}-\sum a_{iy}(a_{ix}\dot{q}+a_{iy}\dot{q}+a_{iz}\dot{r})\,I_i+rp(A-C)=M_{py}+\\
&+M_{ry}+\sum a_{iy}(M_{ai}+M_{ci})-r\sum\omega_i a_{ix}I_i+p\sum\omega_i a_{iz}I_i;\\
&C\dot{r}-\sum a_{iz}(a_{ix}\dot{p}+a_{iy}\dot{q}+a_{iz}\dot{r})\,I_i+pq(B-A)=M_{pz}+\\
&+M_{rz}+\sum a_{iz}(M_{ai}+M_{ci})-p\sum\omega_i a_{iy}I_i+q\sum\omega_i a_{ix}I_i.
\end{aligned}\right\}\qquad(6.5)$$

The last two summands in the right-hand sides of the equations are the projections of the gyroscopic moments (onto the axes indicated in the subscripts applied to the satellite. They are caused by the forced precession of the flywheels. The terms $M_{r\,x}$, $\Sigma a_{i\,x}$-M_{ai}, and so on are the projections of the control moments generated by the actuators.

Let us examine the case of three flywheels [55] with axis of rotation coinciding with the direction along the axes Ox, Oy, and Oz. For the direction cosines we will have

$$\begin{bmatrix} a_{1x}a_{1y}a_{1z}\\ a_{2x}a_{2y}a_{2z}\\ a_{3x}a_{3y}a_{3z}\end{bmatrix}=\begin{bmatrix}1&0&0\\0&1&0\\0&0&1\end{bmatrix}.$$

We denote /309

$$\begin{aligned}
&\omega_1=\omega_x;\quad \omega_2=\omega_y;\quad \omega_3=\omega_z;\\
&M_{a1}=M_{ax};\quad M_{a2}=M_{ay};\quad M_{a3}=M_{az};\\
&M_{c1}=M_{cx};\quad M_{c2}=M_{cy};\quad M_{c3}=M_{cz}.
\end{aligned}$$

In addition, let us set $I'_1 = I_2 = I_3 = I$. The equations of satellite motion about its mass center (6.5) become:

$$
\begin{aligned}
&(A-I)\dot{p}+(C-B)qr=\\
&=M_{px}+M_{rx}+M_{ax}+M_{cx}-\omega_z q I+\omega_y r I;\\
&(B-I)\dot{q}+(A-C)rp=\\
&=M_{py}+M_{ry}+M_{ay}+M_{cy}-\omega_x r I+\omega_z p I;\\
&(C-I)\dot{r}+(B-A)pq=\\
&=M_{pz}+M_{rz}+M_{az}+M_{cz}-\omega_y p I+\omega_x q I.
\end{aligned}
\qquad (6.6)
$$

The right-hand sides of these equations coincide with the right-hand sides of Euler's equations written for the spacecraft hull. They contain projections of all moments that are external with respect to the hull (the moments $\overline{M}_p$, $\overline{M}_r$, $\overline{M}_{ai}$, and $\overline{M}_{ci}$, and the gyroscopic moments of the flywheels).

In contrast to Euler's equations, the axes Ox, Oy, and Oz with respect to the satellite hull are not the principal and central axes of inertia, and the quantities A, B, and C, where the differences A - I, B - I, and C - I, to which we can readily convert, do not coincide with the moments of inertia of the spacecraft hull about these axes.

For motion along an orbit, the perturbing moments acting on the satellite are very small and in many cases I can in general be neglected. For example, these moments include the regimes of programmed turns [55].

Before proceeding to analyzing these regimes, let us introduce the angles that associate the running [mobile] coordinate system Oxyz with the selected inertial system of reference $Ox_0y_0z_0$.

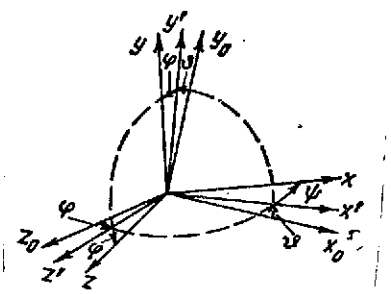

Fig. 6.2. Scheme of rotation of the coordinate system by the angles ϑ, ψ and ϕ

Let us determine the angle ϑ as the angle between Ox', the projection of the Ox axis onto the plane x_0Oy_0, and the Ox_0 axis. Let us define ψ as the angle between Ox' and the Ox axis. The angle ϕ will be between the Oy axis and the line of intersection of the planes x_0Oy_0 and yOz (Fig. 6.2).

This choice of angles relating both coordinate systems,

compared to the ordinary Euler angles in the case considered, is more advantageous since it enables us to get simple equations of motion of a body for small angles of rotation. /310

Table 6.2 gives the direction cosines for the axes associated with the satellite, and the inertial axes.

TABLE 6.2

Axes of inertial system	Axes of bound system		
	x	y	z
x_0	$\cos\psi\cos\vartheta$	$-\cos\varphi\sin\vartheta + \sin\varphi\sin\psi\cos\vartheta$	$\cos\varphi\sin\psi\cos\vartheta + \sin\varphi\sin\vartheta$
y_0	$\cos\psi\sin\vartheta$	$\cos\varphi\cos\vartheta + \sin\varphi\times\sin\psi\sin\vartheta$	$\cos\varphi\sin\psi\sin\vartheta - \sin\varphi\cos\vartheta$
z_0	$-\sin\psi$	$\sin\varphi\cos\psi$	$\cos\varphi\cos\psi$

The projections of the angular rate of the spacecraft hull in terms of the angles ϑ, and ψ can be expressed thusly:

$$\left.\begin{aligned} p &= \dot{\varphi} - \dot{\vartheta}\sin\psi; \\ q &= \dot{\psi}\cos\varphi + \dot{\vartheta}\sin\varphi\cos\psi \\ r &= \dot{\vartheta}\cos\varphi\cos\psi - \dot{\psi}\sin\varphi. \end{aligned}\right\} \qquad (6.7)$$

If external moments are not applied to the satellite, that is, $\overline{M} = 0$, obviously $\overline{K} = \overline{C}$, where $\overline{C}$ is a constant vector. Let us denote its projections onto the axes Ox_0, Oy_0, and Oz_0 by Cx_0, Cy_0, and Cz_0.

Using the rule of determination of the direction cosines, we get:

$$\left.\begin{aligned} C_{x_0} &= K_x\cos\psi\cos\vartheta + K_y(\sin\varphi\sin\psi\cos\vartheta - \cos\varphi\sin\vartheta) + \\ &+ K_z(\cos\varphi\sin\psi\cos\vartheta + \sin\varphi\sin\vartheta); \\ C_{y_0} &= K_x\cos\psi\sin\vartheta + K_y(\sin\varphi\sin\psi\sin\vartheta + \cos\varphi\cos\vartheta) + \\ &+ K_z(\cos\varphi\sin\psi\cos\vartheta - \sin\varphi\cos\vartheta); \\ C_{z_0} &= -K_x\sin\psi + K_y\sin\varphi\cos\psi + K_z\cos\varphi\cos\psi, \end{aligned}\right\} \qquad (6.8)$$

where K_x, K_y, K_z are the projections of the kinetic moment onto the bound axes.

Obviously,

$$C_{x_0}^2 + C_{y_0}^2 + C_{z_0}^2 = K_x^2 + K_y^2 + K_z^2.$$

Assume the Ox and Oy axes of the running system lie in a plane parallel to the Ox_0y_0 plane. Then in unperturbed motion $\psi = \phi = 0$ and for C_{x_0}, C_{y_0}, and C_{z_0}, we get /311

$$\left.\begin{aligned} C_{x_0} &= K_x \cos\vartheta - K_y \sin\vartheta; \\ C_{y_0} &= K_x \sin\vartheta + K_y \cos\vartheta; \\ C_{z_0} &= K_z. \end{aligned}\right\} \qquad (6.9)$$

Let us further assume that the angle ϑ is an assigned periodic function of time. An example of this motion is the case of Earth flyby with constant direction of one of the satellite axes lying in the plane Oxyz (parallel to the orbital plane) toward the center of attraction. Obviously, in the case of this motion K_x and K_y will also be periodic functions of time, where

$$\left.\begin{aligned} K_x &= C_{xy} \sin[\vartheta(t) + \theta]; \\ K_y &= C_{xy} \cos[\vartheta(t) + \theta], \end{aligned}\right\} \qquad (6.10)$$

and

$$C_{xy} = \sqrt{C_{x_0}^2 + C_{y_0}^2} \quad \text{and} \quad \theta = \operatorname{arctg} \frac{C_{x_0}}{C_{y_0}}.$$

In the case of unperturbed motion, $\psi = \varphi = 0$, $p = 0$, $q = 0$, $r = \dot{\vartheta}$, and, as follows from Eq. (6.8), the nonzero projections of the kinetic moments K_x and K_y are projections of the kinetic moments of the flywheels. Generally speaking these acquired some angular rates during the time preceding the moment under study. The rpm of

the flywheels must periodically vary. In the case of three flywheels with axes of rotation parallel to the axes Ox, Oy, and Oz, the revolutions per minute vary for those flywheels whose axes are parallel to the Ox and Oy axes. If the projections of the kinetic moment of the hull onto the axes Ox and Oy are zero, we have

$$K_x=\omega_x I_x \quad \text{and} \quad K_y=\omega_y I_y,$$

where I_x and I_y are the moments of inertia of the flywheels, and ω_x and ω_y are the flywheel angular rates.

Referring to the last formulas, we can state that ω_x and ω_y are periodic functions of time. This is explained by the fact that when $r \neq 0$, based on Eqs. (6.6) the angular flywheel rates ω_x and ω_y will yield nonzero gyroscopic moments. They must be damped by the appropriate acceleration or slowing down of the flywheel angular rate, which is necessary to meet the requirement $p = 0$ and $q = 0$.

These accelerations and decelerations associated with energy expenditure are not necessary for ordered motion in an orbit. If we assume at the initial moment that the projections of vector K onto the orbital plane (plane $Ox_0y_0z_0$) are zero, that is, $C_{x_0} = C_{y_0} = 0$, then $\omega_x = \omega_y = 0$ during the entire motion in the orbit. So to reduce the energy expenditures we must retard the flywheels whose axes are in the orbital plane. /312

By analyzing the kinetic energy of the flywheels we can conclude that to reduce the energy losses the moments of flywheel inertia I_x and I_y must be selected as large as possible and as similar in magnitude as possible.

Let us examine the case of satellite stabilization about a given invariant attitude in space, that is, maintenance of the directions of the Ox, Oy, and Oz axes along the Ox_0, Oy_0, and Oz_0 axes [28].

We will neglect the magnitude of the axial moment of inertia of the flywheels I compared to the moments of inertia A, B, and C. Thus, we will take $\bar{M}_p = \bar{M}_r = 0$ and we will neglect the moments of drag and gyroscopic moments compared to the magnitudes of the control moments M_{ax}, M_{ay}, and M_{az}. Assume that the deviations

of the axes are small. Under these assumptions, we have

$$p = \dot{\varphi};\ q = \dot{\psi};\ r = \dot{\vartheta}.$$

We will assume further that $\dot{p}$, $\dot{q}$, and $\dot{r}$ are quantities of the same order of smallness as p, q, and r. Then the second summands in the left-hand sides of the equations of satellite stabilization Eq. (6.6) can be discarded, and the equations become

$$A\ddot{\varphi} = M_{ax};\ B\ddot{\psi} = M_{ay};\ C\ddot{\vartheta} = M_{az}. \tag{6.11}$$

Let us further assume that the moment on the shaft of a reaction flywheel is a function of the angular rate it develops and, moreover, depends on the angle ϕ and on $\dot{\phi}$, that is,

$$\begin{aligned} A\ddot{\varphi} &= -M'_{ax}(\omega_x,\ \varphi,\ \dot{\varphi});\\ B\ddot{\psi} &= -M'_{ay}(\omega_y,\ \psi,\ \dot{\psi});\\ C\ddot{\vartheta} &= -M'_{az}(\omega_z,\ \vartheta,\ \dot{\vartheta}). \end{aligned}$$

Here it is obvious that oscillations of the satellite about the axes Ox, Oy, and Oz will be independent.

Let us expand M_{ax} into a series close to the point (ω_{x0}, 0, 0) corresponding to the unperturbed regime. With an accuracy to the linear terms we get

$$M'_{ax}(\omega_x, \varphi, \dot{\varphi}) = M'_{ax}(\omega_{x0}, 0, 0) + \left(\frac{\partial M'_{ax}}{\partial \dot{\omega}}\right)_0 \delta\omega_x + \left(\frac{\partial M'_{ax}}{\partial \varphi}\right)_0 \varphi + \left(\frac{\partial M'_a}{\partial \varphi}\right)_0 \dot{\varphi},$$

and the equation of satellite motion in the plane yOz will become:

$$A\ddot{\varphi} + \left(\frac{\partial M'_{ax}}{\partial \dot{\varphi}}\right)\dot{\varphi} + \left(\frac{\partial M'_{ax}}{\partial \varphi}\right)\varphi + \left(\frac{\partial M'_{ax}}{\partial \omega}\right)\delta\omega_x = M_{ax}(\omega_{x0}, 0, 0).$$

Using Eq. (6.9) for the projection C_{x_0} and discarding terms of the first and higher orders of smallness, we get /313

$$C_{x_0} = K_x = A\dot{\varphi} + I\omega_x.$$

Varying about the point (ω_{x0}, 0, 0), we have

$$\delta\omega_x = -\frac{A}{I}\dot{\varphi}.$$

Finally, the equation of motion becomes

$$A\ddot{\varphi} + \left(\frac{dM_{ax}}{d\dot{\varphi}} - \frac{A}{I}\frac{dM'_{ax}}{d\omega_x}\right)_0 \dot{\varphi} + \left(\frac{dM_{ax}}{d\varphi}\right)_0 \varphi = M_{ax}(\omega_{x0}, 0, 0). \qquad (6.12)$$

The term $M_{ax}(\omega_{x0}, 0, 0)$ expresses the displacement action and is responsible for the static error of the system

$$\varphi_{st} = \frac{M_{ax}(\omega_{x0}, 0, 0)}{\frac{dM'_{ax}}{d\varphi}}.$$

It is important to note that when $\frac{dM'_{ax}}{d\varphi} < 0$, the dependence of the moment M_{ax} on flywheel angular rate ω_x promotes damping of the perturbation.

Thus, this theory can solve specific problems associated with employing reaction flywheels as AES stabilization devices. The orientation systems in which flywheels are used, owing to the small expenditure of reaction mass, must provide for extended existence of the controlled satellite in space.

6.3. Dependence of Information Content of Radio Link on Orientation Accuracy

Let us consider the case when a narrowly focussed parabolic antenna is installed on a satellite. This antenna can considerably boost the energy potential of the "onboard-Earth" radio link and, therefore, increase the information content of this radio link.

In recent years adequate experience in developing and using parabolic antennas and methods of orienting these antennas for a spacecraft was accumulated. In particular, this type of antenna was installed on Molniya communication satellites.

The information content of the "onboard-Earth" radio link is determined by the coefficient of oriented action of the parabolic antenna. If there is no automatic variation in the data transmission rate as a function of the instantaneous coefficient of directed action, the information content is defined as the minimum, guaranteed value of this coefficient during a single period of spacecraft oscillation about its mass center. /314

This minimum value of the coefficient of directed action is defined in turn by the geometry of the parabolic antenna and by the maximum angle of deviation of the direction toward the receiving station [point] from the antenna's electrical axis, that is, from the direction corresponding to the maximum coefficient of oriented action. This angle of deviation is determined by the accuracy with which the craft is oriented toward the receiving station.

The orientation accuracy determines, depending on the variant under which the control moments are produced, the mass flow of the reaction mass to the gas-jet system or the required power of the flywheel system.

A combined analysis of all these factors is of interest in selecting the size of the parabolic antenna and the accuracy with which the craft is pointed to the receiving station, ensuring maximum volume of transmitted data.

First of all, let us look at the dependence of the coefficient of oriented action of the parabolic antenna on antenna diameter for a given angle of deviation from the antenna's electrical axis. This problem can be of separate significance in those cases when the accuracy of craft orientation and antenna orientation is not selected, but is assumed given.

From the theory of parabolic antennas we know [2] that the coefficient of oriented action depends on the angle θ between the direction toward the receiving station and the electrical axis of the antenna, as follows:

$$D=D_{\max}F(\theta x), \tag{6.13}$$

where D_{max} is the maximum coefficient of oriented action, corresponding to $\theta = 0$,

$x = \frac{d}{\lambda}$ (d is the antenna diameter and λ is the wavelength), and

$F(\theta x)$ is a continuously differentiable function of the product θx satisfying the conditions:

$F(0) = 1$ and $\frac{dF}{d(\theta x)} \leqslant 0$ in the θx range under study.

Further, we have

$$D_{max} = \pi^2 k x^2, \tag{6.14}$$

where k is a coefficient that depends on the shape and configuration of the radiator of the parabolic antenna and on the parameter $y = d/f_A$, where f_A is the focal length of the paraboloid.

Thus, the coefficient of oriented action of the parabolic antenna is defined by the function

$$D = \pi^2 k(y) x^2 F(\theta x). \tag{6.15}$$

In the theory of parabolic antennas, the dependence of the coefficient k -- called the use coefficient of the paraboloid aperture surface -- on the parameter y is analyzed in detail. In developing an antenna, the maximum value of this coefficient is achieved by selecting the radiator and the parameter y. The actual values of the coefficient k in spacecraft parabolic antennas are 0.5-0.6, and $y_{opt} = 1.6\text{-}3.0$. /315

Analysis of the dependence of D on parameter x for fixed angle θ shows that D reaches a maximum value when the following condition is satisfied:

$$2F(\theta x) = (\theta x) | f(\theta x) |, \tag{6.16}$$

where $f(\theta x) = \frac{dF(\theta x)}{d(\theta x)}$, and here $f(\theta x) < 0$ when $x > 0$, $\theta > 0$.

By solving Eq. (6.16) for (θx), we get

$$(\theta x) = Q, \text{ where } Q \neq Q(\theta x)$$

and, therefore, the optimal value is

$$x_{opt} = \frac{Q}{\theta}. \tag{6.17}$$

Here

$$D_{opt} = \pi^2 k \frac{Q^2 F(Q)}{\theta^2}. \tag{6.18}$$

Let us call the parabolic antenna with parameter x defined by Eq. (6.17) the optimal antenna for an assigned angle θ, where here and in the following by θ we will mean the maximum deviation of the direction toward the receiving station from the antenna's electrical axis.

The function $F(\theta x)$ is defined by a complex expression in terms of Bessel functions, which do not enable us to arrive at simple formulas for design calculations. So we will use this approximation:

$$F(\theta x) \quad \frac{D}{D_{max}} = \exp\left[-\alpha\left(\frac{\theta}{\theta_{0.5}}\right)^2\right], \tag{6.19}$$

where $\alpha = 0.69$;

$\theta_{0.5}$ is the value of θ at which $D = 1/2\ D_{max}$. The value of the angle $\theta_{0.5}$ is given by the formula

$$\theta_{0.5} = \frac{\beta}{x}, \tag{6.20}$$

where β is a coefficient that depends on the shape and construction of the radiator and on the parameter y.

As follows from exact calculations, β depends immaterially on these factors and when y = 1.6-3.2, β lies in the range 0.5-0.7. /316 So we need not consider the dependence of β on y and we can take $\beta = 0.6$, as is usually done when designing spacecraft antennas.

Fig. 6.3 presents this approximation (curve 1), as well as the theoretical radiation patterns in relative quantities for an antenna with a radiator in the form of an elementary vibrator with a plane reflector for two characteristic, mutually perpendicular planes E (curve 2) and H (curve 3) when d/f = 2.4. Shown in the same graph is the radiation pattern of the parabolic antenna of the Zond-3 (curve 4).

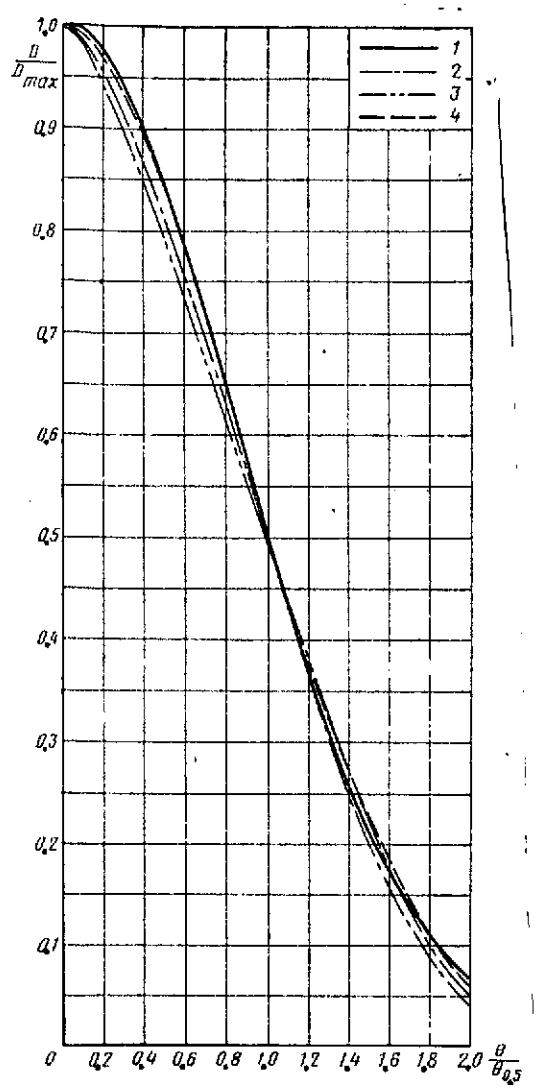

Fig. 6.3. For estimating the accuracy of the adopted approximation when calculating the coefficient of the antenna radiation pattern

As follows from the plots, the approximation is wholly suitable when $\theta < 2\theta_{0.5}$.

Based on Eqs. (6.14), (6.19), and (6.20), for the approximation adopted we have

$$D = \pi^2 k \left(\frac{d}{\lambda}\right)^2 \exp\left[-\frac{\alpha}{\beta^2}\left(\frac{d}{\lambda}\theta\right)^2\right]. \qquad (6.21)$$

Here Eq. (6.17) and (6.18) take on the following form:

$$x_{\text{opt}} = \left(\frac{d}{\lambda}\right)_{\text{opt}} = \frac{\beta}{\sqrt{\alpha}} \cdot \frac{1}{\theta}, \qquad (6.22)$$

$$D_{\text{opt}} = \frac{\pi^2}{e} \cdot \frac{k\beta^2}{\alpha} \cdot \frac{1}{\theta^2}. \qquad (6.23)$$

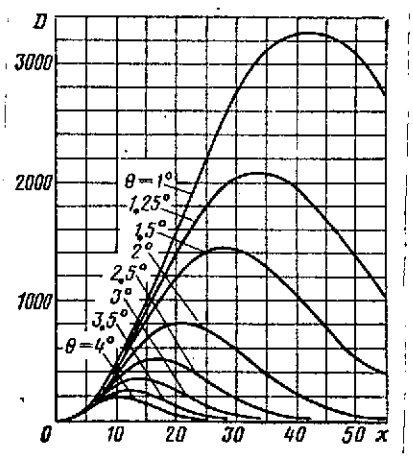

Fig. 6.4. Dependence of coefficient of antenna oriented action on parameter x for different θ /317

In designing parabolic antennas, the parameter d/λ can be determined for a given angle θ by Eq. (6.22) when $\alpha = 0.69$ and $\beta = 0.6$. This parameter determines the diameter of the paraboloid. Then using customary techniques in antenna engineering the focal length of the paraboloid ensuring the attainment of the maximum coefficient k is determined,

and the value of β in Eq. (6.20) is revised. When necessary, a second approximation can be made, correcting based on Eq. (6.22) the optimal diameter for the revised value of β.

Fig. 6.4 shows the dependence of D on the parameter x for different θ. The calculations were made for $\alpha = 0.69$, $\pi^2 k = 5$, and $\beta = 0.61$. As follows from the graphs, D depends strongly on the parameter x. Incorrect choice of the parabolic antenna diameter can lead to a large loss in the oriented action coefficient and in antenna weight (if the antenna diameter was selected as larger than the optimal).

When selecting the parabola antenna and the accuracy of its orientation [pointing] toward the receiving station with reference to all the constraints appearing in the course of spacecraft design, it is convenient to use a series of D(d) curves constructed according to Eq. (6.21) for different θ at a given wavelength.

Here, from the standpoint of obtaining the maximum coefficient of oriented action, one must strive to have θ as small as possible, and the parabola diameter as close as possible to the optimal value corresponding to this θ.

In several cases, determined by the purpose of the spacecraft, it can prove useful to assign the guaranteed coefficient of oriented action of the parabolic antenna and to find the antenna diameter that brings this value about at the smallest orientation accuracy. For this case, based on Eq. (6.21), we get

$$\theta = \frac{\beta}{x}\sqrt{-\frac{1}{\alpha}\ln\frac{D}{\pi^2 k x^2}}. \qquad (6.24)$$

It is not difficult to see that the last expression reaches a maximum when /318

$$x = x_{opt} = \frac{1}{\pi}\sqrt{\frac{De}{k}}. \qquad (6.25)$$

Further, let us take note of the following. Let us assume that for a given θ we have found the optimal parabola with $x = x_{opt} = \frac{\beta}{\sqrt{\alpha}}\cdot\frac{1}{\theta}$. For this parabola, we have

$$\theta_{0.5} = \frac{\beta}{x_{opt}} = \sqrt{\alpha}\theta \cong 0{,}83\theta, \qquad (6.26)$$

that is, the working value of the angle is about 20 percent larger than $\theta_{0.5}$.

By comparing the optimal coefficient of oriented action determined by Eq. (6.23) with a maximum coefficient corresponding to the position of the receiving station along the axis of the optimal parabolic antenna, we get

$$D_{opt} = \frac{1}{e} D_{max}. \tag{6.27}$$

Eqs. (6.26) and (6.27) can be used to determine the optimal parabola for a given angle θ, for an adopted approximation of the radiation pattern.

All the foregoing essentially shows how the volume of the transmitted information can be increased by correctly selecting the parabolic antenna for a given accuracy of antenna orientation. However, as was already pointed out, the mass flows of reaction mass (or electric energy) needed in orientation depend on the orientation accuracy. So for the case of restricted onboard reserves, increasing orientation accuracy can necessitate cutting down on data transmission time.

The amount of data transmitted in the time τ, for parameters of the onboard and ground radio systems constant during this period and for a constant distance from the ground communication station, and also with unchanged data transmission rate, can be expressed by the formula (in standard units)

$$M = AD\tau, \tag{6.28}$$

where A is a parameter dependent on the characteristics of the onboard and ground radio systems and on the distance to the satellite, and
D is the coefficient of oriented antenna action guaranteed during the time τ.

First let us examine the case when onboard the spacecraft is an optimal parabolic antenna whose diameter and maximum angle of deviation from the electrical axis are related by Eq. (6.17). For this case, based on Eq. (6.18) we find /319

$$M = \pi^2 Ak \frac{Q^2 F(Q)}{\theta^2} \tau. \tag{6.29}$$

Let us further look at two variants of producing the control moments needed to orient the craft toward the ground station. Here we will assume that during the time τ the parabolic antenna is fixed relative to the craft.

The first variant provides that onboard there is only a gas jet system imparting controlling impulses to the craft when there are angular deviations corresponding to the boundaries of the insensitivity zone of the orientation system. Here the weight of the reaction mass needed to orient the craft during the time τ can be expressed by the following formula, with an accuracy sufficient for our purposes:

$$G_{r.m} = B_1 \frac{\tau}{\varphi}, \qquad (6.30)$$

[r.m = reaction mass]

where B_1 is a parameter dependent on the moments of inertia of the craft and the characteristics of the orientation system and the gas jet system, and

ϕ is half of the insensitivity zone of the orientation system or (which amounts to virtually the same thing), the maximum deviation of the direction toward the receiving station (ground station) from the axis of the insensitivity zone in the established natural oscillatory regime.

Eq. (6.30) is valid for equal maximum deviations in the corresponding control channels.

The second variant of producing the control moments provides, in addition to the gas jet system, a system of flywheels whose kinetic moments are parallel to the craft axes. In the case of axial deviations determine by the boundaries of the insensitivity zone of the orientation system, to the appropriate flywheel is applied a constant moment of appropriate sign that modifies the angular rate of the flywheel and, therefore, the angular rate and attitude of the craft itself. The change in the angular rate of the flywheel halts when the craft is again within the insensitivity zone.

Characteristic of this variant is the fact that in the steady-state natural oscillatory regime only the electrical energy in changing the flywheel angular rate is dealt with. The working body of the gas jet system is expended only in periodic elimination of the consequences of the action of external perturbing moments, since the action of these moments can lead to an unbounded rise in the flywheel angular rate. Here the mass flow of the reaction mass is virtually independent of orientation accuracy.

In the second variant the amount of electrical energy needed /320
to orient the craft during the time τ can be expressed by the following approximate formula:

$$P = B_2 \frac{\tau}{\varphi}, \tag{6.31}$$

where B_2 is a parameter dependent on the moments of inertia of craft and flywheels, and on the characteristics of the orientation system and the electric power supply system, and
ϕ has the same significance as in Eq. (6.30).

The quantities ϕ and θ in Eqs. (6.29)-(6.31) are associated by the relation

$$\theta = \varphi + \delta, \tag{6.32}$$

where δ is the maximum mismatch between the axis of the insensitivity zone of the orientation system and the electrical axis of the parabolic antenna.

The mismatch δ is determined by the design of the spacecraft, the method of mutual adjustment of the antenna and the orientation system, the accuracy of determination of the electrical axis of the antenna, and several other electrical and dynamic parameters of the orientation system. For craft thus far developed, δ = = 10'-60'.

We note that we have examined the worst case, when the plane extending through the electrical axis of the antenna and the axis of the insensitivity system (the plane of the angle δ) coincides with the plane of the maximum deviation in the orientation system.

Let us further introduce the concept of specific information $\overline{M}$. By the latter we will mean the ratio of the amount of information transmitted in the time τ to the weight of the reaction mass expended during this same time, or to the amount of electrical energy expended in the time τ to orient the craft (for the first and second variants of producing the control moments, respectively). Below we will examine several practical applications of the concept of specific information.

Under Eqs. (6.29)-(6.32), we find

$$\overline{M} = \pi^2 \frac{AkQ^2F(Q)}{B_i} \cdot \frac{\varphi}{(\varphi + \delta)^2}, \tag{6.33}$$

for the case when an optimal parabolic antenna is installed, where i = 1, 2 -- depending on the variant of producing the control moments.

The quantity $\overline{M}$ reaches a maximum when

$$\varphi=\varphi_{opt}=\delta. \tag{6.34}$$

Note that since in deriving Eq. (6.33) we used the general formula (6.18), the result does not depend on the kind of approximation of the radiation pattern. However, this is characteristic only for the case of an optimal parabolic antenna we have been considering. We also note that this derivation does not depend on the scheme of orienting the parabolic antenna toward the ground receiving station, that is, on whether this is done by orientation toward the Sun and a reference star or directly, using optical or radio direction-finders. /321

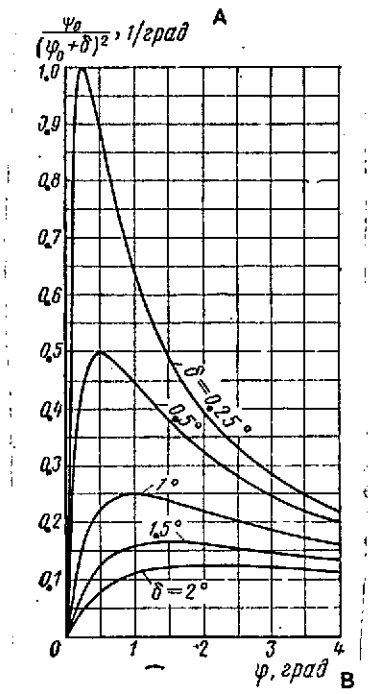

Fig. 6.5. $\frac{\varphi}{(\varphi+\delta)^2}$ as a function of half the insensitivity zone of the orientation system ϕ

Key: A. deg^{-1}
B. deg

Fig. 6.5 shows the dependence of

$$m=\frac{\varphi}{(\varphi+\delta)^2}$$

on ϕ for different δ. The quantity m is the ratio of the information volume transmitted in the time τ to the volume of information transmitted for the same mass flow of the reaction mass or electrical energy, but for $\delta = 0$, $\phi = 1$ deg (for an optimal parabola).

As follows from the curves in Fig. 6.5, for small δ the specific information depends strongly on ϕ.

When $\delta = 0°.25$-$0.5°$, the incorrect choice of the orientation accuracy can reduce the specific information by several-fold. On the other hand, when $\delta = 1°$-$2°$ the change in ϕ over a wide range has virtually no effect on the specific information.

For the approximation of the radiation pattern adopted above, the diameter of the parabolic

antenna, when optimal orientation accuracy is assumed, will be

$$d_{opt} = \frac{\lambda\beta}{2\delta_{\gamma}\bar{\alpha}}. \qquad (6.35)$$

based on Eqs. (6.22), (6.32), and (6.34).

In some cases it may turn out that the optimal orientation accuracy is determined by Eq. (6.34) cannot be realized for technical reasons. So let us introduce the concept of the technically feasible orientation accuracy -- $\bar{\phi}$. If ϕ_{opt} proves to be smaller than $\bar{\phi}$, naturally we take the value $\bar{\phi}$. However, in this case to increase the volume of the transmitted information, the diameter of the parabolic antenna should be chosen optimal for the quantity $\bar{\phi} + \delta$. /322

Finally, there can be a variant in which the optimal orientation accuracy is realized, but the diameter of the optimal parameter determined by Eq. (6.35) cannot be assumed for design or weight considerations.

Let us derive a more general formula for the optimal orientation accuracy for such cases, with a given parabolic antenna diameter $\bar{d}$. This diameter, in particular, can become the limiting diameter by reason of design or weight considerations. Here we must use the approximation (6.19). Based on Eqs. (6.21), (6.28), (6.30), (6.31), and (6.32), we get

$$\bar{M} = \frac{A}{B_i}\pi^2 k\varphi\left(\frac{\bar{d}}{\lambda}\right)^2 \exp\left[-\frac{\alpha}{\beta^2}\left(\frac{\bar{d}}{\lambda}\right)^2(\varphi+\delta)^2\right]. \qquad (6.36)$$

The quantity $\bar{M}$ reaches a maximum when

$$\varphi = \bar{\varphi}_{opt} = \frac{1}{2}\left(\sqrt{\delta^2 + 2\frac{\beta^2}{\alpha}\left(\frac{\lambda}{\bar{d}}\right)^2} - \delta\right). \qquad (6.37)$$

In this case $\bar{\phi}_{opt}$ is determined only by the quantities δ and $\bar{d}/\lambda$, and also by the known coefficients α and β.

The Eq. (6.34) derived above for the optimal parabolic antenna can be readily obtained from Eq. (6.37) if in accordance with Eq. (6.22) we assume in the latter

$$\frac{\bar{d}}{\lambda} = \frac{\beta}{\gamma\bar{\alpha}} \cdot \frac{1}{\bar{\varphi}_{opt} + \delta}$$

and solve the resulting expression for $\bar{\phi}_{opt}$, that is, Eq. (6.34) for the approximation (6.19) is a particular case of Eq. (6.37).

Note that $\bar{\phi}_{opt}$ determined by Eq. (6.37) is always larger than the technically feasible value. Actually, if the diameter $\bar{d}$ in accordance with the mission posed is smaller than the optimal value, based on Eq. (6.35), we have $\frac{\bar{d}}{\lambda} < \frac{\beta}{2\delta\sqrt{a}}$. Under this condition Eq. (6.37) yields $\bar{\phi}_{opt} > \delta$. But δ is equal to the optimal orientation accuracy, which under our assumption can be realized.

In conclusion, let us look at practical applications of these results for a number of spacecraft types.

1. Only a gas-jet system was installed on a spacecraft. In this case

$$M = \bar{M} G_{r.m}, \tag{6.38}$$

Hence it follows that the maximum $\bar{M}$ corresponds to the maximum volume of transmitted information for a given reserve of reaction mass or a minimum required reserve for a given volume of data transmitted. Essentially, achieving maximum specific information implies the most effective use of the reaction mass. Referring to Eq. (6.32), we can cancel out θ from Eqs. (6.29) and (6.30). Here we get the following relations: /323

$$M = \frac{c\tau}{\left(\frac{B_1\tau}{G_{r.m}} + \delta\right)^2}, \tag{6.39}$$

or

$$G_{r.m} = \frac{B_1\tau}{\sqrt{\frac{c\tau}{M}} - \delta}, \tag{6.40}$$

where $c \neq c(\tau)$.

From Eqs. (6.39), (6.40), and (6.33) it follows that the optimal ϕ realizing the maximum $\bar{M}$ corresponds to the optimal

transmission time τ realizing the maximum M for given $G_{r.m}$ of Eq. (6.39), or minimum $G_{r.m}$ for given M of Eq. (6.40). From Eq. (6.39) it also follows that if the duration of transmission ϕ is given, there will be no optimal orientation accuracy since the smaller the ϕ (the greater the $G_{r.m}$), the larger then will be the volume of transmitted information. In the latter case we must adopt the minimum feasible ϕ, which can be determined either by the technical capabilities of the orientation system or by the weight of the gas-jet system. Here, it is useful to install on the spacecraft the optimal parabola for this ϕ, since this will produce the maximum coefficient of the oriented action of the parabolic antenna.

2. A system of flywheels powered from electric storage batteries was installed on a spacecraft, in addition to the gas-jet system. In this case we have

$$M = \overline{M}P, \tag{6.41}$$

where P is a quantity proportional to the capacity of the storage batteries.

This variant coincides with the first if instead of the reaction mass reserve we have in mind the capacity of the storage batteries, that is, in this variant the optimal orientation accuracy realizing the maximum specific information $\overline{M}$ has an engineering meaning.

3. A system of flywheels was installed on a spacecraft, but they were powered by a solar battery. Obviously, in this case $\overline{M}$ is the ratio of the data transmission rate dM/dt to the mean power N collected from the solar battery to sustain the orientation. Here we can write the following formulas: /324

$$\overline{M} = \frac{\frac{dM}{d\tau}}{N}; \quad N = \frac{B_3}{\varphi}; \quad \frac{dM}{d\tau} = \frac{c}{\left(\frac{B_3}{N} + \delta\right)^2},$$

where B_3 is a parameter dependent on the moments of inertia of the craft and the flywheels and on the characteristics of the orientation system and the electric power system.

In this case the effort to obtain the maximum $\overline{M}$ by selecting the optimal orientation accuracy does not have engineering

significance, since the smaller the ϕ (the greater the N), the greater also is the data transmission rate dM/dt. Therefore, here as in the first variant, when τ = const it is best to assume the minimum allowable value ϕ determined by the technical capabilities of the solar battery (by weight or area). Here, naturally, the parabolic antenna optimal for the given ϕ should be installed on the satellite, since this would ensure the maximum coefficient of the directed action of the antenna and the maximum data transmission rate that is possible under the existing constraints.

REFERENCES

/325

1. Akim, E. L. and Eneyev, T. M., "Determination of Parameters of Spacecraft Motion from Trajectory Measurements," Kosmicheskiye issledovaniya 1/1, 5-50 (1963).

2. Ayzenberg, G. Z., Antenny ul'trakorotkikh voln [Antennas for Ultrashort Waves], Moscow, State Publishing House on Problems of Communications and Radio, 1957, 699 pp.

3. Alekseyev, K. B., Bebenin, G. G., and Yaroshevskiy, V. A., Manevrirovaniye kosmicheskikh apparatov [Maneuvering of Spacecraft], Moscow, "Mashinostroyeniye" Press, 1970, 416 pp.

4. Andreyevskiy, V. V., Dinamika spuska kosmicheskikh apparatov na Zemlyu [Dynamics of Deorbiting of Spacecraft to Earth], Moscow, "Mashinostroyeniye" Press, 1970, 232 pp.

5. Appazov, R. F., Lavrov, S. S., and Mishin, V. P., Ballistika upravlyayemykh raket dal'nego deystviya [Ballistics of Long-Range Guided Missiles], Moscow, "Nauka" Press, 1966, 120 pp.

6. Bazhinov, I. K. and Pochukayev, V. N., "Estimation of Flight Trajectory Parameters of a Spacecraft for an Unknown Matrix of Second Moments of Navigation Measurement Errors," Kosmicheskiye issledovaniya 9/2, 173-178 (1971).

7. Bazhinov, I. K. and Pochukayev, V. N., "Geometrical Interpretation of Problems of Estimating the Accuracy of Determining Spacecraft Trajectories," Kosmicheskiye issledovaniya 9/2, 179-187 (1971).

8. Bazhinov, I. K. and Pochukayev, V. N., "Optimal Distribution of Navigation Measurements," Kosmicheskiye issledovaniya 9/2, 188-194 (1971.

9. Baxhinov, I. K., Pochukayev, V. N., and Serdyukov, A. N., "Selecting Parameters to be Measured when Determining Spacecraft Trajectories," Kosmicheskiye issledovaniya 10/4, 467-476 (1972).

10. Bazhinov, I. K., Aleshin, V. I., Pochukayev, V. N., et al., Kosmicheskaya navigatsiya [Space Navigation], Moscow, "Mashinostroyeniye" Press, 1974, 352 pp.

11. Batrakov, Yu. V., and Proskurin, V. F., "First-Order Perturbations in the Motion of Artificial Earth Satellites Caused by Compression of the Earth," in: Iskusstvennyye sputniki Zemli [Artificial Earth Satellites], Moscow, USSR Academy of Sciences Press, No. 3, 1968, pp. 32-38.

12. Batrakov, Yu. V. and Proskurin, V. F., "Orbital Perturbations of Artificial Earth Satellites," in: Iskusstvennyye sputniki Zemli, Moscow, USSR Academy of Sciences Press, No. 3, 1959, pp. 39-46.

13. Beletskiy, V. V., Dvizheniye iskusstvennogo sputnika otnositel'no tsentra mass [Motion of Artificial Satellite Relative to Mass Center], Moscow, "Nauka" Press, 1965, 416 pp.

14. Beletskiy, V. V., "Classification of Motions of Artificial Earth Satellite About Mass Center," in: Iskusstvennyye sputniki Zemli, Moscow, USSR Academy of Sciences Press, No. 6, 1961, pp. 11-32.

15. Vatson, G. N., Teoriya besselevykh funktsiy [Theory of Bessel Functions], Part 1, Moscow, Foreign Literature Publishing House, 1949, 798 pp.

16. Gantmakher, F. R., Teoriya matrits [Matrix Theory], Moscow, "Nauka" Press, 1966, 576 pp.

17. Gurko, O. V. and Slabkiy, L. I., "Use of Force Effects of Gravity and the Light Fields of the Sun in Spacecraft Orientation," in: Iskusstvennyye sputniki Zemli, Moscow, USSR Academy of Sciences Press, No. 16, 1963, pp 34-45.

18. Demidovich, B. P. and Maron, I. A., Osnovy vychislitel'noy matematiki [Fundamentals of Computational Mathematics], Moscow, "Nauka" Press, 1970, 664 pp.

19. Dikusar, V. V. and Shilov, A. A., "Optimization of Craft Flight Range in Atmosphere with Reference to g-Loads," Uchenyye zapiski TsAGI [Scientific Notes of the Central Institute of Aerohydrodynamics imeni N. Ye. Zhukovskiy], 1/2, 75-83 (1970), Moscow.

20. Duboshin, G. N., Vvedeniye v nebesnuyu mekhaniku [Introduction to Celestial Mechanics], Moscow, ONTI, 1938, 256 pp. /326

21. Dubyago, A. D., Opredeleniye orbit. [Orbit Determination], Moscow-Leningrad, Fizmatgiz, 1949, 444 pp.

22. Yegorova, A. B., "Effect of Attraction of Moon and Sun on Motion of Artificial Earth Satellite," in: Iskusstvennyye sputniki Zemli, Moscow, USSR Academy of Sciences Press, No. 8, 1961, pp. 46-56.

23. Yegorov, V. A., "Determining True Anomaly in Perturbed Motion," Astronomicheskiy zhurnal 35/1, 166-168 (1958).

24. Zhelnin, Yu. N. and Shilov, A. A., "Minimum-Range Trajectories in the Entry of Spacecraft Into the Earth's Atmosphere at Supersonic Velocity," Uchenyye zapiski TsAGI 1/1, 8-13 (1970).

25. Yershov, V. G., "Optimization of Program of Trajectory Measurements," Kosmicheskiye issledovaniya 8/1, 6-12 (1970).

26. Zhongolovich, N. A., "External Gravity Fields of the Earth and Fundamental Concepts Associated with It," Trudy Instituta teoreticheskoy astronomii [Transactions of the Institute of Theoretical Astronomy], Leningrad, USSR Academy of Sciences Press, 1952, pp. 1-128.

27. Zenger, Ye. K., K mekhanike fotonnykh raket [Mechanics of Photon Rockets], Moscow, Foreign Literature Publishing House, 1958, 144 pp.

28. Idel'son, N. I., Sposob naimen'shikh kvadratov [Method of Least Squares], Moscow, Geodezizdat, 1947, 352 pp.

29. Idel'son, N. I., Teoriya potentsiala s prilozheniyami k teorii figury Zemli i geofizike [Theory of Potential with Applications to the Theory of the Figure of the Earth and Geophysics], Moscow-Leningrad, ONTI, 1936, 348 pp.

30. Ivanov, N. M., Nogov, O. A., and Bazhinov, I. K., "An Algorithm for Controlling the Descent of the Spacecraft from AES Orbit," Kosmicheskiye issledovaniya 10/4, 510-514 (1972).

31. Ishlinskiy, A. Yu., Inertsial'noye upravleniye ballisticheskimi raketami [Inertial Control of Ballistic Missiles], Moscow, "Nauka" Press, 1968, 142 pp.

32. Kislik, M. D., "Motion of Artificial Satellite in Normal Gravity Field of Earth," in: Iskusstvennyye sputniki Zemli, Moscow, USSR Academy of Sciences Press, No. 4, 1960, pp. 3-17.

33. Kolegov, G. A., "Variations in Density of Upper Atmosphere Based on Data of Variations in Periods of Artificial Earth Satellites," in: Iskusstvennyye sputniki Zemli, Moscow, USSR Academy of Sciences Press, No. 4, 1960, pp. 31-34.

34. Kondrat'yev, K. Ya., Meteorologicheskiye issledovaniya c pomoshch'yu raket i sputnikov [Meteorological Studies Using Rockets and Satellites], Leningrad, Gidrometeoizdat, 1962, 251 pp.

35. Kondratyuk, Yu., Zavoyevaniye mezhplanetnykh prostranstv [Conquest of Interplanetary Space], Moscow, Oborongiz, 1947, 81 pp.

36. Kibardin, Yu. A., Kuznetsov, S. I., et al., Atlas gazodinamicheskikh funktsiy pri bol'shikh skorostyakh i vysokikh temperaturakh vozdushnogo potoka [Atlas of Gas-Dynamic Functions at High Air-Flow Velocities and Temperatures], Moscow-Leningrad, Gosenergoizdat, 1961, 328 pp.

37. Kugayenko, B. V., and El'yasberg, P. Ye., "Influence of Diurnal Effect in the Distribution of Atmospheric Density on Braking of an AES," in: Matematicheskiye metody modelirovaniya v kosmicheskikh issledovaniyakh [Mathematical Methods of Simulation in Space Research], Vol. 1, Moscow, "Nauka" Press, 1971, pp. 73-105.

38. Lantsosh, K., Prakticheskiye metody prikladnogo analiza [Practical Methods of Applied Analysis], Moscow, Fizmatgiz, 1961, 524 pp.

39. Lidov, M. L., "Determining Atmospheric Density from Observed Braking of First Artificial Earth Satellites," in: Iskusstvennyye sputniki Zemli, Moscow, USSR Academy of Sciences Press, No. 1, 1958, 9-20 pp.

40. Lidov, M. L., "Apriori Estimates of Accuracy of Determining Parameters by the Least-Squares Method," Kosmicheskiye issledovaniya 2/5, 713-715 (1964).

41. Linnik, Yu. V., Metod naimen'shikh kvadratov i osnovy teorii obrabotki nablyudeniy [Method of Least Squares and Essentials of Observation Processing Theory], Moscow, Fizmatgiz, 1958, 333 pp.

42. Lokh, U., Dinamika i termodinamika spuska v atmosfere planet [Dynamics and Thermodynamics of Descent into Planetary Atmospheres], Moscow, "Mir" Press, 1966, 114 pp.

43. Lur'ye, A. I., Analiticheskaya mekhanika [Analytical Mechanics], Moscow, Fizmatgiz, 1961, 824 pp.

44. Osnovy teorii poleta kosmicheskikh apparatov [Fundamentals of Spacecraft Flight Theory], edited by G. S. Narimanov, Moscow, "Mashinostroyeniye" Press, 1971, 607 pp.

45. Orlov, B. V., et al., Osnovy proyektirovaniya raketno-pryamotochiykh dvigateley [Fundamentals of the Designing of Ramjet Rocket Engines], Moscow, "Mashinostroyeniye" Press, 1967, 421 pp.

46. Okhotsimskiy, D. Ye. and Eneyev, T. M., "Some Variational Problems Associated with the Launch of an Artificial Earth Satellite," UFN 13/1a, 5-32 (1957).

47. Okhotsimskiy, D. Ye., Eneyev, T. M., and Taratynova, G. P., "Determining Lifetime of Artificial Earth Satellite and Studying Secular Perturbations of Its Orbit," UFN 13/1, 33-50 (1957).

48. Okhotsimskiy, D. Ye., Bel'chanskiy, G. I., Bukharkina, A. P, et al., "Optimal Control for Atmospheric Entry," Kosmicheskiye issledovaniya 6/1, 31-48 (1968).

49. Okhotsimskiy, D. Ye., Bukharkina, A. P., and Golubev, Yu. F., " Control of spacecraft motion in atmospheric entry," Kosmicheskiye issledovaniya 7/2, 171-178 (1969).

50. Okhotsimskiy, D. Ye., Bukharkina, A. P., and Golubev, Yu. F., "Algorithm of Autonomous Control of Bringing Spacecraft to Given Landing Site," Kosmicheskiye issledovaniya 8/2, 169-188 (1970).

51. Pogorelov, D. A., Teoriya keplerovykh dvizheniy letatel'nykh apparatov [Theory of Keplerian Motions of Spacecraft], Moscow, Fizmatgiz, 1961, 107 pp.

52. Polyakova, Ye. N., "Light Pressure and Motion of Earth Satellites," Byulleten' instituta teoreticheskoy astronomii 9/1(104), 15-45 (1963).

53. Pontryatin, L. S., et al., Matematicheskaya teoriya optimal'nykh protsessov [Mathematical Theory of Optimal Processes], Moscow, "Nauka" Press, 1969, 455 pp.

54. Ponomarev, V. M., Teoriya upravleniya dvizheniyem kosmicheskikh apparatov [Theory of Control of Spacecraft Motion], Moscow, "Nauka" Press, 1965, 455 pp.

55. Raushenbakh, B. V. and Tokar', Ye. N., "Several Problems of Control in Interplanetary Space," in: Iskusstvennyye sputniki Zemli, Moscow, USSR Academy of Sciences Press, No. 5, 1960, pp. 41-53.

56. Subbotin, M. F., Kurs nebesnoy mekhaniki [Course in Celestial Mechanics], Vol. 2, Moscow, ONTI, 1937, 414 pp.

57. Reaktivnyye dvigateli [Sbornik statey] [Jet Engines (Collection of Articles)], edited by O. Ye. Lancaster, translated from the English, Moscow, Voyenizdat, 1962, 667 pp.

58. Suslov, G. K., Teoreticheskaya mekhanika [Theoretical Mechanics], Moscow-Leningrad, Gostekhizdat, 1946, 655 pp.

59. Tablitsy vremennoy standartnoy atmosfery(VSA-60) [Tables of Provisional Standard Atmosphere (VSA-60)], Computer Center of the USSR Academy of Sciences, 1960.

60. Taratynova, G. P., "Methods of Numerical Solution of Equations in Finite Differences and Their Application to Calculations of Orbits of Artificial Earth Satellites," in: Iskusstvennyye sputniki Zemli, Moscow, USSR Academy of Sciences Press, No. 4, 1960, pp. 56-81.

61. Taratynova, G. P., "Motion of Artificial Satellites in Noncentral Gravity Field of Earth When Atmospheric Drag is Present," UFN 63/1, 51-58 (1957).

62. Tsiang, H. Sh., "Aerodynamic of Rarified Gases," in: Gazovaya dinamika [Gas Dynamics], Moscow, IL, 1950, pp. 310-340.

63. Tsander, F. E., Problema poleta pri pomoshi reaktivnykh apparatov. Mezhplanetnyye polety [Problem of Jet Device-Assisted Flight, Interplanetary Flights], Moscow, Oborongiz, 1961, 459 pp.

64. Tsiolkovskiy, K. E., Trudy po raketnoy tekhnike [Works on Rocket Engineering], Moscow, Oborongiz, 1947, 368 pp.

65. Charnyy, V. I., Birzgal, A. P., Borisenko, V. I., et al., "Use of Direct Methods in Algorithms for Control of Craft Descent in the Atmosphere," Kosmicheskiye issledovaniya 7/6, 814-818 (1969).

66. Chapman, D. R., Priblizhennyy analiticheskiy metod issledovaniya vkhoda tel v atmosfery planet [Approximate Analytical Method of Investigating Entry of Bodies into Planetary Atmospheres], Moscow, IL, 1962, 114 pp.

67. Shapiro, I. I., Raschety trayektoriy ballisticheskikh snaryadov po dannym radiolokatsionnykh nablyudeniy [Calculations of Ballistic Missile Trajectories from Radar Observation Data], Moscow, IL, 1961, 314 pp.

68. El'yasberg, D. Ye., "Determination of Density of Upper Atmosphere from Secular Measurements of Orbital Elements of the First Two Artificial Earth Satellites," in: Iskusstvennyye sputniki Zemli, Moscow, USSR Academy of Sciences Press, No. 1, 1958, pp. 21-24.

69. El'yasberg, P. Ye., "Dependence of Secular Changes in Orbital /328
Elements on Air Drag," in: Iskusstvennyye sputniki Zemli, Moscow, USSR Academy of Sciences Press, No. 3, 1959, pp. 54-60.

70. El'yasberg, P. Ye. and Yastrebov, V. D., "Determination of Density of Upper Atmosphere from Observations of the Flight of the Third Artificial Earth Satellite," in: Iskusstvennyye sputniki Zemli, Moscow, USSR Academy of Sciences Press, No. 4, 1960, pp. 18-30.

71. El'yasberg, P. Ye., Vvedeniye v teoriyu poleta iskusstvennykh sputnikov Zemli [Introduction to Flight Theory of Artificial Earth Satellites], Moscow, "Nauka" Press, 1965, 540 pp.

72. Yaroshevskiy, V. A., "Approximate Calculation of Atmospheric Entry Trajectories," Kosmicheskiye issledovaniya 2/4-5, 507-531 (1964).

73. Yatsunskiy, I. M., "Determination of Conditions of Illumination and Residence Time of Artificial Earth Satellites in the Umbra and in the Sun," in: Iskusstvennyye sputniki Zemli, Moscow, USSR Academy of Sciences Press, No. 4, 1960, pp. 35-42.

74. Yatsunskiy, I. M., "Effect of Geophysical Factors on Satellite Motion," UFN 13/1a, 59-71 (1957).

75. Citron, S. J. and Meir, T. C., "An Analytic Solution for Entry into Planetary Atmospheres," AIAA Journ. No. 3, (1965).

76. Citron, S. J., "Reply by author to A. N. Nauich," AIAA Journ. No. 4, (1966).

77. Lees, Hartweg, and Cohen, "The Use of Aerodynamic Lift During Entry into the Earth's Atmosphere," ARSJ, No 29, (1959).

78. Kaula, W. M., "Analysis of Gravitational and Geometric Aspects of Geodetic Utilization of Satellites," The Geophysical Journal of the Royal Astronomical Society 5/2, July (1961).

79. Kaula, W. M., Journ. of Geophys. Researches 64/12, 2271-2279 Dec (1959).

80. Kozai, J., Astr. Journ 64/9, 367-377 (1959).

81. Tolle, H., Haseloff, J., Overesch, E., and J-k Boch., "Development of the Configuration of an Aerodynamic Re-entry Test Flight Vehicle with Special [sic] and Maneuverability," International Council of the Aeronautical Sciences, 7th Congress, Rome, Italy, 1970, Paper ICAS 70-02, 15 pp.

82. Vinti, I. P., Journal of Research of the National Bureau of Standards, Mathematics and Physics, 62, (1959).

83. Zimmi, W. F., Hoffman, I. P., and Ratz, E. A., "Thermal Loading of an Aerodynamic Reentry Body and the Resulting Optimization and Design Criteria," German Society of Aeronautics and Astronautics, Annual Congress, Bremen, West Germany, Sept. 22-24, 1969, Paper 45, p. 31.

84. Elfing, "Allocation in Linear Regression Theory," Annals of Mathematical Statistics, 23, (1952).

INDEX

Acceleration due to gravity 55
Active orientation system 323
Aerodynamic coefficients 28,297
Aerodynamic force
-- lift 28,276
-- of drag 28,276
Aerodynamic landing 316
Aerodynamic maneuver 316
Altitude
-- of apogee 20
-- of orbit 126
-- of perigee 20
Angle of atmospheric entry 288
Angle of attack 27
Angle of roll 28
Angular range of flight 282
Atmosphere 153
Atmospheric section
-- of descent 286,290
-- of insertion 27

Ballistic coefficient 158
Ballistic descent 254
Bessel functions of imaginary argument 171,180

Calculation formulas for unperturbed elliptical orbit 16
Characteristic velocity of SC 72
Circular velocity 21
Coasting descent 289
Coefficient of directed action of parabolic antenna 342
Conjugate system of differential equations 31
Control of SC motion 316
Controlled coasting descent 298
Convex covering of navigation vector-function 248
Coordinate system
-- geocentric Greenwich 274
-- launch 55
-- orbital 160
-- velocity 27

Cosines, direction 18

Draconic period 130
Deorbiting of satellite 273
Descent control systems of continuous action 308
Determination of AES orbits 215
Deviations of altitudes of orbital perigee and apogee 88
Deviations of circular orbit 98
Disturbing function 135

Eccentric anomaly 13
Eccentricity of orbit 9
Effect of AES motion
-- of gravitational anomalies 131
-- of initial perturbations 94
-- of sunlight pressure 211
Elements of orbit 88
Ellipsoid of revolution 116
Engine thrust 28
Equations of SC motion
-- in Greenwich coordinate system 274
-- in osculating elements 114
Errors in knowledge of forces acting on AES in flight 154
Euler's angles 324
Extra-atmospheric section
-- of descent 281
-- of insertion 27,55,72

Finite formulas of elliptical theory 15
Force of sunlight 211
Formulas of transformation
-- from osculating elements to rectangular 18
-- for rectangular to osculating 126

G-loads in ballistic descent 276
General problem of insertion of SC into orbit [text page not given]
Geod 131
Gravitational constant 2
Gravitational field of Earth 105

Inclination of orbital plane 6
Information content of radio communication link 340
Initial conditions
-- of AES motion 215
-- of entry 278
Insertion into orbit
-- with additional fuel combustion 71
-- without additional fuel combustion 54
Integral
-- of areas 4
-- of energy 7

Kepler's equation 13
Kinetic energy of AES 7

Landing accuracy 281
Lagrange's equations 135
Longitude of ascending node 6

Method
-- of least squares 221
-- of maximum likelihood 220
-- of orbit determination 229
-- of variations of arbitrary constants 107
Method of hit trajectories 311
Minimum required available lift-to-drag ratio 300
Moon 148

Navigational measurements 215

Optimal control 35
Optimal parabolic antenna 350
Optimal transfer point 72
Orbit
-- circular 14
-- hyperbolic 12
-- elliptical 12
-- parabolic 14
Orientation of SC 323
Osculating elements 106

Parameters of orbit 18
Passive orientation and stabilization 323
Period of revolution 15
Position of orbital plane 23
Potential
-- of gravitational force 116
-- of perturbing forces 105
Potential energy 7
Prediction of AES motion 153,192
Principle of the maximum 30

Reaction flywheels 352

Secular perturbations of orbit 120,123,130
Semi-major axis of orbit 9
Small initial perturbations of circular orbit 98
Specific thrust 28
Staging 41
Standard atmosphere 155

Tesseral harmonics 132
Temperature
-- equilibrium 27
-- of Earth atmosphere 157
Thermal flux
-- convective 293
-- radiative 293
Transfer ellipse 97
True anomaly 19

Uncontrolled coasting descent 300
Unperturbed orbital elements 117

Vernal equinox 17

Zonal harmonics 132

TABLE OF CONTENTS

Annotation iii

Preface iv

Foreword to First Edition vi

Foreword to Second Edition viii

Chapter 1. Insertion of Satellite into Orbit 1
1.1. Unperturbed satellite motion 2
1.2. General problem of inserting spacecraft into orbit 25
1.3. Method of inserting satellite into orbit without additional combustion of fuel 54
1.4. Method of inserting satellite into orbit with additional combustion of fuel 71

Chapter 2. Deviations of Orbit Caused by Errors in Insertion 87
2.1. Orbital deviations due to deviations in the parameters of motion at the end of the powered section 88
2.2. Determination of initial perturbations due to the deviations in final acceleration parameters 94
2.3. Deviations of circular orbit 98

Chapter 3. Analysis of Effect of Perturbing Forces Acting on an Orbit 105
3.1. Method of osculating elements 105
3.2. Orbital perturbations caused by the effect of compression of the terrestrial ellipsoid 116
3.3. Perturbing influences of anomalies in gravity on the satellite orbit 131
3.4. Perturbations caused by the influence of Moon and Sun 135
3.5. Estimate of perturbing action of atmosphere in determination of satellite lifetime 153
3.6. Effect of sunlight pressure 211

Chapter 4. Determination of Orbits from Navigational Measurements 215
4.1. Main concepts. Measured and determined parameters. Measurement errors 215

Chapter 4 [continued]
4.2. Method of maximum likelihood 220
4.3. Estimates of errors in determining orbital parameters 229
4.4. Space of trajectory parameters 245
4.5. Several geometrical interpretations in the space G 250
4.6. Optimal distribution of measurements 260

Chapter 5. Deorbiting of Satellite to Earth 273
5.1. Ballistic descent 274
5.2. Coasting descent 289
5.3. Coasting descent of a satellite with low lift-to-drag ratio 297
5.4. Aerodynamic method of descent 316

Chapter 6. Some Problems in Satellite Orientation 323
6.1. General equations of motion about mass center 324
6.2. Active stabilization of AES 330
6.3. Dependence of information content of radio link on orientation accuracy 340

References 354

Index 362

Table of Contents 364